Faculty of Science and Engineering

Department of Spatial Sciences

Determination of the High Water Mark and its Location Along a Coastline

Xin Liu

This thesis is presented for the degree of
Doctor of Philosophy
of
Curtin University

April 2013

Declaration

To the best of my knowledge and belief this thesis contains no material previously published by any other person except where due acknowledgement has been made.

This thesis contains no material which has been accepted for the award of any other degree or diploma in any university.

Signature……..

Date……..

ABSTRACT

The High Water Mark (HWM) is an important cadastral boundary that separates land and water. It is also used as a baseline to facilitate coastal hazard management, from which land and infrastructure development is offset to ensure the protection of property from storm surge and sea level rise. However, the location of the HWM is difficult to define accurately due to the ambulatory nature of water and coastal morphology variations. Contemporary research has failed to develop an accurate method for HWM determination because continual changes in tidal levels, together with unimpeded wave runup and the erosion and accretion of shorelines, make it difficult to determine a unique position of the HWM. While traditional surveying techniques are accurate, they selectively record data at a given point in time, and surveying is expensive, not readily repeatable and may not take into account all relevant variables such as erosion and accretion.

In this research, a consistent and robust methodology is developed for the determination of the HWM over space and time. The methodology includes two main parts: determination of the HWM by integrating both water and land information, and assessment of HWM indicators in one evaluation system. It takes into account dynamic coastal processes, and the effect of swash or tide probability on the HWM. The methodology is validated using two coastal case study sites in Western Australia. These sites were selected to test the robustness of the methodology in two distinctly different coastal environments.

At the first stage, this research develops a new model to determine the position of the HWM based on the spatial continuity of swash probability (SCSP) or spatial continuity of tidal probability (SCTP) for a range of HWM indicators. The indicators include tidal datum-based HWMs, such as mean high water spring or mean higher high water, and a number of shoreline indicators, such as the dune toe and vegetation line. HWM indicators are extracted using object-oriented image analysis or Light Detection and Ranging (LiDAR) Digital Elevation Modelling, combined with tidal datum information. Field verified survey data are used to determine the swash heights and shoreline features, and provide confidence levels against which the swash height empirical model and feature extraction methods are validated. Calculations of inundation probability for HWM indicators are based solely on tide

data for property management purposes; while swash heights are included for coastal hazard planning.

The results show that the accuracy of swash height calculations is compromised due to gaps that exist in wave data records. As a consequence, two methods are utilised to interpolate for gaps in the wave data records: the wavelet refined cubic spline method and the fractal method. The suitability of these data interpolation methods for bridging the wave record data gaps is examined. The interpolation results are compared to the traditional simple cubic spline interpolation method, which shows different interpolation methods should be applied according to the duration of the gap in the wave record data.

At the second stage of this research, all the HWM indicators, including the two new HWM indicators, SCSP and SCTP, are evaluated based on three criteria: precision, stability and inundation risk. These indicators are integrated into a Multi-Criteria Decision Making model to assist in the selection and decision process to define the most ideal HWM position. Research results show that the position of the dune toe is the most suitable indicator of the HWM for coastal hazards planning, and SCTP is the most ideal HWM for coastal property management purposes.

The results from this research have the potential for significant socio-economic benefits in terms of reducing coastal land ownership conflicts and in preventing potential damage to properties from poorly located land developments. This is because the methodology uses a data-driven model of the environment, which allows the HWM to be re-calculated consistently over time and with consideration for historical and present day coastal conditions.

ACKNOWLEDGEMENTS

For the duration of this study, I have been fortunate to receive support, encouragement and advice from a number of people, to whom I wish to express sincere gratitude. Firstly and foremost my supervisor, Dr Jianhong (Cecilia) Xia who has provided constant support, encouragement and has challenged and discussed my research throughout the study program. I also appreciate my supervisors Professor Graeme Wright and Dr Lesley Arnold for their time and contribution in strengthening the methodology development in this study, and in editing and improving this thesis. My three supervisors' critical thinking on details was very helpful in submitting a sound thesis.

I would also like to acknowledge Ric Mahoney and Murray Dolling who acted as consultants to the research and provided advice on any issues based on their vast experience. Without their assistance, I would not have taken up the challenge and dipped into the unknown 'high water'.

A research project is hardly feasible without the necessary funding and there are a number of institutions I want to thank for their support. I would not have come to Australia without the Curtin International Postgraduate Research Scholarships offered by Curtin University and Landgate. I am also indebted to the Cooperative Research Centre for Spatial Information, activities of which are funded by the Commonwealth of Australia Cooperative Research Centres Programme.

Thanks to all the staff members and postgraduate students in the Department of Spatial Sciences, Curtin University, for providing help and encouragement in times of need. Particularly I would like to thank Professor Bert Veenendaal, Associate Professor Michael Kuhn, Dr Tom Schut, Dr Robert Corner, and Dr Mick Filmer for their encouragement and assistance, including many hours discussing this research. Thank you to Caroline Rockliff, Pam Kapica, and Meredith Mulcahy for their assistance with my study life, especially to Lori Patterson, for her assistance with formatting, editing and associated issues.

Special thanks also go to Val Macduff, Dr Sten Claessens, Saud Aboshiqah, Ting Lin, Xiaoying Wu, Chunmei Chen, Qian Sun, Robert Odolinski, Amir Khodabandeh, Dr Christian Hirt and many others for their friendship that did not stop at the lab

door. The often very welcome distractions such as the rogaining and soccer training and barbecues will never be forgotten.

Thanks are also extended to John Fenner, Russell Teede, Aaron Thorn, Doug Hardman, Allan Campbell, Rodney Hoath, Tia Byrd and other staff from Landgate, Department of Transport and Department of Planning for their assistance in providing the necessary data required for this research and advice and help on the questionnaire and methodology design. I would also like to acknowledge the Department of Water, Tremarfon Pty Ltd. and the many nameless participants who provided the data which provided the basis for this research. Their efforts are very much appreciated. My sincere thanks also go to Associate professor Jennifer Whittal at University of Cape Town, for the insights she has provided.

Finally, I would like to thank all my family, especially to my parents, for their encouragement, love and support throughout this study.

RELATED PUBLICATIONS

Refereed Conference Papers:

Liu, X., J. Xia, G. Wright, L. Arnold, and R. Mahoney. 2011. Identification of onshore features for delineation of the land water interface and their spatial-temporal variation using high resolution imagery. *Proceedings of 2011 IEEE International Geoscience and Remote Sensing Symposium (IGARSS)*, 24-29 July 2011, Vancouver: IEEE.

Liu, X., J. Xia, G. Wright, R. Mahoney, and L. Arnold. 2011. High water mark determination based on the wave runup height distribution and spatial continuity. *Proceedings of Coasts and Ports 2011: Diverse and Developing: Proceedings of the 20th Australasian Coastal and Ocean Engineering Conference and the 13th Australasian Port and Harbour Conference*, 28-30 September 2011, Perth: Engineers Australia.

Journal papers:

Liu, X., J. Xia, M. Kuhn, G. Wright, and L. Arnold. 2013. Assessment of Spatial and Temporal Variations of High Water Mark Indicators. *Ocean & Coastal Management*. In press.

Liu, X. et al.. 2013. Comparison of Wave Height Interpolation with Wavelet Refined Cubic Spline and Fractal Methods. Submitted to *Ocean Engineering*.

Liu, X., J. Xia, C. Blenkinsopp, L. Arnold, and G. Wright. 2012. High Water Mark Determination Based on the Principle of Spatial Continuity of the Swash Probability. *Journal of Coastal Research.* In press, doi: 10.2112/jcoastres-d-12-00061.1.

TABLE OF CONTENTS

LIST OF FIGURES

LIST OF TABLES

TERMS AND ACRONYMS

Below is a list of terms and acronyms used in the thesis:

AHD	:	Australia Height Datum
AHP	:	Analytic Hierarchy Process
ANNs	:	Artificial Neural Networks
ANTT	:	Australian National Tide Tables
ARIMA	:	Auto-Regressive Integrated Moving Average
ARMA	:	Auto-Regressive Moving Average
BFAST	:	Breaks For Additive Seasonal And Trend
CR	:	Consistency Ratio
CWT	:	Continuous Wavelet Transform
DEM	:	Digital Elevation Modelling
DoT	:	Department of Transport
DWT	:	Discrete Wavelet Transform
ELECTRE	:	Elimination and Choice Translating Reality
ESRI	:	Environmental Systems Research Institute
FD	:	Fractal Dimension
FEMA	:	Federal Emergency Management Agency
GIS	:	Geographic Information System or Science
GNSS	:	Global Navigation Satellite Systems
HA	:	Hellden Accuracy
HHW	:	Higher High Water
HWL	:	High Water Line
HWM	:	High Water Mark
ICSM	:	The Intergovernmental Committee on Surveying and Mapping
ICSM	:	The Intergovernmental Committee on Surveying and Mapping

IFS	:	Iterated Function System
KIA	:	Kappa Index of Agreement
K-S	:	Kolmogorov-Smirnov
Landgate	:	Western Australian Land Information Authority
LiDAR	:	Light Detection And Ranging
LLW	:	Lower Low Water
LSQ	:	Least Squares Quadratic
MADM	:	Multi-Attribute Decision Making
MAUT	:	Multi-Attribute Utility Theory
MCDM	:	Multi-Criteria Decision Making
MHHW	:	Mean Higher High Water
MHW	:	Mean High Water
MHWS	:	Mean High Water Spring
MLE	:	Maximum Likelihood Estimation
MLLW	:	Mean Lower Low Water
MODM	:	Multi-Objective Decision Making
NOAA	:	National Oceanic and Atmospheric Administration
OA	:	Overall Accuracy
OHW	:	Ordinary High Water
OHWM	:	Ordinary High Water Mark
OOIA	:	Object-Oriented Image Analysis
PA	:	Producer Accuracy
PCM	:	Pairwise-Comparison Method
PCTMSL	:	Permanent Committee For Tidal and Mean Sea Level
PROMETHEE	:	Preference Ranking Organization Method for Enrichment Evaluation

RMSE	:	Root Mean Squared Error
RTK	:	Real-Time Kinematic
SA	:	Short Accuracy
SCDB	:	State Cadastral Data Base
SCSP	:	Spatial Continuity Of Swash Probability
SCTP	:	Spatial Continuity Of Tidal Probability
U.S.	:	United States
UA	:	User Accuracy
WA	:	Western Australia
WPM	:	Weighted-Product Model
WSM	:	Weighted Sum Model

CHAPTER 1 INTRODUCTION

1.1 The Definition of the High Water Mark (HWM)

The determination of the High Water Mark (HWM) is important for coastal management and planning, as the HWM is considered as a cadastral boundary to separate land and water (Whittal 2011). It is used to denote public and private land, and as a reference from which development is offset to limit the exposure of properties to potential coastal hazards.

Generally, the HWM has been defined from two aspects: either a height determined using a tidal datum calculated from water level observations or from shoreline features in the coastal zone on the landward side. The origin of using tide levels to define the HWM can be traced back to the sixteenth century (Cole 1997). In the following years, a number of definitions and methods were developed based on the tidal datum and legislated in law or for other practical purposes, such as ordinary high water mark (OHWM), mean high water spring (MHWS) and mean higher high water (MHHW).

However, when tide information is not available or not sufficient, field evidence is preferred as the boundary to accurately delineate the HWM (Morton and Speed 1998). The water level, which includes the effect of wave runup (swash), is one such piece of evidence. Alternatively, shoreline features, which indicate the position of the water level in some way, are another type of HWM indicator. They include, but are not limited to, the vegetation line (Guy Jr 1999; Priest 1999), frontal dune toe (Coutts 1989) and high water line (HWL) (Crowell *et al.* 1991).

As indicated by Morton and Speed (1998), the actual water level is systematically underestimated by nearby tide gauges due to the impact of wave runup. In general, wave runup causes an offset which is the difference between tidal datum-based HWM indicators and the indicators based on shoreline features. This difference (offset) makes it difficult to determine a single discrete line for HWM delineation.

Nonetheless, a single discrete HWM is often not realistic as its location is influenced by the application for which it is used, such as coastal property management or coastal hazard planning. Here a single HWM that suits both purposes is not practical.

For example, historically, tidal datum-based HWM indicators have their roots in the development of common law for property management; while the origin of measuring water level and its indicators can be traced back to Roman civil law (Cole 2007), and the wave runup height is an essential criterion for coastal hazard protection (Hubbert and McLnnes 1999; Short and Hogan 1994).

There is currently no consistent method for HWM determination and this has led to discrepancies in scientific analysis and differences in its application in management fields. HWM determination is often complex and results will vary depending on the indicators unique to the location. There are also inconsistencies in the definition of what constitutes the HWM, no procedural methods for its determination (Cole 1997), and inaccuracies in measurement due to the dynamic nature of the coastal environment (Hughes *et al.* 2010; Masselink and Russell 2006). A method to consistently determine the HWM line is urgently required by land and coastal administrators in order to reduce conflicting findings and time-consuming rework for specific purposes.

This research develops a consistent and robust methodology for HWM determination. The method includes two components: determination of the HWM position and evaluation of changes in the HWM over time and space. This methodology takes into account the dynamic processes of the coastal system, and importantly, integrates the land and water system as a whole by calculating the swash or tidal probability of each HWM indicator.

1.2 Problem Formulation

The HWM is one type of water boundary. The HWM boundary between water and land is not explicit, and the definitions of the HWM are ambiguous and can be interpreted in different ways (Coutts 1989). For example, in a statutory definition, the use of the term ‘ordinary’ in OHWM as applied in tidal waters is not mathematically ideal (Horlin 1994) and is not part of the tidal lexicon (R. Mahoney, personal communication 5 December 2009). Therefore, the interpretation of the word ‘ordinary’ has altered since its earliest inception, and the HWM position defined by OHWM varies over time and space (see Section 2.2).

The HWM, as a natural boundary, is also uncertain. It is not stable and will change over time (Burrough and Frank 1996), mainly due to the dynamic coastal morphology which can modify the location of the interface between water and land (Cole 1997). This can partially explain why there is no standard method for determining the position of the HWM in most jurisdictions, including Western Australia.

Current methods for determining the HWM are expensive and only appropriate in localised areas. In the main, determinations of the HWM are only conducted for new land developments to determine land ownership extent or for potential hazard assessments. When there is conflict concerning property boundaries, people are concerned with an exact 'HWM boundary'. However, the HWM line can only be determined precisely in areas that are in close proximity to a tidal control station.

HWM determination was traditionally achieved using medium- to long-term tidal records (Cole 2007). However, there is no consensus on the most appropriate tidal datum-based HWM indicators to represent the position of the HWM. As a consequence, there is a need for critical examination on the tidal datum-based HWM indicators.

Furthermore, the spatial information of shoreline features indicating the position of the HWM can be captured by a number of methods. Field surveys using Real-Time Kinematic (RTK) based Global Navigation Satellite Systems (GNSS) receivers are considered the most accurate determination tool. However the method is labour- and time-consuming when collecting high resolution data along long segments of the shore. Also, the value of the data, in terms of accuracy, will vary depending on the nature and slope of the coast. In contrast, aerial photography interpretation offers substantial time and labour savings. However, if the aerial photography is of poor quality, precise boundary detection is not possible. High-resolution optical remote sensing imagery overcomes this limitation and the precision of the features captured is enhanced. However, the process of classifying shoreline features using high resolution images may result in overly finely distributed classification results on the classified image (Blaschke 2010; Dragut and Blaschke 2006; Marpu 2009; Walter 2004), which makes identification of shoreline features difficult using traditional supervised or unsupervised classification methods.

Other factors have impeded HWM determination and require further analysis. These relate to the ambiguity of the meaning of the HWM, how to manage data gaps, accuracy of imagery, and lack of a multi-criteria decision making perspective for HWM determination. The following questions arise:

- What is the correct meaning of 'high water' or 'high tide'? This is a key issue for HWM determination; however, this has not been definitively addressed (Briscoe 1983). A fundamental question is how to relate HWM indicators to the water-land interface? This requires an understanding of how to integrate the water and land information and how to define the water-land interface. This aspect is considered in this research.

- Should the effect of wave runup be considered in HWM determination? The tidal datum-based HWM indicators exclude the runup height from the determination, while features present on the shoreline usually include the height of wave runup in the determination process. However, the effect of wave runup on HWM determination has rarely been quantitatively assessed. This is often due to limited data because of buoy breakdowns during poor weather conditions or computing problems. Many data gaps occur in the wave information records and these are not always small (Kalra and Deo 2007). Data gaps are addressed in this research.

- When using image analysis to determine the position of HWM indicators, how do the classification accuracy, imagery accuracy and random errors influence the robustness of HWM determination? Also, how does the variation of HWM position over space and time influence the consistency of HWM determination? These aspects have not been previously analysed and are investigated in this research.

- What are the methods for quantitative analysis that can be applied to systematically incorporate and evaluate multiple HWM indicators into a single HWM determination methodology? This research develops a method of evaluation from a multi-criteria perspective and for different determination purposes. The development of such a method has not been undertaken previously.

1.3 Research Objectives

The overall aim of this research is to develop a consistent and robust HWM determination methodology. This model will facilitate decision-making processes for both property management and for hazard planning in coastal areas. To achieve this goal, the primary objectives of the project include:

- To develop a model integrating both land and water information to determine the position of ‘high’ water;
- To develop a computer model to assess all HWM indicators in the one evaluation system.

To address these primary objectives the following secondary objectives are applied:

- To resolve data gaps by interpolating the missing data that are required for HWM determination and evaluation processes;
- To identify the positions of existing HWM indicators using tidal and image analysis, including tidal datum-based HWM indicators from the seaward side, and shoreline features lying in the coastal zone from the landward side;
- To determine the spatial continuity distance of swash/tidal probability for a range of HWM indicators;
- To assess the confidence level for image analysis on shoreline feature identification and water level modelling;
- To evaluate the spatial and temporal variation (precision and stability), and rank the inundation risk for each HWM indicator using three criteria for HWM determination; and
- To determine the HWM using multi-criteria decision making methods.

1.4 Significance and Benefits of the Research

1.4.1 Social and Economic Benefits

The determination and representation of the HWM is an important aspect of both planning and implementation phases of coastal zone management. After developing a statistically reliable method to determine the HWM, not only can surveyors operate within guidelines to guarantee consistency and to maintain integrity, regulations and legislation on the HWM can also be applied with certainty. Other benefits stemming from the ability to consistently and repeatedly determine the HWM include:

- Ability to locate the HWM cost effectively in the field or on digital maps in the cadastral database system;
- Ability to apply Digital Elevation Modelling (DEM) and image analysis to improve the working efficiency of HWM determination;
- Providing scientific evidence to assist in jurisdictional agreements related to HWM boundaries;
- Supporting research and development into data harmonisation through the determination of consistent and robust coastal cadastral boundaries;
- Supporting decision making particularly in the area of town planning and land valuations;
- Supporting risk assessment studies in relation to the impact of erosion and climate change on our coastline and coastal infrastructure; and
- Provide a baseline to which predictive modelling can be applied and forecasts on the effects of sea level rise determined.

1.4.2 Research Contributions

In addition to the new methodology for the determination and evaluation of HWM position, other contributions of the research include:

- Providing a solution to wave record gaps using intelligent interpolation algorithms, thus making recorded information more useful through the improvement of interpolation accuracy, especially for large data gaps;

- Extending the application of spatial analysis to the coastal boundary determination by addressing the difficulty of applying spatial autocorrelation analysis on linear objects, thereby enabling the identification of the 'high' water position;

- Providing a new way for assessing the spatial and temporal variation of shoreline position from both a 'precision' and 'stability' point of view; and adding depth to the visualisation understanding of shoreline variation by applying high resolution imagery in representing the results;

- Proposing a systematic model that can be applied to evaluate the shoreline positions for different purposes.

1.5 Research Methodology

The study comprises three major stages—determination, evaluation and decision, in which the major applied methods are outlined below:

- Determination of HWM indicators, through:

    i. Review of relevant literature on the development of HWM determination;

    ii. Constituent analysis for the tidal datum-based HWM indicators;

    iii. Image analysis for shoreline features using object-oriented image analysis (OOIA);

    iv. Wave information, including heights and periods, interpolation using cubic spline, wavelet refined spline, and fractal method for different sizes of recording gaps;

    v. Calculation of the spatial continuity distance of the tidal/swash probability on the shore by applying the semi-variogram function.

- Evaluation of HWM indicators, through:

i. Measurement of the stability of HWM indicators using the extended Hausdorff distance;

ii. Identification of the random error in the HWM determination process by applying Monte Carlo simulation;

iii. Assessment of the topographic complexity of HWM indicators by calculating the fractal dimension.

- Decision on the position of the HWM, through:

i. Determination of the weights for each criterion using survey feedback from experts using the pairwise-comparison method (PCM);

ii. Establishment of a Multi-Criteria Decision Making (MCDM) model to integrate the three criteria—precision, stability and inundation risk for evaluating HWM indicators in one system.

Two study areas in Western Australia were chosen to test the evaluation methodology. Both sites have distinctive shoreline characteristics (see Section 3.3) and were chosen as being representative of many other coastlines with similar shore conditions, in terms of tidal types, wave characteristics, coastal morphology and coastal types, and therefore pertinent for testing the methods being developed.

1.6 Thesis Structure

This thesis comprises eight chapters. The research model and its relationship to the chapters in this thesis are depicted in Figure 1.1.

Chapter 1 briefly introduces the problems and provides relevant background information on HWM determination. The objectives of the research and its significance are outlined.

Chapter 2 reviews the development of HWM determination, the existing HWM indicators and their determination methods, and investigates the possible factors that influence the variation of the HWM position. An overview of the difficulties in HWM determination is provided, and the limitations of previous determination methods are discussed.

Chapter 3 establishes and depicts a theoretical framework for HWM determination, in which the main processes for the HWM determination and evaluation are discussed. Also included in this chapter are the characteristics of the selected study areas, the required data and software for implementing the methodology, and their limitations.

Chapter 4 develops a method for interpolating the recording gaps in wave information, including wave heights and periods, using wavelet refined cubic spline and fractal methods. These methods are also evaluated and compared with the cubic spline method.

Chapter 5 illustrates the process for identifying HWM indicators based on tidal datum and shoreline features using image analysis. A new method of HWM modelling integrating both land and water information is established by applying the theory of spatial continuity of tidal/swash probability on the shore. The position of shoreline features derived from the image analysis and the swash probability calculated from the empirical model are validated against data obtained from a field survey.

Chapter 6 applies the Kriging method to fill in DEM data gaps and evaluates the precision and the stability (spatial and temporal variation) of HWM indicators as two criteria for HWM determination.

Chapter 7 presents a Multi-Criteria Decision Making (MCDM) model integrating the criteria—precision, stability and inundation risk to evaluate the HWM indicators, followed by discussions on the position of the HWM for both coastal property management and coastal hazards planning purposes.

The thesis is concluded in **Chapter 8**, with a summary of the major findings and the limitations of the research in relation to the stated objectives and recommendations for future research.

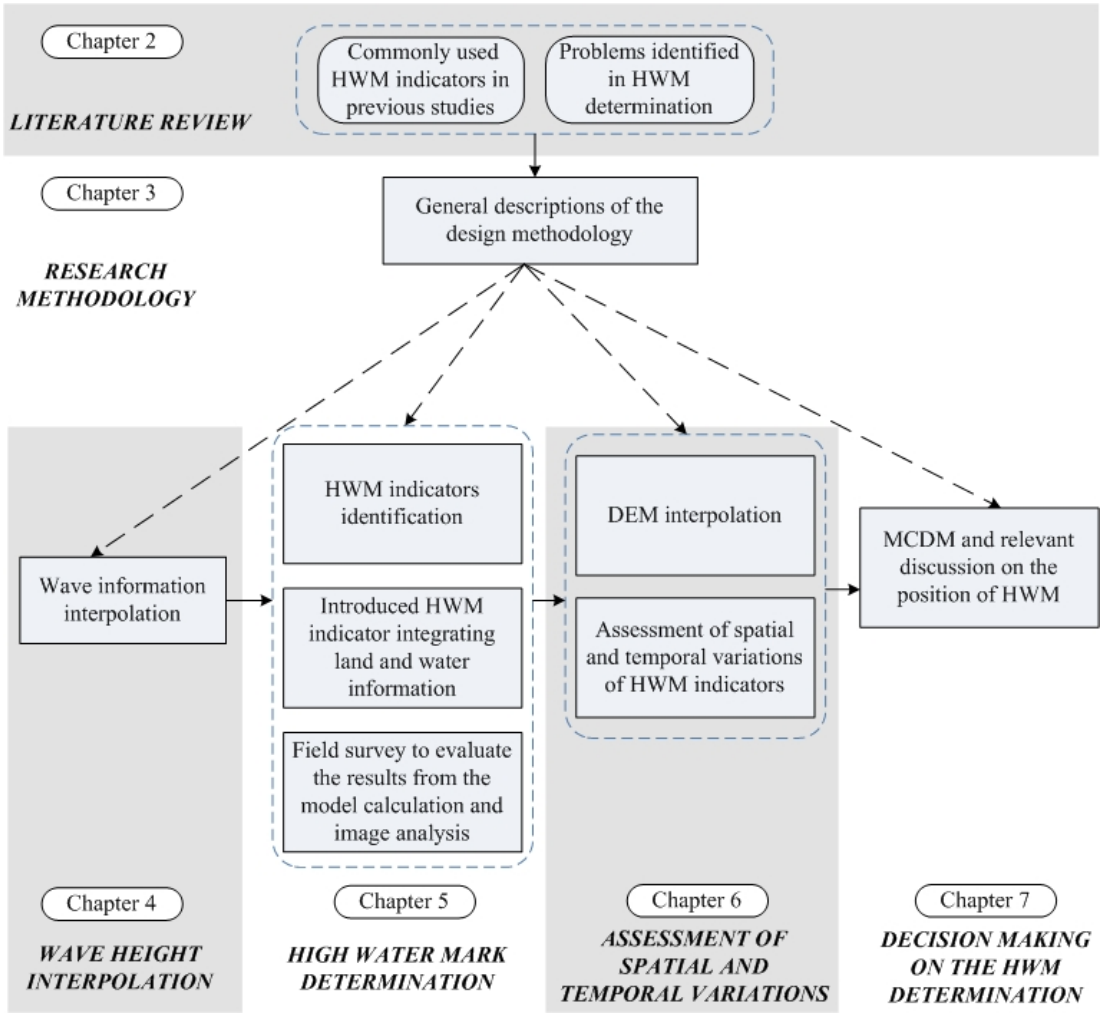

Figure 1.1 Research structure and relationship to the chapters of this thesis

CHAPTER 2 LITERATURE REVIEW

2.1 Introduction

This chapter reviews the legal definition of the HWM based on tidal data. All its variations in different jurisdictions, countries, states and even departments, are presented. The chapter also identifies the different methods for determining the position of the HWM. In addition, a review of the literature concerning factors that affect the position of the HWM and problems associated with its determination, is presented in order to formulate a new, consistent and robust HWM determination methodology.

2.2 Tidal Datum-based Legal Definition of the HWM

2.2.1 Development of the Legal Definition of the HWM in Common Law

The use of tide to delineate the seaward extent of private land is well established in common law (Cole 2007; Horlin 1994; Maloney and Ausness 1974b). The origin of the law can be traced back to the sixteenth century during the reign of Queen Elizabeth I, when Thomas Digges a lawyer, engineer and surveyor, first cited the theory of royal ownership of foreshore areas (Cole 1997). According to Digges, the land beneath tidal waters and the foreshore, which is the submerged land of the kingdom, should be held by the Crown (Maloney and Ausness 1974b). In seventeenth century England, Digges's theory was revived by the treatise of Lord Mathew Hale, who declared that the foreshore 'between the high water mark and the low water mark' belonged to the Crown (Maloney and Ausness 1974b, 199).

However, in early law, there was no clear definition of the HWM. While Hale's doctrine firmly established ordinary high water mark (OHWM) as the boundary between privately-owned property and public beach (Cole 2007; Horlin 1994; Maloney and Ausness 1974b); the definition in his doctrine incorrectly equated the concept of 'neap tides' with 'ordinary tides', leaving the definition ambiguous.

In 1854, the OHWM was clarified in common law by a case in which it was defined as 'the average of the medium tides in each quarter of a lunar evolution during the year (in which the line) gives the limit, in the absence of all usage, to the rights of the Crown on the seashore' (Cole 1997, 3). In the following years, this common law

model and definition of OHWM was widely adopted by most of the United States (U.S.) and commonwealth countries such as Australia, for delineating property boundaries (Gay 1965; Hamann and Wade 1990; Humbach and Gale 1975; Landgate 2009c; Maloney 1977; Simon 1993). The OHWM is also considered synonymous with the term 'the line of mean high water mark (MHWM)' (Coutts 1989; Horlin 1994; Land Services 2008; Maloney and Ausness 1974b).

2.2.2 The Mean and Ordinary High Water Mark

In areas with tidal variations, Gay (1965) suggested that ordinary or mean high water mark should apply as the boundary between privately owned uplands and the submerged lands which are subject to public ownership. In order to locate MHWM accurately, survey regulations in New Zealand require a record of tide information over a period of 370 days (Kearns 1980). This is particularly important in areas with seasonal tidal change, where a mean annual height of high water is appropriate (Cole 1997). In contrast, Gay (1965) insisted that a period of nineteen years as appropriate for the determination of MHWM at any given place, as it takes into account most of the significant tide constituent effects (Australian Hydrographic Service 2010; Doodson 1921; Pawlowicz *et al.* 2002). Thus, the time span to calculate mean high water (MHW) is not fixed but it is apparent that the more tide information that is collected, the more precise the MHW will be.

Mean high water is defined as the average height of all high water marks over a long period of time (The Intergovernmental Committee on Surveying and Mapping (ICSM) 2012). It can be interpreted in different ways (Coutts 1989). Interpretations are complicated by certain tidal characteristics and conditions.

There are three possible types of tide (Gill and Schultz 2001): diurnal, semidiurnal and mixed. A tide is considered semidiurnal when there are two high and two low tides within a single day; whereas a diurnal tide has only one tidal cycle per day. A mixed tide is similar to the semidiurnal tide; however the two high waters and low waters, occurring daily, have significant differences in height. Thus, technically, the term 'mean high water spring' (MHWS) applies only to those areas with a semidiurnal type; while the term 'mean higher high water' (MHHW) applies only to diurnal tidal regimes (Pugh 1996). Generally, the definition of MHWS is the average

of all high water observations at the time of spring tide over a period of time (The Intergovernmental Committee on Surveying and Mapping (ICSM) 2009). Whereas, MHHW is the mean of the higher of the two daily high waters over a period of time (The Intergovernmental Committee on Surveying and Mapping (ICSM) 2009).

Land and property administrative organisations use different interpretations of the HWM to define land ownership boundaries. Hicks (1985) points out that both MHW and MHHW can be interpreted as property boundaries between privately-owned uplands and publicly-owned tidelands. In the U.S., each State has adopted MHW and mean lower low water (MLLW) as the boundary delimiting privately and publicly owned land. The exceptions here, are the states of Hawaii, Louisiana and Texas, which consider that MHHW provides a more reliable datum for surveying and engineering purposes (Cole 2007; Fowler and Treml 2001) (Figure 2.1). Similarly in Australia, boundaries are defined in two main ways: MHW in South Australia (Land Services 2008) and New South Wales (Clerke 2004), and MHWS in Queensland (Collier and Quadros 2006; Dunphy 2010) and Western Australia (WA) (Landgate 2009c).

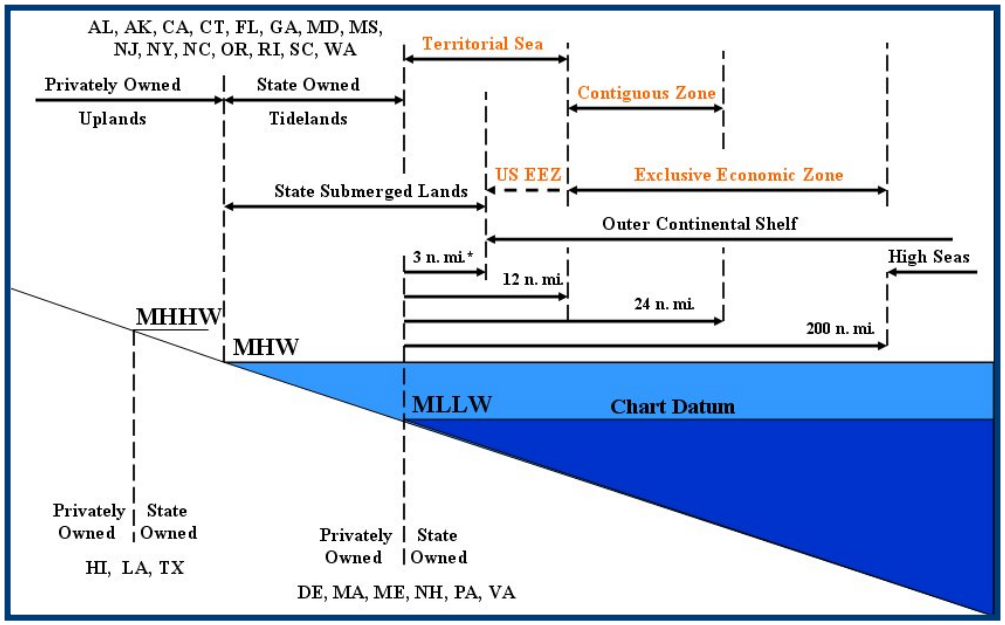

Figure 2.1 The extents of the U.S. maritime zones (National Oceanic and Atmospheric Administration 2012)

In WA, the statutory definition of the HWM is the ordinary high water (OHW) at spring tide. This is generally accepted as equivalent to the definition of MHWS in the

Australian National Tide Tables (Landgate 2009c). The height of MHWS is defined as ‘the average, throughout a year when the average maximum declination of the moon is 23.5 degrees, of the heights of two successive high waters during those periods of 24 hours when the range of the tide is greatest’ (Department of Defence 2008, xxvii). However, because the WA coast also experiences diurnal and mixed tidal characteristics (Pattiaratchi and Sarath Wijeratne 2009), the MHHW is correspondingly applied (Figure 2.2).

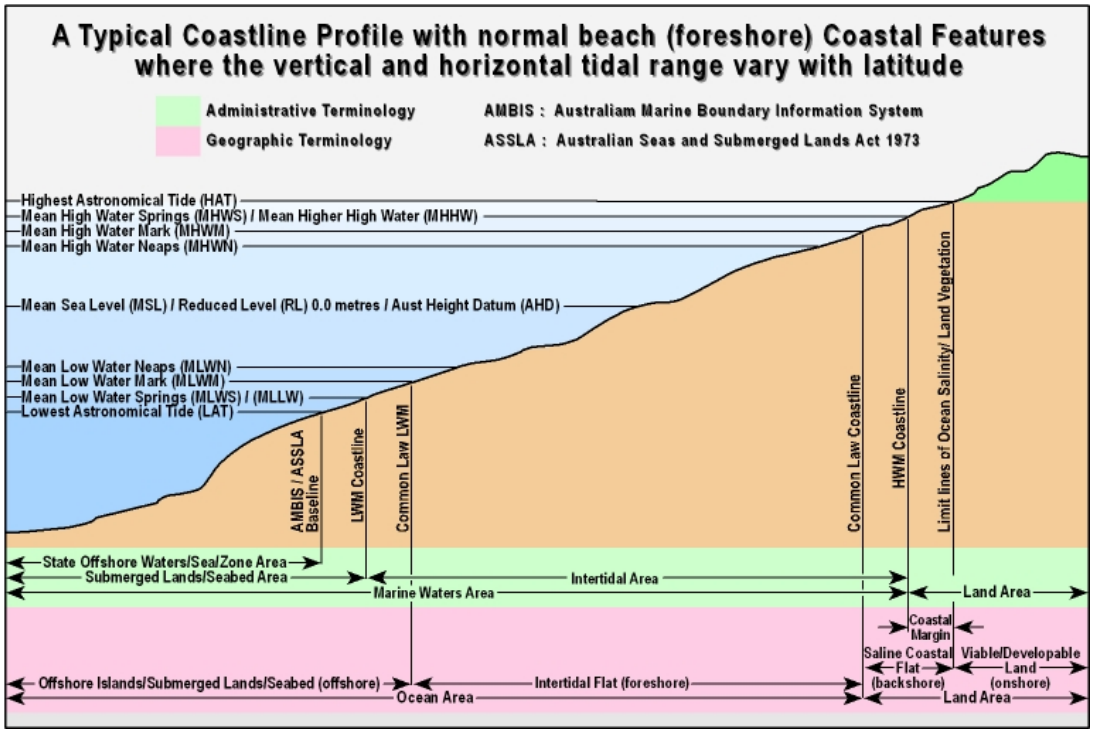

Figure 2.2 HWM determination concepts (Fenner 2010)

The HWM using mean or ordinary high water is not consistent even in the same location. This is because the OHW, defined as ‘the average of the medium tides in each quarter of a lunar evolution during the year’ (Cole 1997, 3), may be lower than the mean high water in normal situations. Furthermore, the time span for calculating ordinary and mean high water is not necessarily the same.

As a consequence, authorities who are responsible for defining the coastal boundaries have gradually adopted MHW as being equivalent to the OHW, as defined under English common law (Horlin 1994). This approach has become widely accepted because the definition is less ambiguous. Nevertheless, because the category of private property is defined as the land above the position of lands beneath tidal waters, there is not yet a consensus as to whether MHW can represent

the ‘true’ landward boundary of tide water. This question remains unanswered and requires further evaluation. Furthermore, the meaning of ‘high water’ or ‘high tide’ has not been definitively addressed (Briscoe 1983). This continues to be a key issue and is fundamental to HWM determination.

The HWM, including the tidal datum-based HWM, should usually be related to a recoverable datum (Clerke 2004). Normally, mean sea level is used as such a reference point (Gay 1965). In Australia, the Australia Height Datum (AHD) is adopted (Landgate 2009c), as the establishment of the AHD is equal to mean sea level at its initial establishment (R. Mahoney, personal communication 5 December 2009).

2.3 Harmonic Analysis and Tidal Datum Computations

The development of tidal analysis, especially harmonic analysis, provides a full description and sufficient information for tidal datum determination (Pugh 1996). Harmonic tidal analysis was introduced by William Thomson in the 1860s (National Oceanic and Atmospheric Administration (NOAA) 2010a), and was further elaborated by Darwin (1883) and Doodson (1921). Most tidal data analysis is based on the harmonic model and was adopted by the Australia National Tidal Centre and other agencies in Australia (Australian Hydrographic Service 2010).

Harmonic tidal analysis considers the tidal datum as a sum of the constituents’ cosine waves (Australian Hydrographic Service 2010; Foreman 1977; Phillips 1999; The Virginia Institute of Marine Science 2010):

$$H\left(t_i\right) = h_0 + \sum_{j=1}^{m} A_j \cos\left[2\pi\left(\sigma_j t_i - \phi_j\right)\right] \tag{2.1}$$

$H\left(t_i\right)$ represents the tidal height at time *i*; h_0 is the height of mean sea level; *m* is the number of constituents chosen for the particular area; A_j, σ_j and ϕ_j represent the amplitude, frequency and phase of constituent *j*, respectively. Since the frequency of every constituent is known in advance, the formula demonstrates that the key to harmonic analysis and constituent calculation is to calculate the amplitude and phase of the individual constituent cosine curves.

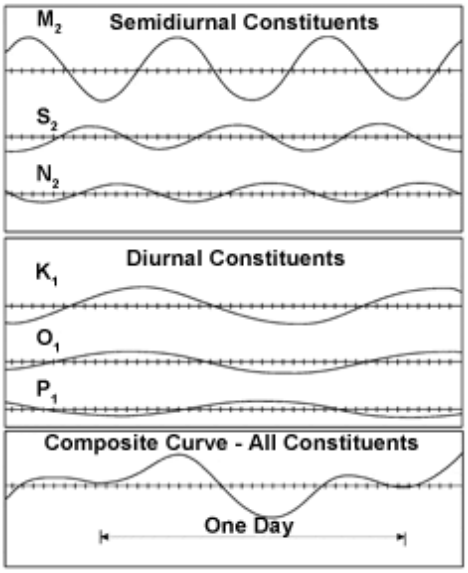

Figure 2.3 Sum of tidal constituents (Department of Oceanography 2007)

Two methods are commonly used together to calculate these elements: Fourier analysis (Korner 1989; Phillips 1999) and the least squares technique (Foreman 1977). The summary of the calculation process is (1) to transform the $\sum_{j=1}^{m} A_j \cos\left[2\pi\left(\sigma_j t_i - \phi_j\right)\right]$ as $\sum_{j=1}^{m}\left[C_j \cos\left(2\pi\sigma_j t_i\right) + S_j \sin\left(2\pi\sigma_j t_i\right)\right]$ in which

$$2\pi\phi_j = \arctan S_j / C_j \tag{2.2}$$

$$\text{and } A_j = \left(S_j^2 + C_j^2\right)^{1/2}; \tag{2.3}$$

(2) to apply the least squares technique and minimise $\sum_{i=1}^{n}\left[y\left(t_i\right) - h_0 - \sum_{j=1}^{m}\left[C_j \cos\left(2\pi\sigma_j t_i\right) + S_j \sin\left(2\pi\sigma_j t_i\right)\right]\right]^2$

where n represents the number of observed tidal recordings and $y\left(t_i\right)$ is the tidal height at time t_i.

Once the value of S_j and C_j are determined, ϕ_j and A_j can be calculated by the Equations 2.2 and 2.3.

In an analysis of 146 constituents, 45 reflect the astronomical arguments while the remaining 101 constituents are commonly referred to as the shallow water constituents (Cartwright and Edden 1973; Foreman 1977).

The astronomical constituents are considered the main constituents and represent the periodic variation at a certain relative location of sun, earth and moon (National Oceanic and Atmospheric Administration (NOAA) 2010b); while the shallow water tidal constituents are produced by the interaction of the main tidal constituents when the tide enters shallow water and is affected by bottom friction (Foreman 1977; The Intergovernmental Committee on Surveying and Mapping (ICSM) 2010b). The shallow water constituents distort the normal tidal profile, and at some sites the distortion can be significant (Foreman 1977). Therefore, a long period of tidal observation is suggested to take into consideration all the possible shallow water effects.

To determine which constituents are the most significant (each site has its own energy signature), the Rayleigh comparison constituent method can be used (Foreman 1977), although in general, of 146 constituents, only 37 of them are considered major constituents (National Oceanic and Atmospheric Administration (NOAA) 2010c). Furthermore, four major constituents are most important: K1 is the diurnal principal declination tide; O1 is the diurnal principal lunar tide; M2 is the semidiurnal principal lunar tide; and S2 is the semidiurnal principal solar tide. S_2 and M_2 are the basic sun and moon tides, whereas K_1 and O_1 are the main effects of the declination of the sun and the moon (Horlin 1994).

Besides calculating the tidal datum, the application of these four constituents also includes quantitatively analysing the type of tides by calculating their ratio (Dietrich and Kalle 1963; Foreman 1977):

$$F = \frac{K1 + O1}{M2 + S2} \tag{2.4}$$

F is called the form number. The tide can be precisely classified as follows:

i. Semidiurnal if $0 \le F \le 0.25$,

ii. Mixed if $0.25 < F \le 3.00$,

iii. Diurnal if $F > 3.00$.

2.4 Other HWM Indicators

When tidal information is unavailable or insufficient, land surveyors prefer to use field evidence to establish the position of boundaries to separate private from public ownership (Morton and Speed 1998). Normally, the area between the vegetation line and the berm crest is defined as the beach (Bauer and Allen 1995; Rooney and Fletcher 2000). Correspondingly, most features lying on the coast, such as scum or an oil line left on the shore and the debris or fine shell continuously deposited on the berm or foreshore (Briscoe 1983), can be considered HWM indicators (Pajak and Leatherman 2002) and be used to define the HWM. These physical markings indicate the general HWM line attained by the runup of high water (Hicks *et al.* 1989; Simon 1993; Williams-Wynn 2011). However, these indicators tend to be present only for short periods and are not present on every beach, while most physical indicators include the impact of wave runup (swash), typical tidal analysis excludes the runup factor.

Previous studies considered several other common types of HWM indicators in addition to tidal records, including the boundary between dry and wet sand, referred to as the high water line (HWL) (Moore *et al.* 2006), dune toe (Williams-Wynn 2011) and the seaward limit of vegetation (Williams-Wynn 2011). These shoreline features are good indicators of water level and are therefore sometimes used as boundary indicators of land and water (Coutts 1989; Gay 1965; Maiti and Bhattacharya 2009; Moore 2000; Morton and Speed 1998). Admittedly, not all of these indicators are available on all coasts, and choosing which one to use for a specific area generally depends on the physical coastal characteristics and data availability (Boak and Turner 2005).

2.4.1 High Water Line

Unlike morphological features, the HWL is the intersection of land with a water surface at its highest point (Hicks *et al.* 1989). It is the best indicator of the water-land interface (Crowell *et al.* 1991). HWL is generally located landward of the last high tide (Anders and Byrnes 1991; Crowell *et al.* 1991; Shalowitz 1964; Stockdon

et al. 2002) and seaward of the berm during normal weather and tidal conditions (Morton and Speed 1998; Pajak and Leatherman 2002).

In the past, HWL was identified by the visible signs of 'high tides' and the discoloration of sand or rocks on the shore (Boak and Turner 2005; Shalowitz 1964). Nowadays, with the development of remote sensing technology, HWL is defined as the line separating dry and wet beach and can be identified in aerial photographs by the sudden change of colour (Moore 2000; Morton and Speed 1998). However, Pajak and Leatherman (2002) mentioned that there might be more than one high water line left on the beach; the previous days' marks are sometimes still visible, so the most recent high water line needs to be surveyed in the field. Fortunately, the previous marks are often not as clear as the recent one and the contrast is different. Although, McBeth indicates that even when a HWL is exposed to the sun after the tide recedes, it will remain stable on the beach (Boak and Turner 2005; McBeth 1956).

In addition to wave runnup, HWL is also affected by a collection of phenomena and complex and varying situations. This is because, its position is related to the tidal level, geomorphology and wave energy; not just field observation (Morton and Speed 1998; Ruggiero *et al.* 2003), and requires further investigation.

Shalowitz suggested that the offset between the position of MHW and HWL as identified in the field and on aerial photographs was insignificant (Crowell *et al.* 1991; Shalowitz 1964). By contrast, other scientists argued that the relationship between these two can only be interpreted as being correlated to each other, and that HWLs seldom coincide with the MHW or the berm crest (Morton and Speed 1998). The MHW is normally seaward of the HWL because of wave runup, (Morton *et al.* 2004; Pajak and Leatherman 2002; Ruggiero *et al.* 2003). This phenomenon is more significant on flat beaches, where even the high water lines themselves are likely to change significantly day by day (Morton and Speed 1998; Pajak and Leatherman 2002).

Although HWL is easily identified on the shore and is convenient to use as an indicator, its position is not stable, especially on gently sloping beaches (Pajak and

Leatherman 2002). Also, the position of HWL usually corresponds to coastal morphology, water level and wave characteristics (Morton and Speed 1998).

2.4.2 Vegetation Line

The vegetation line is a biological feature established by either regular floods of water or storms that destroys the existing vegetation (Morton and Speed 1998; Shalowitz 1964). Therefore, the vegetation line indicates the position of high water in some way. Parker (2003) states that the vegetation line and most geomorphological indicators are landward, away from the mean high water line. The vegetation line was also chosen as an indicator for marine boundaries because it is the most stable natural boundary, controlled by the wash associated with extreme high water (Guy Jr 1999; Priest 1999).

Usually, the vegetation line appears in two positions: one is the inland dense vegetation, and the other is young and sparse, lying on the back shore. The dense vegetation is considered a more stable boundary indicator than the sparse vegetation (Morton 1974); most storm surges cannot reach the position beyond it (Morton and Speed 1998). This makes the vegetation line the most landward water boundary. However, in some wetlands where plants require continuous wash to survive, the vegetation line is seaward of the high water line and lower in elevation (Shalowitz 1964).

However, there are two disadvantages to using vegetation lines as a marine boundary. First, this line is easily subject to artificial manipulation, either intentionally or unintentionally. Second, sometimes a vegetation line is irregularly and/or indistinctly distributed along the shore and is difficult to identify (Morton and Speed 1998). Although drawbacks exist with the vegetation line, it is still an important indicator of the HWM location.

2.4.3 Beach Morphological and Biological Features

Other coastal features that could indicate the position of the HWM include cliff-top edge, berm crest and frontal dune toe. The cliff-top edge is the best evidence of where a horizontal HWM should be, and there should be no conflict about land in these areas (Crowell *et al.* 1991). However, cliffs are only one type of shoreline, and

an uncommon type as well. Morton (1998) supported this opinion and argued that the berm crest is the best physical evidence of the location of OHWM associated with wave runup. Pajak and Leatherman (2002) indicate that the HWL will not be highly dynamic in its position when a well-defined berm exists, as it stops the landward swash to some extent. However, this feature is not very apparent on every coast and may disappear in extreme situations (Hsu *et al.* 1989). Cole even suggested using biological indicators as water boundaries (Cole 1997); for example, the top of oysters appearing on a pier shows where the MHW is located (Songberg 2004), but the accuracy of this has not been proven. Compared with these indicators, the dune toe is more common and relatively stable on most coasts, and MHW usually exists to the waterside of the frontal dune (Coutts 1989).

2.4.4 Water Level

The use of water level to delineate coastal property boundaries has its roots in Roman civil law, in which the coastal boundary was not defined in terms of daily tide, but rather in terms of water level. This definition might be because the Mediterranean Sea, where Roman civil law code developed, has a minimal daily tidal range and is dominated by the effect of wave runup (Cole 2007). Such definition has been formally adopted by some countries whose legal system is based on Roman civil law, such as Puerto Rico, in which the upland limit of public property is considered to be reached by the great storm wave (Cole 2007).

In South Australia, the MHWM contour is sometimes set out by observing the water edge and the information from the nearby tide gauge at the appropriate time (Land Services 2008). However, as indicated in Morton and Speed's (1998) study, the actual water level is systematically underestimated by the tide gauges due to the exclusion of wave runup, and this results in the property boundary position increasing the area claimed by the upland owners. Similarly, HWL may represent the previous position of high water but may not indicate the most recent maximum runup limit (Boak and Turner 2005). Thus, the following questions remain:

- Should water level that includes the runup be used as a coastal boundary?
- Can MHW or HWL be equivalent to the water level and if not;

- Is there any shoreline feature that can represent the position of the water level?

2.4.5 The HWM Defined in Different Departments

Besides the most common definitions of the HWM, the methods of determining the position of the HWM varies across both jurisdictions and also between responsible authorities within the same jurisdiction. Two heights suggested by the Western Australian Land Information Authority (Landgate) and Department of Transport (DoT), WA, were obtained from experienced surveyors' long-term observation of the shoreline features as well as tide and wave effects on the coastal area.

2.4.5.1 The HWM Defined by Landgate

The statutory definition of the HWM is the MHWS or MHHW, depending on the tidal type. These levels have been determined from the Australian National Tide Tables, based on which new levels have been adjusted and are available at any part of the state with the assistance of long-term field observation of water level and coastal features (Landgate 2009c).

2.4.5.2 The HWM Defined by Department of Transport (DoT)

Different from the definition from Landgate, Department of Transport (DoT) suggests determining the HWM based on the statistics of tide information. Don Wallace, the former Chief Hydrographic Surveyor at the DoT, introduced a method to calculate lower low water (LLW) following many years of experience as a surveyor (Mahoney 2007). He suggested that LLW is equal to the 19^{th} low water occurrence from the cumulative frequency in the approved 19-year epoch of tide height observations, minus 1.5 times the standard deviation of the residuals (Equation 2.5).

$$\text{LLW} = 19^{th} \text{ Low Water Occurrence} - 1.5\sigma \qquad (2.5)$$

Note:

- A residual value results from the observed tide minus the predicted tide from constituents' analysis method.

- The '- 1.5 σ ' lowers the low water occurrence.

The higher high water (HHW) can be calculated by using the mirror image of Wallace's formula. This HHW height could be adopted as the position of the HWM (Mahoney 2007):

$$\text{HHW} = 19\text{th high water occurrence} + 1.5\sigma \quad (2.6)$$

Note:

- The '+ 1.5 σ ' raises the high water occurrence.

This method has the advantage of operating independent of tide types, and it takes into account the signal noise caused by factors, such as cyclones (Wood 2005). The limitation of this approach is that the method was determined only on the water side and ignores the effect of localised geomorphology, thereby isolating the water and land for HWM determination.

Although every HWM indicator has its drawbacks, including those determined based on tidal datum, each indicator shows the potential position of the HWM based on one particular purpose or viewpoint.

2.5 The HWM for Different Purposes

There are two fundamental different functions of the HWM—coastal property management and coastal hazard planning. These have always been integrated into one, although this is a misunderstanding in most cases. Differences exist among the positions of different HWM indicators. These are most significant between boundaries based on tidal datums versus high water indicated by water level or its feature indicators. The position of HWM indicators varies with the prevailing wind and wave conditions in different areas. Crowell *et al.* (1991) and McBeth (1956) pointed out that the difference between MHW and high water indicated by physical features is minimal for mapping purposes in moderate weather. However, an American case study showed that the MHHW line calculated by tidal signals was located many miles seaward of a boundary determined by physical features on the beach (Cole 1997). Morton and Speed (1998) also estimated that the actual water level reach on the beach was higher than predicted from the nearby tidal gauges. This indicates inconsistencies in the different definitions of the HWM, which are mainly

due to the wave runup effects. Therefore, the question of whether wave runup should be included in HWM determination is left unanswered.

2.5.1 Extent of Private Ownership of Coastal Zones

The HWM is recognised as the boundary separating private and public property rights under normal water conditions (Gay 1965). Coutts (1989) also acknowledged that the HWM can be used to confer ownership of land, where the land stops and the sea begins. Such a definition, including OHWM, MHWM, MHHW and MHWS, is determined from a land property management point of view, and does not take into account the effect of wave runup. Such tidal datum-based HWM determinations, as mentioned before, have their roots in the development of common law for property boundary delineation.

2.5.2 Coastal Hazard Planning

Coastal hazards are any phenomena that threaten coastal structures, property and the environment under extreme weather and water conditions. Coastal hazard planning aims to minimise these risks or hazard (Short and Hogan 1994). The origin of measuring the water level, which includes the effect of wave runup, or the features indicating the water level to determine the position of the HWM, can be traced back to Roman civil law (Cole 2007). The U.S. Federal Emergency Management Agency (FEMA) calls this type of HWM ‘wave runup coastal HWM’. FEMA identified this water level to improve disaster preparedness and prevent future hazards (URS Group Inc. 2006). The effect of wave runup, which is of particular interest to coastal emergency planners (Papathoma and Dominey-Howes 2003), was also analysed for coastal hazard protection by Bellomo *et al.* (1999). Most of the time, coastal boundaries are analysed for hazard planning purposes, the wave runup height is one of the most important criterion of these studies (Hubbert and McLnnes 1999; Short and Hogan 1994).

Thus, from the view of functionality, the HWM can be divided into two different purposes, property management and hazard planning. The difference between the two is whether the effect of wave runup on the tidal datum plane is included or excluded.

However, one of the factors impeding further investigation on the effect of wave runup on HWM determination is the many gaps that exist in wave information records. Therefore, interpolation on wave record information is required to increase the accuracy of HWM calculations.

2.6 Wave Information Interpolation

The modelling of significant wave information is important to coastal and ocean engineering applications, such as ocean resource management. It is a necessary component in the design and planning of coastal structures, harbours, waterways and shore protection. Time series analysis of wave information provides long-term prerequisite knowledge about the local wave climate and is essential for coastal management and environmental impact studies. However, due to the complexity and uncertainty of wave generation, it is difficult to interpolate and model wave information using deterministic equations.

Two categories of approaches have been studied previously. Firstly, by using an ocean wave model to simulate wave information and secondly, by analysing wave data patterns using interpolation methods. The former may provide time-series with no gaps. However, this is only accurate enough for site-specific analyses where detailed ancillary data are available (Deo *et al.* 2001). Ancillary data refers to wind data and bathymetry around a site (Bouws *et al.* 1998; Kinsman 2002). However, it is often difficult to collect (Altunkaynak and Özger 2004). Moreover, the wave model needs to be validated against observations, and significant computing time may be required to generate a long time-series.

The latter technique, wave data analysis, is relatively more reliable and accurate (Deo and Kumar 2000); however data gaps can only be filled using historical wave data. The time-series extension method is sensitive to the rule that determines the correlation pattern (Makarynskyy 2004). Hence it is necessary to develop an appropriate model to represent the rule and increase the accuracy of wave information interpolation and prediction. In addition, the gaps in data for wave recording are often at different scales. While some are relatively small, many breaks in data availability can be as large as one month or more, and these data gaps are difficult to interpolate with any degree of accuracy. There has been considerable research into wave characteristics and information determination. Of the models

developed, none accurately fill the data gaps in wave information models at different scales.

The most common wave interpolation methods that have been applied in studies are the stochastic models employing the auto-regressive moving average (ARMA) or the auto-regressive integrated moving average (ARIMA) (Agrawal and Deo 2002). These take into account short-term (Spanos 1983) and long-term period variability (Scheffner 1992). Deo and Sridhar Naidu (1998) and Agrawal and Deo (2002) have developed an improved model using artificial neural networks (ANNs). These techniques improved on the short-term wave information prediction method originally developed in Makarynskyy's studies (Makarynskyy 2004; Makarynskyy *et al.* 2005). In addition, Fuzzy logic methods have been applied in predicting wave information using wind speed information (Kazeminezhad *et al.* 2005; Özger and Şen 2007). A comparison of methods shows that ANN interpolation methods are more reliable than the genetic programming interpolation method developed by Ustoorikar (2008), but the results are still not satisfactory.

2.7 Vertical and Horizontal HWM

The HWM, depending on its usage and the way it is measured and defined, can be divided into two types: vertical and horizontal HWM. The tidal datum-based HWM belongs to the vertical HWM category. However, the HWM is not always tied to a specific high water height; sometimes a cadastral boundary that represents the HWM is mapped as a horizontal line between buildings or land features (Mahoney 2009). Moreover, a vegetation, debris or high water line left on the beach can be viewed as a natural representation of horizontal HWM.

Although the HWM may exist in two different forms (horizontal and vertical), the aim of HWM determination coincides with delineating the coastal boundary. When the HWM is defined vertically, it is possible to derive its horizontal HWM position on the coastal zone or in the imagery with spatial information. This means that, to some extent, a transformation can be used to derive one form of HWM from another. However, the two may be inconsistent; for instance, the State Cadastral Data Base (SCDB) in Western Australia (at certain locations) has large offsets between the equivalent horizontal location of HWM defined by height (vertical 'position') and

the displayed location of HWM defined as a horizontal boundary (horizontal position).

The difference between the tidal datum and its equivalent horizontal location is an important topic in marine science (Cole 1997). Even though the tidal datum may be constant over years in a certain location, the intersection of this datum with data representing the coastal morphology, such as digital elevation model (DEM), might be ambulatory (Figure 2.4) as the coastline changes by eroding or accreting (Coutts 1989). Therefore, the horizontal location of a tidal datum on a beach should be related to a specific time (Cole 1997).

Besides the uncertainty of the tidal plane, the slope of shore land is another factor causing significant offsets between the tidal datum and its horizontal location on the beach (Center for Operational Oceanographic Products and Services 2003). The vertical tidal datum error may lead directly to uncertainty in determining the horizontal HWM (Clerke 2004). This situation will be exacerbated on relatively flat coastal areas, and a centimetre of difference can cause an extension of many metres horizontally (Center for Operational Oceanographic Products and Services 2003;Morton *et al.* 2004). Thus, defining a coastal boundary in low lying beach areas and quantifying the spatial uncertainty and variation are difficult research issues that should be addressed (Quadros and Collier 2008).

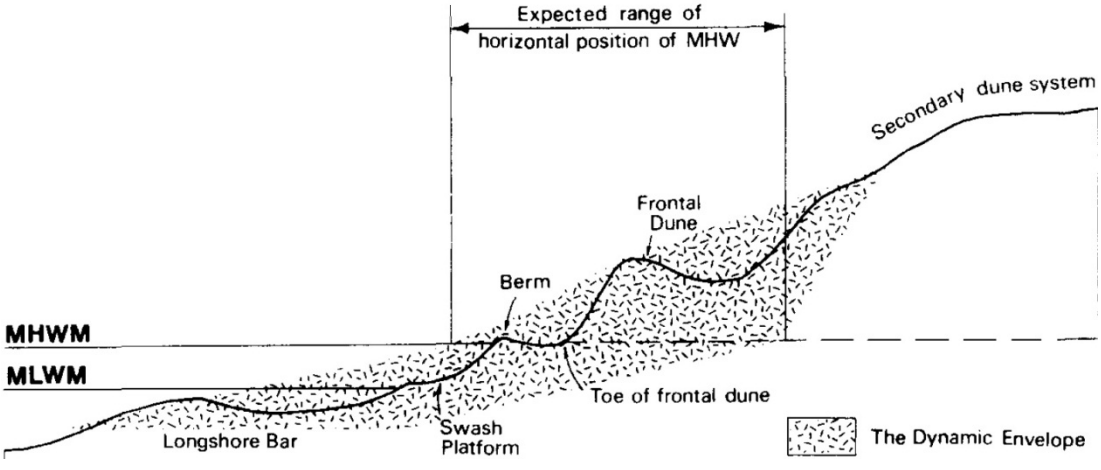

Figure 2.4 Illustration of the horizontal variation of the tidal datum on the beach (Coutts 1989)

2.8 Methods of HWM Determination

One of the challenges in coastal studies is to develop a methodology and procedure to determine the coastal boundaries with available data that is sufficiently repeatable and robust (Boak and Turner 2005). The process of determining the HWM can involve two approaches:

- Select a definition of the HWM and choose the appropriate indicators or datum to calculate the HWM with the available data; and
- Detect the location of the HWM on the field or in the imagery with spatial information.

Methods used to determine the HWM can generally be divided into three groups: survey methods, remote sensing methods and statistical methods.

2.8.1 Survey Methods

Because the HWM is self-evident at particular times, HWMs can be obtained by marking the water's edge, HWL and vegetation line in a field survey (Nunley 2002). This is the most convenient method, as the physical line on the ground can be easily observed (Cole 1997). Although the HWM location can be observed through these physical features, the certainty in its horizontal position is very weak (Hirst and Todd 2003). It is in the order of metres, or even tens of metres if the terrain is close to horizontal. As such, the accuracy of the surveyed position is limited by the knowledge of the position of the feature, rather than limited by the survey instrumentation and methods used. Modern survey field techniques can rapidly determine positions on the ground to a centimetre or less using Real-Time Kinematic (RTK) based Global Navigation Satellite Systems (GNSS) or electronic angle and distance measuring equipment (total stations). As a boundary or real property, the HWM is understood to be an ambulatory (moving) boundary and is temporal. A survey today does not determine the extent of rights to land and seashore tomorrow. It is also understood that the location of the HWM is not to the order of accuracy that other fixed boundaries are located due to the nature of the boundary.

Field survey work is not limited to determining coastal features. After determining the height of the HWM at a tide gauge, the HWM contour value in close proximity to

that gauge can be set out by spirit levelling from a nearby benchmark related to a recoverable datum—AHD in Australia. Landgate in WA recommend it as good survey practise to determine the HWM (Landgate 2009c) based on the assumption that MHW is a contour (Cole 1997). Clerke (2004) stated that the mean high water boundary levelling from the tidal elevation should follow the contour on the foreshore. However, the HWM is only a 'contour' when in close proximity to the tidal control station (R. Mahoney, personal communication 5 December 2009), since the actual elevation of the HWM may vary over longer distances. In WA, a similar type of survey method was introduced by Cribb and Horlin (R. Mahoney, personal communication 5 December 2009) and is considered a practical and convenient way to determine the position of the HWM. Cribb and Horlin (R. Mahoney, personal communication 5 December 2009) determined the general height of the HWM relative to AHD in major ports based on many years of field observations and reviews of hard-copy tide records. Surveyors at Landgate can thus survey the vertical HWM directly on the beach.

However, this is generally a labour- and time-consuming method for getting data of long segments along the shore with sufficient resolution and density, and the value will also vary depending on the nature and slope of the coast. The popular use of GNSS provides rapid measurement of onshore features, and it is moderately inexpensive to monitor both the horizontal and vertical positions (Guariglia *et al.* 2006; Mitasova *et al.* 2002; Morton *et al.* 1993; Uunk *et al.* 2010). Also, the coast is usually a suitable area to conduct GNSS surveys because of the unobstructed view of the sky (Morton *et al.* 1993). However, the point capture method by GNSS cannot cover large areas in a short time.

2.8.2 Remote Sensing Methods

Since the 1920s, aerial photography and photogrammetric methods have been used to determine marine boundaries and document topographic information along coasts (Anders and Byrnes 1991; Crowell *et al.* 1991; Overton *et al.* 1996; Stockdon *et al.* 2002). Surveyors have also used their judgment to accept certain topographic features on the photographs as the position of the HWM (Horlin 1994). These works often include manual interpretation of photography (Boak and Turner 2005; List and Farris 1999) together with field surveys, including shoreline feature analysis, the

testimony of eye witnesses and sand colour analysis (Cole 1997; Nunley 2002). For instance, Crowell *et al* (1991) stated that HWL as an indicator of land-water interface is a line that can be detected by the change in colour or grey tone in aerial photographs caused by differences in the content of the sand. Similarly, Anders and Byrnes (1991) asserted that HWL could be recognised by wet/dry contact on a beach caused by an abrupt or subtle change in contrast. The wet/dry line on aerial photographs was considered as the most prominent feature dividing land and water by Cole (1997). One definition that enhanced the edge detection was the zone of variance of high-pixel brightness in imagery (Shoshany and Degani 1992). A more common and practical method is for the analyst to detect the shore markings on photography by the last preceding high water (Pajak and Leatherman 2002; Shalowitz 1964) and its accuracy is dependent on photography being taken at high tide. Furthermore, the location of salt-resistant marshes and mangroves shown on aerial photographs are also used as indicators of the HWM in the U.S. (Horlin 1994).

However, many studies show that interpreting marine boundaries from photography introduces significant errors in locating shorelines (Anders and Byrnes 1991; Boak and Turner 2005; Moore 2000; Pajak and Leatherman 2002; Stockdon *et al.* 2002). Hirst and Todd (2003) argued that it is difficult to determine the high tide line on a beach within a few metres, and even more so from a plane using aerial photographs. Crowell *et al.* (1991) wrote that errors in determining coastal boundaries from aerial photography arise from two processes: (1) identification or interpretation of the boundary, and (2) mapping the interpreted line as part of topographic information.

Compared with field surveying, manual interpretation of shoreline features as HWM indicators may be less accurate and more subjective because it relies heavily on the photogrammetrist's individual skills and judgement (Anders and Byrnes 1991; Boak and Turner 2005; Crowell *et al.* 1991; McBeth 1956), and so the method cannot guarantee precise determination of the HWM. Also, precise boundary detection depends on high quality aerial photography (Boak and Turner 2005). When one cannot see the water boundary clearly because of poor contrast or a fuzzy transitional zone of tonal change, it is difficult to determine the exact location of HWM indicators (Crowell *et al.* 1991).

However, this does not mean that even good quality aerial photography will necessarily result in a satisfactory boundary. Sometimes large scale high resolution data can also make it difficult to obtain a well-defined boundary to delineate objects because the overly finely distributed details make it difficult to distinguish the target classes from others during the classification process (Burrough and Frank 1996). This is called 'salt-and-pepper effect' (Blaschke *et al.* 2008). Therefore, the result of traditional pixel-based image analysis is unsatisfactory for shoreline feature detection using high-resolution imagery (Antunes *et al.* 2003).

Satellite imagery taken by remote sensing techniques is an alternative to aerial photography. It has also been widely applied in coastal boundary determination. Both MHW and MLW can be located by the satellite imagery using an infrared band which can detect wet and dry sand (Horlin 1994), while another potential application of satellite imagery is to detect biological profiles (Cole 1997). Because of flooding, wind or other effects, vegetation zones can be distinct on the shore and indicate the high water level in an extreme situation. Thus, it is helpful to look at vegetation information by enhancing the 'vegetation band' to help detect vegetation lines (Nunley 2002).

However, the degree of utility is questioned. This is because satellite images such as SPOT and Landsat have large ground cell sizes of more than 1 metres; therefore, they show no potential for accurately identifying the shoreline features (Nunley 2002). The identification of shoreline features on both satellite images and aerial photography can become more objective when using unsupervised classifications such as neural networks that distinguish land and water classes (Boak and Turner 2005; Kingston *et al.* 2000). However, there is no unanimous agreement about how to make a consistent interpretation of features when applying remote sensing techniques (Pajak and Leatherman 2002).

Airborne Light Detection And Ranging (LiDAR) systems are optical remote sensing techniques that are mainly used to measure dense clouds of three dimensional data, including topography (Mitasova *et al.* 2002; Stockdon *et al.* 2002), while GNSS can be used to determine the elevation of discrete points on a corresponding tidal datum such as a transect (Nunley 2002). Airborne LiDAR techniques can be used to capture onshore features over large areas in a short time frame (Armaroli *et al.* 2004), thus it

is a complementary technique used to fill data gaps between ground profiles. Moreover, when applied in a repetitive manner, LiDAR enables three-dimensional analysis of temporal beach profile variations.

With the use of LiDAR topographic data, it is possible to create a DEM of the foreshore, with which a tidal datum-based HWM can be easily identified (Boak and Turner 2005; Hapke and Richmond 2000; Morton *et al.* 2004). More potential applications of LiDAR-derived DEMs for studying the coastal morphology have been illustrated in studies by Hapke and Richmond (2000) and Mitasova *et al.* (2002). Landgate in Western Australia recommend the use of modern survey equipment, such as LiDAR (Landgate 2009c), especially when it is necessary to obtain data on a broad shore, and quickly obtain data over a large area (Boak and Turner 2005). However, this does not mean the HWM position obtained from LiDAR is reliable. The nature of the beach, such as its morphology, and the resolution of the data captured by this technique also influence the precision of the determined HWM indicators (Stockdon *et al.* 2002). This may contribute to the variation in the determined HWM position.

2.8.3 Statistical Methods

Statistical methods are well-established approaches often used to determine tidal datums using long-term tidal records and are considered objective ways to determine coastal boundaries (Boak and Turner 2005). This is because statistical methods usually observe the tide over a considerable period of time, thereby taking a number of necessary factors into account (Gay 1965). Cole (1997) stated that the method of using tidal datum records is the best approach to determining the position of the HWM, especially where landform change over a period of time is insignificant. The most popular statistical method is to calculate the ‘mean’ tidal datum over a period.

For surveys to locate the position of tidal datum-based HWM for one site, especially at a standard port (also known as a ‘primary port’) for which sufficient tidal data is available (The Intergovernmental Committee on Surveying and Mapping (ICSM) 2009), the tide tables such as Australian National Tide Tables (ANTT) in Australia, can be consulted. These tables provide the information of tidal constituents (Land

Services 2008), which are essential to calculate the tidal datum-based HWM. The relevant tidal datums are derived as follows (Horlin 1994):

$$MHWS = Z_0 + (M_2 + S_2) \quad (2.7)$$

$$MHHW = Z_0 + (M_2 + K_1 + O_1) \quad (2.8)$$

where Z_0 represents the mean sea level (MSL). For practical purposes, the MSL is equivalent to an AHD value of 0 metres in Australia (Horlin 1994). The equations illustrate that the tide is actually the composite sum of factor constituent cycles, which usually last 18.6 years (Cole 1997). During this time, all the major tidal variations have been taken into account (Gay 1965), excluding only those in extreme conditions (Center for Operational Oceanographic Products and Services 2003).

Early surveyors rarely used statistical methods to determine the HWM based on the tide datum, especially those who had no knowledge of tides (Clerke 2004). Recently, statistical methods have been widely applied and show that water level can be objectively recorded by tide information in some areas. However, offsets still exist between the tide gauge records and the actual positions that water reaches on the shore because the tide gauge excludes the influence of wave runup. This situation will be exaggerated on gently sloping sandy beaches, making it difficult to transform a tidal elevation to the horizontal position of MHM (Morton and Speed 1998; Pajak and Leatherman 2002). Also, an accurate statistical method is not available when distant from tide gauges, as the estimation of tidal information can only be reached by interpolation methods (Greenfeld 2002). Furthermore, the tidal datum-based statistical method isolates the water from the land, which ignores local spatial information, such as geomorphology and variation through time.

2.9 Variation of the HWM Position

The HWM is considered ambulatory, that is, it may shift over time both horizontally and vertically because of artificial or natural factors. Tide is produced by the gravitational forces of the moon and sun, but additional non-astronomical factors such as cyclones, air pressure, artificial structures, wind, wave height, types of coast, sea level change, and El Nino and La Nina are factors that may influence the position of the HWM (Dolan *et al.* 1980; Hicks *et al.* 1989; Moore 2000; Morton and Speed

1998; Pajak and Leatherman 2002). Furthermore, accretion and erosion of coastal morphology will physically move coastal boundaries (Figure 2.5).

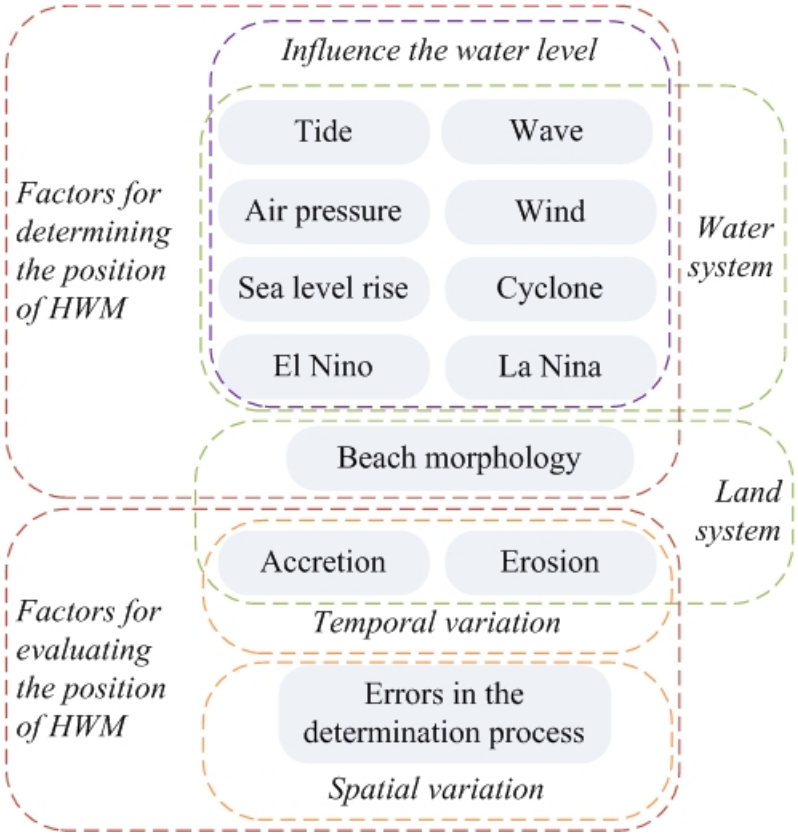

Figure 2.5 The factors influencing the position of the HWM and its relation to the determination process

2.9.1 Factors Influencing the Position of the HWM

Tides are most strongly affected by the gravitational force of the moon and, to a lesser degree, the sun (Cole 1997). Rahmstorf (2007) estimated that global warming is the main cause of the current rise in the sea level, which by 2100 will be 0.5 to 1.4 m above the 1990 level.

Generally, the tidal range in summer is greater than that in winter, since the air pressure is lower in summer, and this leads to abnormally high water levels (R.Mahoney, personal communication 12 May 2010). Sudden and distinct changes in the tidal datum are mainly caused by storm events (Pajak and Leatherman 2002). These changes are normally larger than those produced by astronomical tides (Morton and Speed 1998).

Changing depth, width and the course of estuaries, as well as the distance from the ocean, are all relevant to the variation of the tide datum (Cole 1997). The dynamic nature of seawater continuously affects the coast in the form of waves and tides, but these also act variously on different kinds of coast (Anthony and Orford 2002).

To determine the unbiased position of the HWM, long-term observation of tides and waves can identify most of the above factors and include them in statistical calculations. Comparing results from study areas with different coastal features can reveal how coastal types may influence the position of the HWM. Even if the vertical position of a tidal datum-based HWM is determined by the long-term observation of tides and waves, its horizontal position may vary through time as the coastal morphology changes. This is similar to most corresponding shoreline features.

2.9.2 Temporal Variation of the Beach Profile—Stability

Generally, HWM indicators such as berm crest or vegetation line are located on the swash (wave runup) zone, a transitional zone between the subaqueous (below water) and subaerial (above water line) zone of the beach, intermittently covered and exposed by wave action (Hughes *et al.* 2010). Both engineers and coastal researchers are interested in the swash zone since the process of swash could result in coastal inundation. Of particular interest to HWM studies is the variation of coastal boundaries due to relatively higher cross-shore sediment transportation rates in the swash zone (Hughes *et al.* 2010; Masselink and Russell 2006). Alsina and Cáceres (2011) also indicate that the beach close to the shoreline is a highly dynamic zone where coastal sediment transport takes place frequently, and yet this dynamic mechanism remains poorly understood (Masselink and Russell 2006).

A significant number of quantitative analysis studies have been conducted on the seasonal changes in beach profiles (Aubrey 1979; Aubrey and Ross 1985; Shepard 1950; Weishar and Wood 1983; Winant *et al.* 1975). These studies show that seasonal morphology changes cause the most dominant temporal variations (Masselink and Pattiaratchi 2001), with large changes of the beach profile often occurring between summer and winter. Changes between spring and autumn beach profiles are often almost identical (Larson and Kraus 1994). However, the results of these temporal variation studies are limited as they are only based on two-

dimensional parameters (e.g. transection lines), which may result in large data gaps between established profiles (Hapke and Richmond 2000).

The most traditional way to examine changes in coastal morphology is through field surveys (Austin and Masselink 2006; da Fontoura Kle and de Menezes 2001; Eliot *et al.* 2006), and the tools to study change have improved over time. Today, the most commonly used equipment for GNSS field surveys is based on Real-Time Kinematic methods(RTK) with centimetre accuracy (Dail *et al.* 2000; Travers 2009). However, field surveys are very time consuming and labour intensive and cannot cover large areas in a short time frame.

Alternatively, video techniques can be used to monitor the evolution of coastal morphology (Lippmann and Holman 1989, 1990). However, video is costly in terms of setup and maintenance of the video system. In addition, video techniques are highly sensitive to field conditions, such as lighting conditions.

Another technique for quantifying the variation of spatial objects over time is to use time series image analysis. Most recently, time series analysis has been developed to detect temporal changes of coastal morphology using a series of remotely sensed images. The (periodic) time series is usually analysed in terms of general trends, seasonal variations and residual components (Herold 2011; Jacquin *et al.* 2010; Jong *et al.* 2011). One of the models developed to illustrate this idea is the ‘Breaks For Additive Seasonal and Trend’ (BFAST) (Verbesselt *et al.* 2011; Verbesselt *et al.* 2012).

However, the application of this model depends highly on whether a sufficient number of images are available as input data (e.g. more than two per year when analysing seasonal variations and annual variation). When image data is limited (e.g. only two images), a simplified method can be used to identify temporal variations by comparing the two different images (Andrews *et al.* 2002). While this is a relatively simple method, the results may be highly biased due to seasonal and longer-term variations.

2.9.3 Spatial Variation of Shoreline Features—Precision

The variation in the position of a shoreline feature between successive monitoring as a result of the measurement process can be expressed as spatial precision, thus indicating apparent spatial variations. When using remote sensing techniques, variations in extracted shoreline features can be expressed by their comparison with features on a geographically registered map and the corresponding position on the Earth's surface.

Spatial variations of shoreline features may arise from data source inaccuracies and interpolation errors (Ruggiero and List 2009). The errors from interpolation processes can occur in the pre-processing stages of the determination process, such as identification of the shoreline position on aerial photography, and post-processing stages when it is represented on the map to display the data (Shi 2009). When image analysis is applied in shoreline feature position determination, pre-processed spatial variations are mainly determined by the classification accuracy and image registration; while if the shoreline position, including the HWM, is calculated from a statistical model, the variations are mostly due to the accuracy of the model itself.

During post-processing, the HWM in Australia is usually determined as a height above the AHD. When the HWM is positioned on the ground, as is the horizontal cadastre, any inaccuracies (including errors and uncertainties) of the digital elevation model (DEM) used to extract beach profiles based on the AHD can lead to spatial variations that can affect the position of derived results such as the beach slope and contour lines (Hunter and Goodchild 1997; Oksanen and Sarjakoski 2005).

Traditionally, these errors and uncertainties are categorised into three groups: (1) gross errors, (2) systematic errors and (3) random errors (Cooper 1998; Wise 2000). Due to their magnitude, gross errors are easily detected and removed prior to data processing. These errors are often associated with faulty equipment and errors in the data collection process (Wechsler and Kroll 2006). Systematic errors follow a consistent pattern and are often inherent in the procedures used to generate the DEM (Fisher and Tate 2006), and are normally characterised by the Root Mean Squared Error (RMSE).

In contrast to systematic errors, random errors can only be quantified through repeated experiments. Currently, due to the complexity of processing algorithms, it is not well understood how random errors are introduced and propagated through a DEM (Wechsler and Kroll 2006). Therefore, the uncertainty present in derived products from the DEM cannot be easily determined. Furthermore, due to topographic data complexity, the determination of HWM indicators is not straightforward, and this may also influence spatial variation in HWM indicators (Thompson *et al.* 2001). Therefore, the effects of the topographic complexity of the HWM indicator on the spatial variation in HWM determination require further investigation.

In summary, factors influencing the determination of the position of the HWM are usually considered separately and have not been integrated into a single system for coastal boundary determination. In this research, factors influencing the spatial and temporal variations of the HWM are considered in a holistic or whole system to evaluate their effects on HWM determination.

2.10 Difficulties in HWM Determination

Due to inconsistencies in the definition, there are no reliable techniques nor generally accepted methods to determine the HWM worldwide or even in Australia (Cole 1997). Therefore, the analysis of various HWM data (called HWM indicators), along with analysis of the methods of determination of the horizontal position of the HWM, is required. This would inform future data collection (tidal datum, terrain morphology, etc.) and data processing (statistical, survey calculations, processing of remote sensing) phases of large-scale HWM mapping. It is likely that, from a better understanding of data and processing, a formal definition for the HWM can be derived for Australia and countries with a similar legal system and understanding of the boundaries of coastal rights.

Indeed, Landgate has been involved in several disputes over the last few years involving the need to defend the definition of water boundaries in Western Australia's Spatial Cadastral Database (SCDB). Users need to be fully aware of the limitations of the SCDB for precise boundary definition on the one hand, and on the other hand, precise and up-to-date land and water boundary information is essential,

but may not be easy to obtain for either property management or coastal hazard planning purposes.

Traditionally, MHWM was determined using medium- to long-term tidal records (Cole 2007). Although determined with mathematical precision, the MHWM using a tidal datum is not suitable as a permanent boundary for property rights (Cole 1997) because neither the ocean level nor the coastal geomorphology are stationary over long periods. The HWM is difficult to determine accurately due to the ambulatory nature of both water and coastal morphology (Whittal and Fisher 2011).

Contemporary research has failed to develop a robust method of determining the HWM because of the continuous changes in tidal levels together with unimpeded wave runup, as well as the erosion and accretion of beaches. This explains, in part, why there is no official or widely recognised definition of the HWM. It is important to identify, evaluate and integrate various factors into the process of determining the HWM, yet there is currently no consensus as to how to do so.

Furthermore, the use of tidal records ignores wave runup and, as such, will always underestimate the HWM in coastal regions (Whittal 2011). For example, in areas where there is a small tide range and significant wave action, the actual landward water level will be further inland than the HWM level determined using only tide records due to the effects of setup and wave runup. The effect of wave runup in HWM determination has rarely been quantitatively assessed. Yet some studies have indicated that the water level (swash or wave runup) is more appropriate for the HWM used for coastal hazard planning, while the tide water is suitable for coastal property management (Bellomo *et al.* 1999; Maloney and Ausness 1974a).

If this is the case, further quantitative analysis is required to evaluate all the indicators based on this assumption. However, analysis is often impeded by limited data because of either buoy breakdowns during cyclones or computing problems. As a consequence there are many gaps in the wave information records, and these are not always small gaps (Kalra and Deo 2007). Moreover, because of the complexity and uncertainty of wave generation, it is difficult to interpolate and model wave information using deterministic equations.

Boak and Turner (2005) suggested that researchers have not considered all indicators in their methods for determining shorelines. The same can be said of HWM determination, and this has affected results. However, the fundamental question of the relationship of each HWM indicator to the water-land interface is still not resolved. Further knowledge of how to integrate the water and land system as a whole and how to define the water-land interface is required. For instance, MHW has been recognised as a concept isolated from the whole coastal system; however, besides knowledge of tides, it is also important to understand the geomorphology of the coast to locate the HWM (Coutts 1989).

Although LiDAR DEMs have proven useful in coastal studies, some researchers have identified a low accuracy of data in various applications (Bater and Coops 2009; Hodgson and Bresnahan 2004; Hodgson *et al.* 2005). This is most significant with data captured when the technology was first introduced. Therefore, data collection protocols and proper spatial interpolation methods are needed to fill in data gaps.

An acceptable method of determining coastal boundaries should satisfy the following criteria: repeatable, consistent and reliable (Leon and Correa 2006; Pajak and Leatherman 2002). Moreover, as an administrative boundary, the HWM tends to be used as though it has been precisely defined (Burrough and Frank 1996). A cliff edge was considered a much more stable boundary than the instantaneous HWL and berm crest on a beach (Moore 2000; Morton 1991); and if conditions permit, these stable features should be given priority as indicators when determining the HWM.

Morton and Speed (1998) point out that, although the determination of MHW considers most of the factors influencing its position over a long period, it is not as stable as a vegetation line, but the higher precision makes it as good an indicator option as the vegetation. However, quantitative analysis and comparison of the variation for each HWM indicator in one system has not been conducted; thus more research on this topic is required. Even if the factors that influence the determination of the HWM were identified and quantified, a rule for the criteria to evaluate the HWM indicators would also be necessary to make a final decision about the proper position of the HWM for different purposes.

2.11 Summary

The determination of the HWM has a long history. Its definition, the mean and even the corresponding determination methods have changed through time.

Nowadays, the definition of the HWM is still ambiguous worldwide, due to the diversity of coastal types, different determination purposes and the limitations of observation techniques and data. The definition of the HWM is different for different countries as their legal systems and the understanding of rights in the coastal zone and especially the shoreline are different. Moreover, the land and water systems have always been considered separately, which leads to inconsistent results in the determination of land/water boundaries from the water-side and land-side.

Therefore, an improved method to determine the position of the HWM is required. This should be an analytical system that integrates all factors. In addition to the HWM position determined by the improved methods, all HWM indicators should be assessed in one evaluation system that can provide a consistent and robust HWM determination methodology.

Based on the investigation of previous studies explored in this chapter, a methodology to solve the HWM determination problems is presented in the next chapter.

CHAPTER 3 RESEARCH METHODOLOGY FOR HWM DETERMINATION

3.1 Introduction

The difficulties of determining the HWM have been discussed in the previous chapter. Industry requires that a consistent and robust methodology for HWM determination is developed and this requires further research.

The methodology proposed in this chapter provides a solution for consistent and robust determination of the HWM. It also includes an overview of the research method, and the implementation of the method in the form of a workflow.

The methodology is evaluated in two case study areas located in Western Australia—Fremantle and Port Hedland. Finally, this chapter describes the data and the software used to implement the new methodology.

3.2 Research Method

The research method comprises two major components—the determination and evaluation of HWM indicators (Figure 3.1). The research methodology includes the following key steps:

- accurate identification of the shoreline features using remote sensing image analysis;
- exploration on the effect of wave runup in the HWM determination;
- integration of both land and water information to determine the position of the HWM; and
- evaluation of HWM indicators in one quantitative system.

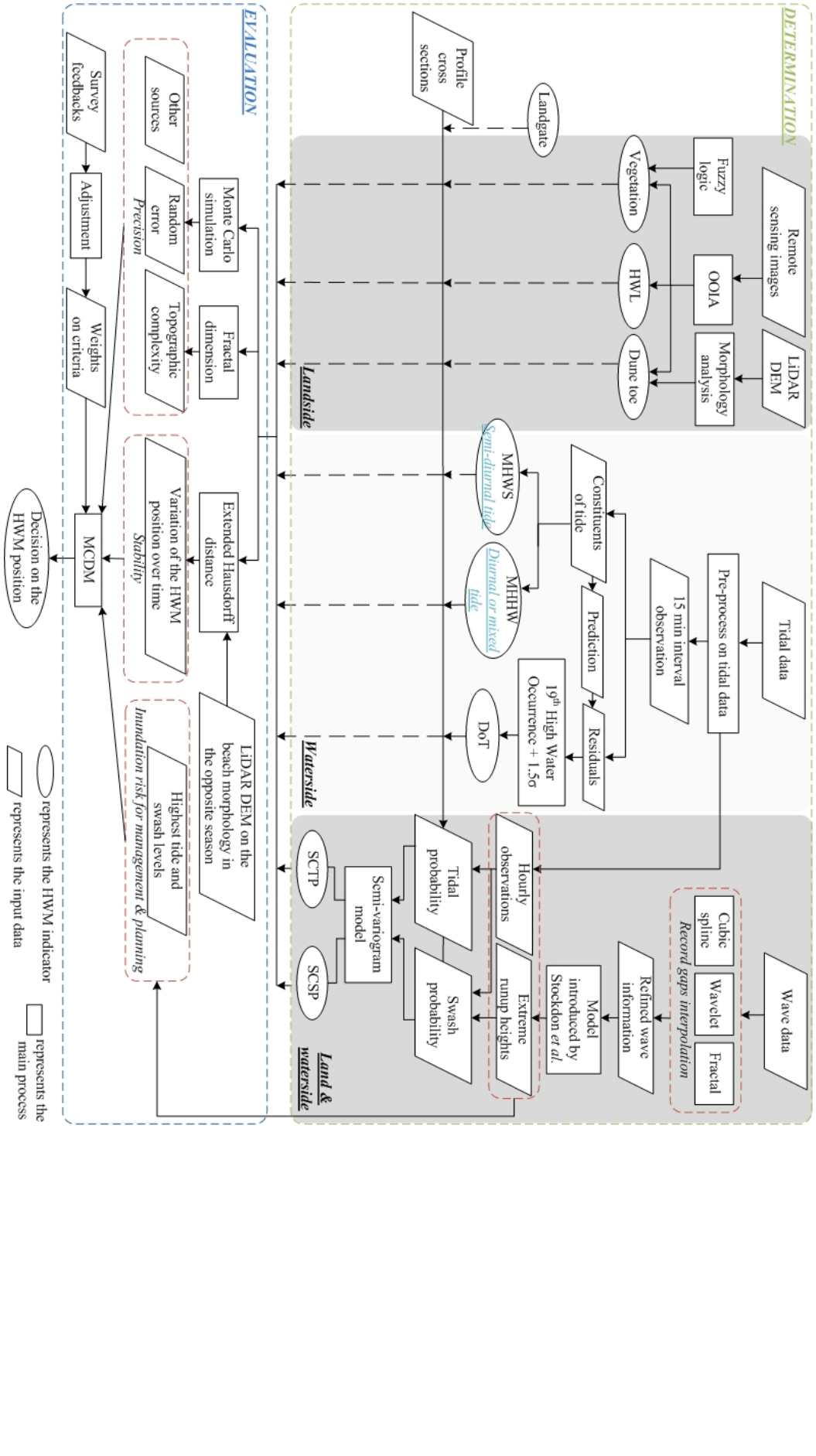

Figure 3.1 Workflow for HWM determination

3.2.1 Determination of HWM Indicators

In this study, the HWM indicators are divided into three primary categories:

- shoreline features from the landward side, including HWL, vegetation line and the position of the dune toe (Section 2.3);
- tidal datum-based HWM indicators located towards the waters edge, including MHWS, MHHW and the HWM suggested by DoT (Section 2.2 and 2.3); and
- indicators introduced in this study including the positions of the HWM based on the spatial continuity of swash probability (SCSP) or spatial continuity of tidal probability (SCTP) for a range of HWM indicators that integrate both land and water information into the determination system.

3.2.1.1 Shoreline Features

The determinations for landside and waterside HWM indicators are two relatively independent processes. The image analysis techniques and classification methods were applied to identify the position of landside shoreline features.

In the process of classification, pixel-level analysis is based on the information contained in each pixel; while for the object-oriented image analysis (OOIA), the image is partitioned into meaningful regions based on pixel values and region shapes, and then the classification process is conducted on these regions. Classification on the homogeneous regions avoids the salt-and-pepper effect obtained using traditional pixel-level analysis (Blaschke *et al.* 2008), which results in overly finely distributed classification results on the classified image, especially for high-resolution imagery.

The pixel-based image analysis has not proven satisfactory for high-resolution imagery classification and feature detection (Antunes *et al.* 2003). Therefore, OOIA is used in this research for the classification of shoreline features. This method is more accurate and effective than pixel-level analysis on high-resolution images (Blaschke 2010). Vegetation is considered to be either sparse or dense. It is easy to identify the boundary of dense vegetation, but the position of sparse vegetation is fuzzy and difficult to differentiate from beach sand in the imagery. However,

because the sparse vegetation zone is always further seaward than the dense vegetation zone, the most seaward position of vegetation and the average height of the sparse vegetation located on the beach are considered as the position of the vegetation line.

In this study, an objective oriented fuzzy logic method was applied to identify the position of the vegetation line, due to its efficiency to derive good results where feature extraction is necessarily vague as indicated by Benz *et al.* (2004). The position of the dune toe was identified by the OOIA integrated with the morphology analysis using DEM. More details are illustrated in the Section 5.4.

3.2.1.2 Tidal Datum-based HWM Indicators

The tidal datum-based HWM indicators on the waterside were all determined using a series of software and methods developed by the DoT, WA. During the determination process, the constituents of tide were extracted from long-term tidal information to calculate MHWS and MHHW for the two different tidal types—semi-diurnal tide and diurnal tide, respectively. The prediction of tidal heights during the recording period can also be calculated from the constituents. Residuals between predications and recordings, required to calculate the HWM suggested by the DoT method, were also derived. More details can be found in the Section 5.3.

3.2.1.3 The Indicators Introduced in This Study—SCTP and SCSP

Boak and Turner (2005) suggested that when attempting to determine shorelines more accurately, researchers have not considered all the indicators, and this has impacted results. Furthermore, the landside and waterside information is always used separately to determine the HWM position. This ignores the fact that water and land are one integrated system for HWM determination. For example, the spatial distribution of swash/tidal probability, which is the chance of inundation on the beach face over a specified time period, is a significant criterion for determining HWM position and it is commonly ignored. However, one of the factors impeding further investigations on the effect of swash on HWM determination is the gaps existing in wave recordings. Many gaps exist in the records and they are not necessarily small. Although, a number of previous studies have attempted to fill the

gaps in wave information (height and period) records, most of the interpreted results are not satisfactory.

Nonetheless, the irregular pattern of the time series of wave information has two main features: multi-frequencies and self-similarity. These features enable the application of the wavelet and fractal methods. In this research, the wave information was interpolated using these two methods: wavelet refined cubic spline and fractal models. These were examined to assess their capability of filling various data gaps for different size gaps. These methods aim to interpolate missing data in wave recordings, particularly where there are lengthy time lapses.

To start with, the initial hourly interpolation of significant wave information used the cubic spline method over 1-1255 hours time intervals. A correction to this interpolation was made using the wavelet method, which separates the time series of wave information into high and low frequencies for the cubic spline interpolation. This method achieved improved interpolation results; however, large data gaps still could not be calculated with any degree of confidence. To overcome this problem, the fractal method was used to map and simulate the whole time series pattern to more accurately portray data where there are large gaps. Next, the effects of two new methods on different sized gaps were discussed and compared with the cubic spline method. The details of the method are illustrated in Chapter 4.

Swash/tidal probability at different locations along one beach profile (cross-section) tends to be spatially autocorrelated, which means two locations nearby along a profile tend to have similar swash probability compared with those that are farther apart (Cliff and Ord 1970). However, for two locations, such autocorrelation only takes effect within a certain distance. This is called the range or spatial continuity distance, which can be estimated by the basic moment of geostatistics—the semivariogram (Jian *et al.* 1996; Oliver and Webster 1990).

In this research, ten-year hourly swash/tidal heights were fitted into a cumulative distribution function. The probability that swash will reach the various HWM indicators over a 10 year period is then estimated. The spatial continuity distances of the swash/tidal probability of HWM indicators were calculated using semivariogram models that measure similarity of swash/tidal probability. The spatial continuity

distance was defined as the distance between the lower bound of sampling position (the most seaward HWM indicator) and the position where autocorrelation, or the similarity of swash/tidal probability of the various HWM indicators, approaches zero. The latter is considered as the HWM position.

The positions of the HWM based on the spatial continuity of swash or tidal probability (SCSP or SCTP) are for the purposes of coastal hazard planning and coastal property management, respectively in this study. Generally, the processes can be described by the following three key steps, which are explained in detail in Chapter 5. These are:

- Fitting swash/tidal heights to a cumulative distribution function;
- Determining the probability of inundation due to swash/tide of HWM indicators by the determined cumulative distribution function;
- Calculating the spatial continuity distance of swash/tidal probability to determine the position of the HWM based on the semivariogram.

Field verified GNSS survey data from RTK methodswere used to determine the position of water level and shoreline features at two study areas. These provided confidence levels against which the empirical model and feature extraction methods were validated.

3.2.2 Evaluation of the HWM Indicators

The determined HWM indicators were evaluated from three perspectives: precision, stability, and inundation risk for the coastal hazard planning and coastal property management. The importance of precision and stability in HWM determination is illustrated in Sections 2.8 and 2.9. The risk for the HWM means the chance of a property at risk of inundation from the tidal water and wave runup over a long period of time. The inundation risk was estimated by the long-term cumulative distribution of water levels in a 10 year period. As illustrated in Section 2.4, the difference between the two different functionalities of the HWM is whether the effect of the wave runup on the tidal datum plane is included or not.

Therefore, the highest *tidal* level derived from the long-term tidal records was adopted as the 'benchmark' for the inundation risk of the HWM for the purpose of coastal property management; while the swash level derived from the long-term *tidal* and *wave* records was adopted as the 'benchmark' for the inundation risk of the HWM for the purpose of coastal hazard planning. The further the HWM indicators are away from this level, the lower they were ranked. For more detail refer to Section 7.3.2.

3.2.2.1 The Precision of HWM Indicators

The factors influencing the precision of HWM indicators mainly arise from data source inaccuracies (pre-process stages) and shoreline interpolation error (post-process stages) during the HWM determination process (Ruggiero and List 2009). Random error and topographic complexity cannot be easily determined and this is illustrated in the Section of 2.8.3.

The classical approach to examine the uncertainty is through error propagation. This can be done in two ways: (1) developing analytical error models, and (2) constructing stochastic simulation models (Zhang and Goodchild 2002). As indicted by Fisher and Tate (2006), the analytical error models are a relatively simple way to represent the uncertainty of a land feature from imagery, while stochastic simulation models are more realistic for modelling the occurrence of error by introducing random functions. These can be divided into two groups: unconditioned and conditioned models.

By considering the observations at the same sample location, the conditional simulation model using geostatistical methods, which takes into account the spatial autocorrelation of the simulated features, are more widely used (Fisher 1998; Holmes *et al.* 2000; Kyriakidis *et al.* 1999). In the stochastic simulation process, previous studies mainly focus on the Gaussian error model combined with the Monte Carlo method, especially when analysing DEM uncertainties (Davis and Keller 1997; Holmes *et al.* 2000; Oksanen and Sarjakoski 2005; Wechsler and Kroll 2006).

Therefore, the Monte Carlo method was adopted to evaluate the random errors in DEM data for determination of HWM indicators in this study. To determine the random error, 100 DEM simulations were carried out, from which the corresponding

HWM indicators were re-extracted. Then, the original DEM pixels were compared with the simulated values by Root Mean Squared Error (RMSE). This will be further discussed in Chapter 6.

Another factor influencing the precision of HWM indicators is the topographic complexity of HWM lines. A way to quantify the topographic complexity is using the fractal dimension (FD). The FD method has been extensively applied to understand the complexity of spatial patterns and their variation (Burrough 2006; Palmer 1988). The fractal concept was first introduced by Mandelbrot (1967) in order to illustrate irregular patterns that cannot be analysed by traditional Euclidean geometry. Euclidean geometry only allows dimensions with an integer number; however the important concept of the FD is that it also allows for non-integer dimensions. The FD increases as the complexity of the spatial pattern increases. This has been applied in studies such as measurement of plant development (Corbit and Garbary 1995) and variation (Palmer 1988), characterising complexity in earthquake slip and identifying regressive ecological succession (Alados *et al.* 2003).

One of the most commonly used examples to illustrate the fractal concept is to measure the length of a coastline (Jiang and Plotnick 1998; Mandelbrot 1967; Phillips 1986; Schwimmer 2008). Because all HWM indicators can be considered as different representations of the coastline, the FD was considered suitable to capture the topographic complexity of the HWM indicators. For more detail refer to Chapter 6.

3.2.2.2 The Stability of HWM Indicators

In this research, the stability of the HWM indicators refers to the seasonal variation of the HWM position on the coast. Studying the spatial variation of complex but linear objects such as the horizontal HWM requires the quantification of their spatial relationship (e.g. distance).

Various methods are available to measure the spatial distance between two linear objects, such as minimum Euclidean distance (Peuquet 1992) and surface ‘in between’ (McMaster 1986). However, neither of these methods are able to determine the true mathematical distance (Hangouët 1995). In this regard, the Hausdorff distance was introduced as a ‘safe and systematic’ distance to calculate the largest

minimum distance (refer to Chapter 6) between two vector polylines (Hangouët 1995). However, the Hausdorff distance can be rather unstable when there is a local sudden change in the shape of the measured objects (Min *et al.* 2007).

Therefore, an extended Hausdorff distance was introduced by Min *et al.* (2007) by removing (smoothing) sudden changes before calculation of the Hausdorff distance. This is considered as a more accurate measure, and as reflected in Section 2.8.2, will accommodate the large changes of the beach profile that often occur between summer and winter. This research adopted the extended Hausdorff distance method to assess spatial distances between HWM lines captured in summer and winter seasons based on different indicators. The input data required to assess the stability of HWM indicators were the two DEMs representing the coastal morphology in summer and winter.

Inherent in all the monitoring techniques identified in Section 2.8.2 is the occurrence of large data gaps (Bater and Coops 2009; Hodgson and Bresnahan 2004; Hodgson *et al.* 2005). Therefore, spatial interpolation methods are needed to fill in these data gaps because the information existing in the data gaps may still be useful for further analysis, especially for the DEM.

The Kriging method can be used to successfully interpolate data gaps in ground profiles. Compared to other interpolation methods, such as nearest neighbour, spatial averaging and inverse distance weighting, Kriging (Bailey and Gatrell 1995; Griffith 1988) has been proven to provide more accurate (minimum variance) and produces less biased estimates when applied to coastal morphology (Oliver and Webster 1990; Wong *et al.* 2004). Therefore, it was applied in this study to interpolate the data gaps in the DEM (Section 6.3), and to predict the missing data by summation of surrounding weighted observations (Oliver and Webster 1990).

The weights were estimated using a semivariogram model based on autocorrelation theory. However, Kriging may rely on the smoothness assumption of the interpolated surface (Li and Heap 2008) and it is restricted to the first and second order effects in spatial analysis (Emery 2006). Nonetheless, Li and Heap (2008) state that when observations are insufficient to compute variograms, the gap in sparse data can be satisfactorily interpolated using the Kriging method.

3.2.2.3 The Multi-Criteria Decision Making (MCDM) Model

Finally, the Multi-Criteria Decision Making (MCDM) model was adopted to score each HWM indicator. This model integrates the three criteria mentioned above to assist the selection and decision process for the best HWM indicators for two different purposes—coastal property management and coastal hazard planning, respectively. The HWM indicator with least score is chosen as the ideal HWM position. Survey methods were used to determine the weight for each criterion. Experts from different fields were asked to evaluate the criteria using a pairwise-comparison method (PCM). The inconsistency of the evaluation is adjusted by the method introduced by Ergu *et al.* (2011). Before being applied in the MCDM, all the assessed values of the three criteria were normalised. Based on the final evaluation results at two study areas, decisions and discussions on the position of the HWM for both hazards planning and property management were presented.

3.3 Characteristics of the Study Areas

Two study areas in Western Australia were chosen to test the developed method. These were Coogee Beach in South Fremantle and Cooke Point in Port Hedland (Figures 3.2 and 3.3). Table 3.1 summarises the basic coast features of these study areas (Gozzard 2011), which indicate distinctive differences between the two study areas and therefore they are considered appropriate for testing the developed methods under varying conditions. The two sites for implementing the research method were also selected due to the significant difference in their tidal and wave characteristics. Both sites had long-term tidal and wave observations available.

Table 3.1 Beach information on the two study areas (Gozzard 2011)

	Near shore	**Fore shore**	**Back shore proximal**	**Back shore distal**	**Geology substrate**	**Coastal exposure**
Coogee Beach	sand and sea grass meadows	low tide terrace	foredune - stable to prograding	prograded barrier	Unclassified	low
Cooke Point	rock pavement	rock platform / tempestite / segmented beach	low calcarenite cliff	transgressive dune barrier	Calcarenite	moderate / high

3.3.1 South Fremantle

The South Fremantle is a wave-dominated reflective straight beach with a diurnal tidal feature and a micro tidal range of 0.7 m (Short 2004). The site chosen extends approximately 500 m along the coast and is 70 m in cross-shore width. The wave breaking types at South Fremantle are either plunging (81.06%) or spilling (18.94%) and were estimated as shown below.

The Iribarren number, ξ_0, is an important parameter that indicates the dynamic beach steepness and is used to determine the nature of wave breaking on a beach slope (Stockdon *et al.*, 2006), which is defined as (Battles 1974):

$$\xi_0 = \frac{\tan\beta}{(H_0 / L_0)^{1/2}} \tag{3.1}$$

in which β is the average beach steepness calculated from the digital elevation model (DEM) of the study area (Burrough and McDonnell 1998), and H_0 and L_0 are the deep-water wave height and length, respectively. Based on the value of ξ_0, Battles (1974) pointed out that different wave-breaking types occur. Due to the fact that the wave information applied in this study was recorded from offshore, the criteria are slightly different from those of breaking waves (Galvin Jr 1968). Based on the 10 year records of wave height and period, the wave-breaking types were estimated in the two study areas.

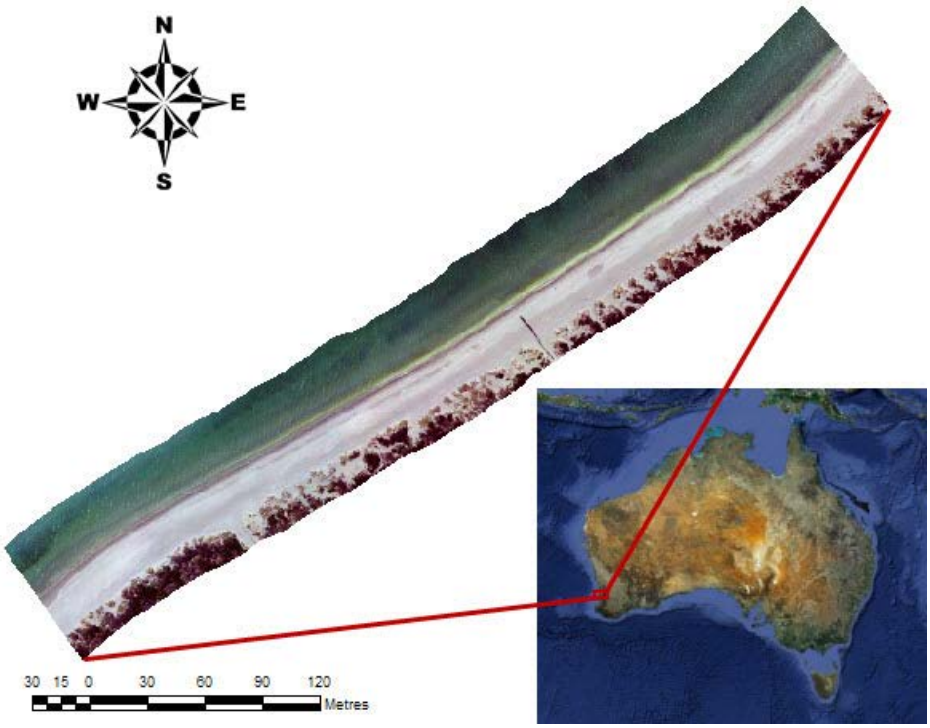

Figure 3.2 Map of the study area (South Fremantle)

3.3.2 Port Headland

In contrast, Port Hedland is a tidal-dominated sand-flat headland (Cooke Point), where the tide type is semi-diurnal, and the macrotidal range is 6 m (Short 2004). The Port Hedland site extends approximately 2300 m along the coast and 200 m in cross-shore width. The wave-breaking types, based on an analysis of 10 years of historic wave data, are either plunging (92.07%) or spilling (7.93%).

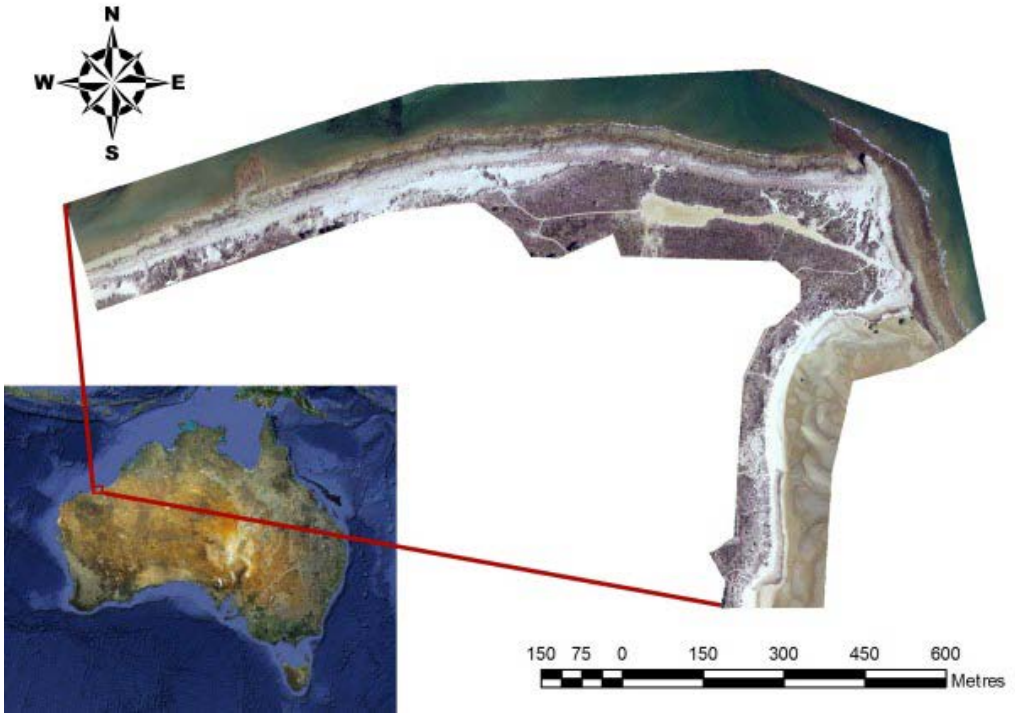

Figure 3.3 Map of the study area (Port Hedland)

3.4 Data and Their Format Requirements

3.4.1 Tide

A period of 19 years is usually considered as a standard tidal cycle when research is conducted, as it reflects the principle lunar node of 18.6 years. The decision as to which years will be the beginning and end of the standard cycle epoch is made, in Australia, by the Permanent Committee for Tidal and Mean Sea Level (PCTMSL). Their decision conforms to international standards; the current epoch commenced in 1992 and finishes at the end of 2010 (The Intergovernmental Committee on Surveying and Mapping (ICSM) 2010b).

Therefore, tidal data in the period between 1992 and 2010 were selected for this research. Tidal data were regularly recorded using the tide gauges by Department of Transport during this period in the form of one specific time with one corresponding tidal height. The tide data applied in this research were recorded every 5 minutes at Fremantle (about 8 km from the study area at South Fremantle). For the Port Hedland region, the tide data were also recorded in a uniform format in terms of tidal datum recording period and recording intervals by the Department of Transport (DoT) (Department of Transport 2010b).

3.4.2 Imagery and Digital Elevation Model (DEM)

The imagery used in this study to extract HWM indicators was captured by Landgate using Leica ADS80 Digital Camera. The South Fremantle region was captured in February 2010 with a ground resolution of 0.1 m (Landgate 2010). The DEM for the same area, also reflecting the summer coastal morphology, was derived from LiDAR data captured in February 2008 and produced by WA Department of Water (Department of Water 2008). The DEM has a vertical accuracy of 0.15 m and horizontal accuracy of 0.6 m. Another DEM (with a vertical accuracy of 0.3 m and horizontal accuracy of 0.5 m), reflecting winter coastal morphology, was generated by Landgate (Landgate 2012) from digital aerial photography captured in August 2011.

Imagery for the Port Hedland study area was captured in November 2009 at a ground resolution of 0.2 m (Landgate 2009b). The DEM, representing the summer coastal morphology, was created by Landgate (Landgate 2009a) from airborne LiDAR data with a vertical and horizontal accuracy of 0.2 m and 1.0 m, respectively. As the point density of LiDAR data captured at South Fremantle (both seasons) and Port Hedland (November 2009) is very high, the Inverse Distance Weighting algorithm was used to resample the point cloud to a grid. This is considered sufficient to provide a high quality DEM. However, the LiDAR points captured to represent the coastal morphology at Port Hedland in winter (July in 1995) were not dense enough (Figure 3.4) to provide a high quality DEM, so further interpolation is required (Landgate 1995).

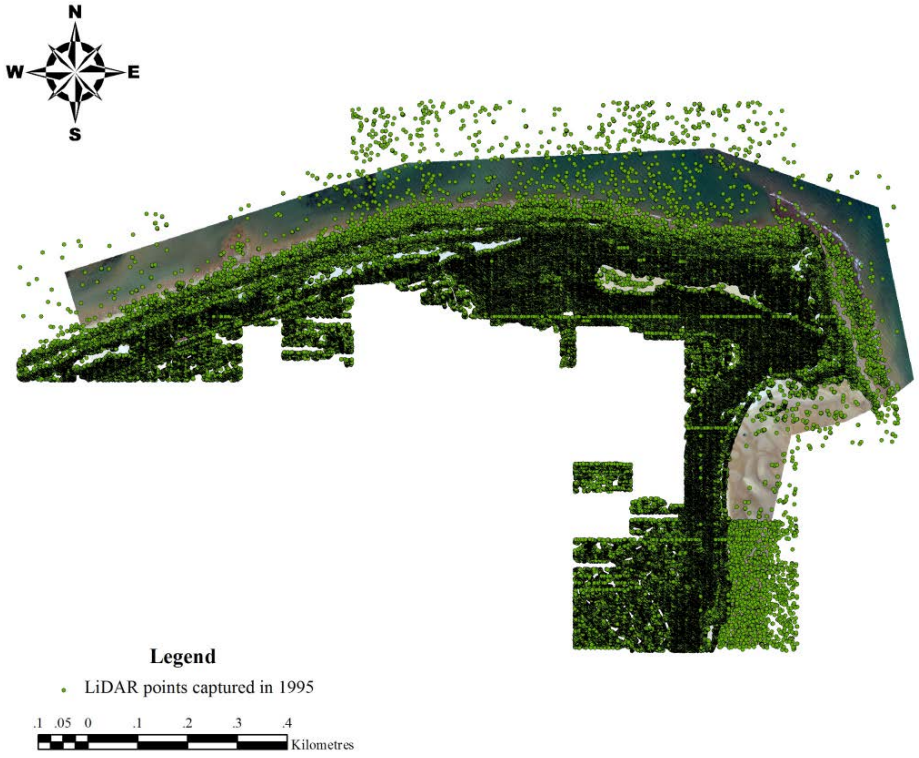

Figure 3.4 Original LiDAR points captured at Port Hedland 1995

3.4.3 Real-Time Kinematic (RTK) Land Survey Data

A centimetre accuracy RTK GNSS receiver is used in the field to survey the position and elevation of shoreline features and the water level. The advantage of RTK, with a standard deviation from the mean of about 10 mm (Cordesses *et al.* 2000), enables the captured position and elevation information of ground reference points to be more reliable. The surveys are tied back to control points near each study area to assess the confidence of the whole survey process.

3.4.4 Wave

The time series of hourly wave information (significant heights and periods) for South Fremantle and Port Hedland, Western Australia were recorded by the Cottesloe wave rider buoy (approximately 16 km from South Fremantle) and Beacon 16 (approximately 19 km west of Port Hedland), respectively (Tremarfon Pty Ltd. 2011). The wave heights and wave period are recorded at the same time. The range for the wave heights are from 0.18 m to 3.67 m at Cottesloe and from 0.16 m to

4.85 m at Port Hedland; while the range for the wave periods are from 2.6 seconds to 12.5 seconds at Cottesloe and are from 1.8 seconds to 13.9 seconds at Port Hedland.

There are missing data in the recordings for both locations. This reduces the whole wave information records dataset in Cottesloe and in Port Hedland by 2.15% and 7.91%, respectively. The largest recorded gap for Cottesloe is 835 hours (from 19th February 2009 to 25th March 2009) and for Port Hedland it is 1255 hours (from 22rd October 2001 to 13th December 2001) (Figures 3.5 and 3.6).

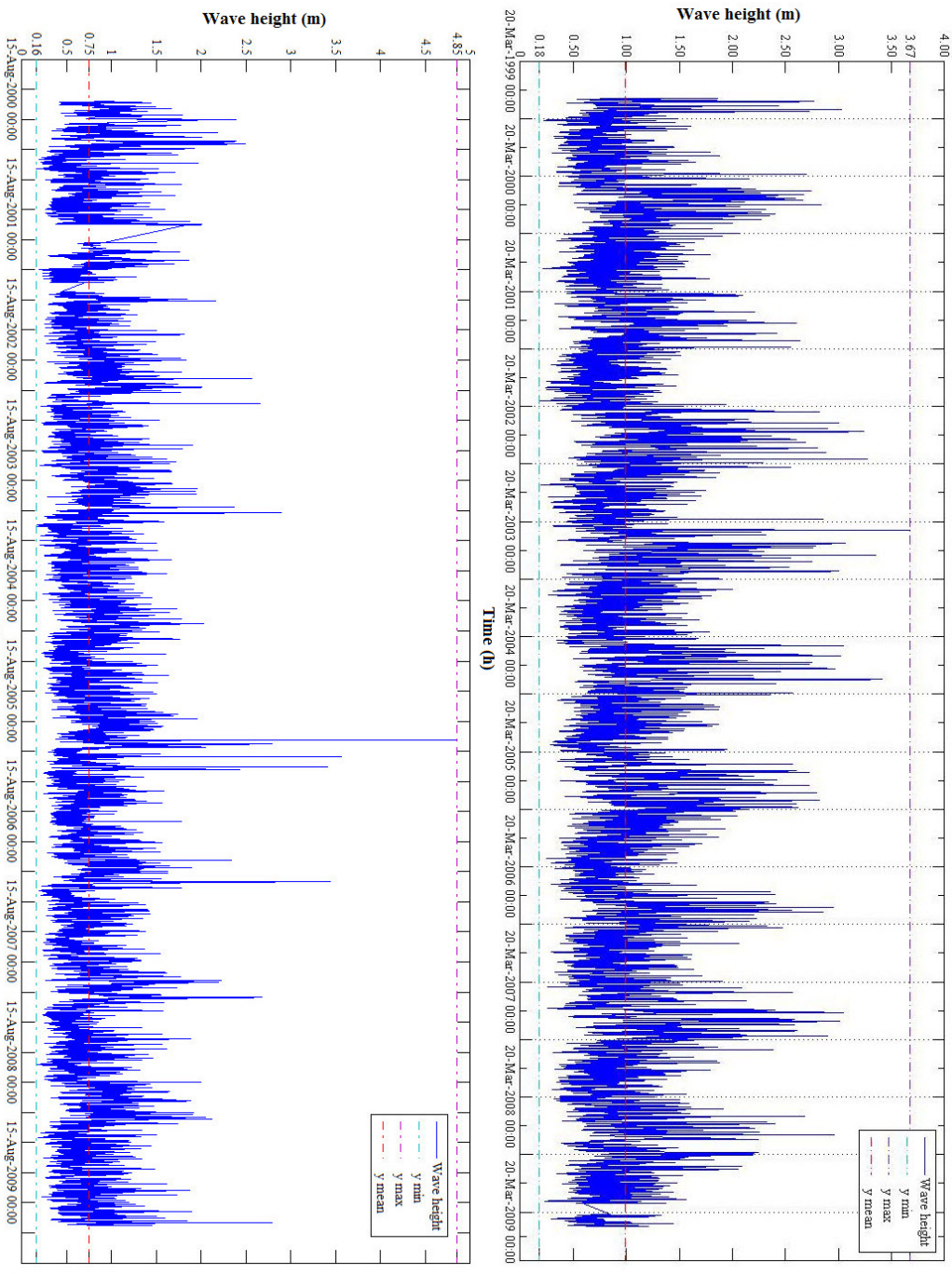

Figure 3.5 Wave height records from Sept 1999 to Apr 2009 at Cottesloe (above) and at Port Hedland (below)

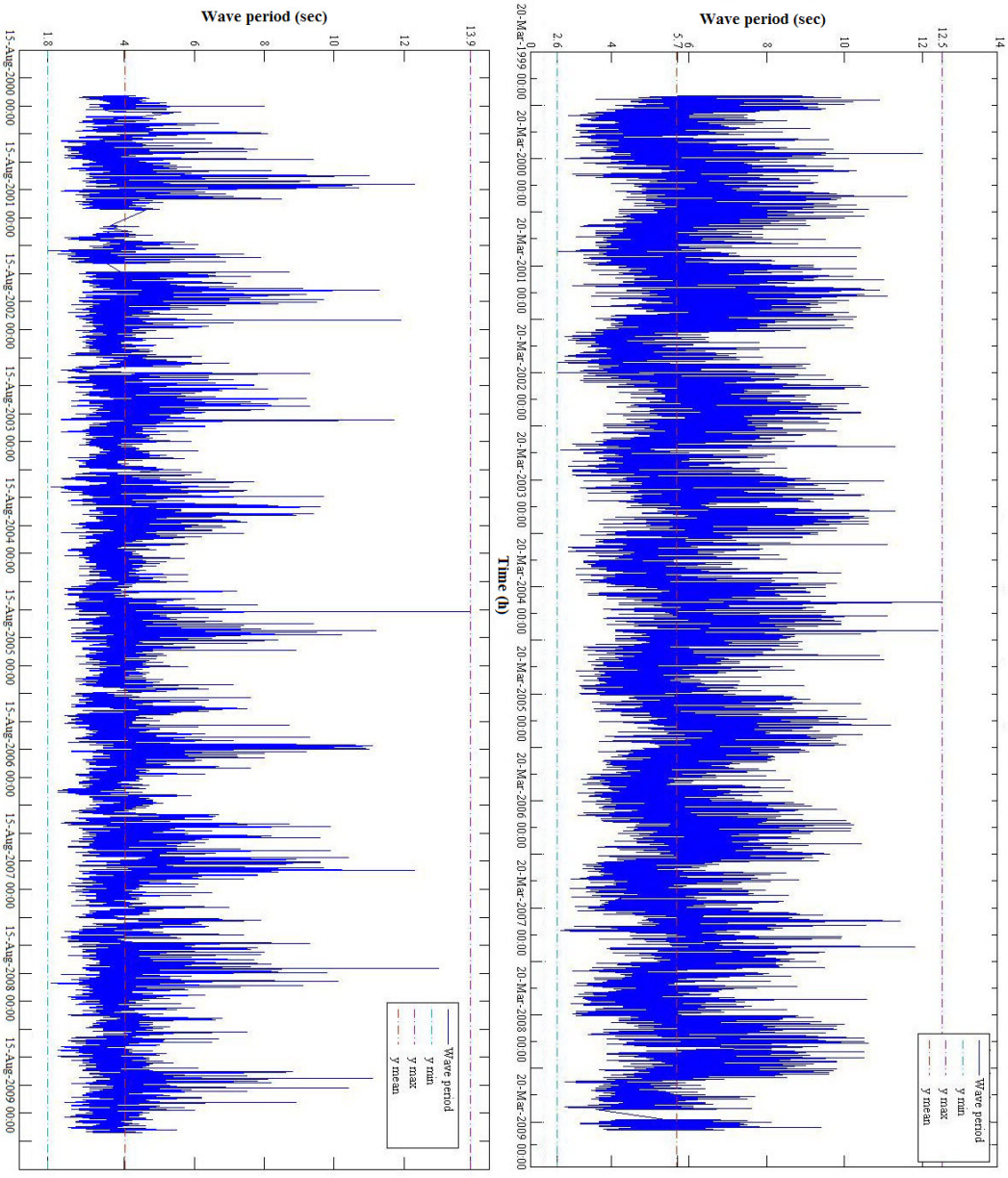

Figure 3.6 Wave Period records from Sept 1999 to Apr 2009 at Cottesloe (above) and at Port Hedland (below)

3.5 Software

3.5.1 GIS, Remote Sensing and Data Processing Software

The integrated image analysis solution development environment eCognition Developer 8.0.2 (Trimble Germany GmbH 2010) was used as the test-bed environment to develop the object-oriented approach for image analysis on shoreline identification.

The geodata stored in a shapefile format are developed by the Environmental Systems Research Institute (ESRI). The shapefile data are important input and output information that indicates the spatial relationship between different spatial features. For example, the classification results of the coastal features and all of the HWM indicators are in the format of shapefile, when they are required to be represented on digital maps. The LiDAR points and the RTK based GNSS survey data are also represented as shapefile to show their spatial positions (ESRI Inc. 2010).

Most of the data processing and spatial features representation were implemented in ArcGIS 10.1 (ESRI Inc. 2010). Tools to automate the analysis processes have been developed using Python scripts. These tools were developed specifically for this research and to automate the steps for accessing the spatial and temporal variation (precision and stability) of HWM indicators.

3.5.2 Statistical Software

The Matlab (MathWorks 2010) and R (R Development Core Team 2012) for numerical computing and graphics was applied throughout the research to interpolate the wave information (Chapter 4), and identify and adjust the inconsistent survey feedback in modelling MCDM (Chapter 7).

The analysis of tide data was conducted using software developed by the Department of Transport (DoT), WA (Department of Transport 2010a). ‘TIDINT’ (TIDe INTerpolation), ‘TIDPTU’ (TIDe Packed To Unpacked), and its reverse ‘TIDUTP’ were used for pre-processing the tide records. The software ‘TANS’ and ‘TIDSTAT’ (TIDe STATistic) were used to calculate the tidal constituents and high water statistical occurrences, respectively. Other software used in this research includes the

@RISK for Excel (Palisade Corporation 2009), which simulated the cumulative distribution of swash and tidal heights, respectively, when determining the SCSP and SCTP.

3.6 Summary

This chapter describes the methodology to address the difficulties and problems in two sequential stages—HWM determination and HWM evaluation. The key steps to determine the positions of the HWM based on spatial continuity of swash probability (SCSP) or spatial continuity of tidal probability (SCTP) are described. This model integrates the information both seaward and landward of the HWM.. A Multi-Criteria Decision Making (MCDM) model is developed with consideration to precision, stability and inundation risk. This model assists in the selection and evaluation of the most accurate positions of the HWM for two different purposes. The distinctive features between the two study areas are correspondingly compared in terms of beach type, tidal and wave characteristics.

In addition, the data and their formats required for implementing the methodology are identified. It was found that recording gaps in wave information significantly limits the ability to derive the HWM indicators. A solution to this problem is explored in the next chapter using interpolation methods.

CHAPTER 4 WAVE INFORMATION INTERPOLATION WITH WAVELET REFINED CUBIC SPLINE AND FRACTAL METHODS

4.1 Introduction

Wave information is important for the calculation of wave runup as an input to calculate the swash probability for each HWM indicator, which is critical to the determination of the HWM. However, gaps often exist in wave recordings, and this impacts on the accuracy of HWM determination. Wave information interpolation is used to interpolate across gaps in the recorded wave information to provide input to the calculation of wave runup.

This chapter presents two methods for wave information interpolation, namely, wavelet refined cubic spline and fractal methods. These methods are then compared with the original cubic spline method used for wave information interpolation. The methods are implemented and compared at South Fremantle and Port Hedland study areas, which have distinct wave types and coastal features.

Furthermore, this chapter presents conclusions about the effects of recording gap sizes on the interpolation process.

4.2 Outline of Wavelet and Fractal Methods

The basis of the wavelet method is a ‘small wave’ that essentially decays and grows in size over a limited time (Percival and Walden 2006). Some mathematical methods, such as Fourier analysis, can decompose general time series data into simpler pieces of information in the frequency domain. These methods work on the assumption that the underlying process, such as wave information time series, is stationary (Gu and Bollen 2000). The wavelet transform provides the localised information in both time and frequency domain for the process.

Broadly speaking, there are two main classes of wavelets: the Continuous Wavelet Transform (CWT) and the Discrete Wavelet Transform (DWT). The CWT is usually applied when working with time series data over the entire real axis and is ideal for feature extraction (Subasi 2007). In contrast, the DWT is designed to deal with time series over integer space. DWT has been applied successfully in the study of noise reduction (Borsdorf *et al.* 2008). DWT enables the separation of high and low

frequency signals in a time series and is used in this research to separate the high and low frequency of wave information in a time series record. The DWT method is discussed in Section 4.4.

The fractal method has been applied to analyse the correlation of time series data for various studies ranging from physiology (Stubsjøen *et al.* 2010) and economy (Muzy *et al.* 2000), to hydrology (Jayawardena and Lai 1994). For the wave research, Reikard (2009) forecasted the wave energy by determining the wave parameter's fractal dimension. However, the concept of fractal was not directly involved in the interpolation. In this research, fractal methods are applied to interpolate wave information where data gaps occur, and in particular larger gaps where data are missing.

Both wave height and wave period are important wave information, and are required by the wave runup (swash) height modelling. Therefore, the interpolation of wave height and period is essential to examine the effect of wave runup in the determination of the HWM. Since the periods of record gaps are the same and time series patterns of the records are similar for wave height and wave period (see Chapter 3.4.5), the principle of interpolating record gaps of the wave period is essentially the same as the wave height. Therefore, the implementation process was only illustrated on the wave height interpolation. In this study, the wave height refers to the significant wave height.

4.3 Stationarity Test and the Feature of the Wave Height Records

4.3.1 Stationarity Test

The time series of the wave height records require a stationarity test before performing any interpolation. Stationarity of the time series is the basic requirement for most interpolation methods. To conduct this test the Least Squares Quadratic (LSQ) fit between the wave heights ($Wh(t)$) and the null model were identified from the regression. This is called the partial sum process of the residuals (Kwiatkowski *et al.* 1992):

$$S(t) = \sum_{i=1}^{t} e_i , \quad t = 1, 2, \ldots, T \tag{4.1}$$

in which e_t is defined as the residuals from the regression, and T is the number of observed records. The test of the null hypothesis of the level stationary is defined as (Kwiatkowski *et al.* 1992):

$$\hat{\eta}_{\mu} = \sum_{t=1}^{T} \left(S(t)\right)^2 \Big/ \left(S_{nw}^2 T^2\right) \tag{4.2}$$

where S_{nw}^2 is the 'long-run variance' Newey-West estimator (Newey and West 1987) and is used to overcome autocorrelation that could be easily identified in the time series (Müller 2007). The statistical significance of the stationary test of the wave heights is indicated by the *p*-value and the critical values with the $\hat{\eta}_{\mu}$.

4.3.2 Feature of the Wave Height Records

The time series of the hourly recorded significant wave height are calculated to be non-stationary at the 0.01 significance for both of the study areas (Table 4.1); therefore, the commonly used interpolation, such as cubic spline interpolation, cannot be successfully applied on the wave height time series, and improved methods are required.

Table 4.1 The test of null-hypothesis of stationary trend

	$\hat{\eta}_{\mu}$	**Critical value**	**Decision**
Cottesloe	19.34	0.146	Rejected
Port Hedland	4.86	0.146	Rejected

4.4 Wavelet Adjusting on Cubic Spline Interpolation

4.4.1 Discrete Wavelet Transform (DWT)

The DWT of the time series of wave height records is defined as the transformation of the wave heights $f_D(t)$ multiplied by the wavelet (Thyagarajan 2011):

$$Wf_D(m,n) = \lambda_0^{-m/2} \int f_D(t)\Psi(\lambda_0^{-m} t - nt_0)dt \tag{4.3}$$

where λ_0 is the fixed dilation step greater than 1, m is an incremental step, λ_0^m is a magnification, t_0 is the initial position of the wavelet, and is moved to another location by n. A family of discrete wavelets are defined as:

$$\Psi_{m,n}(t) = \frac{1}{\sqrt{\lambda_0^m}} \Psi\left(\frac{t - nt_0\lambda_0^m}{\lambda_0^m} \right). \tag{4.4}$$

4.4.2 Multi Components Analysis on Wave Heights

In this research, results have shown that the components of the data pattern are in some cases more revealing than the data pattern itself. For example, the time series of wave heights act like a series of signals composed of a number of sub-level signals with different frequencies, which means that both long-term trend and localised variation exist in the time series of wave heights.

However, in a large number of studies using Fourier analysis on time series signals, researchers have failed to separate the different frequencies in the series (Kumar and Foutoula-Georgiou 1997), and thereby making the interpolation of wave heights impossible. However, a wavelet has the property of time-frequency location, which is indicated by the time location *n* and scale m. This means that the components, with different frequencies, can be identified and separated by the wavelet analysis.

In this research, the linear combination of the wavelet $\Psi_{m,n}(t)$ was applied to approximate any square-integrable function $f_D(t)$, and is expressed as:

$$f_D(t) = \sum_{m=-\infty}^{\infty} \sum_{n=-\infty}^{\infty} D_{m,n} \Psi_{m,n}(t) \tag{4.5}$$

where, the $D_{m,n}$ is the coefficient and measures the contribution of scale λ_0^m at the location $nt_0\lambda_0^m$ to the function $f_D(t)$, and can be obtained as $D_{m,n} = \int f_D(t)\Psi_{m,n}(t)dt$.

One important application of the wavelet method applied in this research is the analysis of the patterns of signals at the different frequencies. This was an important

step as the wave height records captured over time are mixed with high frequencies (big waves followed by calm water or *vice versa* and low frequencies (constant big wave or constant calm water). This irregular change is a major reason why the wave height is 'impossible' to interpolate.

This problem has been resolved by decomposing the irregular changes by introducing the wavelet multi-frequencies method:

$$f_m(t) = f_{Am}(t) + f_{Dm}(t) \tag{4.6}$$

where $f_m(t)$ is a function that represents how the wave height changes in time, and $f_{Am}(t)$ and $f_{Dm}(t)$ are functions representing the approximate trend and the detail change of the wave heights in time.

The $f_{Am}(t)$ can be further decomposed into a more detailed function as $f_{Dm-1}(t)$ and approximated as $f_{Am-1}(t)$ with a smaller scale filter, and thus higher resolution, so that broader trends appear. In such multi-resolution framework, the $f_{Am}(t)$ is formulated as:

$$f_{Am}(t) = \sum_{n=-\infty}^{\infty} C_{m,n}\phi_{m,n}(t) \tag{4.7}$$

in which $\phi_{m,n}(t)$ is the smooth function (or scale function) and is defined as $\phi_{m,n}(t) = \frac{1}{\sqrt{\lambda_0^m}}\phi\left(\frac{t - nt_0\lambda_0^m}{\lambda_0^m}\right)$; whereas $C_{m,n} = \int \phi_{m,n}(t) f(t) dt$ are the coefficients of $f(t)$ at the time location *n* and scale m. $\phi(t)$ is used for scaling, like a sampling function, and related to the $\Psi(t)$, which is defined as:

$$f_{Dm}(t) = \sum_{n=-\infty}^{\infty} D_{m,n}\Psi_{m,n}(t)\,. \tag{4.8}$$

In order to improve the interpolation, the time series was separated into high and low frequency data using the wavelet method. In this research, the wave height records time series were decomposed into three levels in the form of Equation 4.6. This process is illustrated in Figure 4.1.

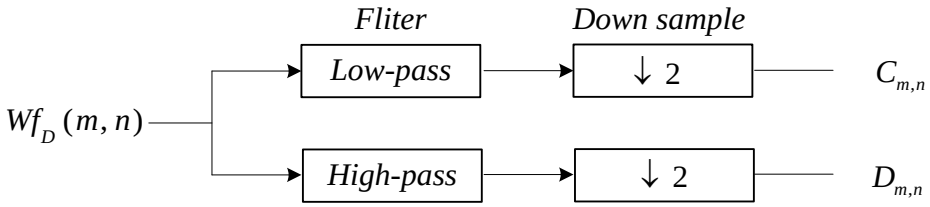

Figure 4.1 High and low frequency wave height interpolation using the wavelet method

The cubic spline interpolation can be used to draw the smooth curve through the points and is expressed as a combination of a series of third degree polynomials. In this research, a pair of wave height records is defined as $(Wh(i), Wh(i+1))$, and the third degree polynomial between them is $f_i(t) \quad i = 1, 2, \cdots, l-1, t \in [i, i+1)$. Firstly, the approximate (low frequencies) and detail (high frequencies) function at the scale m are fitted into a piecewise function separately:

$$f_{Am}(t) = \sum_{i=1}^{l-1} f_{Ami}(t) \qquad t \in [i, i+1) \tag{4.9}$$

and

$$f_{Dm}(t) = \sum_{i=1}^{l-1} f_{Dmi}(t) \qquad t \in [i, i+1) \tag{4.10}$$

where $f_{Am}(t)$ and $f_{Dm}(t)$ are defined as a third degree polynomials:

$$f_{Ami}(t) = a_{Ai}(t - x_{Ai})^3 + b_{Ai}(t - x_{Ai})^2 + c_{Ai}(t - x_{Ai}) + d_{Ai} \tag{4.11}$$

and

$$f_{Dmi}(t) = a_{Di}(t - x_{Di})^3 + b_{Di}(t - x_{Di})^2 + c_{Di}(t - x_{Di}) + d_{Di} \quad i = 1, 2, \ldots, n-1. \tag{4.12}$$

Therefore, the next step of this interpolation is to calculate the coefficients. These have been determined by McKinley and Levine (1998) and are as follows:

$$a_i = \frac{M_{i+1} - M_i}{6h} \tag{4.13}$$

$$b_i = \frac{M_i}{2} \tag{4.14}$$

$$c_i = \frac{Wh(i+1) - Wh(i)}{h} - (\frac{M_{i+1} + 2M_i}{6})h \tag{4.15}$$

$$d_i = Wh(i) \tag{4.16}$$

in which, M_i denotes the second derivative of $f_{mi}(i)$ as $f''_{mi}(i)$. The cubic spline interpolation was applied on high frequencies and low frequencies of the wave height time series separately at different scales *m*, and then $f_m(t)$ was reconstructed according to the Equation 4.6. In this research, the interpolation started from level three (*m*=3). When m equals one, the $f(t)$ is the final cubic spline function refined by the wavelet method to interpolate the wave heights in recording gaps.

4.4.3 Wavelet Selection

There are a number of wavelets available. The most commonly used are the Haar, Symlets, Coiflets, Biorthogonal and Meyer (Zhou and Paul 2005). All of these methods satisfy the features of the wavelet, but are different from each other in terms of the attributes of the wavelet and scale functions.

The selection of the wavelet in this research has been determined using a sampling test. Of the wave height records, 20% have been used as the test sample, and the wave heights have been interpolated using most of the common wavelets. The RMSE of the cubic spline interpolation method was calculated for different wavelets: the smaller the RMSE, the higher the accuracy of the cubic spline method for a given wavelet.

4.5 Fractal Interpolation on 'Large' Record Gaps

The results of this research proved that the wavelet refined spline method alone would not fill the larger wave record gaps accurately. As a consequence, it was determined that other interpolation methods were needed.

As wave height records over time have a pattern of self-similarity, the fractal method uses this to interpolate wave heights in the record gaps. One of the most important

concepts in the fractal method is the Iterated Function System (IFS), which is a type of transformation. The points (t, $Wh(t)$) were used to construct the IFS $\{\Re^2; w_j, j = 1, 2, \cdots, N\}$, N stands for the number of randomly selected records. The results of a general IFS interpolation are quite variable, rather than smooth and continuous (Moore 1999). The general IFS is one type of an affine transformation, and defined as:

$$w_j \begin{pmatrix} t \\ Wh(t) \end{pmatrix} = \begin{pmatrix} a_j & 0 \\ c_j & d_j \end{pmatrix} \begin{pmatrix} t \\ Wh(t) \end{pmatrix} + \begin{pmatrix} e_j \\ f_j \end{pmatrix} \tag{4.17}$$

with the following constraints:

$$w_j \begin{pmatrix} 1 \\ Wh(1) \end{pmatrix} = \begin{pmatrix} j-1 \\ Wh(j-1) \end{pmatrix} \tag{4.18}$$

and

$$w_j \begin{pmatrix} N \\ Wh(N) \end{pmatrix} = \begin{pmatrix} j \\ Wh(j) \end{pmatrix} \tag{4.19}$$

As such, the transformation should obey the four linear equations with five coefficients a_j, c_j, d_j, e_j, and f_j:

$$a_j + e_j = j - 1 \tag{4.20}$$

$$a_j N + e_j = j \tag{4.21}$$

$$c_j + d_j Wh(1) + f_j = Wh(j-1) \tag{4.22}$$

$$c_j N + d_j Wh(N) + f_j = Wh(N) \tag{4.23}$$

where d_j stands for the vertical compression ratio and is randomly selected. The interpreted heights $(Wh'(t'), t')$ can be determined by:

$$\begin{bmatrix} t' \\ Wh(t') \end{bmatrix} = w_j \begin{bmatrix} t \\ Wh(t) \end{bmatrix} = \begin{bmatrix} a_j & b_j \\ c_j & d_j \end{bmatrix} \begin{bmatrix} t \\ Wh(t) \end{bmatrix} + \begin{bmatrix} e_j \\ f_j \end{bmatrix} \tag{4.24}$$

4.6 Interpolation and Test on the Missing Data

The cubic spline method was used to interpolate the record gaps in the whole dataset (Figures 4.2 and 4.3). However, the RMSEs in the two study areas are over 2 m (Table 4.3); therefore, the cubic spline method does not satisfy the requirement of wave height interpolation in terms of high accuracy, and a more refined approach is needed.

The wavelet method was applied to refine the cubic spline method. It separates high frequency and low frequency data in the wave height time series. As shown in Table 4.2, the db3 and db8 were selected as the most suitable wavelets at Cottesloe and Port Hedland respectively, showing the least RMSE (Table 4.2, Figures 4.4 and 4.6). After applying the wavelet method, the results of the cubic interpolation have been significantly improved at Cottesloe (Table 4.3 and Figure 4.5), but not that significantly at Port Hedland (Table 4.3 and Figure 4.7).

However, as shown in Figures 4.5 and 4.7, the interpolation for large intervals of the wave height record gap are not accurate. Hence, the fractal method was introduced to interpolate these larger gaps. The results show that the fractal method is satisfying the statistic test (Table 4.3) and there is no extreme and apparent error in the shape of the wave height record time series in general (Figures 4.8 and 4.9). In comparison to the original cubic spline, the wavelet refined cubic spline and fractal interpolations have significantly improved the results for the whole dataset on average (Table 4.3).

Table 4.2 Wavelet selection for wave height interpolation based on the RMSE test (m)

	db3	db5	db8	sym4	sym5	sym6	sym8	rbio3.3
Cottesloe	0.60	2.71	1.73	1.13	1.39	1.27	1.37	1.26
Port Hedland	3.57	2.71	2.38	4.28	3.64	3.97	3.75	3.93

Table 4.3 RMSE on the different types of wave height interpolation (m)

	Cubic spline	Wavelet refined	Fractal interpolation
Cottesloe	2.77	0.60	0.578
Port Hedland	2.47	2.38	0.456

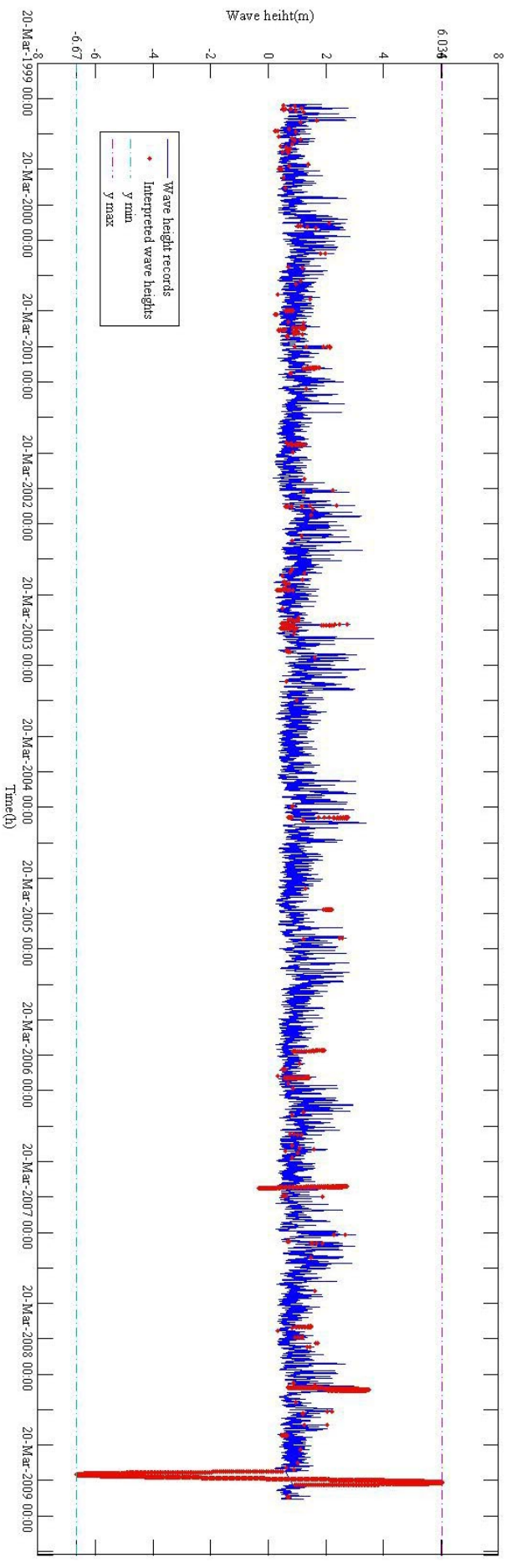

Figure 4.2 Wave height interpreted by cubic spline method at Cottesloe

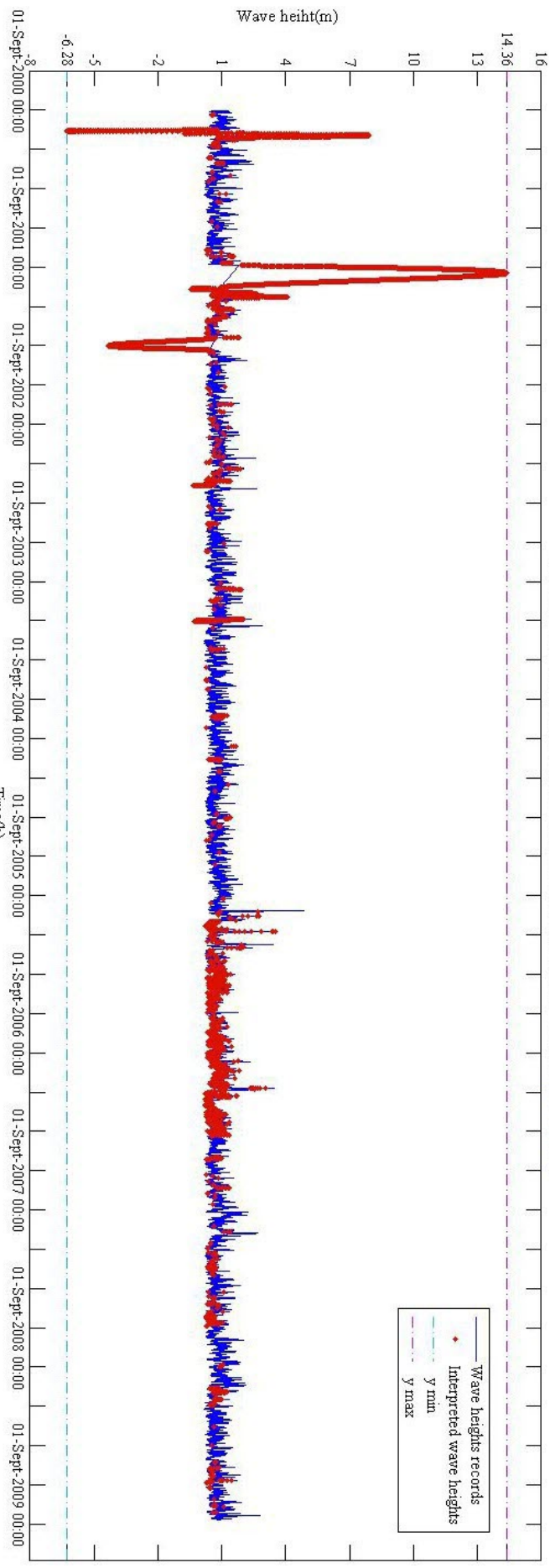

Figure 4.3 Wave height interpreted by cubic spline method at Port Hedland

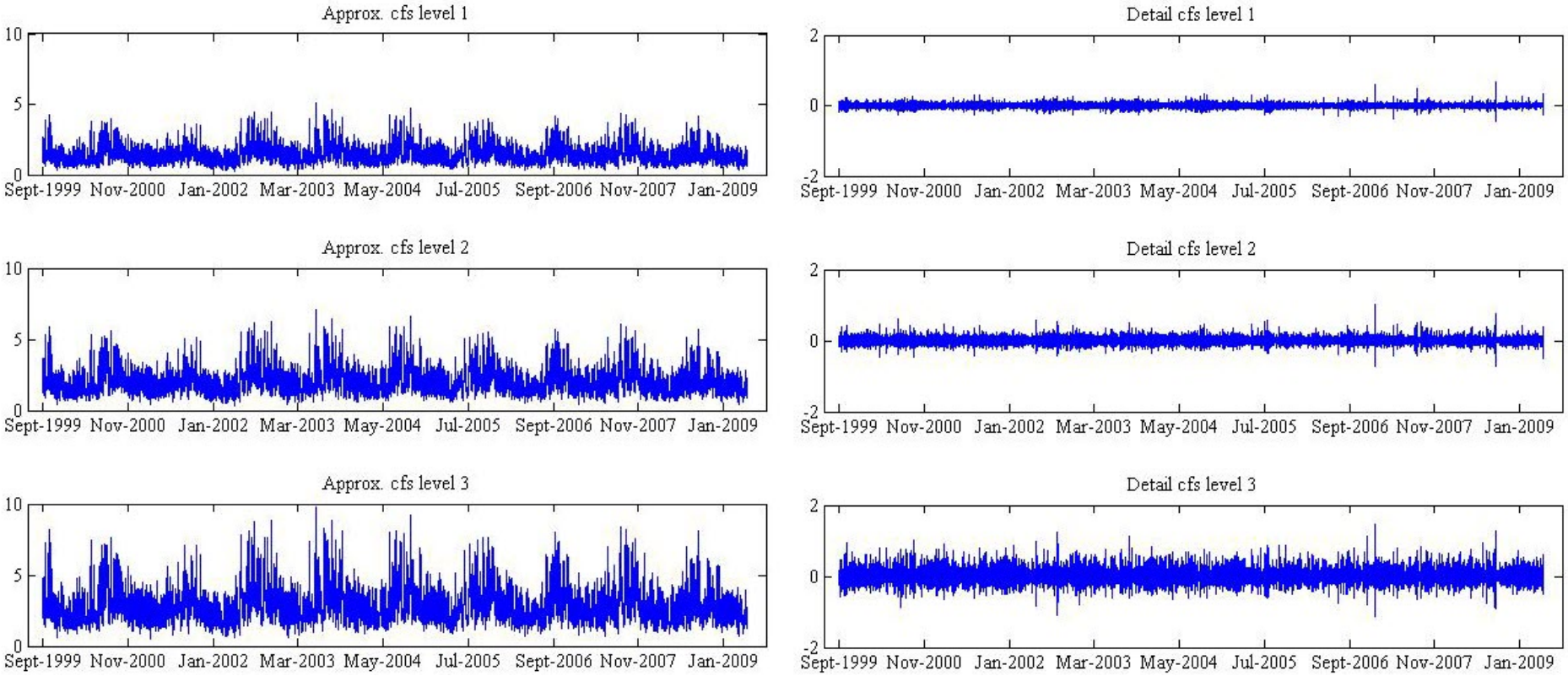

Figure 4.4 Three levels of the wavelet db3 decomposed approximate and detail coefficient on Cottesloe's wave height records

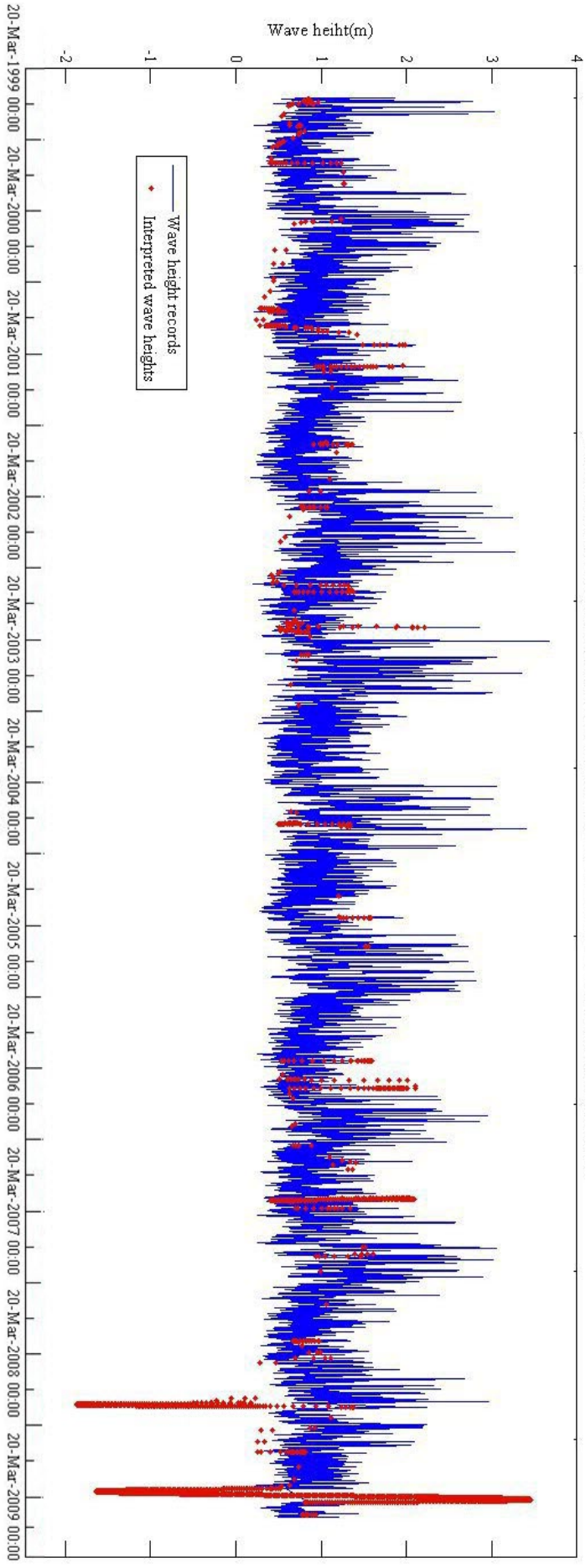

Figure 4.5 Wave heights interpolated by the wavelet refined cubic spline method at Cottesloe

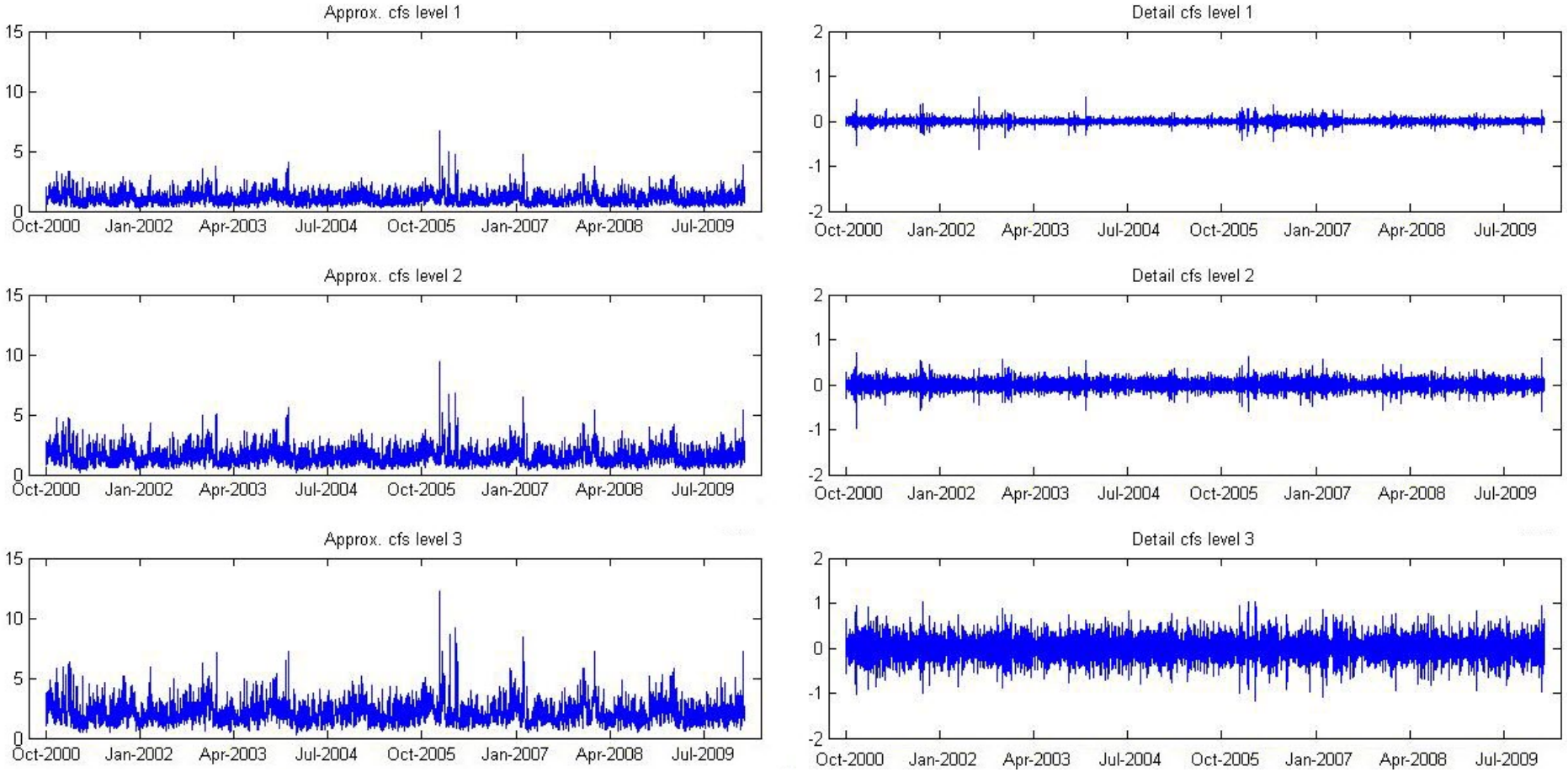

Figure 4.6 Three levels of the wavelet db8 decomposed approximate and detail coefficient on Port Hedland's wave height records

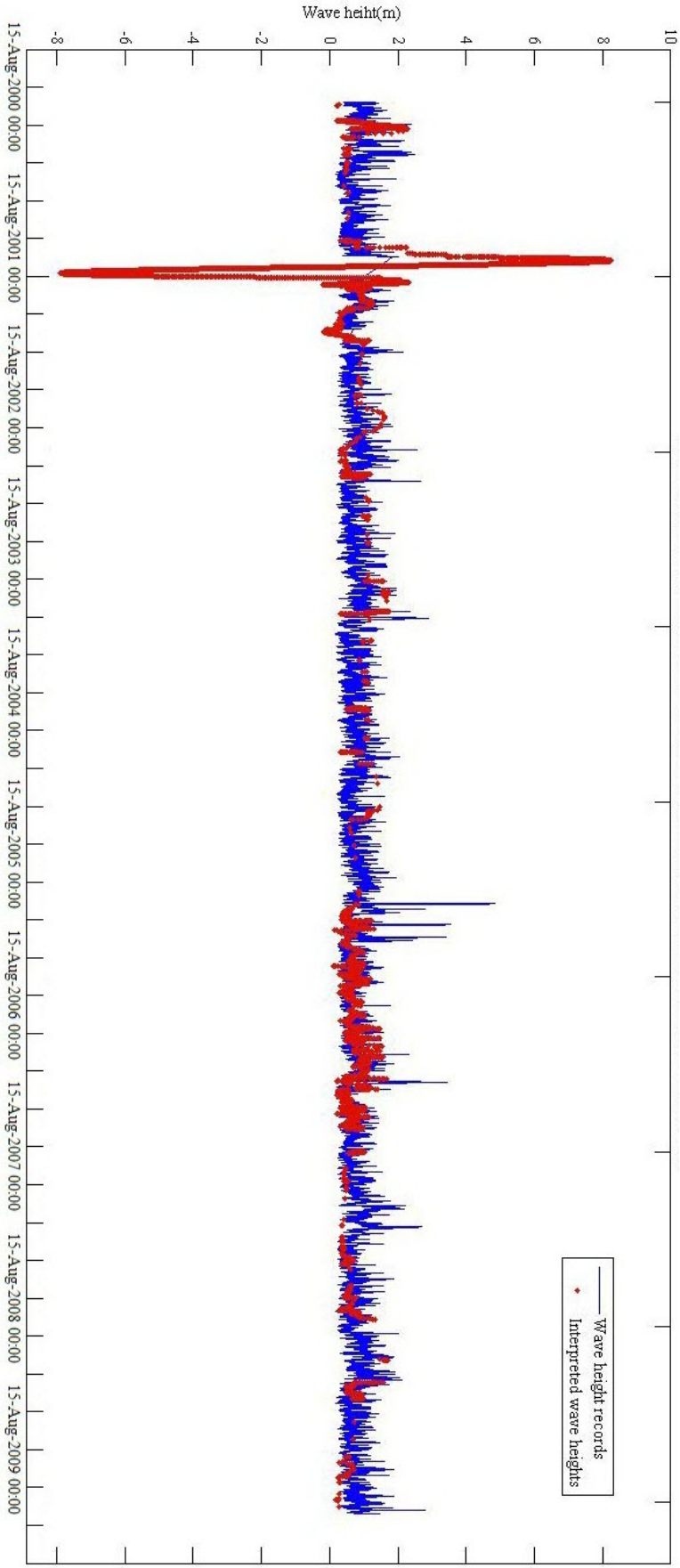

Figure 4.7 Wave heights interpolated by the wavelet refined cubic spline method at Port Hedland

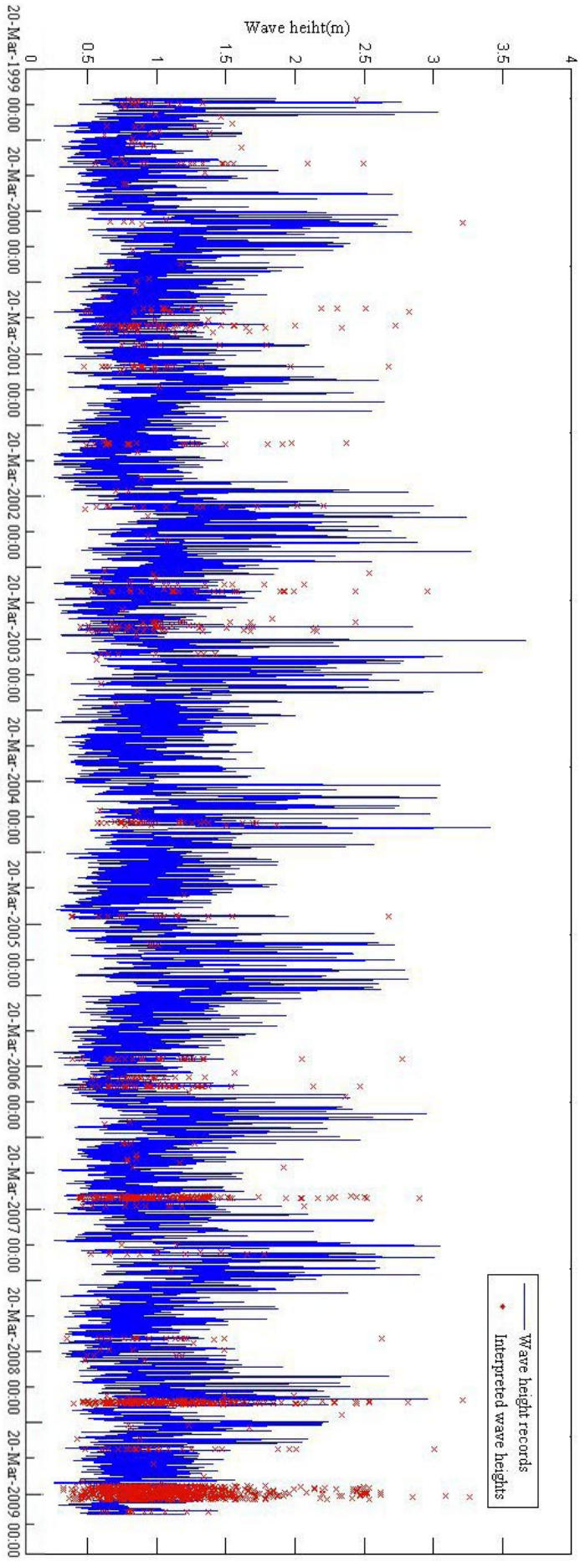

Figure 4.8 The final wave heights interpolation with large gap records interpolated by fractal method at Cottesloe

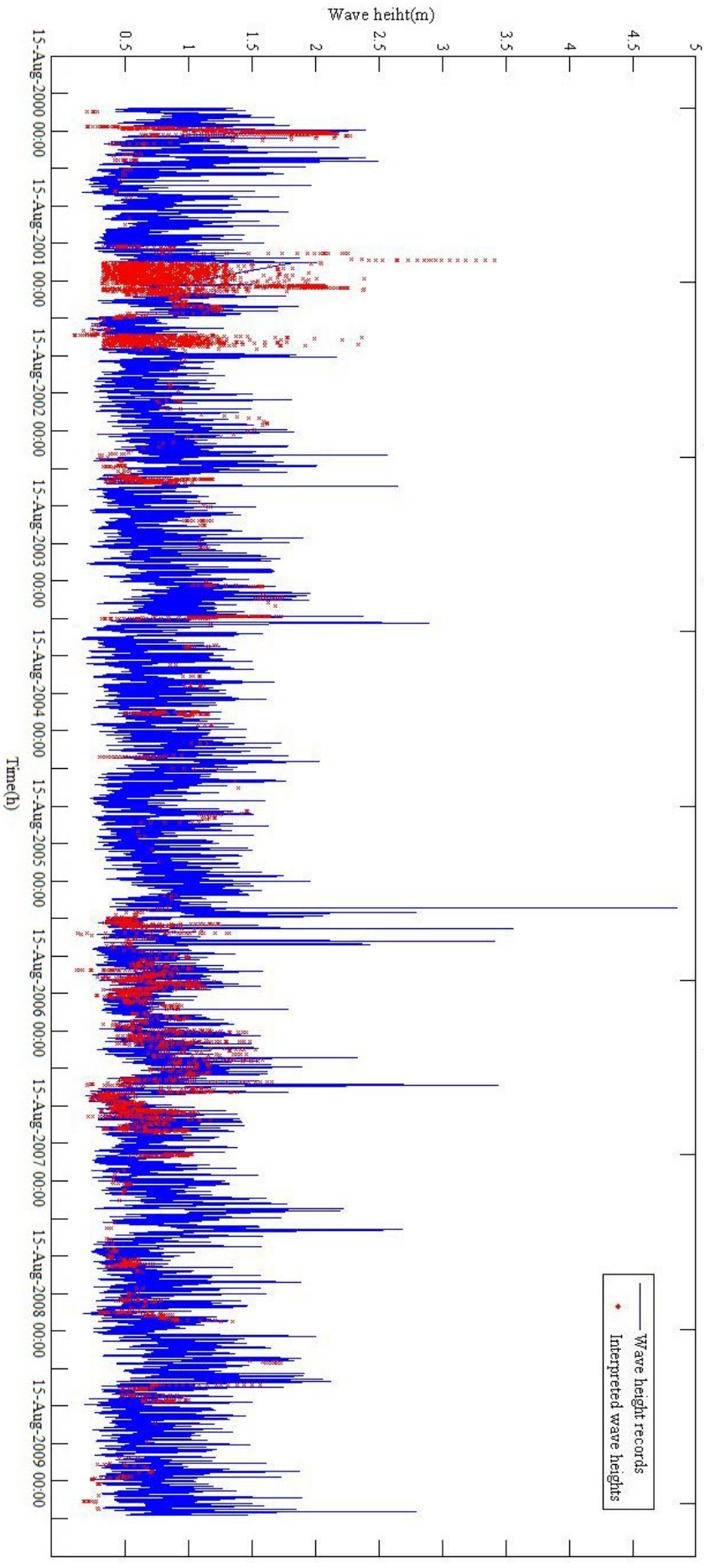

Figure 4.9 The final wave heights interpolation with big gap records interpolated by fractal method at Port Hedland

The time series of wave period records are also identified as non-stationary ($\hat{\eta}_{\mu}$ = 8.86 and 12.23 at Cottesloe and Port Hedland respectively with critical values of 0.146), and therefore the same methods and processes are conducted on the record gaps interpolation. In contrast, rbio3.3, showing the least RMSE, is the ideal wavelet for wave period interpolation at both Cottesloe and Port Hedland (Table 4.4). Similarly, the interpolation results have been substantially improved using the wavelet refined cubic spline and fractal methods (Table 4.5).

Table 4.4 Wavelet selection for wave period interpolation based on the RMSE test (sec)

	db3	db5	db8	sym4	sym5	sym6	sym8	rbio3.3
Cottesloe	2.12	2.56	2.21	1.24	1.42	1.23	1.23	1.21
Port Hedland	1.40	1.76	1.62	1.12	1.18	1.07	1.04	0.89

Table 4.5 RMSE on the different types of wave period interpolation (sec)

	Cubic spline	Wavelet refined	Fractal interpolation
Cottesloe	4.13	1.21	1.86
Port Hedland	8.66	0.89	1.38

4.7 Evaluation and Discussions

In this research, the evaluation process has been illustrated on the wave height data. Table 4.3 depicts the average of the interpolation results, where the cubic spline has the largest interpolation error when applied to the wave height interpolation study. While the fractal method shows the best results in general for the whole data set interpolation, the wavelet refined spline method works better for the Cottesloe wave heights than the Port Hedland wave heights.

Two further questions remain unanswered: (1) Why do different interpolation methods have different levels of performance? and (2) How does the size of data gap interval influence the interpolation results? As a consequence, further analysis was conducted to answer these two questions.

The difference between cubic spline and fractal interpolation is that when the cubic spline is used in interpolating the missing data gap, only the values adjacent to each

side of the data gap were used as the known information for the interpolation. Therefore, the interpolation model is determined only by data in the near vicinity of the data gap. This explains why other similar interpolation methods, like linear and polynomial, also fail on wave height interpolation because they are even more restrictive in terms of the data used to inform the model parameters.

In contrast, the fractal method uses the affine transformation, which takes into account the entire trend of the time series (not just the points adjacent to the gap) and is considered as a simulation process. However, the fractal method may ignore the order effects during the interpolation process and importance of neighbourhood information close to the interpreted data gaps. Usually, the neighbourhood information should be given more weight to inform the interpolation model parameters.

The wavelet refined process separates the main trend and noise in the time series of the wave height records, which makes the cubic spline interpolation easier. By combining the separate interpolation results from high and low frequency, the final interpolation results are more accurate than the pure cubic spline interpolation.

Table 4.3 presents the average results of interpolating the record gaps in the whole dataset. However, the size of the wave record gap influences the interpolation results and this requires further analysis and discussion. Figures 4.10 through 4.13 show the interpolation for relatively large gaps that may happen one or two times in ten years (for example, 224 hours at Cottesloe and 142 hours at Port Hedland) and for medium record gaps (24 hours at Cottesloe and 27 hours at Port Hedland). The wavelet refined spline interpolation on medium gap intervals shows a better shape than the spline interpolation. The spline interpolation fails to fill in the relatively large data gaps for both of the study areas.

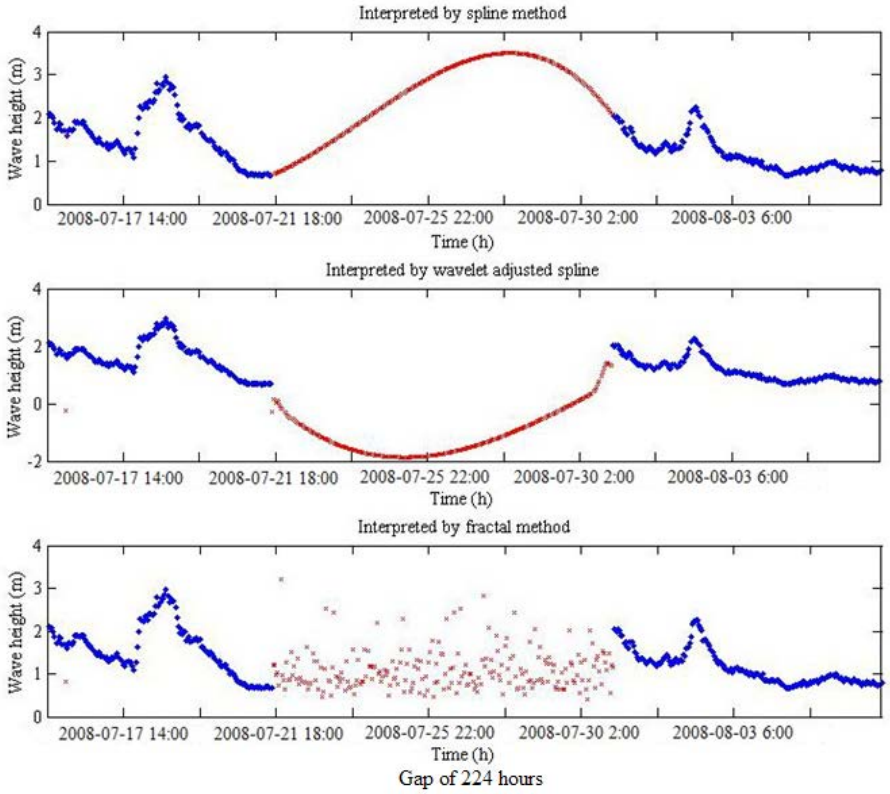

Figure 4.10 Relatively large gap interval interpolation at Cottesloe

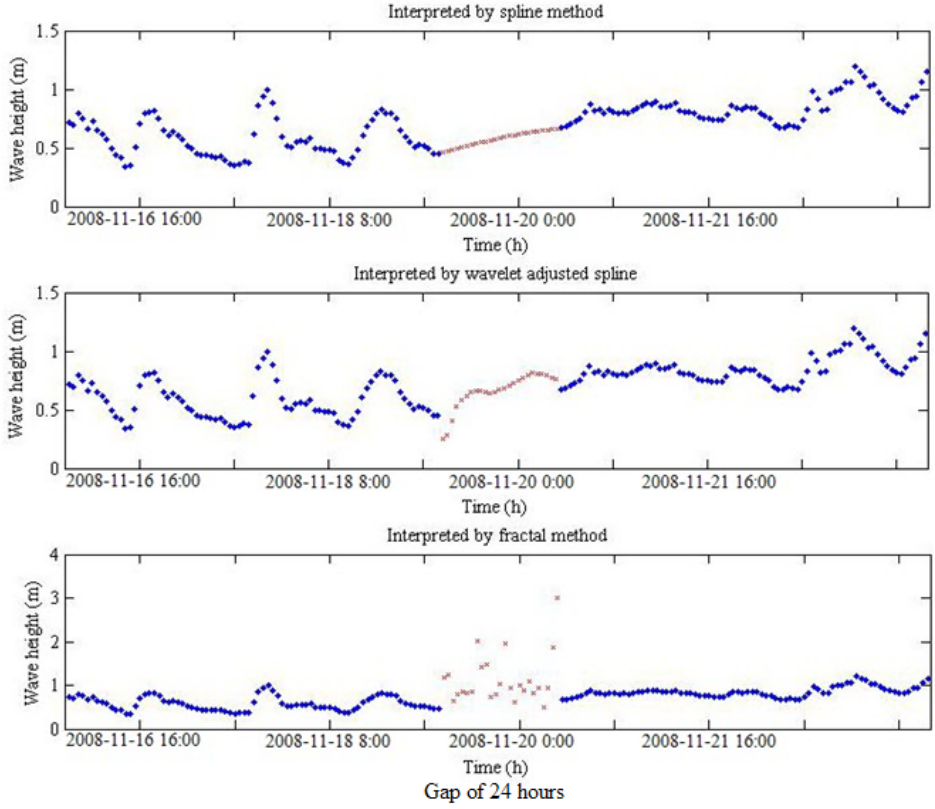

Figure 4.11 Medium gap interval interpolation at Cottesloe

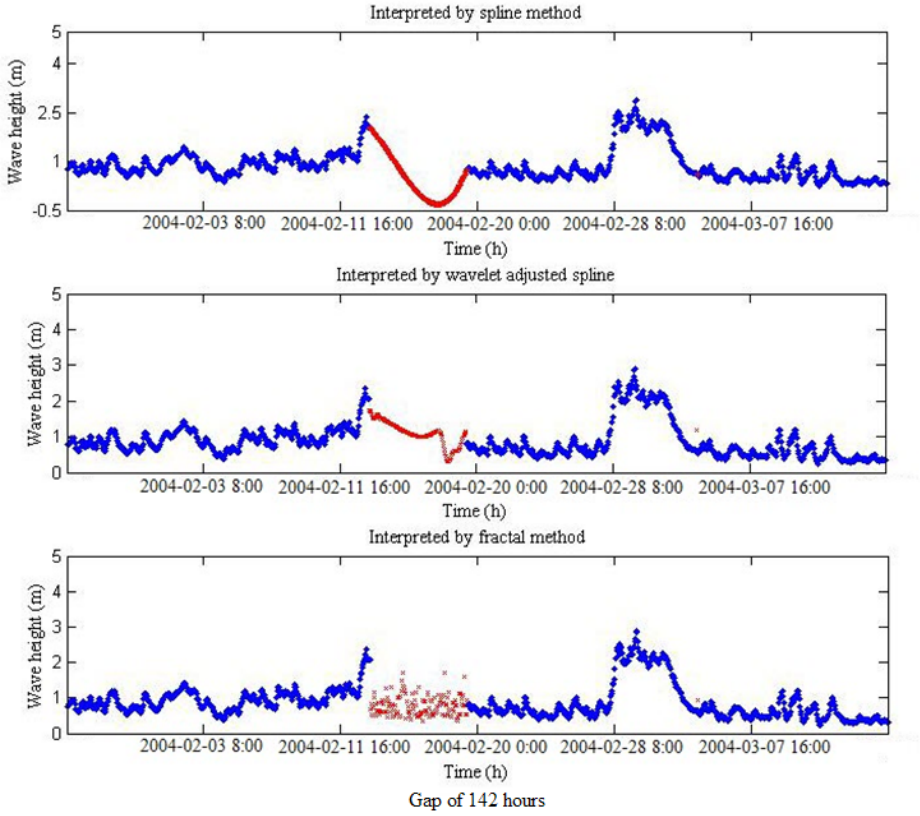

Figure 4.12 Relatively large gap interval interpolation at Port Hedland

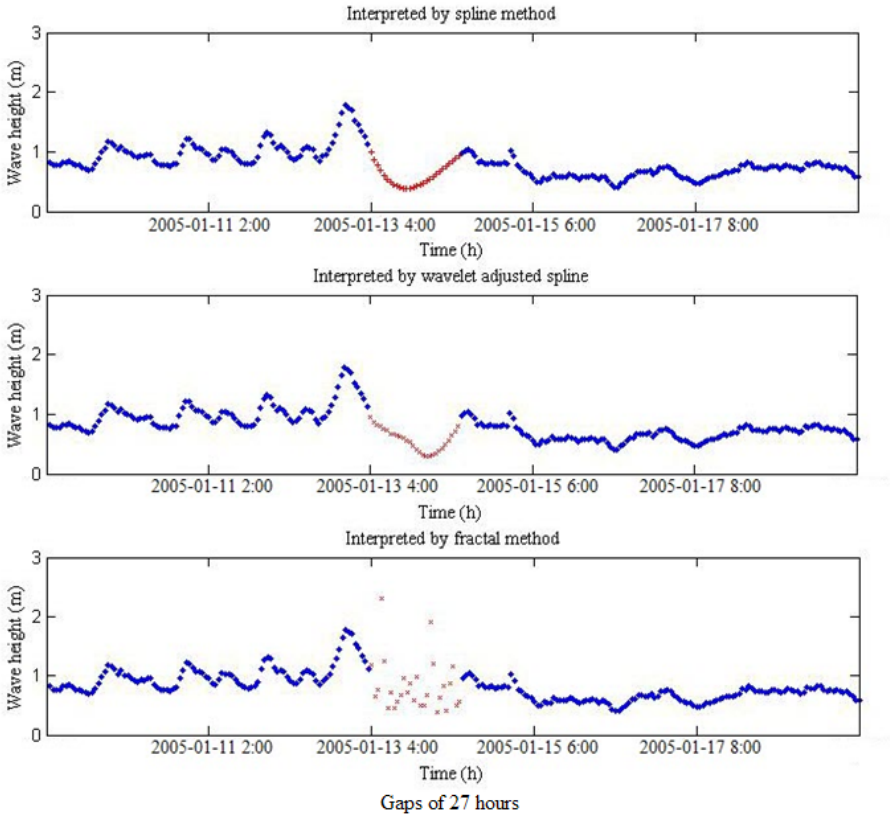

Figure 4.13 Medium gap interval interpolation at Port Hedland

Also, the interpolated results by the wavelet refined spline showed both general trend and detailed variation for relatively large gaps than the ones at Port Hedland, and this is not obvious for the interpolated results at Cottesloe. This might be relevant to the difference of the stationarity level of the two time series at the two study areas. From Table 4.1, the test statistic of wave height trends $\hat{\eta}_{\mu}$ shows that the level of non-stationarity is much higher for the dataset at Cottesloe than those at Port Hedland. That is, the higher energy waves at Cottesloe made the interpolation process more unpredictable.

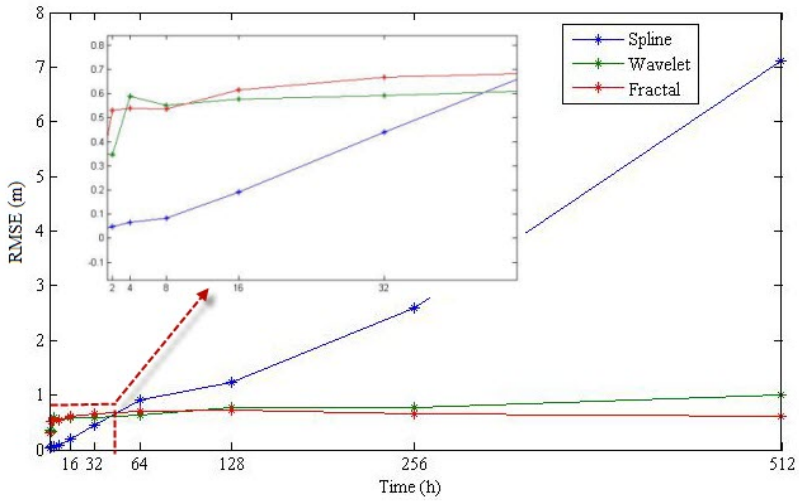

Figure 4.14 Relationship between gap interval and interpolation errors for the wave heights at Cottesloe

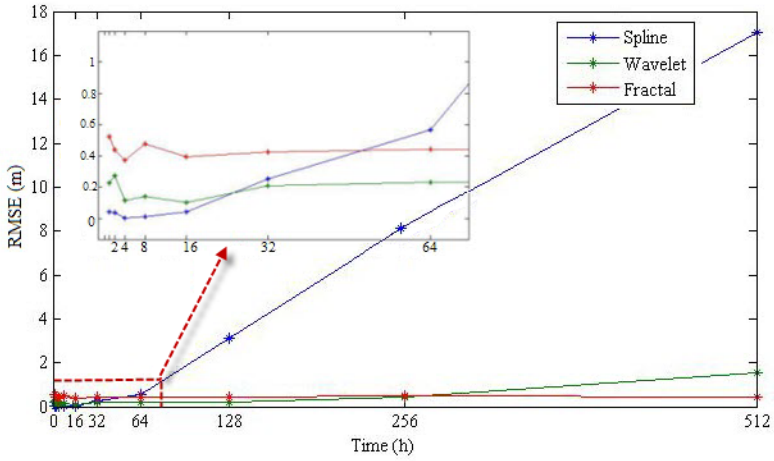

Figure 4.15 Relationship between gap interval and interpolation errors for the wave heights at Port Hedland

The fractal simulation does not represent the time series as a coherent shape, as does the recorded wave height time series. However, the dispersed distribution of the interpolated heights averages the interpolation error and reduces the interpolation risk to some extent (Figures 4.14 and 4.15).

Figures 4.14 and 4.15 compare the effect of wave record gap size on the RMSE for the three interpolation methods. To calculate the RMSE, artificial gaps were created. Then, the actual values were compared with the values interpolated by the three interpolation methods. The gap size ranges from 2^0 to 2^{10}. For each gap size, thirteen groups of test data were used and their RMSE was used as the interpolation level for that gap size. The estimated values are sparsely distributed along the true values and this reduces the accuracy and potential risk of interpolation at same time. However, the gap size does not have a great effect on the fractal interpolation, which can be estimated from the two levelled off red lines in the Figures 4.14 and 4.15.

Although the fractal interpolation is the most stable of the three methods, this method is not recommended when the gap is small (less than 20 hours). This is because the interpolation results from the cubic spline method are far more accurate at this time interval. The fractal method is more suitable for the data set at Cottesloe, where the wavelet refined spline did not improve results. This could also be attributed to the high non-stationarity of the wave heights at Cottesloe, which also caused the average of the wavelet refined spline and fractal interpolation results to be less accurate than those at Port Hedland for small gap intervals.

When the interpolation time interval is larger than 50 hours, the RMSE of the spline method significantly increased at both study areas. It shows the wavelet refined spline is more suitable for medium and relatively large data gap interpolation. However, as the gap size increases to a large interval, this interpolation method is less accurate than the fractal method due to stable interpolation outcomes of the fractal method, as this is irrelevant to the time gap size.

In the study by Deo and Kumar (2000), the cubic spline failed to produce satisfactory estimates in general. However, in this research the suitability of the mathematical function for the interpolation does show that it relates to gap size. Generally, the spline interpolation works well on small data gaps, whereas the wavelet refined

spline performs better than the other methods on the medium and relatively large data gap intervals. The fractal method is shown to be more appropriate for large data gap interpolation in extreme situations.

Finally, in the wavelet refined spline process, the decomposed level is fixed at 3 and it is not clear whether the decomposed level would have any influence on the results. This requires further analysis. Similarly, the fractal method uses a vertical compression ratio, and it is not fully understood if the random selection process of vertical compression ratio has any effect on the results.

4.8 Summary

The interpolation of data gaps in wave records has always been recognised as a challenging task and results are often inaccurate. This is due to the complexity and uncertainty of wave generation and the various gap sizes in wave records. The wavelet refined spline and fractal methods are implemented in this chapter, and they show an improvement on the interpolation accuracy, particularly for large or medium gaps.

After a systematic evaluation of these methods, the cubic spline method was identified to be more effective for interpolating wave data with small gaps. Therefore, different interpolation methods should be applied to fill in data gaps according to the duration of the gap. The next chapter discusses the determination of the HWM position based on the spatial continuity of swash or tidal probability (SCSP or SCTP) for a range of HWM indicators, where the calculation of swash height is based on the wave information interpolated in this chapter.

CHAPTER 5 HIGH WATER MARK DETERMINATION BASED ON THE PRINCIPLE OF SPATIAL CONTINUITY OF THE SWASH/TIDAL PROBABILITY

5.1 Introduction

The recording gaps within the wave information, which is one of the important components required for wave runup (swash) height modelling, were interpolated in the previous chapter. This chapter presents a model that determines the position of the HWM indicators based on analysis of tidal constituents, image analysis and the spatial continuity model. These indicators include tide datum based HWMs, such as MHHW and MHWS, and a number of shoreline features, such as HWL and the vegetation line. The methods developed are implemented at two case study areas, and a field survey was conducted to evaluate effectiveness of the methods.

5.2 The Outline of HWM Determination: Integrating both Landward and Seaward Information

The proposed HWM determination methodology is based on the spatial distribution of swash/tidal probability for HWM indicators and the spatial continuity distance of swash/tidal probability on the beach. It is assumed that the swash/tidal probability of the various HWM indicators has a level of spatial autocorrelation. The calculation of spatial continuity of swash/tidal probability (SCSP/SCTP) required the following steps:

- Identify the HWM indicator lines. The mean higher high water (MHHW) for the diurnal tide at South Fremantle, mean high water spring (MHWS) for the semi-diurnal tide at Port Hedland, and the DoT line (Section 2.4.5.2) can be derived from tide data. The height of the HWM suggested by Landgate was obtained from long-term observation of the shoreline features by experienced surveyors. Identification of another three indicators, HWL, dune toe position and vegetation line, required object-oriented image analysis (OOIA), which is described in the following sections.

- Calculate the probability that swash/tide will reach the HWM indicators over a 10 year period. In this research, the effect of swash was estimated to determine the position of the HWM for coastal hazard planning; while the

effect of tide was applied to determine the position of the HWM for coastal property management. Swash heights were determined using empirical models by taking into account wave and tide records. The swash/tidal heights were then fitted to an appropriate distribution and the probability that swash/tide would reach each HWM indicator was computed.

- Determine the spatial continuity distance of swash/tidal probability. The boundary between the ocean and land is constantly mobile due to swash/tidal motions on the beach face and it is suggested that this motion should be taken into account when defining the HWM. The swash/tidal limit can be considered as the position where the swash/tidal probability begins to discontinuously distribute landward. Such a position can be estimated by the semivariogram model.

The semivariogram model is essential to regionalised variable theory (Burrough 2001; Oliver and Webster 1990). The semivariogram range, for which the upper bound is the level of spatial autocorrelation approaching zero, was used as a benchmark to identify the minimum distance between the lower bound of the sampling position (the most seaward HWM indicator) and the upper bound of swash/tidal probability (i.e. the level at which there is no spatial autocorrelation of swash/tidal probability). Such an upper bound could be considered as the HWM level.

The principle of determining SCTP is as essentially the same as the SCSP, but without taking into account the effect of wave runup. Therefore, the determination model was only illustrated on the SCSP in this chapter (Figure 5.1).

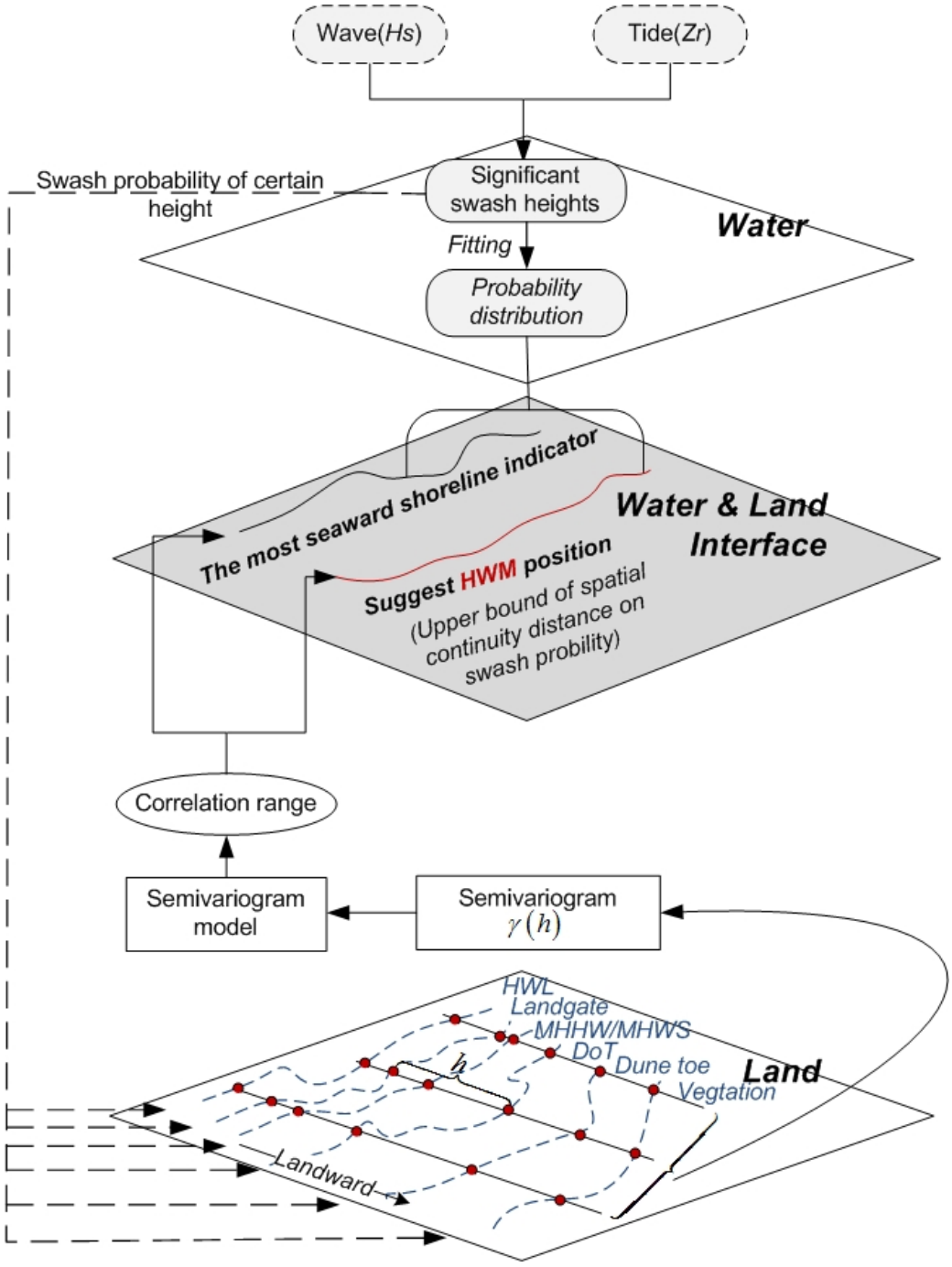

Figure 5.1 Method framework for determination of SCSP

5.3 Tidal Datum-based HWM Indicators Determination

The main objective of this section is to present the method to calculate the tidal datum-based HWM indicators. All of the indicator calculations require, as input, the tidal constituents over a standard tidal cycle. However, the DoT's HWM also requires the tidal constituents in each year to identify the annual variation. The constituents were used to calculate: (1) the height of MHHW at South Fremantle and

MHWS at Port Hedland for a 19 year observation, and (2) 19 years of predicted 15 minute interval tidal heights, from which residuals from observed values can be calculated. To obtain the HWM height using the DoT method, the 19^{th} high water occurrence in a 19 year observation was also calculated.

5.3.1 Standard Tidal Cycle

A period of 19 years is usually considered as a standard tidal cycle for establishment of tidal parameters as it reflects the principle lunar node cycle of 18.6 years. The decision as to which years will be the beginning and end of the standard cycle epoch was made by the Permanent Committee for Tidal and Mean Sea Level (PCTMSL) in Australia. Their decision is aligned with international standards; the current epoch commenced in 1992 and ended at the end of 2010 (The Intergovernmental Committee on Surveying and Mapping (ICSM) 2010b).

Therefore, tidal data in the period between 1992 and 2010 were used for this research. The tidal data were regularly recorded using the tide gauges by DoT during this period in the form of one specific time with one corresponding tidal height. However, the data are not in a uniform format in terms of tidal datum and recording intervals, and standardization of the tidal data had to be conducted before analysing the data.

5.3.2 MHWS, MHHW and the DoT HWM

The formulae to calculate MHWS and MHHW using constituents are $Z_0 + (M_2 + S_2)$ and $Z_0 + (M_2 + K_1 + O_1)$, respectively (Pugh 1996). Z_0 represents the height of mean sea level. The 19 years MHWS and MHHW were calculated by the constituents using the observed tidal data from 1992 to 2010.

The formula for the DoT method to determine the HWM was presented in Section 2.3.5.2 (Equation 2.6), which is: 19 times high water occurrence plus standard deviation of residuals. The 19 times high water occurrence can be directly calculated by statistical methods of tidal recordings, and the residuals were obtained by calculating the differences between observed and predicted values. The method to predict the tide level is to overlap all the tidal constituents in that area. Because every constituent is represented by a curve, the calculated tide is an overlapping curve.

Therefore, the HWM indicator suggested by DoT was obtained using these two values. The workflow to calculate these three tidal datum-based HWM indicators is illustrated in Figure 5.2. The software used to conduct the necessary steps is described in Section 3.5.2.

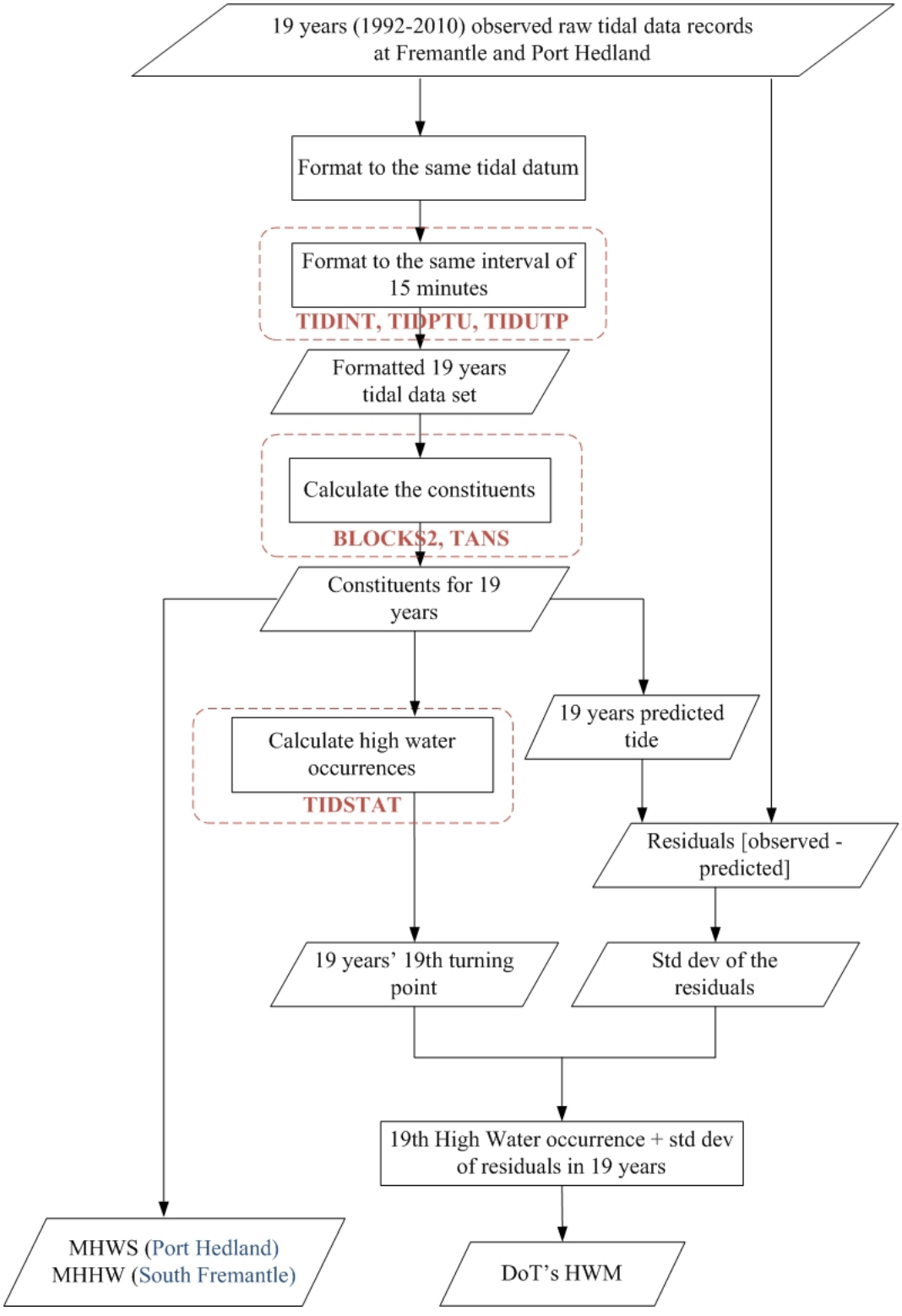

Figure 5.2 Workflow for tidal datum-based HWM indicators determination

5.4 Shoreline Feature based HWM Indicators Generation

5.4.1 Image Classification Using OOIA

The process of OOIA was conducted using eCognition Developer 8.0 as a test-bed environment. Various criteria were applied to complete the classification, including contrasts, colours, reflections, shapes, the steps of 'segmentation,' 'brightness,' 'colour,' 'relationship,' and 'manual modification.'

The results of the classification were tested using:

- Producer Accuracy (PA) (measures the error of omission and exclusion; for example, some vegetation and dry sand pixels were omitted from the wet sand classification);
- User Accuracy (UA) (measures the error of commission, inclusion; for example, some vegetation and dry sand pixels were erroneously included in the wet sand classification);
- Hellden Accuracy (HA) (takes into account the test of Producer and User Accuracy);
- Short Accuracy (SA) (takes into account the test of Producer and User Accuracy);
- Overall Accuracy (OA) (provides a crude measure of accuracy); and
- Kappa Index of Agreement (KIA) (a more robust test on the accuracy of classification than the OA, which is also known as KHAT accuracy) (Gupta *et al.* 2010; NOAA Coastal Services Center 2011).

These are defined as:

$$PA(c_i) = a_{ii} \Big/ \sum_{i=1}^{N} a_{ki} \tag{5.1}$$

$$UA(c_i) = a_{ii} \Big/ \sum_{i=1}^{N} a_{ik} \tag{5.2}$$

$$HA(c_i) = 2a_{ii} \Big/ \sum_{k-1}^{N} a_{ik} + \sum_{i=1}^{N} a_{ik} \tag{5.3}$$

$$SA(c_i) = a_{ii} \Big/ \sum_{k=1}^{N} a_{ik} + \sum_{i=1}^{N} a_{ik} - a_{ii} \tag{5.4}$$

$$OA(c_i) = \frac{1}{n} \sum_{k=1}^{N} a_{kk} \tag{5.5}$$

$$KIA = \frac{P_o - P_c}{1 - P_c} \tag{5.6}$$

where c_i indicates the column i, a_{mn} indicates the accuracy of classification in the column m and row n, P_o is the observed accuracy , and P_c represents the chance of agreement, which is defined as:

$$P_c = \frac{1}{n^2} \sum_{k=1}^{N} \left(\sum\nolimits_{i=1}^{N} a_{ki} * \sum\nolimits_{i=1}^{N} a_{ik} \right). \tag{5.7}$$

In this research, all of the methods described here were used to test the classification accuracy.

5.4.2 Identification of the Vegetation Line

In this analysis vegetation is considered to be either sparse or dense. It is easy to identify the boundary of dense vegetation, but the position of sparse vegetation is fuzzy and the sparse vegetation zone is always further seaward. Therefore, the average elevation of the beach where sparse vegetation starts was considered as the elevation of vegetation line. The vegetation line can be positioned on the map like a contour line using the DEM of the foreshore. Nonetheless, sparse vegetation is difficult to differentiate from beach sand in imagery. Benz *et al.* (2004) suggest that the objective oriented fuzzy logic method is an efficient approach to derive good results where feature extraction is necessarily vague. This research applies the Benz *et al.* (2004) method to sparse vegetation identification.

5.4.3 Identification of the Frontal Dune Toe Position

As previous studies have confirmed, coastal morphology is directly influenced by waves and water levels (Austin and Masselink 2006).

The curvature of the beach landform for each pixel in the study area was calculated using the DEM. Those pixels with curvature of 2.5 standard deviations less than the mean curvature in the dry sand zone, were chosen as identifying the toe of the major frontal dune. This step was conducted based on the following principles (Moore *et al.* 1991): for each pixel cell, the height H_z is fitted into a bivariate quadratic function as a second-degree polynomial of the form given in Equation 5.8 using its *x* and *y* coordinate with all the parameters from *A* to *I*:

$$H_z = Ax^2y^2 + Bx^2y + Cxy^2 + Dx^2 + Ey^2 + Fxy + Gx + Hy + I \tag{5.8}$$

which is fitted to a three-dimensional (3-D) surface composed of 3 × 3 cells around the target pixel, in which each x and y has a corresponding height H_z. The nine points can be exactly fitted into the nine term polynomial. The rate of change of slope for the target pixel is calculated as:

$$\varphi = -2\left(EH^2 + DG^2 + FGH\right)/\left(G^2 + H^2\right). \tag{5.9}$$

The mean elevation of the dune toe was calculated by averaging the elevations of each of the included pixels, which could be used as the elevation of the toe of the frontal dune in this particular area.

5.5 HWM Determination Using the Theory of SCSP

5.5.1 Calculate Extreme Swash Heights

Extreme swash or wave runup height is taken as the highest elevation that water reaches on a beach. The 2% runup exceedance height ($R_{2\%}$) takes into account the effect of both tide and waves (Stockdon *et al.* 2006). Much research on wave runup on beaches has been undertaken by Didenkulova *et al.* (2010), Hughes *et al.* (2010) and Southgate (1989), and numerous approaches for calculating wave runup are available (Holman 1986; Hughes 2004; Mase 1989; Stockdon *et al.* 2006). These are typically based on wave parameters and beach slope.

For the current study, the commonly used empirical formula (Equation 5.10) developed by Stockdon *et al.* (2006) for a range of beach types was applied to calculate wave runup at the two study sites. Their study is based on measurements at 10 diverse field sites (as opposed to laboratory experiments) and is one of the most comprehensive runup studies available. However, while their model provides a good predictor of runup on beaches, there are some variations between estimated and measured runup (Root Mean Square Error [RMSE] = 38 cm in the vertical).

$$R_{2\%} = 1.1\left\{0.35\tan\beta\left(H_0 L_0\right)^{1/2} + \frac{\left[H_0 L_0\left(0.563\tan\beta^2 + 0.004\right)\right]^{1/2}}{2}\right\} \qquad (5.10)$$

where H_0 represents the deepwater wave height, L_0 is the deepwater wavelength derived from the wave period and $\tan\beta$ signifies the beach slope.

To improve the accuracy of estimation on $R_{2\%}$, when the Iribarren number, ξ_0 is less than 0.3 (taking 0.019% and 0.015% of total records at South Fremantle and Port Hedland, respectively), another formula was adopted (RMSE = 21 cm in the vertical) (Stockdon *et al.*, 2006):

$$R_{2\%} = 0.043(H_0 L_0)^{1/2}. \qquad (5.11)$$

Thus the maximum runup elevation on the beaches is defined as (Ruggiero *et al.* 1996; Ruggiero *et al.* 2001):

$$TWL = Z_r + R_{stat} \qquad (5.12)$$

where Z_r is the tidal level, and R_{stat} is the wave runup height as a statistical representation. In this research, the hourly swash runup limit was calculated by adding the hourly mean tide elevation derived from 15 minute interval tidal records using software 'TIDINT' to the hourly 2% exceedance wave runup.

Two of the parameters required by the runup empirical model are the wave height and the wave period. Recording gaps of these parameters are interpolated according to the approach provided in the previous chapter. However, as the propagation mechanism of these two parameters on the runup model is too complex to be

estimated, the effect of the interpolation accuracy on the wave runup modelling was not provided. This is a limitation of this research (See Section 8.4).

5.5.2 Fit Significant Swash Heights into the Cumulative Distribution Function

The cumulative distribution function of swash height can be regarded as the probability that the swash height X is less than x, for any x, denoted as,

$$F(x) = P\{X \leq x\}. \tag{5.13}$$

To try to identify the feature of swash level, the swash heights were fitted into a continuous probability distribution model. The selection of swash probability distribution function was based on the Chi-squared test statistic, and is defined as:

$$\chi^2 = \sum_{i=1}^{k} \frac{\left(N_i - E_i\right)^2}{E_i} \tag{5.14}$$

in which k is the number of bins, and N_i and E_i are the observed and expected number of samples in the i^{th} bin.

To calculate the Chi-squared statistic, it is necessary to break the x axis domain into several bins, the size of which is adjusted based on the fitted distribution, and to associate each bin with an equal probability. To test the significance of the fitting process, which calculates the likelihood that a set of samples drawn from the original data would generate a similar fit statistic, the observed significance level of the test p-value was calculated. The parameters of the distribution model were estimated by the method of maximum likelihood estimation (MLE).

5.5.3 Semivariogram Model of the Swash Probability

Different locations on the beach will be associated with different swash probabilities, but such spatial variation should not be wholly erratic, and a spatial structure may exist based on spatial autocorrelation theory (Anselin and Getis 1992; Burrough 2001; Oliver and Webster 1990). This means that two locations (cross-sections intersected with indicator lines) that are closer together will usually have a smaller difference of swash probability than distant ones. However, autocorrelation should only take effect within a certain distance known as the range (Chiles and Delfiner

1999). Outside this range, the spatial continuity of the swash probability no longer exists, therefore, the range from the lower bound of the sampling position could be considered as the highest level that water can reach in a normal situation, and this would indicate the HWM position.

A semivariogram model was applied to calculate the distance of spatial continuity of swash probability. In order to simulate the semivariogram model, the semivariogram between two positions was calculated (Burrough 2001; Oliver and Webster 1990):

$$\gamma(h) = \frac{1}{2} Var\left\{F(x_i) - F(x_{i+h})\right\} \tag{5.15}$$

where h is the distance between two positions. To measure the relationship between distance and the variation of swash probability, cross-shore transects were defined with spacings to intersect with the different HWM indicators. Each intersected point has a swash probability value, which is used to define the semivariogram model.

5.6 Implementation of the Methods

5.6.1 Identification of Tidal Datum-based HWM Indicators

5.6.1.1 Data Preparation

From the year 2005 onwards, tidal records changed to a new tidal datum at Port Hedland. The new tidal datum was 0.239 m higher than the previous datum, so the data recorded from 2005 onwards was converted back to the previous datum by adding the offset in order to ensure the tidal datum is consistent.

For converting all of the individual tide observations into consistent 15 minute sets, a program titled ‘TIDINT’ (TIDe INTerpolation) (Department of Transport 2010a), was used. The principle of interpolating 15 minute tidal records sets is to simulate the cosine curve by the observed data in a two-dimensional coordinate system. Along the *x* axis is time, and on the *y* axis is the tidal height. The next step is to select the heights with every 15 minute interval. Because of the large amount of tidal records in one year, 15 minute intervals are adequate for this research.

In order to save valuable computer storage space in the past, all the tidal data were compressed into a packed file, in which one row may record several tidal heights at

different times. The software ‘TIDINT’ can only work with the unpacked data, changing data from packed to unpacked was conducted by using software ‘TIDPTU’ (TIDe Packed To Unpacked) (Department of Transport 2010a) and its reverse ‘TIDUTP’ (Department of Transport 2010a).

5.6.1.2 Constituents and High Water Occurrences Calculation

All calculation processes were conducted using the software ‘BLOCKS2’ (Department of Transport 2010a) and ‘TANS’ (Department of Transport 2010a). ‘BLOCKS2’ was used to deal with the raw tidal data, and calculate the main features of the tide data, such as the start recording date and finish date, and to identify the data gaps (no records). ‘TANS’ was used to calculate the constituents. These two software programs were used to analyse the tidal information obtained from the National Tidal Facility Australia and the Coastal Data Centre, DoT, WA. Both are based on Doodson’s theory (The Intergovernmental Committee on Surveying and Mapping (ICSM) 2010a).

In the 19 years tidal data records, high water height occurrences were ordered from the highest level to the lowest level, and the 19 times highest water levels were selected and prepared for the next stage. The high water statistical occurrences were calculated by the software ‘TIDSTAT’ (TIDe STATistic) (Department of Transport 2010a). By calculating the constituents and high water occurrences, the position of MHWS, MHHW and DoT’s HWM were obtained.

5.6.2 Identification of Shoreline Feature based HWM Indicators

Using the images and DEM to identify the HWM shoreline indicators, requires a suitable classification approach. In this study, five feature classes at South Fremantle and six classes at Port Hedland were identified based on significant HWM features on the image (Figure 5.3). The classification of rock could only be found at Port Hedland. The classification at South Fremantle is less difficult than for Port Hedland, where the presence of rock makes the HWL more difficult to identify (Table 5.1), because the features of wet beach and rock are very similar to each other in the imagery. The vegetation at Port Hedland is also more irregularly distributed. Therefore, the classification performed at Port Hedland is thought to be less accurate

than for South Fremantle. Overall, the accuracy of the classification is sufficient to identify the HWM indicators (Figures 5.4 and 5.5 and Table 5.1).

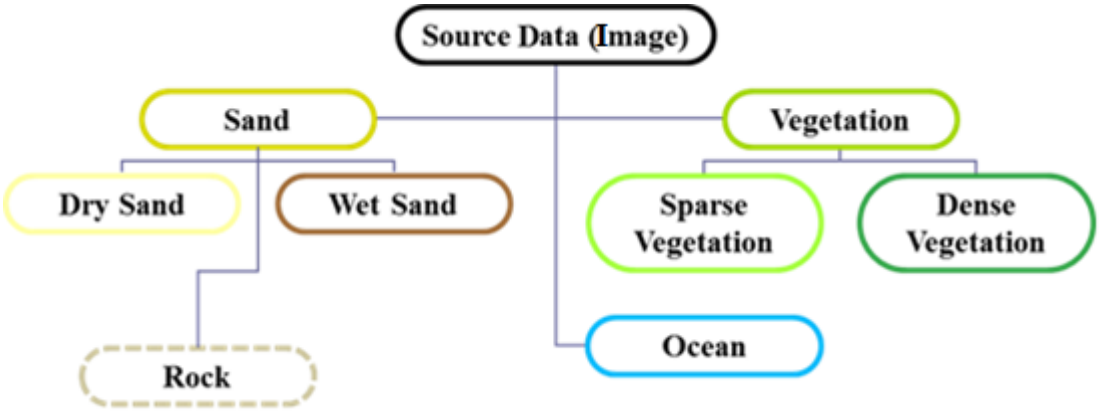

Figure 5.3 Concept classification with objects' hierarchy

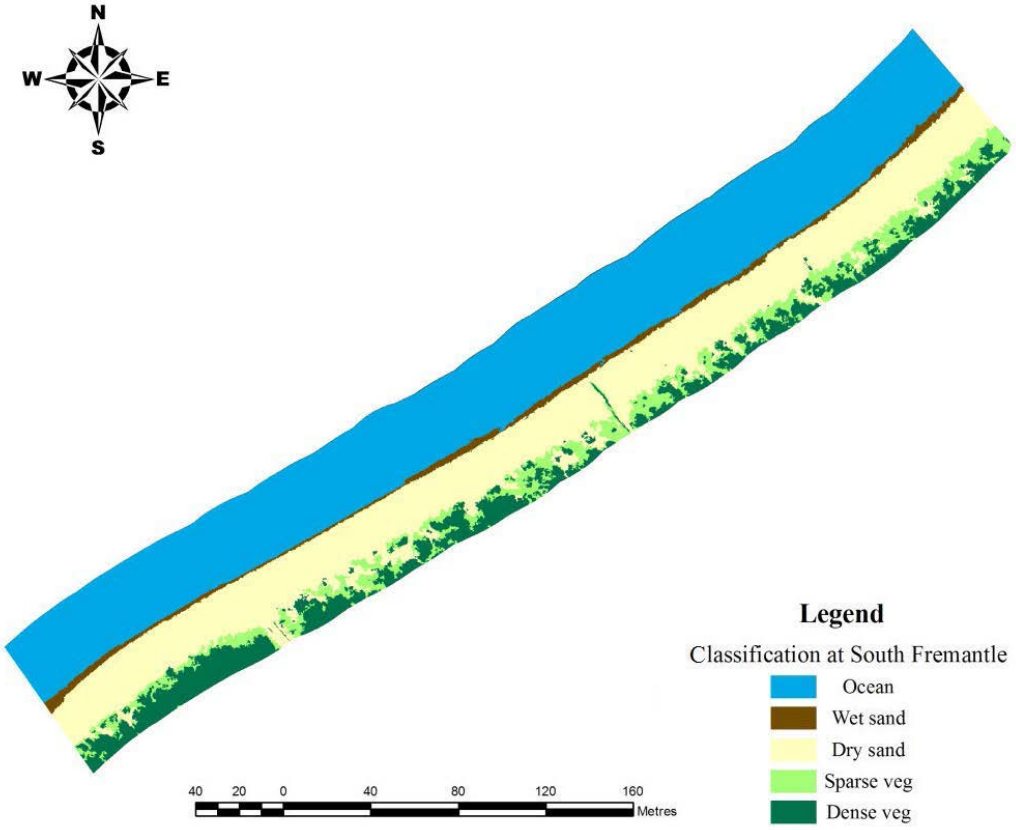

Figure 5.4 Shoreline feature classification at South Fremantle (Source image: Figure 3.2)

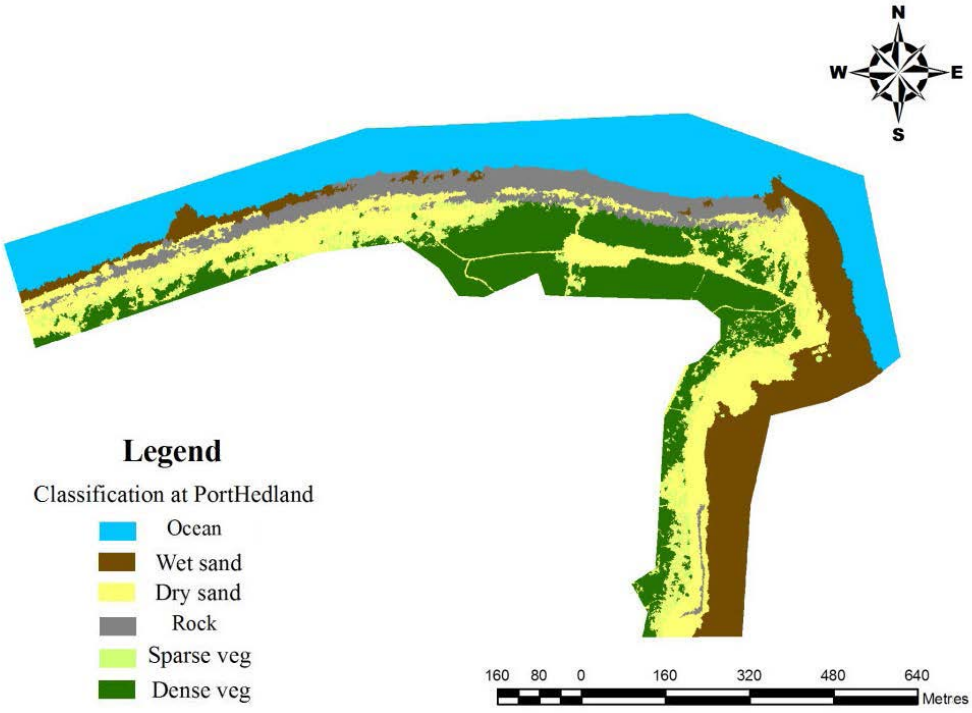

Figure 5.5 Shoreline feature classification at Port Hedland (Source image: Figure 3.3)

Table 5.1 Accuracy test for classification

Accuracy	Ocean	Dry sand	Wet sand	Sparse vegetation	Dense vegetation	Rock
South Fremantle						
Producer	1	1	1	1	0.917	
User	1	1	1	0.839	1	
Hellden	1	1	1	0.912	0.957	
Short	1	1	1	0.839	0.917	
Overall accuracy				0.991		
KIA				0.988		
Port Hedland						
Producer	1	0.908	0.946	0.393	0.937	0.946
User	1	0.782	0.925	0.797	0.931	0.925
Hellden	1	0.840	0.936	0.527	0.934	0.936
Short	1	0.725	0.879	0.358	0.876	0.879
Overall accuracy				0.922		
KIA				0.901		

The HWL position was derived from the interface of wet and dry sand; it is noted that this shoreline indicator has been acknowledged as highly variable, but it still could indicate the landward limit of the previous high tide (Pajak and Leatherman 2002). As the HWL at Port Hedland was broken by the rock areas, the average height of all the identifiable wet and dry sand interfaces were employed as the HWL height, and the corresponding contour line was defined as the horizontal HWL position.

This also applied to the vegetation line. The average elevation of the sparse vegetation was considered as the elevation of the vegetation line. Another HWM indicator, the frontal dune toe, which is indicated by coastal morphology change, was also identified using image analysis (Figures 5.6 and 5.7).

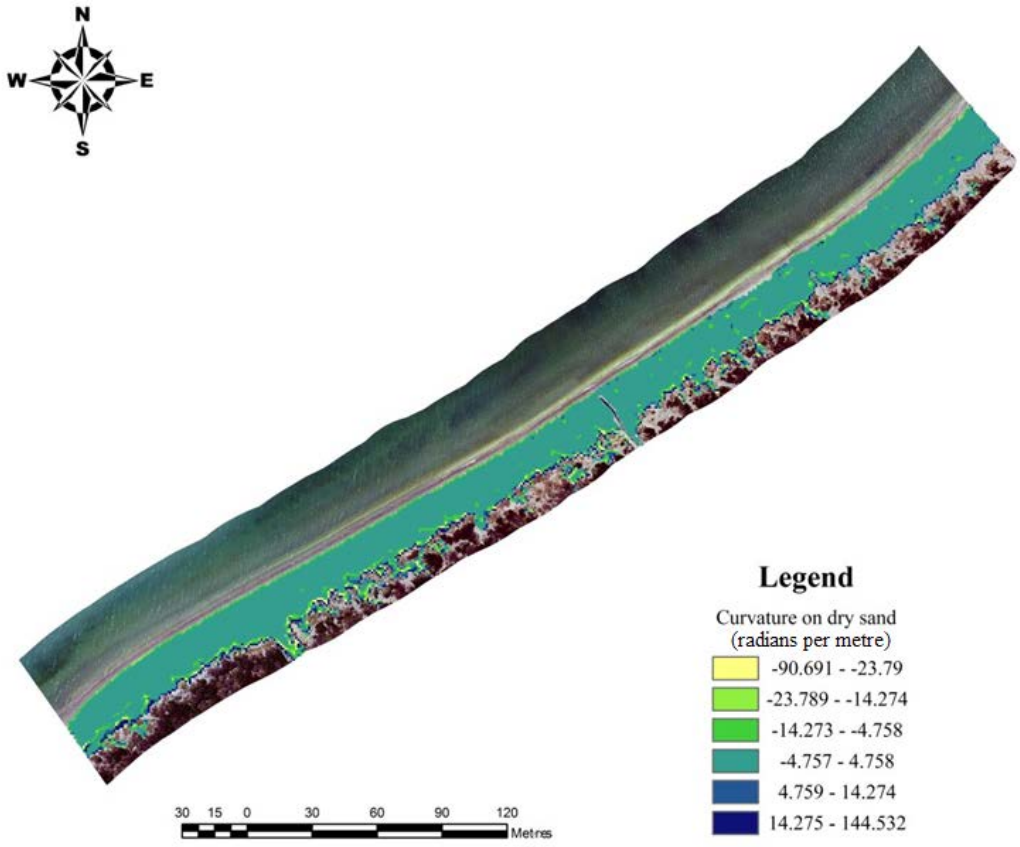

Figure 5.6 Curvature on dry sand at South Fremantle

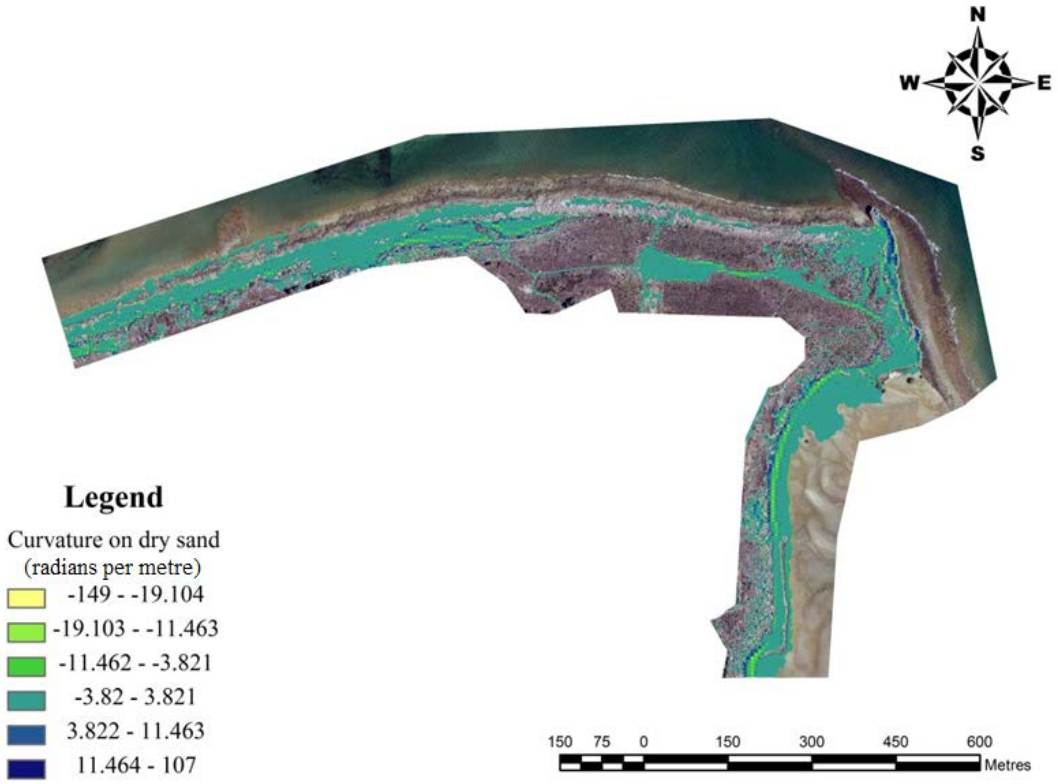

Figure 5.7 Curvature on dry sand at Port Hedland

The HWM indicators examined in this study are defined by both their vertical and horizontal position. However, indicators were initially determined by their horizontal positions and then transposed to their vertical levels. This includes shoreline features, such as HWL, frontal dune toe and the seaward limit of vegetation. The vertical HWM indicators that need to be positioned on the shoreline include MHWS, MHHW and the HWM used by Landgate and suggested by DoT. These indicators can be positioned on the shore like a contour line or integrated into the DEM image. Thus, all the HWM indicators examined in this research have been identified for the two study sites (Figures 5.8 and 5.9).

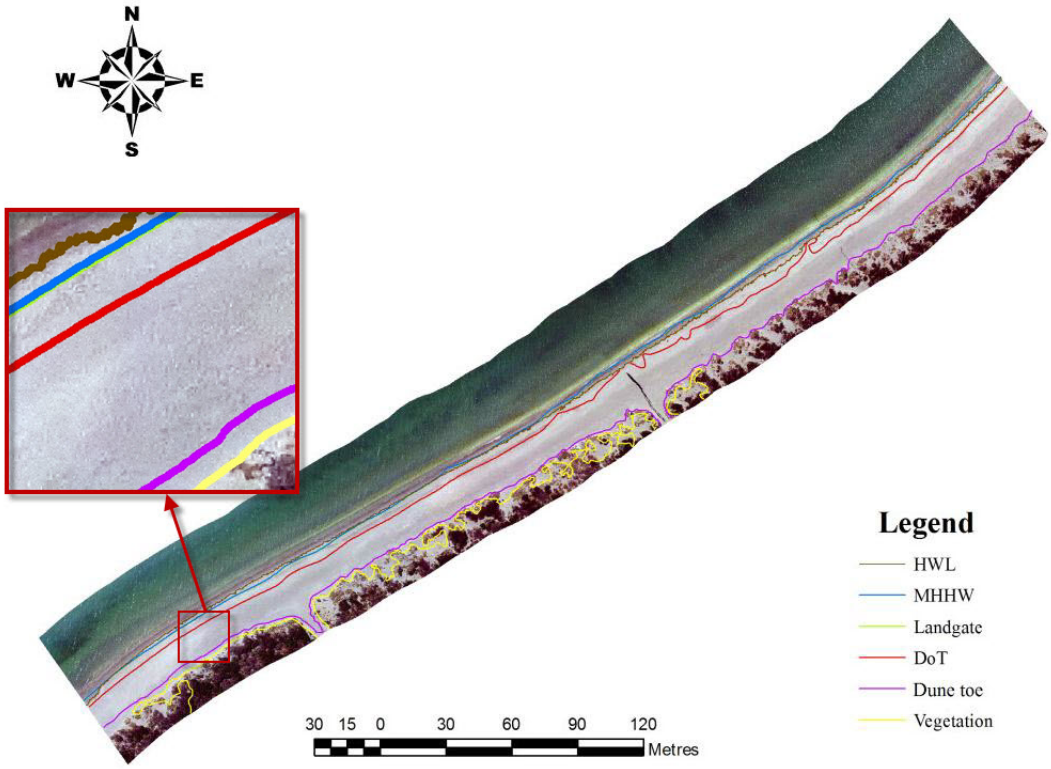

Figure 5.8 HWM indicators at South Fremantle

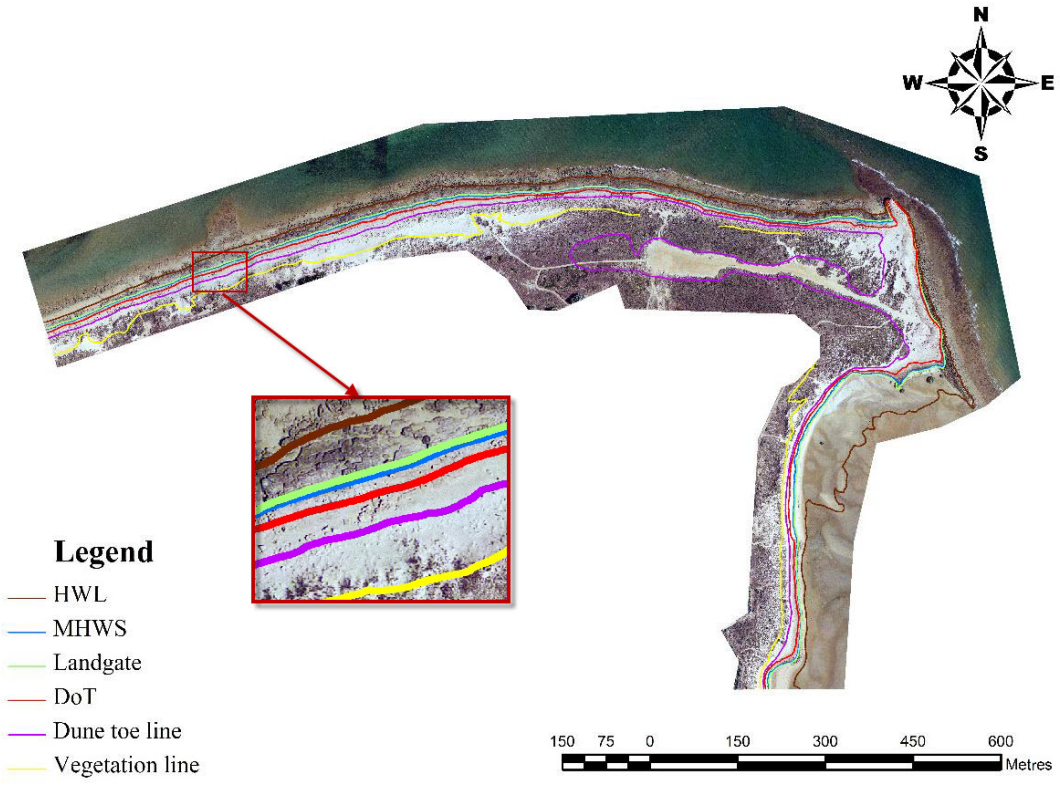

Figure 5.9 HWM indicators at Port Hedland

5.6.3 Comparison of the Swash Probability of HWM Indicators

The 2% swash runup limit was calculated hourly over a 10 year period. These records were fitted using a cumulative distribution function. The top five models, with highest chi-square among the most commonly used distribution models, are listed in Tables 5.2 and 5.3. However, the significance test, as indicated by *p*-value, shows it is less convincing to accept the hypothesis that the fitted distribution could possibly generate the original data set. Therefore, the swash heights could not be fitted into any distribution model, and only the cumulative probability distribution of the swash heights calculated from the original data could be utilised. Equation 5.13 was applied in this study (Figures 5.10 and 5.11).

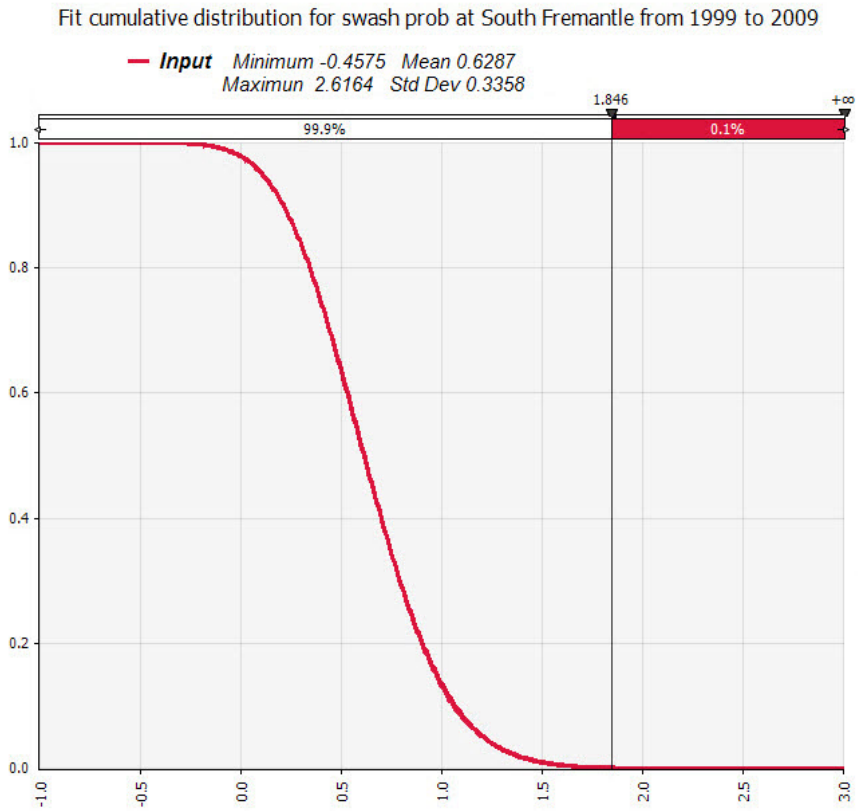

Figure 5.10 Cumulative probability distribution on swash heights at South Fremantle

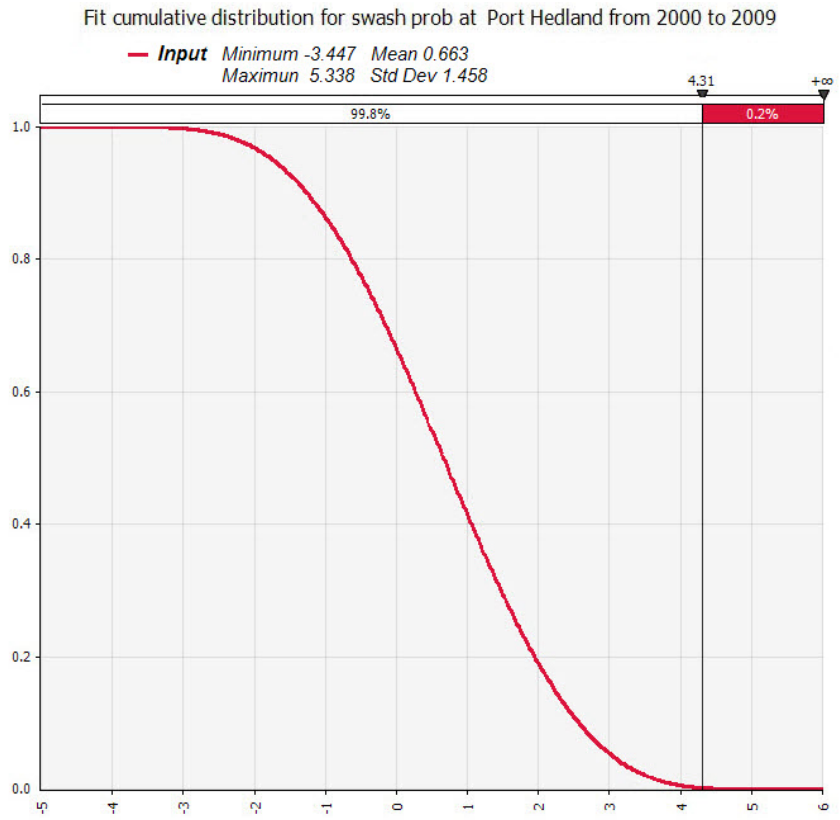

Figure 5.11 Cumulative probability distribution on swash heights at Port Hedland

Table 5.2 Chi-Square test on the model choice at South Fremantle

Model	InverseGauss	Lognormal	Gamma	Normal	Logistic
Chi-Square	217.923	218.274	243.791	1369.351	1707.678
P-value	0.0133	0.0128	0.0004	0	0

Table 5.3 Chi-Square test on the model choice at Port Hedland

Model	BetaGeneral	Normal	Logistic	Chi square	Student
Chi-Square	1107.822	3098.539	6259.065	34876.666	50250.064
P-value	0	0	0	0	0

The swash probability values associated with the various HWM indicators at the two study sites are shown in Tables 5.4 and 5.5. These results indicate that over the 10 year period, the maximum wave runup elevation for South Fremantle is 2.616 m above AHD, while the lowest is 0.458 m below AHD. At Port Hedland, the runup elevation is between 5.339 m above AHD and 3.447 m below AHD. It is clear that

the heights of MHWS, MHHW and the HWM suggested by Landgate are quite similar to each other in both study areas, and the swash probabilities of these indicators at the individual locations do not vary greatly. However, the swash probability of these indicators for Port Hedland is much smaller than that at South Fremantle.

Table 5.4 Compare the swash probability for different HWM indicators at South Fremantle

HWM indicators	Average height	Swash probability
HWL	3.87×10^{-1}m	7.59×10^{1}%
MHHW	3.40×10^{-1}m	8.04×10^{1}%
Landgate	4.00×10^{-1}m	7.46×10^{1}%
DoT	7.20×10^{-1}m	3.75×10^{1}%
Dune toe line	2.11×10^{0}m	1.89×10^{-4}%
Vegetation line	2.67×10^{0}m	0%

Table 5.5 Compare the swash probability for different HWM indicators at Port Hedland

HWM indicators	Average height	Swash probability
HWL	1.18×10^{0}m	3.83×10^{1}%
MHWS	2.83×10^{0}m	7.00×10^{0}%
Landgate	2.67×10^{0}m	9.10×10^{0}%
DoT	3.46×10^{0}m	1.40×10^{0}%
Dune toe line	4.48×10^{0}m	2.40×10^{-2}%
Vegetation line	8.35×10^{0}m	0%

It is commonly accepted that the position of MHHW/MHWS is close to the HWL, but this assumption lacks statistical evidence (Crowell *et al.* 1991; Pajak and Leatherman 2002). In this study, the swash probability at HWL and MHHW are comparable for South Fremantle, while at Port Hedland, the HWL is much lower than the other indicators.

The HWL is the boundary between dry and wet sand. However, its position is highly reliant on high tide elevation and wave conditions on the day when the imagery was taken; thus, while it is a good indicator of maximum runup limit for that particular day, it is likely to have little relevance to the HWM over a longer duration.

This supports the previous finding that the HWL is highly variable (Crowell *et al.* 1991; Pajak and Leatherman 2002) and is not suitable for the robust definition of the HWM. The HWM levels suggested by the DoT method are higher, but the swash probability was significantly lower than MHWS and the HWM used by Landgate. The probability that water can reach the dune toe level in 10 years is very small at both sites, and its swash probability is consistent at the two sites. However, further analysis is required for a credible determination result on the HWM position.

5.6.4 HWM Determination based on the SCSP/SCTP

Tables 5.4 and 5.5 provide an evaluation of the swash probability associated with the identified HWM indicators; however it is difficult to give an objective determination on where the HWM should be located based on this analysis. To provide further insight, a new HWM level was derived from the swash probability of the HWM indicators based on spatial continuity theory.

To identify this position, cross-shore transects were defined at regular intervals along the study sites, intersecting with the calculated indicator lines. These transects were at 50 m intervals along the shore at South Fremantle, and at varying intervals at Port Hedland. These intervals were selected to ensure all shoreline features were captured with the minimum number of cross sections (Figures 5.12 and 5.13). The swash probability was calculated for each intersection point, and the semivariogram curve was fitted to the data to estimate the spatial autocorrelation of the swash probability.

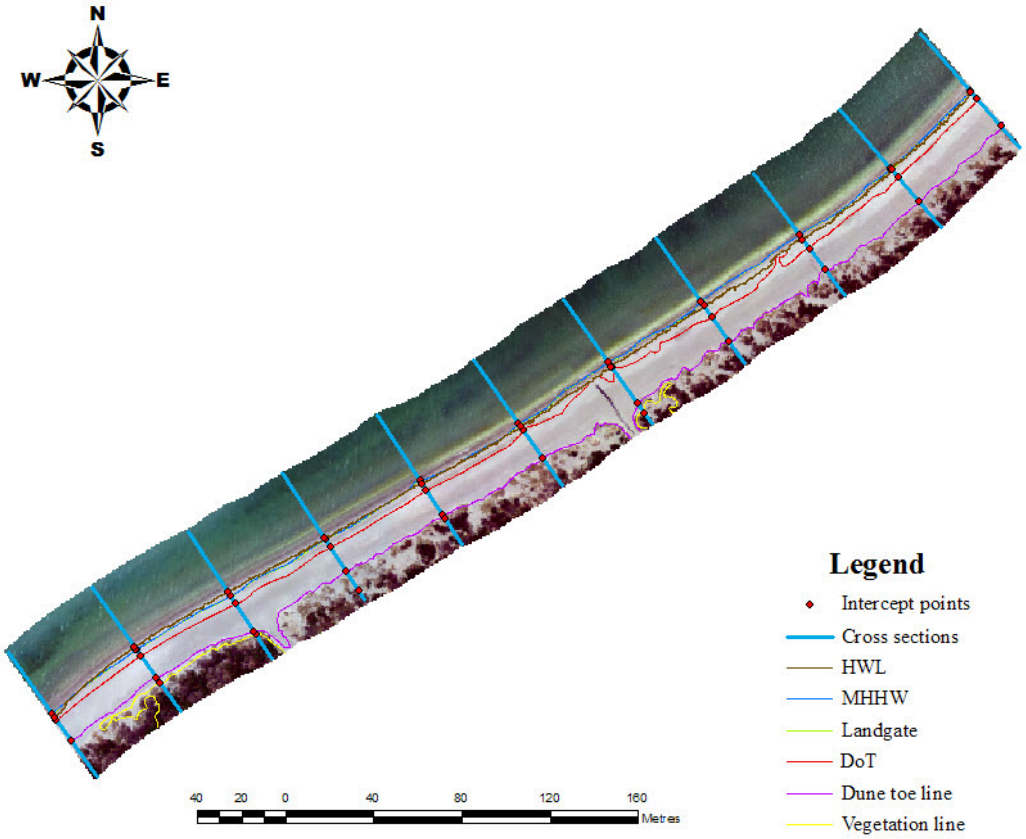

Figure 5.12 HWM indicators with cross sections at South Fremantle

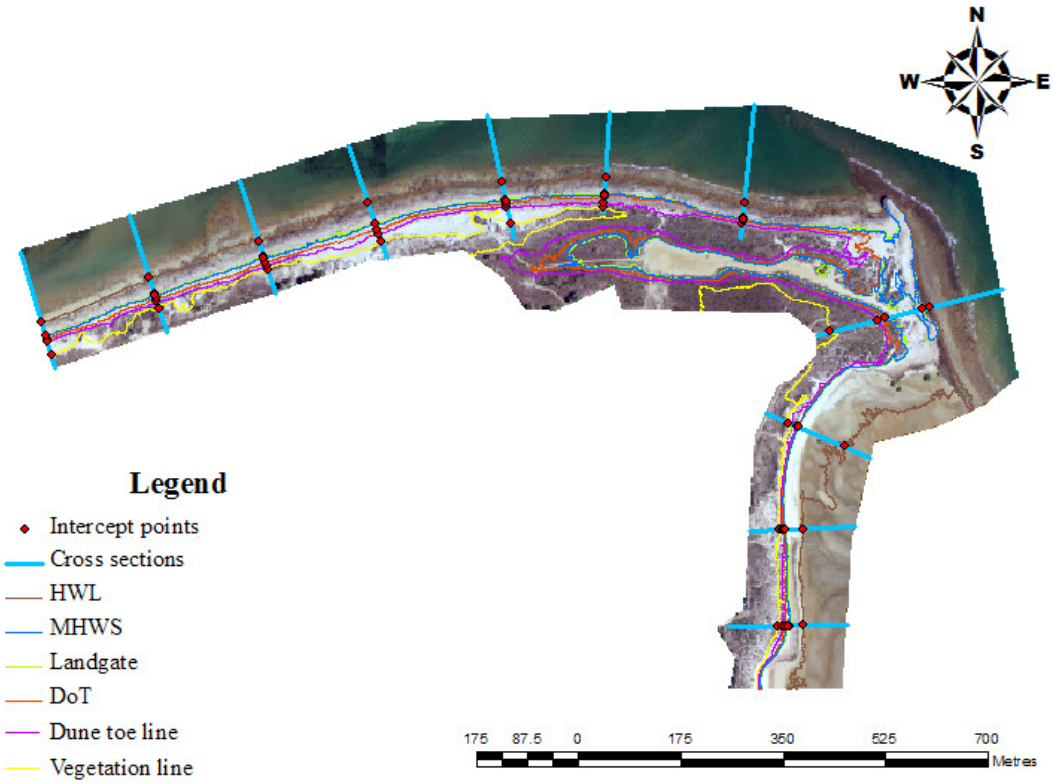

Figure 5.13 HWM indicators with cross sections at Port Hedland

Compared with other semivariogram models of spatial continuity distance calculation, the Gaussian model best fits the empirical semivariogram model (observed values) to the data at the two study sites (Table 5.6). Therefore, the Gaussian model was chosen to describe the spatial autocorrelation pattern (Figures 5.14 and 5.15). The ranges of the semivariogram are 17.2 m and 30.9 m at South Fremantle and Port Hedland, respectively, beyond which no spatial autocorrelation and continuity of the swash probability exist. The range, which is one parameter of the model, was calculated by minimising the RMSE for each model.

Admittedly, the results are sensitive to sampling and measurement errors, which are included in, and estimated by, the nugget effect (0.000290 at South Fremantle and 0.000265 at Port Hedland) (Jaksa *et al.* 1997). The baseline for the spatial autocorrelation distance calculation was the location of the most seaward HWM indicator at which the sampling began to calculate the semivariogram model. Thus, the semivariogram indicates that the HWM is located 17.2 m and 30.9 m landward of the baseline at South Fremantle and Port Hedland, respectively. The lines with 0.148% (South Fremantle) and 0.149% (Port Hedland) swash probability were suggested as the most appropriate HWM levels for coastal hazards planning purposes, and the corresponding elevations on the beach are 1.785 m and 3.990 m for the two sites, respectively.

What should be emphasised here, is that these swash probabilities and heights are lower but very close to the frontal dune toe, which indicates that the position of dune toe is a reasonable indicator of the position of SCSP for coastal hazards planning when insufficient data are available to carry out more complex analysis, such as in remote areas. Figure 5.16 depicts an example at South Fremantle and illustrates the entire process of SCSP determination.

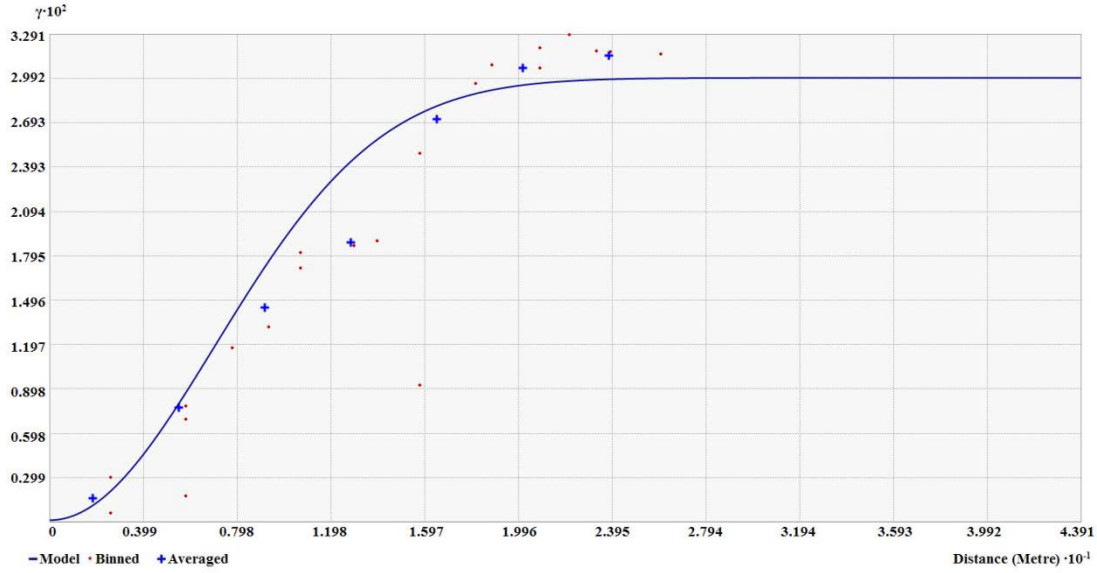

Figure 5.14 Semivariogram Gaussian model to calculate the spatial continuity range at South Fremantle

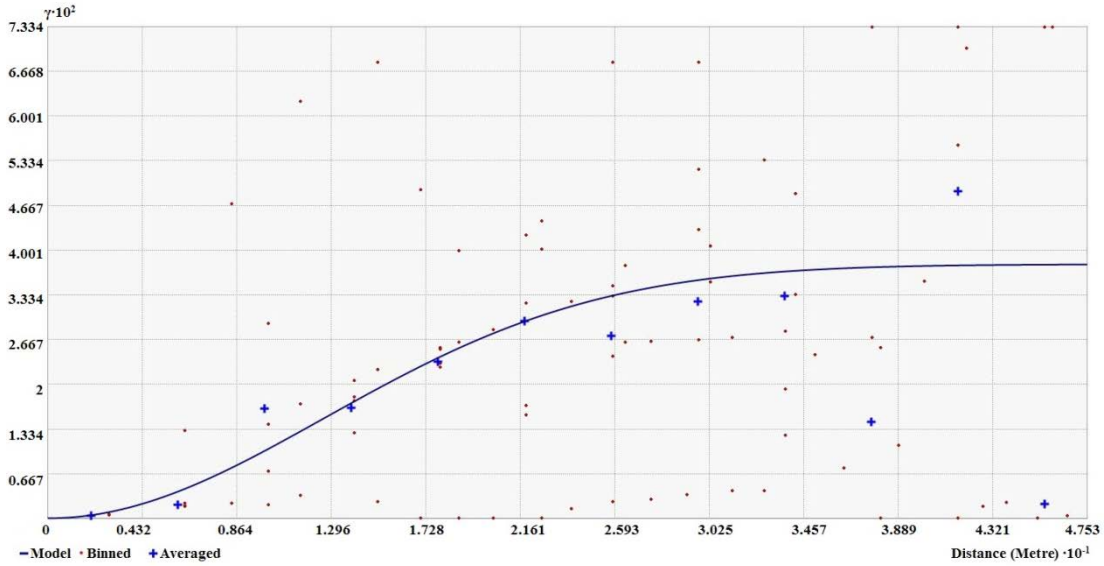

Figure 5.15 Semivariogram Gaussian model to calculate the spatial continuity range at Port Hedland

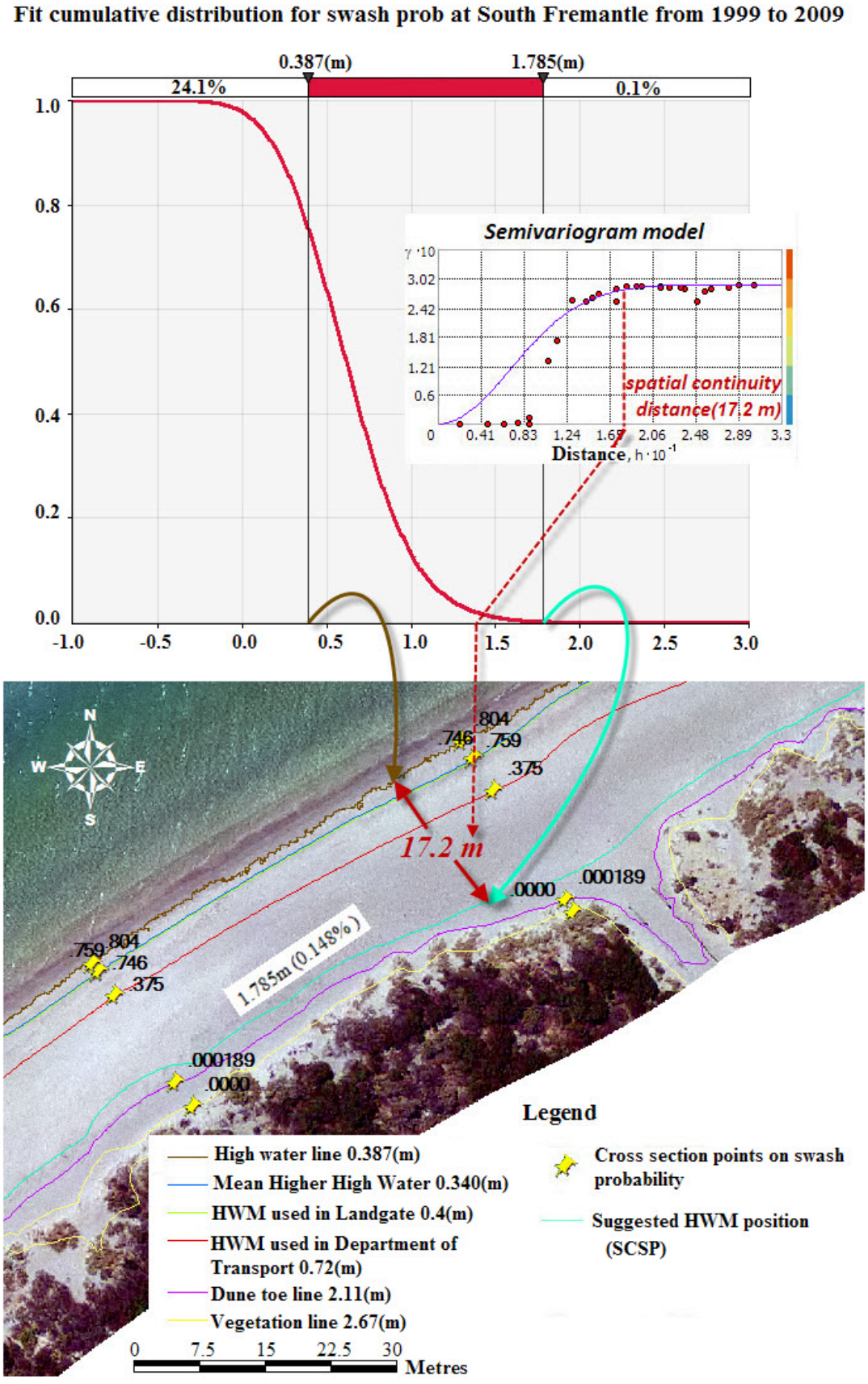

Figure 5.16 Model to illustrate the idea and process to calculate the HWM position

Table 5.6 Compare the different semivariogram models on spatial continuity distance calculation

Model (Optimized range (m))	Mean error	Root-Mean-Square
South Fremantle		
Gaussian (17.2)	0.0167	0.0961
Circular (17.1)	0.0264	0.1430
Spherical (16.6)	0.0305	0.1000
Stable (29.3)	0.0239	0.0972
Port Hedland		
Gaussian (30.9)	0.0278	0.0811
Circular (20.5)	0.0330	0.1030
Spherical (23.5)	0.0334	0.1040
Stable (29.0)	0.0281	0.0832

For coastal property management, the same process was used to model the HWM position by excluding the wave runup parameter regarding the spatial continuity of tide probability (SCTP). The ranges of the semivariogram are 4.59 m and 29.89 m at South Fremantle and Port Hedland, respectively; therefore, the lines with 0.220% and 0.127% tidal probability were suggested as the most appropriate HWM levels for coastal management purposes. Correspondingly, the elevations on the beach are 0.707 m and 3.919 m for South Fremantle and Port Hedland, respectively (Figures 5.17 and 5.18).

The key and fundamental step to achieve accurate shoreline feature identification by OOIA is the segmentation. In this step, the homogeneous image objects are grouped and extracted by the pixel value and object shape. However, the determination on the weights for these two criteria is highly dependent on the experiences of the analyst. This may lead to variations in the classification results, especially for images covering large areas. Furthermore, the interval distance between cross sections is another source of uncertainty introduced to this study. When calculating the semivariogram based on swash/tidal probability and distance of intersection points, the distances between cross sections may have an effect on the calculation of spatial continuity distance of swash/tidal probability.

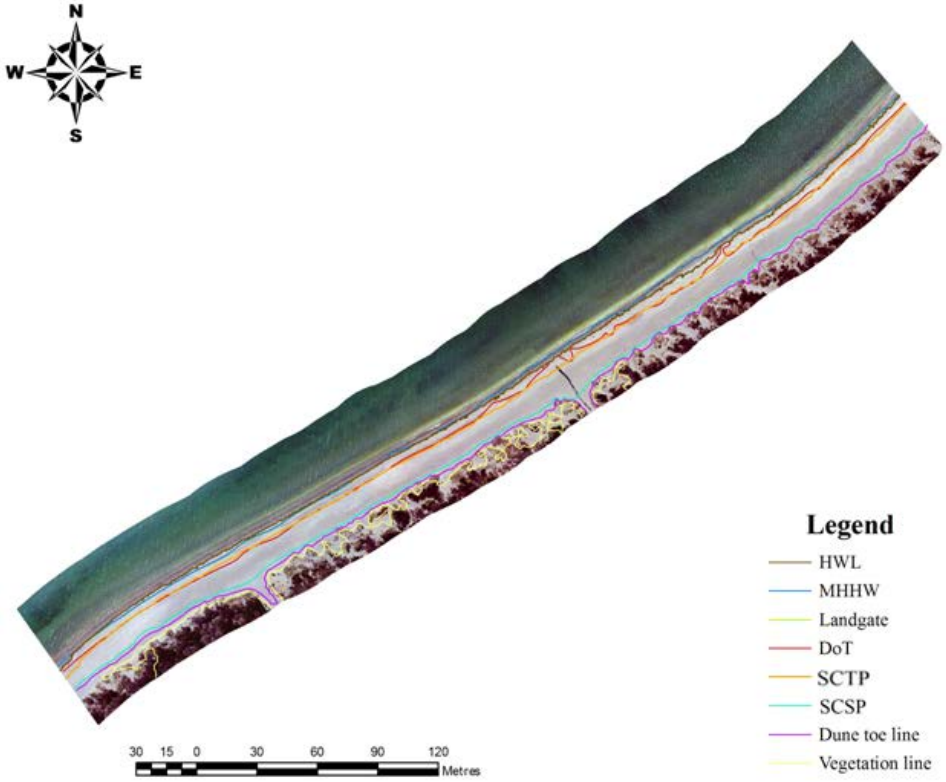

Figure 5.17 The positions of SCSP and SCTP and the other HWM indicators in Fremantle

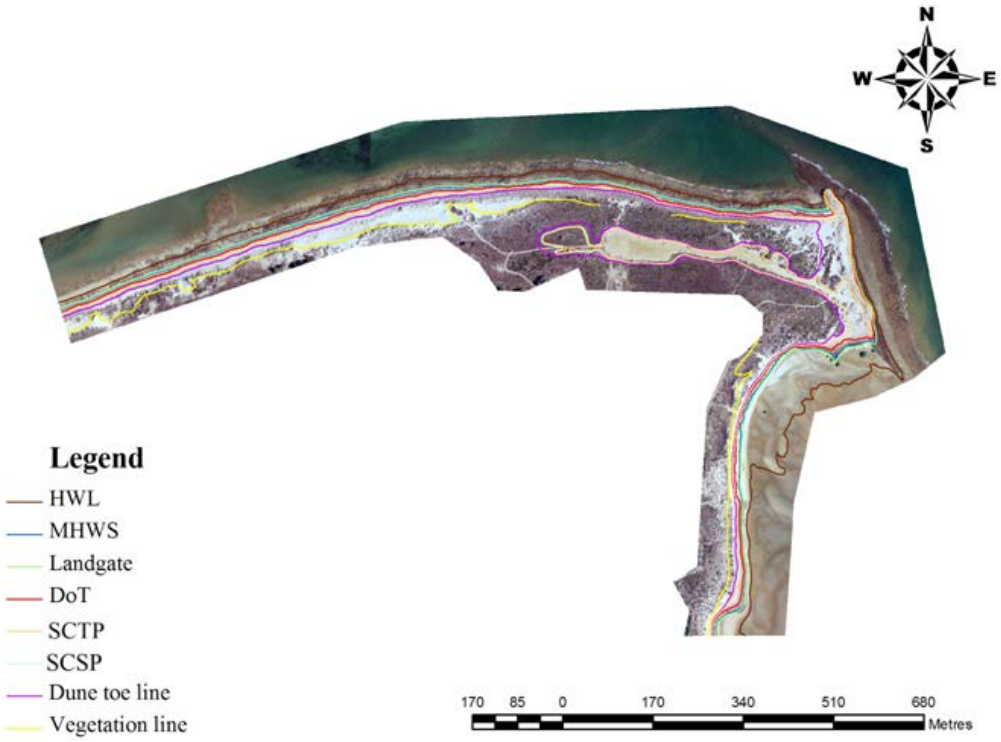

Figure 5.18 The positions of SCSP and SCTP and the other HWM indicators at Port Hedland

5.7 Field Work Evaluation

Two field surveys were conducted in the two study areas to assess the confidence level of shoreline features identified using the image analysis techniques, and the swash height calculated from the empirical model. Plans of the field work for the surveyors' reference are illustrated in the Appendix I. The field work was carried out from 8:30am to 11:30am on 23 August 2012 at South Fremantle and from 9:30am to 2:00pm on 8 July 2012 at Port Hedland, respectively (Figures 5.19 and 5.20). Due to the environmental factors and the limitation of labour resources, the field work at Port Hedland could only be carried out on the south west face of Cooke Point.

Figure 5.19 Field survey at Coogee beach, South Fremantle

Figure 5.20 Field survey at Cooke Point (south west face), Port Hedland

During the survey process, the highest water levels were recorded for three hours in both study areas to validate the hourly 2% significant swash heights calculated from the empirical model for the same time in 10 years. In addition, survey points representing the HWL and frontal dune toe positions were also collected at both study areas. However, since the vegetation zone at Port Hedland was difficult to reach (see Figure 5.20), survey points on the position of vegetation line are only available at South Fremantle (Figures 5.21 and 5.22).

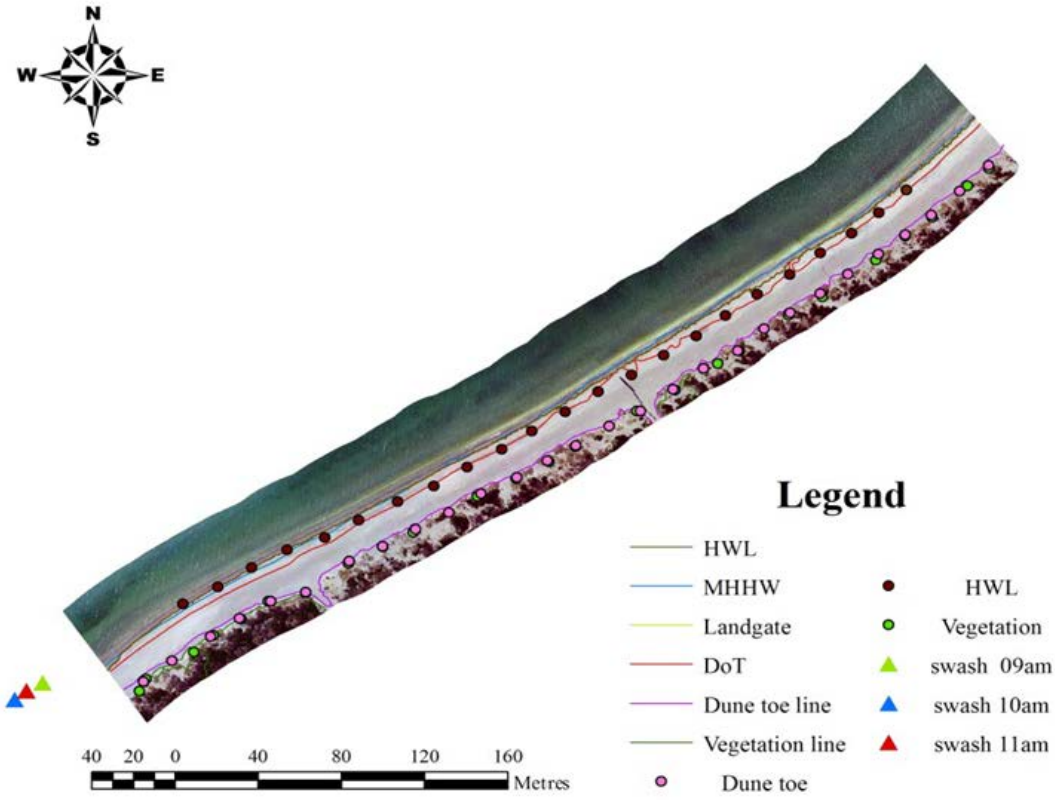

Figure 5.21 Shoreline features' position (points from field RTK survey) and their relationships to HWM indicators at South Fremantle

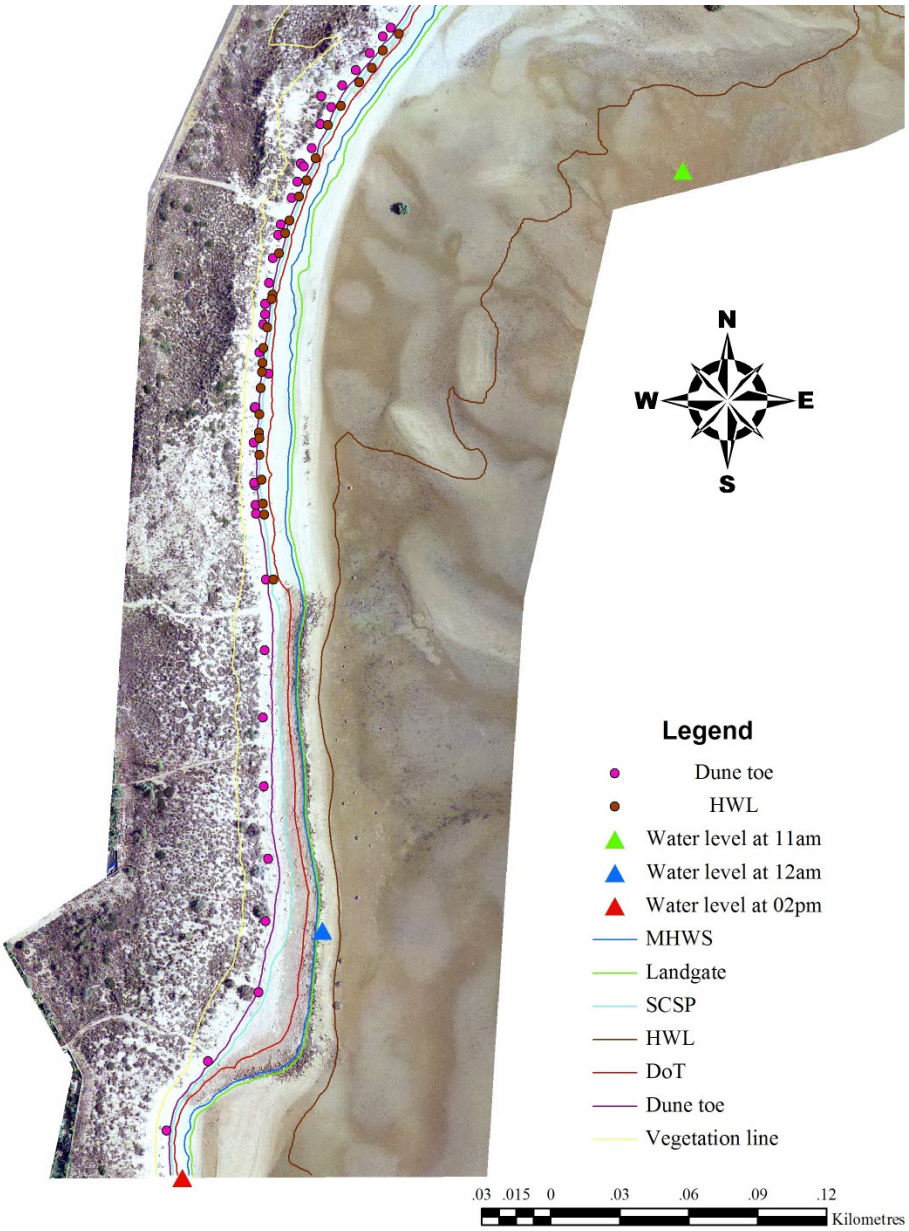

Figure 5.22 Shoreline features' position (points from field RTK survey) and their relationships to HWM indicators at Port Hedland

5.7.1 HWL, Vegetation Line, Swash Heights

To provide a confidence level on the shoreline features and swash height determination, one sample *t*-test (Cressie *et al.* 1984) was applied. The hypotheses are defined as:

> ***Null Hypothesis:*** *There is no significant difference between the observed and estimated mean of data (runup heights determined from the empirical model in the last 10 years and HWL height determined by image analysis).*

Alternative Hypothesis: *There is a significant difference between the observed and estimated mean of data.*

From Tables 5.7 and 5.8, it can be estimated that there are significant differences between the HWL and vegetation positions (not available at Port Hedland) estimated from image analysis and the observed positions on the beach. This confirms that HWL could be the most dynamic feature over time, because of the highly frequent exchange of status between being inundated by water and being exposed to air. Also, half of the swash height estimations are acceptable in the sample test in this study, while the overall runup modelling is more accurate at Port Hedland than at South Fremantle.

Table 5.7 One sample t-test on the positions of HWL, vegetation line and swash heights between observed and estimated values at South Fremantle

	Mean (m)	**t**	**Sig. (2-tailed)**
HWL (0.39m)	0.68	12.59	0.000 (significant difference)
Vegetation line (2.67m)	2.22	-9.636	0.000 (significant difference)
Water level at 09am (0.51m)	0.76	2.24	0.055 (no significant difference)
Water level at 10am (0.46m)	0.74	2.60	0.032 (significant difference at 0.05 level)
Water level at 11am (0.37m)	0.69	3.56	0.007 (significant difference at 0.05 level)

Table 5.8 One sample t-test on the positions of HWL and swash heights between observed and estimated values at Port Hedland

	Mean (m)	**t**	**Sig. (2-tailed)**
HWL (1.18m)	3.41	94.84	0.000 (significant difference)
Water level at 11am (0.52m)	1.18	1.430	0.191 (no significant difference)
Water level at 12am (1.51m)	1.49	-.041	0.968 (no significant difference)
Water level at 1400 (2.54m)	1.43	-2.445	0.040 (significant difference at 0.05 level)

5.7.2 Frontal Dune Toe

One of the limitations of the *t*-test is the sample size cannot be over 30 (Ozmutlu *et al.* 2002). Therefore, two sample non-parametric tests were adopted to compare the positions of high curvatures obtained using the image analysis with the one collected from the field RTK survey. Two of the most well-known non-parametric tests are Kolmogorov-Smirnov (K-S) distance and Mann-Whitney U test, while Kolmogorov-Smirnov (K-S) is more sensitive to differences in shape of the empirical cumulative distribution of the compared samples (Lin *et al.* 2010).

5.7.2.1 Kolmogorov-Smirnov (K-S) Distance

As indicated by Rubner *et al.* (2001), the similarity measure performs well in distance detection using K-S distance statistics. The two sample K-S test is to compare the distributions of the values in two different datasets, which is defined as the maximal discrepancy between two cumulative distributions:

$$D_{n,n'} = \sup_{x} \left| F_{1,n}(x) - F_{2,n'}(x) \right| \tag{5.16}$$

where $F_{1,n}(x)$ and $F_{2,n'}(x)$ are two cumulative distributions of the original samples, which need to be compared. In this study, the two datasets are the frontal dune toe positions calculated by the image analysis techniques and determined by the field survey, respectively. The largest distance on the cumulative probability with the same elevation x_a was defined as the K-S distance $D_{n,n'}$.

5.7.2.2 Mann-Whitney U Test

The Mann-Whitney U test is one of the most common non-parametric significance tests, which evaluates whether independent observations from one sample tend to have a larger value than the other. Also, the distributions of the samples do not necessarily need to be a normal distribution. These features of the Mann-Whitney U test make it suitable for the analysis in this research.

To calculate the U statistic, the combined data from the two groups are sorted and ranked first, and the rank for each sample is (Rosner and Grove 1999):

$$\overline{R_i} = R_i / n_i \tag{5.17}$$

in which n_i is the sample size of the group *i*. The U statistic for the group 1 is:

$$U_1 = n_1 n_2 + \frac{n_1(n_1+1)}{2} - R_1 \tag{5.18}$$

$$U_1' = n_1 n_2 - U_1 \tag{5.19}$$

The U statistic is expressed as:

$$U = \min(U_1, U_2) \tag{5.20}$$

Both the Mann-Whitney U test and the K-S test were used to compare these two datasets. The results (Tables 5.9 to 5.12) indicate that there is a significant difference between the real positions of dune toe and its position determined from the image analysis. This is because the asymptotic significance levels (Asymp. Sig.) from both tests are below the predetermined statistical threshold of 0.05, which is more significant for the shoreline features at South Fremantle.

Table 5.9 Summary about the dune toe position from field survey and image analysis at South Fremantle

	Dune toe	N	Mean	Std. Deviation
Field survey	1	28	1.72	0.13
Image analysis	2	69	2.11	0.29

Table 5.10 Mann-Whitney U and K-S test for dune toe at South Fremantle

Mann-Whitney U	220.000
Asymp. Sig. (2-tailed)	0.000 (significant)
Kolmogorov-Smirnov test	0.652
Asymp. Sig. (2-tailed)	0.000 (significant)

Table 5.11 Summary about the dune toe position from field survey and image analysis at Port Hedland

	Dune toe	N	Mean	Std. Deviation
Field survey	1	39	3.93	0.46
Image analysis	2	91	4.13	0.81

Table 5.12 Mann-Whitney U and K-S test for dune toe at Port Hedland

Mann-Whitney U	1505.000
Asymp. Sig. (2-tailed)	0.171 (not significant)
Kolmogorov-Smirnov test	0.293
Asymp. Sig. (2-tailed)	0.018 (significant at 0.05 level)

Overall, variations exist in the HWM indicators between the positions calculated by image analysis or the empirical model and their corresponding positions on the Earth's surface. Such variations can arise from different scales of the survey on the HWM position. They may also be due to the field survey seasons, which are different from the seasons when the images were captured. However, in this research, the seasonal variation of the position of the HWM indicators, as well as the precision of HWM indicators, may have an influence on the determination of the HWM. This will be further analysed in the next chapter.

5.8 Summary

In this chapter, a new method to determine the location of the HWM was introduced. This model was implemented in two study sites with different coastal features and tidal ranges. OOIA was used for the classification of HWM indicators interpreted from high-resolution images. This was an important step in the determination of the HWM.

The position of the HWM based on the spatial continuity of inundation probability due to swash/tide for a range of HWM indicators, SCSP/SCTP, are introduced for hazard planning and property management purposes, respectively. However, field survey data showed there are variations between the HWM indicators' position calculated by image analysis or empirical model and their corresponding position on the Earth's surface, and indicated that further studies are necessary for assessing the effect of HWM indicators' variations on the determination of the HWM.

CHAPTER 6 ASSESSMENT OF SPATIAL AND TEMPORAL VARIATIONS OF HIGH WATER MARK INDICATORS

6.1 Introduction

Due to the dynamic nature of the coastal environment, the position of the HWM will vary over time. This chapter addresses the methods developed to evaluate the spatial and temporal variation (precision and stability) of HWM indicators using remote-sensing image analysis techniques.

This follows the previous chapter, which focussed on the determination of the position of the HWM indicators. For clarity, the framework for the evaluation process is outlined in Section 6.2 and the interpolation of DEM data presented in Section 6.3. The spatial and temporal variations of HWM indicators are assessed in Section 6.4 and 6.5, followed by a discussion on the implementation of the methods for two case study areas.

6.2 Outline of Evaluation of Spatial and Temporal Variations of HWM Indicators

The dynamic nature of the swash zone is explored in the literature review (Chapter 2). Physical feature markings (or HWM indicators) lying on the swash zone are highly variable over time and tend to be at the same location for short periods only. In addition, these HWM indicators are not always available on every beach. Analysis of tide gauge records show that there is temporal variation of the HWM over different time scales. These variations range from short-term daily changes to seasonal changes and multi-decadal changes (Pugh 1996).

To be acceptable as a coastal boundary, the determined the HWM should satisfy the following criteria: repeatable, consistent and reliable (Leon and Correa 2006; Pajak and Leatherman 2002). These criteria are interpreted as the stability of the HWM.

In addition, the data source inaccuracies and shoreline interpolation error during the HWM determination process may also contribute to the variation of the position of HWM indicators. This variation can be expressed as the difference between the feature on a geographically registered map and its corresponding position on the Earth’s surface.

The methodology applied in this study to evaluate the spatial and temporal variation of the determined indicators is outlined in Figure 6.1. The evaluation determines the precision (spatial perspectives) and the stability (spatial and temporal perspectives) of the HWM indicators.

The seasonal variation of the coastal morphology is the dominant temporal variation. As such the position of each HWM indicator in winter and summer are compared and then measured using the extended Hausdorff distance.

The accuracy of the LiDAR points used, while representing the coastal morphology at Port Hedland in winter time, was of low resolution and subject to inherent error. However, the information in the LiDAR points is still useful, and it is the only available data representing the coastal morphology at Port Hedland in winter time. Therefore, before assessing the seasonal change of the HWM position, the DEM was interpolated using the Kriging method based on these LiDAR points.

The spatial variation of the HWM was evaluated against the precision of the HWM determination process (both pre-process and post-process). This included DEM accuracy, random error, model accuracy and classification accuracy. In addition, the topographic complexity was also analysed to assess its impact on HWM determination (Figure 6.1).

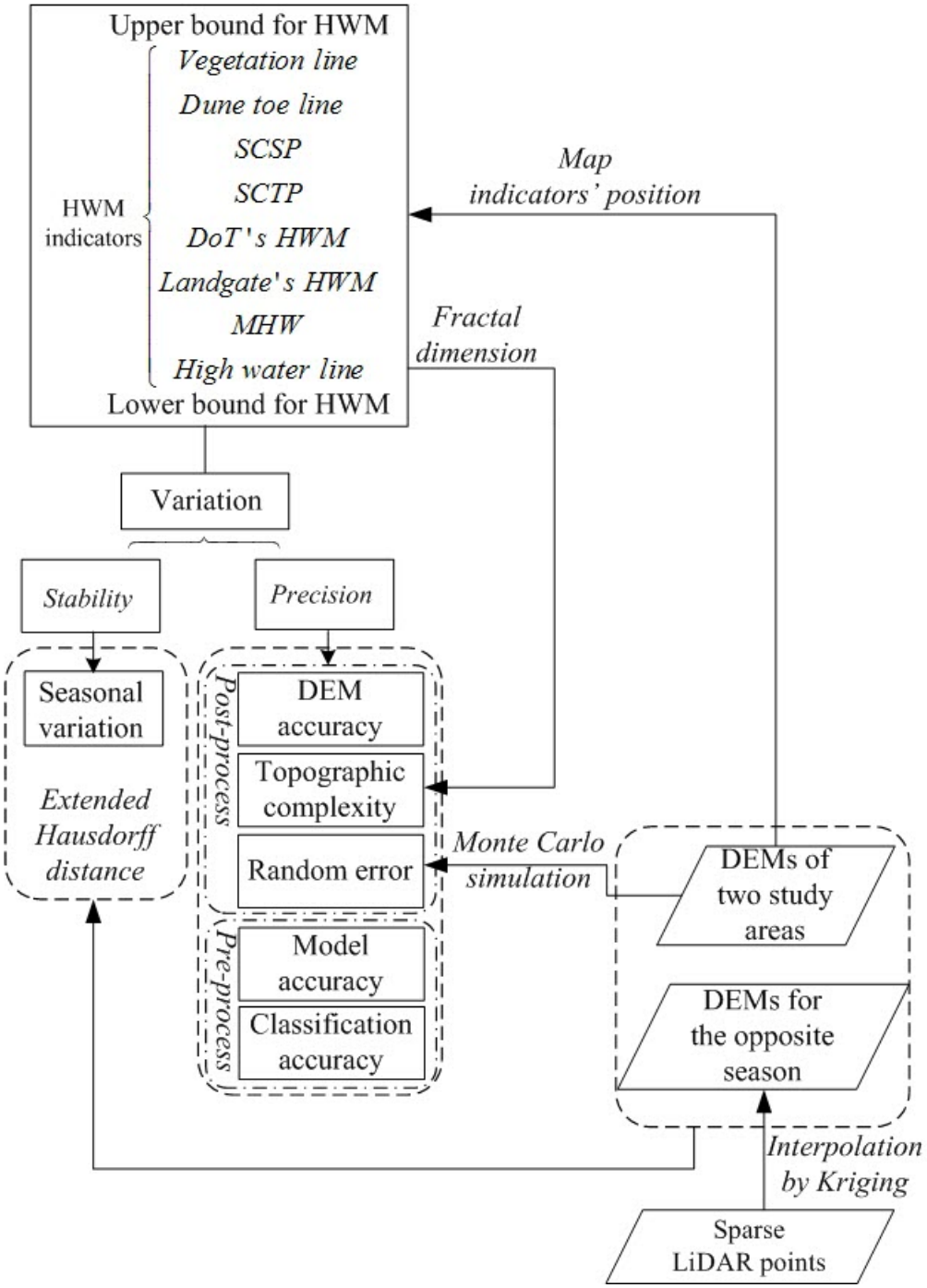

Figure 6.1 Framework for assessing spatial and temporal variations of the HWM

6.3 DEM Data Interpolation by Kriging

The first step of the evaluation process, for spatial and temporal variation of HWM indicators, is to interpolate data gaps using the Kriging method. Kriging is used to predict the values of the missing DEM data by the sum of the surrounding weighted values of the observed DEM data (Oliver and Webster 1990):

$$\hat{Z}(s_0) = \sum_{i=1}^{N} \lambda_i Z(s_i) \quad (6.1)$$

in which, $Z(s_i)$ is the observed value at location *i*, λ_i is the weight at the location *i*, s_0 is the location to be estimated and *N* is the number of observed data used to predict $\hat{Z}(s_0)$.

The weights λ_i were estimated based on spatial autocorrelation theory using semivariogram models as follows (Burrough 2001; Oliver and Webster 1990):

$$\gamma(h) = \frac{1}{2} Var\left\{F(x_i) - F(x_{i+h})\right\} \quad (6.2)$$

where $\gamma(h)$ is the estimated variance between two observed data points, h is the distance between two observed data points and $F(x)$ semivariogram function.

The semivariogram function is derived based on the original data. As shown in the Table 6.1, the 'stable function' model with smallest RMSE and mean error was chosen to represent the spatial dependency of the DEM surface, in which the major range is 401.470 metres (where the blue curve begins to level off), and the partial sill is 8.803 metres (Figure 6.2).

Table 6.1 Semivariogram models used for Kriging interpolation

Model	Mean error (m)	Root-Mean-Square (m)
Rational Quadratic	-0.815×10^{-3}	0.151
Gaussian	-0.100×10^{-2}	0.159
Circular	-0.242×10^{-3}	0.153
Spherical	-0.223×10^{-3}	0.153
Stable	-0.360×10^{-3}	0.151

The cross-validation shows the results of interpolation of the DEM are accurate (Figures 6.3 and 6.4). For example, the points representing the predicted and measured values are distributed intensively along the diagonal; with most of the error and standardised error points close to 0, and with a small standard deviation. One reason that high accuracy interpolation results were achieved is that Port Hedland has a low variation of gradient on the sand beach where sparse LiDAR points exist and this reduced the magnitude of elevation interpolation errors.

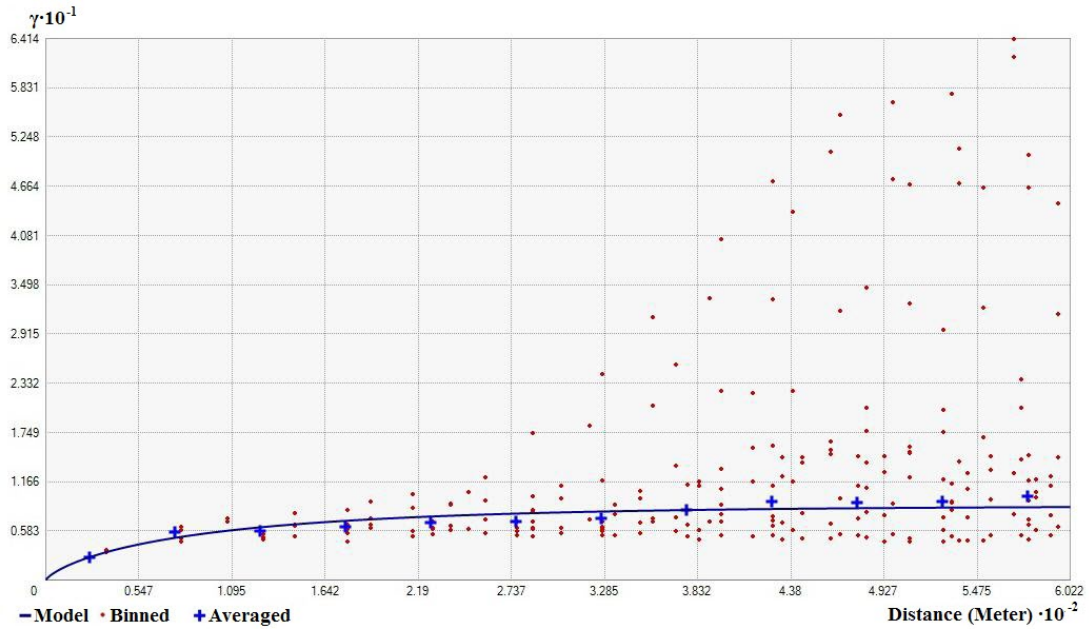

Figure 6.2 Semivariogram model representing the autocorrelation of the original LiDAR data at Port Hedland

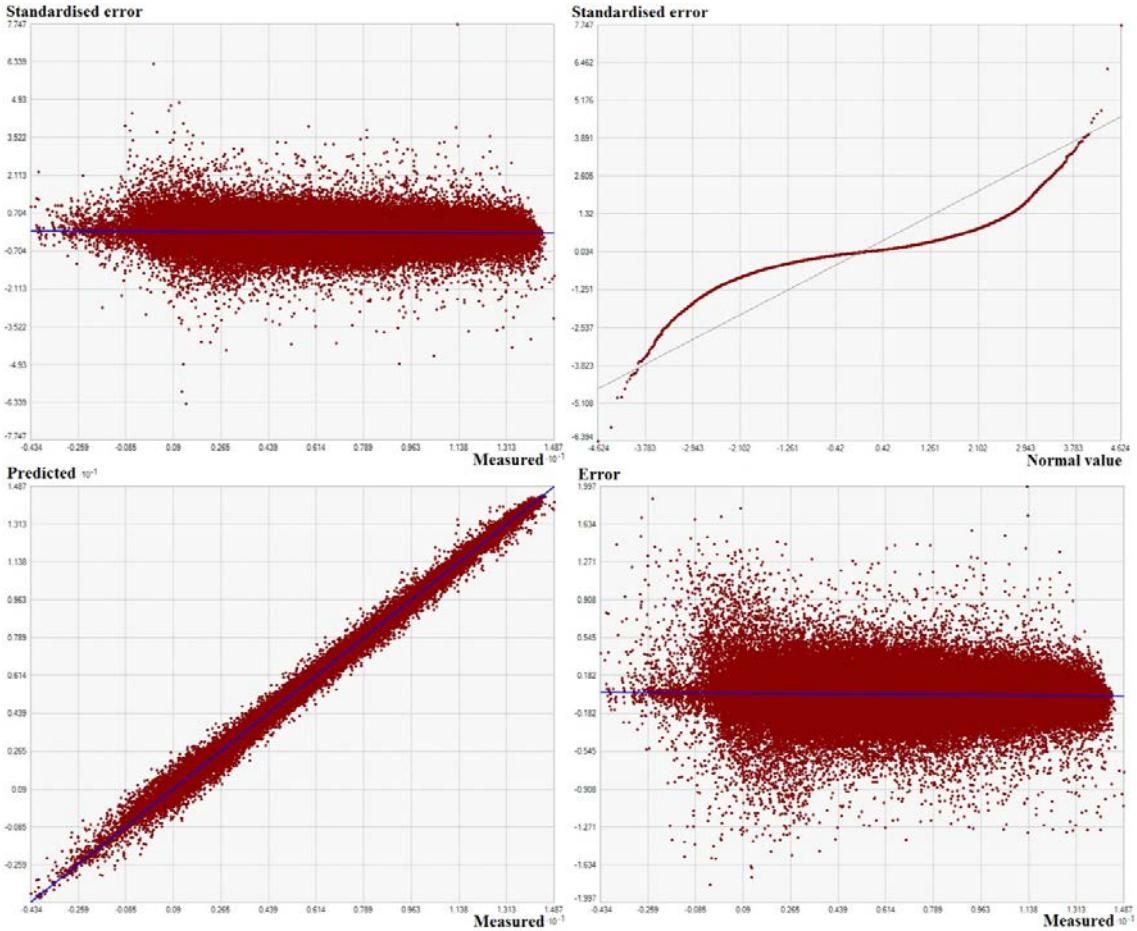

Figure 6.3 Cross-validation on the Kriging interpolation

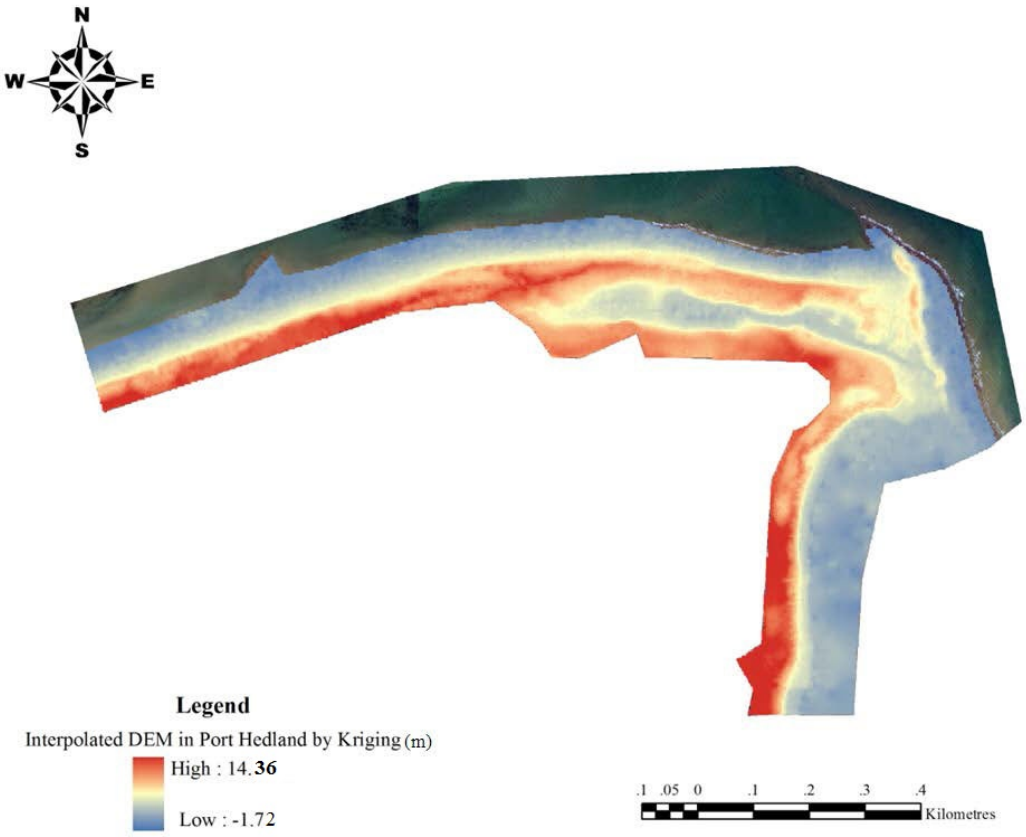

Figure 6.4 Kriging interpolated DEM at Port Hedland

6.4 Spatial Variation due to Errors Resulting from the HWM Determination Process—Precision

As mentioned in Section 2.8.3, errors or uncertainty arising from the data, pre-process or post-process, contribute to the variation of extracted HWM indicators and influence their location. Errors arising from the pre-processing, include the shoreline feature classification and swash height modelling (wave runup model) accuracy. These error types are discussed in the previous chapter. However, the random errors of the indicators derived from the DEM data and the complexity of the HWM indicators, which contribute to the post-process errors, are still unexamined.

In this research, the influence of random error is studied using the Monte Carlo simulation and spatial autocorrelation methods. When the HWM indicators are drawn on the map, spatial variation of the location of the HWM indicators may occur due to the quality/accuracy of the DEM and the complexity of the indicators themselves. Systematic errors in the HWM determination process, such as those

relating to accuracy of the DEM, can be directly understood and evaluated. However, the effects of random errors on the position of HWM indicators and the process of drawing lines on maps have not been sufficiently analysed in previous research. This problem is explored in this chapter using the Monte Carlo simulation method.

6.4.1 Conditional Simulation of DEM Values

The Monte Carlo simulation method is based on the assumption that only random errors are present and that they are normally distributed (Gaussian distribution) with a constant mean value and standard deviation. In this research, for each pixel *i*, the mean and the standard deviation are derived from the simulated DEM data and are expressed respectively as:

$$\bar{U}(p_{ij}^{SIM}) = \sum_{j=1}^{m} p_{ij}^{SIM} \Big/ m \tag{6.3}$$

$$\sigma_U(p_{ij}^{SIM}) = \sqrt{\sum_{j=1}^{m} \left(p_{ij}^{SIM} - \bar{U}(p_{ij}^{SIM}) \right)^2 \Big/ m-1} \tag{6.4}$$

in which *m* is the total number of simulations (here *m*=100), and p_{ij}^{SIM} represents the simulated DEM value for pixel *i* at time *j*. To obtain more realistic random simulation results, the following condition is implicit: that the simulated elevation values, on average, are equal to the elevation values of the original DEM with the standard deviation equal to the given accuracy (RMSE) of the DEM.

Furthermore, the p_{ij}^{SIM} values are usually dependent on neighbouring values. Therefore the elevation simulation model also includes spatial dependency described by the spatial autocorrelation of the simulated values (Hunter and Goodchild 1997). A number of methods have been developed to model such spatial dependencies (Wechsler and Kroll 2006), including neighbourhood autocorrelation, mean spatial dependence and weight spatial dependence. In this study, weight spatial dependence was chosen and implemented in combination with the semivariogram model, because it incorporates the notion of spatial autocorrelation.

For the Monte Carlo method, 100 DEM simulations were carried out to achieve stable results (Heuvelink 2006). The corresponding indicators were re-extracted from

the 100 DEM simulates, and compared with the original DEM pixels intersected with the position of the HWM indicators by the RMSE. This is one of the most common tools to measure the derived simulation differences from the original data (NOAA Coastal Services Center 2011).

6.4.2 The Effects of DEM Random Errors on Derived HWM Indicators

In comparison to the effect of systematic DEM error on the HWM indicators, the random error (expressed as spatial uncertainty) contributed less to the spatial variation (Tables 6.2 and 6.3). As indicated in previous studies (Barber and Shortridge 2005; Vaze and Teng 2007), uncertainty analysis is not necessary for high quality LiDAR DEM data, because of the high accuracy of the data. However, this study shows that uncertainty may lead to spatial variations in the derived results—both large and small.

The first eight simulated DEMs for both the South Fremantle and Port Headland study areas are illustrated and compared with the original DEM in Figures 6.5 and 6.6. Each map in the figures represents one possibility that the DEM may exist, due to the uncertainties, which is not necessarily the same as the original DEM. The apparent spatial variation from such uncertainty is not always small, especially at Port Hedland (Tables 6.2 and 6.3). For example, the uncertainty for the DoT position (0.1140 m) is as large as 57% of the systematic error. This occurs for two reasons: firstly, the accuracy of the DEM at Port Hedland is not as high as at South Fremantle, and this would increase the variation of the simulation for each pixel; and secondly, the coastal land surface at Port Hedland is not as smooth as that at South Fremantle.

Table 6.2 Spatial variation of HWM lines based on different indicators from determination process (precision) at South Fremantle study area

HWM indicators	Classification accuracy	Model accuracy (m)	DSM error (m)		Topographic complexity (FD)	Precision (m)
			Accuracy	Random		
	Pre-process		Post-process			
HWL	1.0000	N/A	0.1500	0.0020	1.0032	0.1525
MHHW	N/A	N/A	0.1500	0.0020	1.0032	0.1525
Landgate	N/A	N/A	0.1500	0.0020	1.0032	0.1525
DoT	N/A	N/A	0.1500	0.0010	1.0582	0.1598
SCTP	N/A	N/A	0.1500	0.0010	1.0127	0.1529
SCSP	N/A	0.38	0.1500	0.0090	1.0021	0.5401
Dune toe line	1.0000	N/A	0.1500	0.0020	1.0836	0.1647
Vegetation line	1.1370	N/A	0.1500	0.0050	1.1840	0.2087
Average						0.2105

Table 6.3 Spatial variation of HWM lines based on different indicators from determination process (precision) at Port Hedland study area

HWM indicators	Classification accuracy	Model accuracy (m)	DSM error (m)		Topographic complexity (FD)	Precision (m)
			Accuracy	Random		
	Pre-process		Post-process			
HWL	1.1140	N/A	0.2000	0.1040	1.1010	0.3729
MHWS	N/A	N/A	0.2000	0.0690	1.0860	0.2921
Landgate	N/A	N/A	0.2000	0.0790	1.0860	0.3030
DoT	N/A	N/A	0.2000	0.1140	1.0890	0.3419
SCTP	N/A	N/A	0.2000	0.0300	1.1840	0.2723
SCSP	N/A	0.3800	0.2000	0.0240	1.1900	0.7188
Dune toe line	1.1860	N/A	0.2000	0.0030	1.1670	0.2810
Vegetation line	1.4810	N/A	0.2000	0.0520	1.1920	0.4449
Average						0.3784

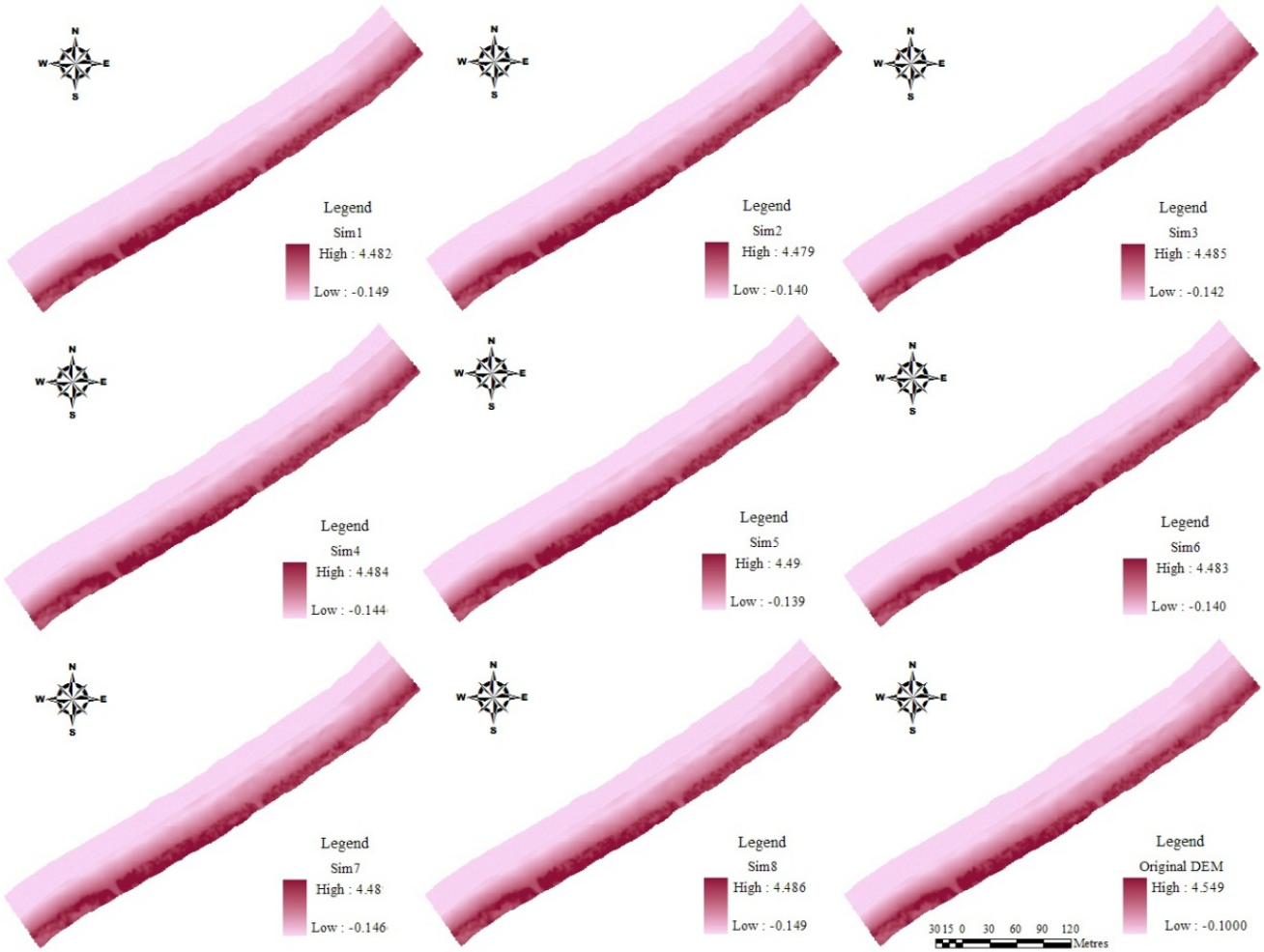

Figure 6.5 Maps of the DEM at South Fremantle (lower-right) and its first eight conditional simulations

Figure 6.6 Maps of the DEM at Port Hedland (lower-right) and its first eight conditional simulations

6.4.3 Fractal Dimension (FD) of HWM Indicators

The FD of the HWM indicators is estimated using the log-log relationship (Theiler 1990):

$$\text{Log}(L(s))=(1\text{-}D)\text{Log}(s)+b \tag{6.5}$$

where $L(s) = N \cdot s$ is the length of the HWM line along a coast, which equals the length of a spatial unit s multiplied by N, the number of units needed to cover the complete HWM line. As the spatial unit decreases in length, the length of the HWM line increases. D is the fractal dimension and b is the residual. As indicated by Mandelbrot (1982), the value (1-D) is assigned to the slope of Equation 6.5, which can be estimated using Least Squares regression for the length of the HWM line and the combined length of all spatial units used.

As the FD of the HWM line increases (e.g. close to 2), the line shows less spatial dependence and becomes more unpredictable; whereas a value approaching 1 indicates there exists a direct spatial relation in the distribution of the HWM line (Palmer 1988). Tables 6.2 and 6.3 show the FD of the HWM lines corresponding to the different indicators selected.

From the results obtained it can be seen that the FD of the vegetation line in both study areas was found to be the largest due to the highly dispersed distribution of the vegetation zone, indicating the highest spatial complexity and variability. Although widely adopted as the position of the HWM, the results show that the vegetation line may not be the most suitable indicator due to its high variability. Figures 6.7 and 6.8 show that the FD will increase as the elevation of the HWM increases and the position located more landward.

However, the FD of the DoT HWM line at South Fremantle was identified higher than the other indicators around it. This does not follow the general trend of the FD. This may be due to the fact that the position of the DoT HWM indictor is located around the berm. The high variation of the berm elevation causes a larger uncertainty of the position of the HWM line around it. The Landgate and DoT HWM lines, as well as, MHWS at Port Hedland, also have smaller FD than HWM lines derived from the other indicators.

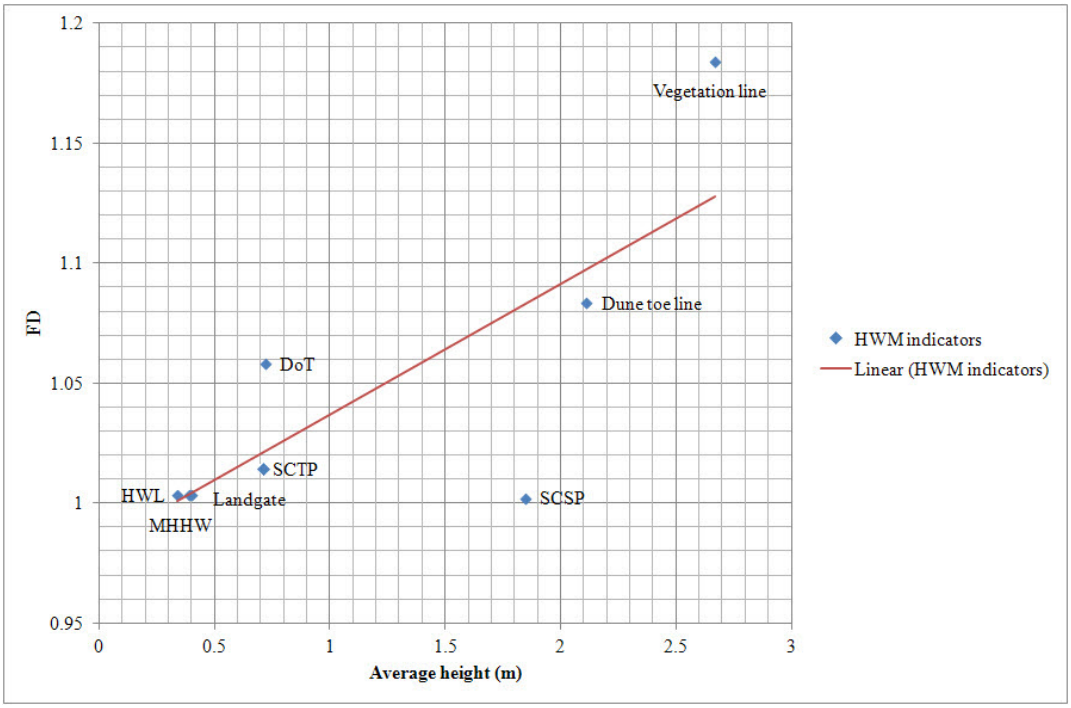

Figure 6.7 FD of HWM indicators at South Fremantle

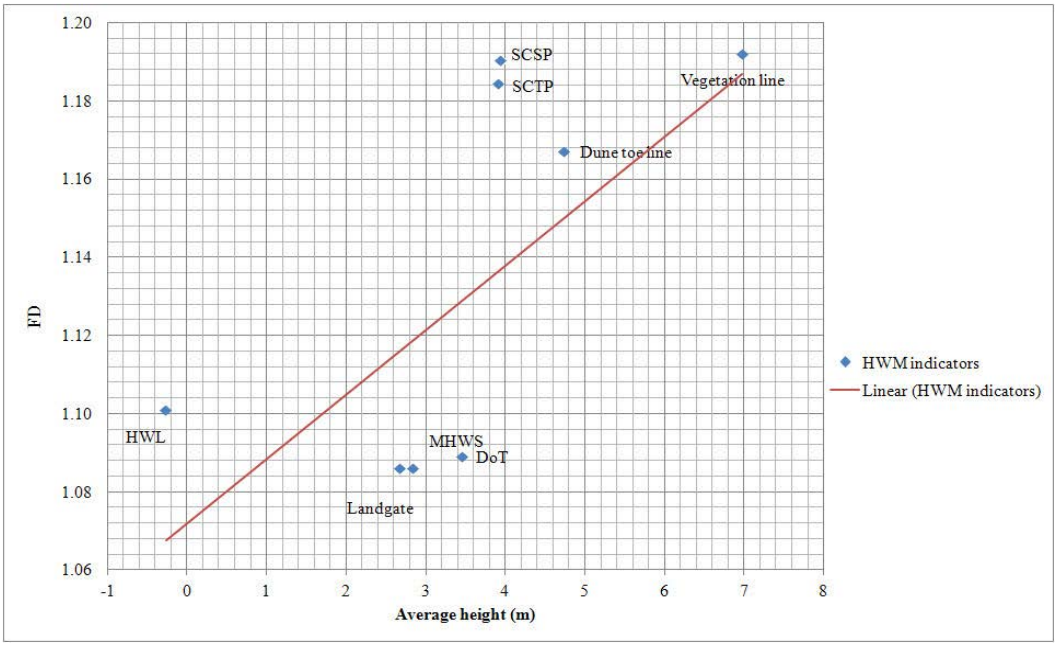

Figure 6.8 FD of HWM indicators at Port Hedland

After determining and assessing all the factors that govern the precision of an extracted HWM line during the determination process, the final spatial variation (precision) was obtained by totalling the absolute error and multiplying this with the relative errors.

It can be concluded that the two most important sources of spatial variation of the HWM arise from the accuracy of the model used to estimate the wave runup heights and DEM error, which made SCSP more variable over space than the other indicators (Tables 6.2 and 6.3).

Similarly, the high value on the classification accuracy test, topographic complexity (e.g. FD), and even uncertainty in the DEM, make the identification of the vegetation line on the beach difficult.

The variation for all the other indicators is less than the average level, and the MHWS, MHHW, SCTP and dune toe line resulted in higher levels of precision in the determination at both study areas. In general, the variation arising from the determination at Port Hedland is larger than that at South Fremantle, due to the higher variation of the coastal morphology and onshore feature distribution.

6.5 Seasonal Variation of the HWM Position—Stability

In this research, the positions of the lines for each HWM indicator were first derived separately from the two DEMs representing summer and winter coastal morphology. The seasonal variation (winter and summer) of the corresponding lines representing the HWM positions was evaluated by measuring spatial distances between them using the extended Hausdorff distance.

6.5.1 Extended Hausdorff Distance

The Hausdorff distance is a max-min distance used in image analysis and was introduced by Huttenlocher (1993). Subsequently, Hangouët (1995) applied this method in the study of spatial variation of vector features in GIS. Given two finite point sets $A=\{a_1,\cdots,a_p\}$ and $B=\{b_1,\cdots,b_q\}$, defining a vector feature, the Hausdorff distance is defined as:

$$H(A,B)=\max\{h(A,B),h(B,A)\} \tag{6.6}$$

where

$$h(A,B)=\sup_{p_a\in A}\left\{\inf_{p_b\in B}\|p_a-p_b\|\right\} \tag{6.7}$$

and

$$h(B,A) = \sup_{p_b \in B}\left\{\inf_{p_a \in A}\left\|p_a - p_b\right\|\right\} \tag{6.8}$$

in which p_a and p_b are the points in the point sets *A* and *B*, respectively, while $\|\bullet\|$ represents 'some underlying metric between points of the sets *A* and *B*' (Min *et al.* 2007).

In this study, the metric used is the classical Euclidean distance. *p* refers to the segment, and *A* and *B* are two segment sets. The length of the segment corresponds to the horizontal accuracy of the DEMs from which the HWM lines are derived. Therefore, the first step to calculate the Hausdorff distance between lines *l* and *n* is to divide each line into segments, then determine the shortest distance from the segment of line *l* to the closest segment of the line *n*, and choose the largest value to the segment as the distance between the corresponding segments. The same process is applied to calculate the distance from line *n* to line *l*, and the larger of the two is adopted as the Hausdorff distance between the two lines.

However, sudden changes of the shape of the lines may significantly influence the calculation. This is a retreat problem for coastal boundaries as the coastal morphology will often protrude and retreat. Thus, the extended Hausdorff distance (Min *et al.* 2007) was applied in this research to mitigate this problem. The extended Hausdorff distance is given by Min *et al.* (2007):

$$H^{f_1 f_2}(A,B) = \max\left\{h^{f_1}(A,B), h^{f_2}(B,A)\right\} \tag{6.9}$$

where

$$h^{f_1}(A,B) = \min\left\{\varepsilon_i : f_1 = \vartheta\left(\left(B \oplus S(\varepsilon_i)\right) \cap A\right) \Big/ \vartheta(A)\right\} \tag{6.10}$$

and

$$h^{f_2}(B,A) = \min\left\{\varepsilon_j : f_2 = \vartheta\left(\left(A \oplus S(\varepsilon_j)\right) \cap B\right) \Big/ \vartheta(B)\right\} \tag{6.11}$$

with ε_i and ε_j indicating the buffer width ($S(\bullet)$) for line *B* and line *A*, respectively; while $\vartheta(\bullet)$ is a metric function to measure the length of a line. For example, $\vartheta\left(\left(B \oplus S(\varepsilon_i)\right) \cap A\right)$ represents the length of line *A* falling inside the dilated region $\left(B \oplus S(\varepsilon_i)\right)$. For $f_1 = f_2 = 1$, the extended Hausdorff distance equals the Hausdorff distance as indicated by Equation 6.6; in contrast, when $f_1 = f_2 = 0$, the extended Hausdorff distance measures the shortest distance between the two lines. In this study, both f_1 and f_2 are assigned the value of 0.5, thus the so called median Hausdorff distance, is obtained. This is recognised as a robust measure by Min *et al.* (2007) and is applied as a metric to evaluate the variation of the position of the HWM lines due to the change in coastal morphology over time (in this instance, between summer and winter).

6.5.2 Seasonal Variation of HWM Indicators' Position

Tables 6.4 and 6.5 illustrate the seasonal variation of position of the HWM indicators at the two study areas. Generally, it can be estimated from the tables that seasonal variation of the HWM position is almost one order of magnitude larger than the spatial variation due to errors from the determination process. Furthermore, there is a larger seasonal variation of the position of the HWM indicators at South Fremantle than at Port Hedland. Although, the data used to analyse the variation at Port Hedland have a temporal gap of 14 years (1995 to 2009) between the summer and winter lines evaluated.

From Table 6.4 and Figure 6.9, it can also be estimated that at South Fremantle the sediment accumulation in the low wave runoff summer months makes the HWM lines 'lower' (moving seaward) than the ones in the high wave runoff winter months. This situation is more apparent on the backshore where indicators of DoT and SCTP lie. In contrast, the occurrence of highly irregular morphology at the foreshore, due to the high energy swash in the winter season, makes the HWM lines lying in this zone not as 'straight' as during the summer time. Three indicators, SCSP, dune toe line and vegetation line, which are close to the vegetation zone, show least temporal variation that is mainly due to the low level of the swash probability.

Table 6.4 Seasonal variation of the position of HWM indicators (stability) at South Fremantle

HWM indicators	Stability (Median Hausdorff distance; m)
HWL	5.91
MHHW	4.61
Landgate	6.50
DoT	9.14
SCTP	8.07
SCSP	3.00
Dune toe line	2.16
Vegetation line	1.70
Average	5.14

Table 6.5 Seasonal variation of the position of HWM indicators (stability) at Port Hedland

HWM indicators	Stability (Median Hausdorff distance; m)
HWL	9.08
MHWS	1.11
Landgate	1.12
DoT	3.13
SCTP	2.21
SCSP	2.17
Dune toe line	1.47
Vegetation line	3.38
Average	2.96

At Port Hedland, the horizontal position offsets of the HWM lines for all indicators are less than 4 m between summer and winter, with the exception of HWL (Table 6.5 and Figure 6.10). Although, the rocky coastal zone at Port Hedland may stabilise the HWM lines, the different effect of tide and wave activity on the coastal morphology and sediment transport is another factor explaining the low variation. This has already been shown by Davis Jr (1985), who states that tide, compared with wave

breaks, plays a passive and indirect role in the beach evolution and its change in profile.

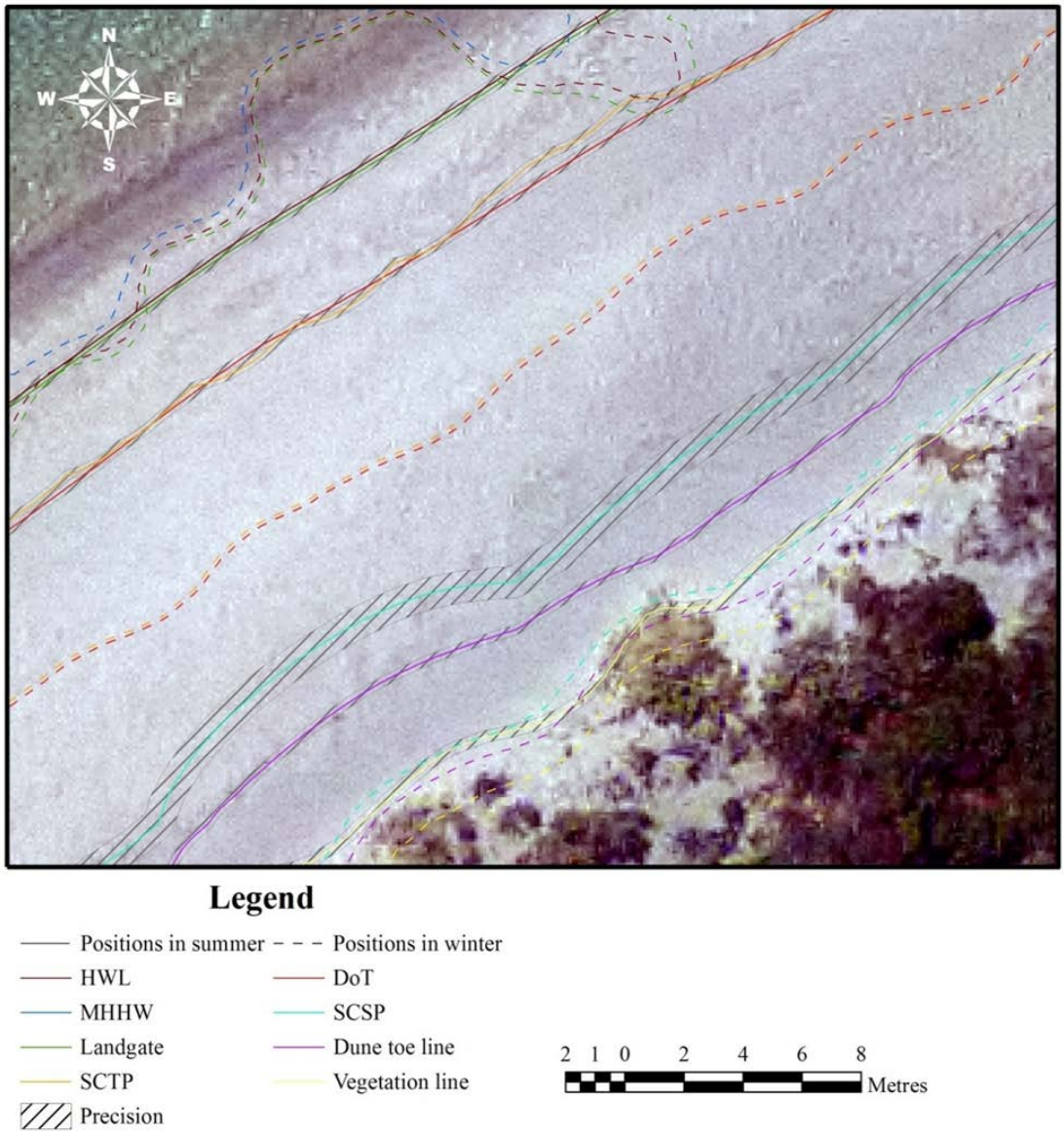

Figure 6.9 Zoom in one detailed area for spatial and temporal variation of HWM indicators at South Fremantle

According to Masselink and Pattiaratchi (2001), seasonal beach cycles are mainly due to the seasonal variation of the wave energy level. This contrasts with the high energy wave-dominated Coogee Beach at South Fremantle, whereas the wave energy at the tide-dominated Cooke Point at Port Hedland is much lower (Short 2004). This may partly explain why there is less apparent seasonal variation of the HWM at Port Hedland. The HWL shows the largest horizontal offset between the two seasons at

both study areas. This concurs with the conclusions of Pajak and Leatherman (2002) that the ‘HWL position can be highly variable’. In contrast, the position of the dune toe shows small variation consistently at both study areas.

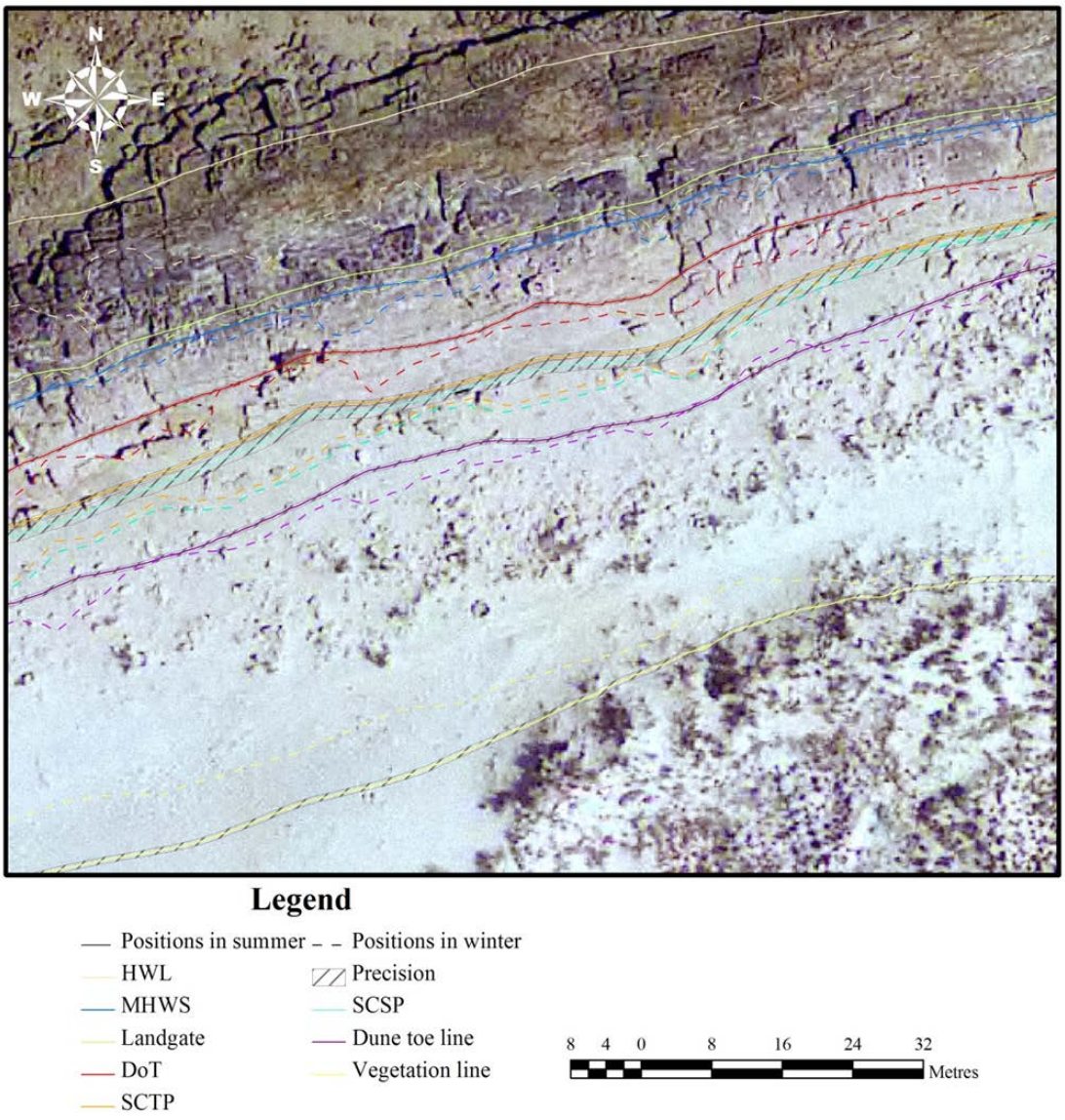

Figure 6.10 Zoom in one detailed area for spatial and temporal variation of HWM indicators at Port Hedland

6.6 Summary

This chapter has evaluated the spatial and temporal variation of HWM lines derived from different HWM indicators using image analysis techniques. The study shows that the seasonal variation of the HWM position is almost one order of magnitude larger than the spatial variation due to errors from the determination process. To visually illustrate the variation of the HWM line corresponding to the different

indicators for both the spatial and temporal view, the variation maps have been presented and analysed.

Results of the study in this chapter indicate that the dune toe line is the best estimate of the HWM position in terms of the small variation over both time and space, while SCSP and HWL are more variable than the other indicators from the point of view of precision and stability, respectively.

This chapter only focuses on the position of the HWM in terms of spatial and temporal variation. This position reflects the precision and the stability of the HWM. Other factors, such as probabilistic estimates (e.g. the risk of inundation), should also be included in the process of establishing the HWM. This approach is explained in the next chapter. Probabilistic estimates and other decision factors derived from experts from different professional fields, such as coastal management and coastal planning, are included in a multi-criteria decision model for HWM determination.

CHAPTER 7 DECISION MAKING ON THE POSITION OF THE HWM

7.1 Introduction

This chapter applies a Multi-Criteria Decision Making (MCDM) model, specifically a pairwise-comparison method (PCM) and weighted sum model (WSM), to evaluate the HWM indicators based on relevant criteria including stability and precision, assessed in the previous chapter, and inundation risk. The results are significant and show that different HWM indicators are suitable for different implementation purposes, such as coastal property management and coastal hazards planning.

7.2 Background

In Section 2.10, the importance of two criteria for the coastal boundary determination—stability and precision, was addressed. In addition, land use, population and coastal properties at a risk of inundation have been discussed in a number of previous studies (Doukakis 2005; Granger *et al.* 1999; Marfai and King 2008). Thus, the inundation risk for the HWM is also an important factor that needs to be considered for HWM determination from both a coastal property management and a coastal hazards planning point of view. HWM determination is inherently complex, involving different decision makers with conflicting priorities and different preferences on the criteria of HWM determination; therefore, MCDM can help to manage this problem by integrating dynamic information and judgements in a systematic framework (Levy *et al.* 2007), and providing evaluation results on HWM indicators as references for the HWM.

MCDM methods are designed for understanding a process of decision making with a number of quantifiable or non-quantifiable decision criteria (Pohekar and Ramachandran 2004). One of the most traditional and common examples is single criterion decision making, which is designed to maximise the benefits with minimisation of cost (Barzilai 1998), but is insufficient when dealing with complex problems (Ehrgott and Gandibleux 2002). Furthermore, in most cases, different groups with different points of view, which should be resolved within a single framework by understanding and compromising, are involved in the decision-making process (Pohekar and Ramachandran 2004).

MCDM can be divided into two different groups: multi-objective decision making (MODM) and multi-attribute decision making (MADM) (Mendoza and Martins 2006). The most significant difference between the two is the decision space associated with research problems; specifically, the former is continuous, while the latter is discrete (Triantaphyllou *et al.* 1998). Determination of the HWM is classified as a process of MADM, in which the HWM indicators can be considered as a number of alternatives to be evaluated against a set of criteria. The best alternative is chosen as the ideal HWM position by comparing the alternatives with respect to every criteria. A number of methods have been developed for such a decision-making process (Table 7.1), and the Weighted-sum Model (WSM) was used in this research because it is a straightforward method that can be easily applied, and produces quality results. Furthermore, the evaluation result for the WSM is in the form of absolute values for each alternative, which makes it possible for direct comparison of the HWM indicators from two different study areas. The drawback of inconsistent units in WSM can be overcome by a procedure of normalisation.

Table 7.1 Comparison of the most commonly used methods for MADM

Method	Main feature	Advantage	Disadvantage
Weighted-sum model (WSM)	This method is based on the assumption of additive utility (Martins *et al.* 1996).	The most straightforward and practical method.	The additive utility assumption does not apply when combining different units of criteria (Triantaphyllou *et al.* 1998).
Weighted-product model (WPM)	Any unit of measure is eliminated in the calculation (Triantaphyllou and Lin 1996).	Dimensionless analysis (Triantaphyllou *et al.* 1998).	The final calculation does not provide absolute evaluation values for each alternative.
Analytic hierarchy process (AHP)	This method decomposes the decision problem into a hierarchy system of sub-problems, each of which is analysed in terms of each criterion (Mendoza and Sprouse 1989; Phua and Minowa 2005).	Hierarchical structure analysis of the criteria.	The potential of internal inconsistency may exist in the AHP (Hu *et al.* 2010).
Preference ranking organization method for enrichment evaluation (PROMETHEE)	It is one type of outranking method, and requires the concordance and discordance indices (Kangas *et al.* 2001; Schmoldt *et al.* 2001).	Flexible selection of preference functions and indifference thresholds (Silva *et al.* 2010).	The final calculation does not provide absolute evaluation values for each alternative.
Elimination and choice translating reality (ELECTRE)	It is one type of outranking method, and each criterion associates a preference function (Kangas *et al.* 2001; Laukkanen *et al.* 2002).	Good performance in the decision making problem with few criteria, but with a large number of alternatives (Goicoecha *et al.* 1982).	The ideal alternative sometimes cannot be identified (Triantaphyllou *et al.* 1998).
Multi-attribute utility theory (MAUT)	The utility function, which indicates the decision maker's preferences, is defined over a number of attributes included in the method (Pukkala 1998).	The transparent aggregation procedure can be easily understood by decision makers (Von Winterfeldt and Fischer 1975).	The decision makers are required to have knowledge of probability theory (Tanadtang *et al.* 2005).

The MCDM may also integrate with other intelligent algorithms, such as fuzzy sets, to estimate the inherent uncertain impacts or preferences (Cheng *et al.* 2009; Kahraman *et al.* 2003; Opricovic 2011; Shemshadi *et al.* 2011), but this is not necessary and is out of the scope of this study.

To evaluate the HWM indicators with WSM, two more steps are required after establishing the criteria: one is to determine the weights for each criterion, and the other is to rank and standardise the HWM indicators for each criterion. Determination of the weights of criteria has been recognised as one of the challenges in MADM (Jassbi and Khanmohammadi 2010). PCM has shown its advantages in ranking and rating the criteria in the decision-making model (Kok and Lootsma 1985). Compared with the most common ranking and rating method, it is more accurate and easier to express one's judgement on only two criteria rather than on all at the same time (Ishizaka and Labib 2011). However, recent studies show inconsistency and contradiction may exist in the matrices of the pairwise comparison on different criteria (Alonso and Lamata 2006; Kwiesielewicz and van Uden 2004), due to the complex nature of the decision process or the limitation of the knowledge and experiences of experts (Ergu *et al.* 2011). A number of improvements on the pairwise comparison, such as separating the subset of inconsistent matrices from the original (Kwiesielewicz and van Uden 2004) or integrating the theory of fuzzy logic with pairwise-comparison matrices (Jaganathan *et al.* 2007), have been developed to refine irrational weights calculation when the comparison matrix is not perfectly consistent.

7.3 Multi-Criteria Decision Making on Evaluation of HWM Indicators

In this study, the HWM indicators will be evaluated by the MCDM based on three criteria—stability, precision and inundation risk, and the HWM indicators are considered as the alternatives. The HWM indicators were evaluated for two different purposes—coastal property management and coastal hazards planning in terms of the criterion of inundation risk. From a property management point of view, it means property at risk of inundation from the tide only; while from a hazards planning point of view also takes the wave runup into account (Figure 7.1).

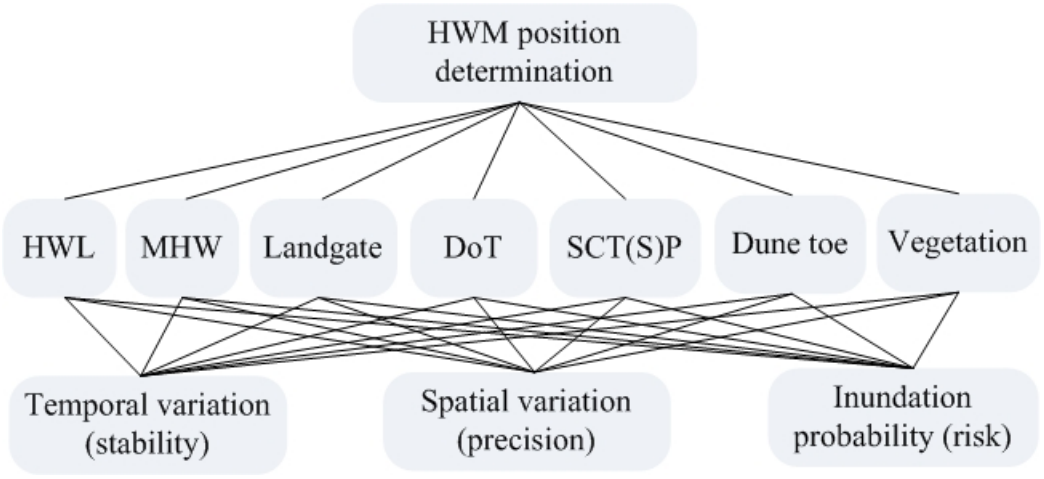

Figure 7.1 Illustration on the HWM determination structure

7.3.1 Criteria Weights Determination by Pairwise-Comparison Method (PCM)

In this study, criteria weights for HWM determination were assessed by eight experts from both industry and academia with a range of backgrounds, including coastal planning, land property management, cartography and coastal risk management. The information sheet and questionnaire (Appendix II) were designed to collect the perspective views of experts on the importance of different criteria for HWM determination, which is in the format of PCM:

$$C = [c_{kl}] = \begin{bmatrix} 1 & 1/c_{21} & 1/c_{31} \\ c_{21} & 1 & 1/c_{32} \\ c_{31} & c_{32} & 1 \end{bmatrix} \tag{7.1}$$

where c_{kl} indicates the ratio of m_k / m_l, and m_k and m_l represent the importance of criteria k and l in the view of experts, respectively, which range from 1 to 9 (Appendix II). According to the Perron-Frobenius Theorem (Perron 1907), a positive eigen value $\lambda_{\max}$, which is greater than or equal to all the other eigen values, exists to ensure there is a corresponding positive eigen vector W satisfying the equation:

$$CW = \lambda_{\max} W \tag{7.2}$$

where the positive eigen vector W is equal to the weights vector for the three criteria in the WSM, and in the form of $[w_1, w_2, w_3]'$ in this study.

However, as estimated by Jaganathan *et al.* (2007), in a practical situation, it is highly unlikely to expect all the experts can provide consistent answers in their pairwise-comparison matrixes; therefore, the consistency check is necessary to ensure the judgements of the experts are neither random nor self-illogical (Kwiesielewicz and van Uden 2004).

The method used to assess the consistency of PCM is defined as (Saaty 1980):

$$\text{Consistency Ratio (CR)} = \frac{\text{CI}}{\text{RI}} \tag{7.3}$$

where RI refers to the random index, which has been evaluated by a number of previous studies (Alonso and Lamata 2006); while CI means the consistency index and defined as (Saaty 1980):

$$\text{CI} = \frac{\lambda_{\max} - n}{(n-1)} \tag{7.4}$$

where n indicates the size of the PCM. If CR < 0.10, the ratio indicates a reasonable level of consistency in the data in the pairwise-comparison matrices; otherwise, it is considered there is inconsistent judgement. In most cases, although some of the questionnaire feedback has been shown to be inconsistent, the information in the experts' feedback may still be useful for the evaluation of each criterion; therefore, adjustments to the inconsistent pairwise-comparison matrices were conducted to ensure all of the feedback can be included in the determination of the criteria weights.

To improve the consistency of the comparison matrix, a simple method introduced by Ergu *et al.* (2011), which was developed based on the definition of consistency in PCM and requires a series of transforms using matrix multiplication and vector dot products, was applied in this study. Generally, two steps are involved in the method: (1) indentifying the inconsistent element in the comparison matrix, and (2) adjusting the inconsistent elements with a slight change of the experts' logical relationship on the criteria.

In this study, RI is equal to 0.525, as this number has been tested as the most stable value under large numbers of random simulations (Aguaron and Moreno-Jiménez 2003; Alonso and Lamata 2006). For the eight feedback responses, three are

identified as inconsistent and adjusted using the method introduced by Ergu *et al.* (2011) without significantly changing the logical relationship between the criteria (Table 7.1). After the adjustment, the average of the weights for each criterion from the eight experts (ensuring the CRs are less than 0.1) was calculated as the final criteria weights in the WSM.

Table 7.2 Criteria weights determination by PCM and their CR

		Stability	**Precision**	**Inundation risk**	**CR**
Feedback1	*original*	0.225	0.638	0.137	0.330>0.1
	improved	0.192	0.677	0.131	0.080<0.1
Feedback2	*original*	0.106	0.261	0.633	0.040<0.1
	improved				
Feedback3	*original*	0.072	0.232	0.697	0.180>0.1
	improved	0.078	0.234	0.688	0.070<0.1
Feedback4	*original*	0.261	0.633	0.106	0.040<0.1
	improved				
Feedback5	*original*	0.062	0.701	0.236	0.070<0.1
	improved				
Feedback6	*original*	0.072	0.697	0.232	0.180>0.1
	improved	0.078	0.688	0.234	0.070<0.1
Feedback7	*original*	0.243	0.669	0.088	0.010<0.1
	improved				
Feedback8	*original*	0.071	0.748	0.180	0.030<0.1
	improved				
Average	CR<0.1	**0.136**	**0.576**	**0.287**	

7.3.2 Ranking and Normalising the Value of Each Criteria for HWM Indicators

The spatial and temporal variations (precision and stability) have been evaluated for each HWM indicator as two criteria for HWM determination in the previous chapter, but the inundation risk was left undiscussed. For the two different purposes, the interpretation of risk can be dissimilar: when it refers to the coastal property management or for hazards planning (Section 2.5). The risk for the HWM means the chance of a property at risk of inundation from the tidal water and wave runup, respectively, over a long period of time. In this study, due to the availability of wave data, the statistics on the wave runup and the corresponding tidal water were calculated for approximately 10 years in both study areas. In this period, the highest levels that wave runup and tidal water reached were recognised as the ‘benchmark’

of the inundation risk for coastal hazard planning and coastal property management, respectively. The HWM indicators above this level are considered further from the optimum position for minimising the inundation risk and maximising the usage of coastal land for management or planning purposes; therefore, the further away from this level, the lower they would be ranked. To include the ranking of inundation risk as one criterion in the WSM, a normalisation step is required:

$$IR_i = \frac{r_i + 1}{\sum (r_i + 1)} \tag{7.5}$$

where IR_i is the normalised ranking for the inundation risk, and r_i indicates the original ranking for the HWM indicator *i*. The final results for the inundation risk ranking for the HWM indicators at the two study areas are presented in Tables 7.3 and 7.4. Before applying WSM in the calculation, normalisation is also required for the spatial and temporal variations (stability and precision) of each HWM indicator, which have been calculated in the previous chapter (Table 7.5).

Table 7.3 Ranks and their normalisation of the inundation risk for each HWM indicator at South Fremantle

HWM indicator	Height (m)	Ranking for planning	After normalisation	Ranking for management	After normalisation
No risk position		*2.62 m*		*1.20 m*	
HWL	0.39	7	0.182	5	0.136
Landgate	0.40	6	0.159	4	0.114
MHHW	0.34	8	0.205	6	0.159
DoT	0.72	4	0.114	1	0.046
SCTP	0.71	5	0.136	2	0.068
SCSP	1.79	3	0.091	3	0.091
Dune toe	2.11	2	0.068	7	0.182
Vegetation	2.67	1	0.045	8	0.205

Table 7.4 Ranks and their normalisations of the inundation risk for each HWM indicator at Port Hedland

HWM indicator	Height (m)	Ranking for planning	After normalisation	Ranking for management	After normalisation
No risk position		*5.34 m*		*3.85 m*	
HWL	1.18	8	0.205	7	0.182
Landgate	2.67	6	0.159	6	0.159
MHWS	2.83	5	0.136	5	0.136
DoT	3.46	4	0.114	3	0.091
SCTP	3.92	3	0.091	1	0.045
SCSP	3.99	2	0.068	2	0.068
Dune toe	4.48	1	0.045	4	0.114
Vegetation	8.35	7	0.182	8	0.205

Table 7.5 The normalised value for the other two criteria at two study areas

HWM indicator	Stability	Precision	Stability	Precision
	South Fremantle		*Port Hedland*	
HWL	0.141	0.119	0.318	0.125
Landgate	0.153	0.119	0.067	0.118
MHHW or MHWS	0.114	0.119	0.067	0.117
DoT	0.207	0.120	0.130	0.122
SCTP	0.185	0.119	0.101	0.115
SCSP	0.081	0.159	0.100	0.156
Dune toe	0.064	0.120	0.078	0.116
Vegetation	0.055	0.125	0.138	0.131

7.3.3 Evaluation on the HWM Indicators by WSM

WSM is one of the most common MCDMs, and has been illustrated in a number of previous studies (Triantaphyllou and Lin 1996; Triantaphyllou and Mann 1989). Two components—the weights vector for the criteria (Table 7.2) and the value on each criterion for the alternatives, which are necessary for the WSM analysis, have been calculated. The next step is to evaluate each alternative—HWM indicator—and identify the ideal HWM position for hazard planning and property management, respectively, at the two study areas. The best HWM should be minimised on the sum of the three criteria values—stability, precision and the inundation risk, which can be defined as (Fishburn 1967):

$$P^* = \min_{M \geq i \geq 1} \sum_{j=1}^{N} c_{ij} w_j \quad (7.6)$$

where c_{ij} indicates the value of alternative i (HWM indicator i in this study) on the criterion j, and w_j refers to the weight on the criterion j. M and N are the number of alternatives and criteria, respectively. The final evaluations on all the HWM indicators are illustrated in Table 7.6.

Table 7.6 Final evaluations of the HWM indicators from the two study areas

HWM indicator	Evaluation score on planning	Evaluation score on management	Evaluation score on planning	Evaluation score on management
	South Fremantle		*Port Hedland*	
HWL	0.1400	0.1268	0.1741	0.1675
Landgate	0.1350	0.1221	0.1227	0.1227
MHHW or MHWS	0.1429	0.1297	0.1155	0.1155
DoT	0.1300	**0.1103**	0.1207	0.1141
SCTP	0.1327	**0.1133**	**0.1061**	**0.0929**
SCSP	0.1287	0.1287	0.1230	0.1230
Dune toe	**0.0973**	0.1301	**0.0903**	**0.1101**
Vegetation	**0.0924**	0.1383	0.1465	0.1531

* and * represent the best and second best HWM indicators, respectively.

7.4 Discussion of the Position of the HWM

HWM determination depends on the implementation purpose. In this study, two purposes were considered: property management and hazards planning. The difference between them lies in whether the effect of wave runup should be included or only the effect of tidal water should be considered, which is reflected in the differences in the HWM indicators ranking for the inundation risk. From Table 7.6, it can be estimated that such a perspective does have an effect on the variation of the HWM position for these different purposes, and such differences are more significant at South Fremantle, which is a high energy beach and is dominated by the wave effect.

7.4.1 For Coastal Property Management

From the view of consistency, SCTP is the ideal HWM indicator for property management purposes, as it was identified to be a good indicator at both of the study areas. The SCTP level was calculated as the significant high tide level on the beach by applying the theory of spatial continuity of the tide probability on the beach, and thereby integrating the characteristics of the land and water system as a whole. However, the limitation of using this indicator as the HWM position for coastal property management is the data availability, because the calculation of this position requires coastal morphology data, such as DEM or field survey data.

If such morphology data are not available, the HWM indicator developed by DoT is another option, as the tide information is sufficient at most standard ports for the calculation of this position. Such a level was found to be very close to the position of SCTP (Table 7.6), and was identified as a good alternative for the position of the HWM in the evaluation, especially at South Fremantle.

7.4.2 For Coastal Hazards Planning

In contrast, the most consistent and ideal HWM indicator is the position of dune toe for the purpose of coastal hazards planning. As the dune toe feature mostly presents itself on undisturbed coasts, the wide availability of methods to define dune toe means it does not need a backup or an alternative option as the HWM does for the property management. However, the results show that the vegetation, which is more apparent on the high energy, narrow and straight beach, can also be used as the HWM for hazards planning.

The results also show that the most commonly used HWM indicators—MHWS or MHHW—are acceptable as the position of the HWM, if the wave energy is small in that area, but is a less suitable option at the high energy beach, especially for hazard planning purposes.

7.5 Summary

This chapter presented the final evaluation on the position of the HWM for two different purposes—coastal property management and coastal hazards management. WSM was one method of MCDM that was used to evaluate the HWM indicators for

different purposes, which provided scientific evidence as a reference for the final determination of the HWM position. The results showed the position of dune toe is a good indicator of the HWM for coastal hazards planning, while the SCTP is more suitable for defining the position of the HWM for coastal property management purposes. If these two positions were not available due to the lack of availability of data or the obscurity of such features, the backup indicators, such as the HWM defined by the DoT method for management purposes and the vegetation line for planning purposes, can be applied as an alternative HWM position for both.

CHAPTER 8 CONCLUSIONS AND RECOMMENDATIONS

8.1 Introduction

This chapter summarises the achievements of the research into HWM determination and gives recommendations for improvements and future research. The research objectives and research questions set out for this thesis are reiterated to show how these were achieved.

Research in this thesis dealt with the development of a consistent and robust HWM determination methodology over space and time. Two primary objectives and five secondary objectives were established at the beginning of the research (Chapter 1). These objectives were achieved by a number of successive steps: The clear understanding of the HWM, in terms of its definition and difficulties in determination were illustrated in Chapter 2. Chapter 3 provided an outline of the research methodology for HWM determination. The questions regarding the data limitations, in terms of wave information and DEM, were answered in Chapter 4 and Section 6.3, respectively. Chapter 5 addressed the question of developing a model identifying the position of 'high' water by integrating both land and water information. To achieve this goal, the spatial continuity distance of swash/tidal probability for a range of HWM indicators was identified. The tidal datum-based HWM indicators and shoreline features were determined using tidal and image analysis, respectively. Also, field survey was applied to assess the confidence level for image analysis on shoreline feature identification and water level modelling. Chapters 6 and 7 assessed the HWM indicators at two study areas, with varying conditions, in a quantitative multi-criteria evaluation system in order to ensure the consistency and robustness of the determined HWM. The criteria include precision, stability and inundation risk for each HWM indicator.

8.2 Conclusions

This section highlights the major findings of the research.

8.2.1 Interpolation of Wave Data Gaps

Wave information is a crucial component of swash (wave runup) height calculations and is required to model the actual water level on the shore. However, typically there

are significant data gaps that occur in the wave records from established recording stations and these can be sizeable. These record gaps will reduce the reliability of the swash height statistic and the subsequent estimation of inundation risk. However, currently there are no wave information interpolation methods that adequately provide a solution for accurate interpolation of gaps in wave information records.

This research introduced and examined three methods for their suitability and accuracy to interpolate wave records for the periods where no data exist. These methods include, cubic spline, wavelet refined cubic spline and fractal methods. Two study areas were chosen as they have distinct wave and coastal features. In this way the robustness of the time series interpolation methods for different coastal environments could be tested.

The results of the tests showed that for the whole dataset both wavelet refined cubic spline and fractal simulation display are far more accurate than the cubic spline method. This is because the application of wavelet and fractal methods enables the interpolation process to capture more information from the irregular pattern of the time series of wave records by multi-frequency and self-similarity analysis.

However, different interpolation accuracies were obtained for the three methods when they were applied to interpolate data gaps at various scales—small, medium and large. In general, the cubic spline is more accurate when data gaps are small. The wavelet refined cubic spline method is more accurate for medium and relatively large data gap intervals. This phenomenon is more apparent at Port Hedland than at Cottesloe where the non-stationary level is higher. The fractal method proved to be a stable interpolation method for large data recording gaps.

Overall, the study demonstrated that the size of the recording gaps in the wave information time series influenced the accuracy of interpolation results. Therefore, gap size should be considered before choosing an interpolation method.

8.2.2 Identification of HWM Indicators

HWM indicators are determined from either a water or land point of view. The land-based HWM indicators are shoreline features, and were identified using image analysis in this research. The image analysis on the shoreline feature position avoids

the labour- and time-consuming work by the field survey. Whereas, the water-based HWM indicators were determined from tidal data.

The accurate classification on the high-resolution imagery is difficult to achieve by traditional pixel-based image analysis, however the object-oriented image analysis (OOIA) adopted in this study aimed to improve the accuracy of the feature classification and overcome the impact of high frequency variations in the distribution of the classification results usually found using pixel-based approaches. Features with fuzzy boundaries, such as the vegetation zone on the beach, can be identified more readily by integrating artificial intelligent algorithms, such as fuzzy logic, as part of the OOIA. Geomorphological features on the beach, such as the calculation of the gradient or curvature from the DEM, can also be incorporated into the OOIA image classification.

The classification of shoreline features at Port Hedland is less accurate than for South Fremantle. This is due to the irregularly distributed and the more diverse shoreline features present at Port Hedland. The accuracy evaluation also indicated that classification of vegetation at both study areas is less satisfactory than the classification on the other features.

Although the overall high accuracy of the OOIA image classification is sufficient to identify the shoreline features, investigations from the field surveys revealed that variations exist in the shoreline features between the positions calculated through image analysis and their corresponding positions on the Earth's surface. Such variation is mainly due to the timing of the field survey seasons, which was confirmed by the stability assessment of the position of the HWM indicators. Therefore, careful attention needs to be paid to the comparison of shoreline feature positions in two seasons, when the image analysis is applied to identify the position of the HWM.

The tidal datum-based HWM indicators on the waterside were all determined using a series of software and methods developed by the DoT, WA. Combination of the LiDAR DEM and the tidal datum information provided an efficient means of identifying the position of tidal datum-based HWM indicators on the coast.

8.2.3 Development of a New HWM Determination using the Theory of Spatial Continuity of Swash/Tidal Probability

Two new methods to determine HWM by integrating both land and water information were introduced in this research. The methods determine the position of the HWM based on the spatial continuity of swash probability (SCSP) or spatial continuity of tidal probability (SCTP) for a range of HWM indicators that are either land-based or water-based. The water information refers to the cumulative distribution of swash (wave runup) and tidal heights abstracted from long-term records of wave and tide information; while the land information is indicated by the spatial relationship among the HWM indicators derived from image analysis of aerial photographs and DEM.

The locations, indicating 'significant' high tide/swash, were determined by identifying the SCSP/SCTP between the lower bound sampling position (the most seaward HWM indicator) and the position where the autocorrelation of swash or tidal probability approaches zero. Compared with other semivariogram models of spatial continuity distance calculation, the Gaussian model best fits the empirical semivariogram model (observed values) to the data at the two study sites. The semivariogram indicates that SCSP is located 17.2 m and 30.9 m landward of the baseline at South Fremantle and Port Hedland, respectively; while the ranges of the semivariogram for SCTP are 4.59 m and 29.89 m, respectively.

The swash probabilities and heights of SCSP are lower but very close to the frontal dune toe at both study areas, which indicates that the position of dune toe is a reasonable indicator of the position of SCSP for coastal hazards planning when insufficient data are available to carry out more complex analysis, such as in remote areas. The positions of SCTP are very close to the position determined by the DoT's method of determining HWM at both study areas. When the land information, such as DEM representing the beach morphology, is not available; DoT's method can be a useful indicator for the position of SCTP.

8.2.4 Evaluation of the Precision of the Position of HWM Indicators

The lack of precision when determining HWM indicators may arise from uncertainties in the input data, and contributes to the variation of the HWM position.

Errors or uncertainty arising from the data, pre-process or post-process, contribute to the variation of extracted HWM indicators and influence their location. Compared with errors arising from the pre-processing, the random errors of the indicators derived from the DEM data and the complexity of the HWM indicators, which contribute to the post-process errors, are more difficult to evaluate.

To counteract this problem, random error and topographic complexity were assessed using Monte Carlo simulation and Fractal dimension techniques, respectively. Although previous studies (Barber and Shortridge 2005; Vaze and Teng 2007) indicated uncertainty analysis is not necessary for high quality LiDAR DEM data, because of the high accuracy of the data, this study shows that uncertainty may lead to spatial variations in the derived results—both large and small. Such uncertainty is more apparent at Port Hedland where the coastal land surface is not as regular as that at South Fremantle. In addition, the accuracy of the DEM at Port Hedland is not as high as at South Fremantle, and this contributes to the variation of the simulation for each pixel. However, in comparison to the effect of systematic DEM error on the HWM indicators, the random error contributed less to the spatial variation.

Although the vegetation line is widely adopted as the position of the HWM, it was identified as the HWM indicator with highest spatial complexity and variability. This is due to the highly dispersed distribution of the vegetation zone. From the analysis result of fractal dimension, this research also demonstrated that the complex beach morphology can cause a large uncertainty of the HWM position on the coast.

However, the two most important sources of spatial variation of the HWM arise from the DEM error and the accuracy of the model used to estimate the wave runup heights. Close attention needs to be paid to these two sources of errors, when the HWM is determined using DEM and wave runup height modelling.

8.2.5 Evaluation of the Stability of the Position of the HWM Indicators

Assessment of the stability of the HWM indicators relies upon a DEM representing the ground profiles of the study areas in two different seasons. However, inherent in all the monitoring techniques is the occurrence of large data gaps, especially in the early 1990s. Therefore, spatial interpolation methods are also needed to fill in these data gaps. The results in the research demonstrate that the gaps in sparse DEM data

can be satisfactorily interpolated using the Kriging method. This effect is more apparent when the approach is applied to the DEM representing the beach with a low variation of gradient.

The most significant variation of the HWM over time was identified between the summer and winter seasons. Studying the spatial variation of complex but linear objects, such as the horizontal HWM, requires the quantification of their spatial relationship. The extended Hausdorff distance measurement increases the reliability of the estimation of the stability of the HWM position over time, especially for the coastal boundaries with sudden changes of the shape.

There were smaller seasonal variations of the position of the HWM indicators at Port Hedland than were identified at South Fremantle, although the data used to analyse the variation at Port Hedland has a temporal gap of 14 years (1995 to 2009) between the summer and winter lines evaluated. This is because the rocky coastal zone at Port Hedland may stabilise the HWM lines, and the tidal-dominated coast at Port Hedland has a passive effect on the beach evolution and profile change, compared with the high energy wave-dominated beach at South Fremantle.

The analysis showed that spatial variations of the HWM due to seasonal changes were approximately one order of magnitude larger than variations due to uncertainties in the input data. This behaviour is more significant on a sandy beach with high wave energy. Of all the HWM indicators, the HWL shows the largest horizontal offset between the two seasons at both study areas. The highly variable nature of the feature makes HWL unsuitable as an indicator of the HWM position. In addition, the dune toe line is shown to be the best HWM indicator in terms of the small variation over both time and space.

8.2.6 Decision of the HWM Position

A Multi-Criteria Decision Making (MCDM) model was developed to make a final evaluation of the position of the HWM. The model included the following decision making criteria—stability, precision and inundation risk. The MCDM proved to be a suitable method for making a decision on the position of the HWM. This is because the decision making process for HWM determination is complex and the multi-

criteria were weighted differently by different authorities and experts according to their business perspective.

Inconsistent answers were identified in the pairwise-comparison matrixes during the weights determination process. The method introduced by Ergu *et al.* (2011) has proved to be effective and efficient to identify and adjust the inconsistency in their feedback.

Finally, an objective decision on the position of the HWM was made by providing a systematic evaluation model. The position of dune toe and SCTP were identified as the ideal HWM for coastal hazards planning and coastal property management purposes; while the vegetation line and the HWM defined by the DoT method were suggested as the HWM backup approaches for coastal hazards planning and coastal property management, respectively.

8.3 Summary of Contributions and Significances

This study fills the research gap of how to develop a consistent and robust HWM methodology by identifying and integrating the environmental factors from both water and land systems that influence the position of the HWM. The advantages of this methodology include: (1) all the determination processes and results are based on the quantified statistical analysis; (2) the algorithms developed to determine the HWM position are capable of providing repeatable results; (3) in the decision making stage, experts from different disciplines are involved to enhance the objectivity of the results.

8.4 Recommendations for Future Research

This section examines the limitations of the HWM determination methods in terms of data inadequacies and implementation of the methods. In addition to future improvements to the model, recommendations and directions for future research are also provided, along with opportunities for strengthening and expanding the current approach.

8.4.1 Research Data

In this study, tidal and wave records were limited to approximately 10 years. Nonetheless, it was possible to extract the variation of water levels during this period,

and the most significant tidal constituents. According to Cole (1997), however, the tidal variations can only be fully understood in 18.6 year cycles. Therefore, investigation of the impact of longer term statistics on the wave runup heights is suggested to reduce the uncertainty of results.

One of the parameters required to estimate the hourly wave runup height is the beach gradient. In reality, the coastal morphology is not stable all the time. However, due to the limitations on the time-series data representing the coastal morphology, such as field survey or DEM, the beach gradient was assumed consistent over the 10 year period. This can cause another uncertainty in the wave runup height calculation.

Furthermore, it is likely that the analysis of the stability of the HWM position will become more accurate when sufficient time series DEM images are available. In this study, the most significant component in temporal variation is the seasonal variation. Although, the effect of annual variation may not be as significant as seasonal variation, the analysis of long-term trends for annual variation, particularly when combined with the study of sea level change, is still worth conducting in the future (Church *et al.* 2006; Jones and Hayne 2002; Kay and Alder 1999; Nicholls 2002; Titus *et al.* 1991).

8.4.2 Research Methods and its Implementation

In the wave information interpolation process, the decomposed levels of wavelet method were fixed at 3, and the vertical compression ratios in the fractal method were randomly selected. The effects of the variation of these input parameters on the interpolation results require further investigation.

Furthermore, the effect of the accuracy of interpolated wave information on the wave runup modelling was not estimated. This was due to the complexity of the uncertainty propagation mechanism of the runup model.

Uncertainties may also exist in the HWM determination process. In Chapter 5, it has been estimated that the variation on the segmentation in OOIA and interval distance between cross sections can contribute to the variation on the determined HWM position. This requires further investigation.

Due to lack of available equipment and high cost of labour, the RTK field survey, applied to evaluate the shoreline features classification, was conducted only once in each study area. Ideally, the coastal zones should be observed at summer and winter times, especially for the season when the image was captured. Furthermore, because of the high standing frontal dune zone at Port Hedland, it was not possible to obtain the position information of the vegetation line. In addition, a longer time period of water level observations from the field survey is suggested, so that the validation of the wave runup model can be adequately tested.

Also, although the selected study areas represent the two most distinctive and typical coasts in Western Australia, more sites are recommended to test the consistency and the robustness of the HWM determination method. The new research would need to account for all factors that may influence the position of the HWM including modelling the long and complex coastline with various shore morphologies, weather regions, tidal features and wave activities.

8.5 Summary

The HWM is an important boundary that separates land and water. However, the position of the HWM is subject to many variables and attempts to serve multiple purposes because the determination of the HWM can be a scientific question, management question, or even a philosophical question. In this research, this question was addressed from the perspective of a spatial analysis system that integrates both water and land information, and an evaluation system based on commonly accepted criteria and under varying coastal conditions. The results of this research have significant benefits from both scientific and socio-economic perspectives.

REFERENCES

Agrawal, J. D., and M. C. Deo. 2002. On-line wave prediction. *Marine Structures* 15 (1):57-74.

Aguaron, J., and J. M. Moreno-Jiménez. 2003. The geometric consistency index: Approximated thresholds. *European Journal of Operational Research* 147 (1):137-145.

Alados, C. L., Y. Pueyo, M. L. Giner, T. Navarro, J. Escos, F. Barroso, B. Cabezudo, and J. M. Emlen. 2003. Quantitative characterization of the regressive ecological succession by fractal analysis of plant spatial patterns. *Ecological Modelling* 163 (1):1-17.

Alonso, J. A., and M. T. Lamata. 2006. Consistency in the analytic hierarchy process: A new approach. *International Journal of Uncertainty, Fuzziness and Knowledge-Based Systems* 14 (4):445-459.

Altunkaynak, A., and M. Özger. 2004. Temporal significant wave height estimation from wind speed by perceptron kalman filtering. *Ocean Engineering* 31 (10):1245-1255.

Anders, F. J., and M. R. Byrnes. 1991. Accuracy of shoreline change rates as determined from maps and aerial photographs. *Shore and Beach* 59 (1):17-26.

Andrews, B. D., P. A. Gares, and J. D. Colby. 2002. Techniques for GIS modeling of coastal dunes. *Geomorphology* 48 (1-3):289-308.

Anselin, L., and A. Getis. 1992. Spatial statistical analysis and geographic information systems. *The Annals of Regional Science* 26 (1):19-33.

Anthony, E. J., and J. D. Orford. 2002. Between wave-and tide-dominated coasts: The middle ground revisited. *Journal of Coastal Research* 36 (Special Issue):8-15.

Antunes, A. F. B., C. Lingnau, and J. C. Da Silva. 2003. Object oriented analysis and semantic network for high resolution image classification. *Boletim de Ciências Geodésicas* 9 (2):233-242.

Armaroli, C., P. Ciavola, Y. Balouin, and M. Gatti. 2004. An integrated study of shoreline variability using GIS and ARGUS techniques. *Journal of Coastal Research* 39 (Special Issue):34-52.

Aubrey, D. G. 1979. Seasonal patterns of onshore/offshore sediment movement. *Journal of Geophysical Research* 84 (C10):6347-6354.

Aubrey, D. G., and R. M. Ross. 1985. The quantitative description of beach cycles. *Marine Geology* 69 (1):155-170.

Austin, M. J., and G. Masselink. 2006. Observations of morphological change and sediment transport on a steep gravel beach. *Marine Geology* 229 (1):59-77.

Australian Hydrographic Service. 2010. *The factors contributing to the level of confidence in the tidal predictions accuracy of tidal predictions*. Wollongong: Intergovernmental Committee on Surveying and Mapping (ICSM).

Bailey, T. C., and A. C. Gatrell. 1995. *Interactive spatial data analysis*. Vol. 413. Essex: Longman Scientific & Technical.

Barber, C. P., and A. Shortridge. 2005. LiDAR elevation data for surface hydrologic modeling: Resolution and representation issues. *Cartography and Geographic Information Science* 32 (4):401-410.

Barzilai, J. 1998. On the decomposition of value functions. *Operations Research Letters* 22 (4):159-170.

Bater, C. W., and N. C. Coops. 2009. Evaluating error associated with LiDAR-derived DEM interpolation. *Computers & Geosciences* 35 (2):289-300.

Battles, J. A. 1974. Surf similarity. *Proceedings of 14th Conference on Coastal Engineering*, 1974, Copenhagen: American Society of Civil Engineers.

Bauer, B. O., and J. R. Allen. 1995. Beach steps: An evolutionary perspective. *Marine Geology* 123 (3):143-166.

Bellomo, D., M. J. Pajak, and J. Sparks. 1999. Coastal flood hazards and the national flood insurance program. *Journal of Coastal Research* (28):21-26.

Benz, U. C., P. Hofmann, G. Willhauck, I. Lingenfelder, and M. Heynen. 2004. Multi-resolution, object-oriented fuzzy analysis of remote sensing data for GIS-ready information. *ISPRS Journal of Photogrammetry and Remote Sensing* 58 (3):239-258.

Blaschke, T. 2010. Object based image analysis for remote sensing. *ISPRS Journal of Photogrammetry and Remote Sensing* 65 (1):2-16.

Blaschke, T., S. Lang, and G. Hay. 2008. *Object-based image analysis: Spatial concepts for knowledge-driven remote sensing applications*. Berlin: Springer.

Boak, E. H., and I. L. Turner. 2005. Shoreline definition and detection: A review. *Journal of Coastal Research* 21 (4):688-703.

Borsdorf, A., R. Raupach, T. Flohr, and J. Hornegger. 2008. Wavelet based noise reduction in CT-images using correlation analysis. *Medical Imaging, IEEE Transactions on* 27 (12):1685-1703.

Bouws, E., L. Draper, E. Shearman, A. Laing, D. Feit, W. Mass, L. Eide, P. Francis, D. Carter, and J. Battjes. 1998. *Guide to wave analysis and forecasting.* No. 702. Geneva: Secretariat of the World Meteorological Organization.

Briscoe, J. 1983. The use of tidal datums in the law. *Surveying and Mapping* 43 (2):115-121.

Burrough, P. A. 2001. GIS and geostatistics: Essential partners for spatial analysis. *Environmental and Ecological Statistics* 8 (4):361-377.

———. 2006. Multiscale sources of spatial variation in soil. I. The application of fractal concepts to nested levels of soil variation. *Journal of Soil Science* 34 (3):577-597.

Burrough, P. A., and A. U. Frank. 1996. *Geographic objects with indeterminate boundaries*. London: Taylor and Francis.

Burrough, P. A., and R. A. McDonnell. 1998. *Principles of geographical information systems*. Vol. 333. Oxford: Oxford university press.

Cartwright, D. E., and A. C. Edden. 1973. Corrected tables of tidal harmonics. *Geophysical Journal of the Royal Astronomical Society* 33 (3):253-264.

Center for Operational Oceanographic Products and Services. 2003. *Computational techniques for tidal datums handbook, NOAA special publication nos co-ops 2*. Silver Spring: National Oceanic and Atmospheric Administration.

Cheng, J. H., C. M. Lee, and C. H. Tang. 2009. An application of fuzzy delphi and fuzzy AHP on evaluating wafer supplier in semiconductor industry. *WSEAS Transactions on Information Science and Applications* 6 (5):756-767.

Chiles, J. P., and P. Delfiner. 1999. *Geostatistics: Modeling spatial uncertainty*. Vol. 497. New York: John Wiley & Sons Inc.

Church, J. A., J. R. Hunter, K. L. McInnes, and N. J. White. 2006. Sea-level rise around the australian coastline and the changing frequency of extreme sea-level events. *Australian Meteorological Magazine* 55 (4):253-260.

Clerke, A. 2004. Determination of mean high water mark within New South Wales. Bachelor's thesis, Engineering and Surveying, University of Southern Queensland, Toowoomba

Cliff, A. D., and K. Ord. 1970. Spatial autocorrelation: A review of existing and new measures with applications. *Economic Geography* 46:269-292.

Cole, G. M. 1997. *Water boundaries*. New York: John Wiley & Sons Inc.

———. 2007. Delineation of coastal boundaries using tidal data *Proceedings of Coastal Areas and Land Administration – Building the Capacity 6th FIG Regional Conference*, 12-15 November 2007, San José: International Federation of Surveyors (FIG).

Collier, P., and N. D. Quadros. 2006. Resolving spatial uncertainty in the tidal interface. *Administering Marine Spaces* 36 (International Issues):36-50.

Cooper, M. 1998. Datums, coordinates and differences. In *Landform monitoring, modelling and analysis*, edited by S. N. Lane, K. S. Richards and J. H. Chandler, 21-36. Chichester: John Wiley & Sons Inc.

Corbit, J. D., and D. J. Garbary. 1995. Fractal dimension as a quantitative measure of complexity in plant development. *Proceedings of the Royal Society of London. Series B: Biological Sciences* 262 (1363):1-6.

Cordesses, L., C. Cariou, and M. Berducat. 2000. Combine harvester control using real time kinematic GPS. *Precision Agriculture* 2 (2):147-161.

Coutts, B. J. 1989. Mean high water as a cadastral boundary. *Ocean and Shoreline Management* 12 (4):309-330.

Cressie, N. A. C., L. J. Sheffield, and H. J. Whitford. 1984. Use of the one sample t-test in the real world. *Journal of Chronic Diseases* 37 (2):107-114.

Crowell, M., S. P. Leatherman, and M. K. Buckley. 1991. Historical shoreline change: Error analysis and mapping accuracy. *Journal of Coastal Research* 7 (3):839-852.

Dail, H. J., M. A. Merrifield, and M. Bevis. 2000. Steep beach morphology changes due to energetic wave forcing. *Marine Geology* 162 (2-4):443-458.

Darwin, G. H. 1883. The harmonic analysis of tidal observations. Scientific papers. Cambridge University Press.

Davis Jr, R. A. 1985. Beach and nearshore zone. In *Coastal sedimentary environments*, edited by R. A. Davis Jr, 379-445. New York: Springer-Verlag.

Davis, T. J., and C. P. Keller. 1997. Modelling uncertainty in natural resource analysis using fuzzy sets and Monte Carlo simulation: Slope stability prediction. *International Journal of Geographical Information Science* 11 (5):409-434.

Deo, M., and C. Sridhar Naidu. 1998. Real time wave forecasting using neural networks. *Ocean Engineering* 26 (3):191-203.

Deo, M. C., A. Jha, A. S. Chaphekar, and K. Ravikant. 2001. Neural networks for wave forecasting. *Ocean Engineering* 28 (7):889-898.

Deo, M. C., and N. K. Kumar. 2000. Interpolation of wave heights. *Ocean Engineering* 27 (9):907-919.

Department of Defence. 2008. *Australian national tide table*. Kent Town: Bureau of Meteorology.

Basic concepts in physical oceanography: Tides. Image. 2007. Department of Oceanography. http://www.oc.nps.edu/nom/day1/partc.html (accessed 27 December 2010).

Department of Transport. 2010a. *Tide analysis software package, version 1.0* (program). Fremantle.

———. 2010b. *Tide heights (dataset)*. Fremantle.

Department of Water. 2008. *Digital elevation of Fremantle (dataset)*. Perth.

Didenkulova, I., E. Pelinovsky, and A. Sergeeva. 2010. Statistical characteristics of long waves nearshore. *Coastal Engineering* 58 (1):94-102.

Dietrich, G., and K. Kalle. 1963. General oceanography, New York. *Inter Science*.

Dolan, R., B. P. Hayden, P. May, and S. May. 1980. The reliability of shoreline change measurements from aerial photographs. *Shore and Beach* 48 (4):22-29.

Doodson, A. T. 1921. The harmonic development of the tide-generating potential. *Proceedings of the Royal Society of London. Series A, Containing Papers of a Mathematical and Physical Character* 100 (704):305-329.

Doukakis, E. 2005. Coastal vulnerability and risk parameters. *European Water* 11 (12):3-7.

Dragut, L., and T. Blaschke. 2006. Automated classification of landform elements using object-based image analysis. *Geomorphology* 81 (3):330-344.

Dunphy, B. 2010. *Redefining land / water boundaries in queensland: The new rules from may 2010. (natural resources and other legislation amendment act 2010)*. High Beam Research [accessed March 2, 2012. Available from http://www.highbeam.com/doc/1G1-225974679.html.

Ehrgott, M., and X. Gandibleux. 2002. *Multiple criteria optimization: State of the art annotated bibliographic surveys, International series in operations research & management science*. Norwell: Kluwer Academic Publishers.

Eliot, M. J., A. Travers, and I. Eliot. 2006. Morphology of a low-energy beach, Como Beach, Western Australia. *Journal of Coastal Research*:63-77.

Emery, X. 2006. Multigaussian kriging for point-support estimation: Incorporating constraints on the sum of the Kriging weights. *Stochastic Environmental Research and Risk Assessment* 20 (1):53-65.

Ergu, D., G. Kou, Y. Peng, and Y. Shi. 2011. A simple method to improve the consistency ratio of the pair-wise comparison matrix in ANP. *European Journal of Operational Research* 213 (1):246-259.

ESRI Inc. 2010. *ArcGIS, version 10.1* (program). Redlands.

Fenner, J. 2010. *A typical coastline profile with normal beach (foreshore) coastal features where the vertical and horizontal tidal range vary with latitude*. In *HWM determination in WA*. Perth: Landgate.

Fishburn, P. C. 1967. Additive utilities with incomplete product set: Applications to priorities and assignments. *Operations Research Society of America*.

Fisher, P. F. 1998. Improved modeling of elevation error with geostatistics. *GeoInformatica* 2 (3):215-233.

Fisher, P. F., and N. J. Tate. 2006. Causes and consequences of error in digital elevation models. *Progress in Physical Geography* 30 (4):467-489.

Fontoura K, A. H., and J. T. Menezes. 2001. Beach morphodynamics and profile sequence for a headland bay coast. *Journal of Coastal Research* 17 (4):812-835.

Foreman, M. G. G. 1977. Manual for tidal heights analysis and prediction. In *Pacific Marine Science Report*. Sydney.

Fowler, C., and E. Treml. 2001. Building a marine cadastral information system for the United States - a case study. *Computers, Environment and Urban Systems* 25 (4):493-507.

Galvin Jr, C. J. 1968. Breaker type classification on three laboratory beaches. *Journal of Geophysical Research* 73 (12):3651-3659.

Gay, N. 1965. High water mark: Boundary between public and private lands. *Florida Law Review* 18:553.

Gill, S. K., and J. R. Schultz. 2001. *Tidal datums and their applications*. Washington: National Oceanic and Atmospheric Administration.

Goicoecha, A., D. Hansen, and L. Duckstein. 1982. *Introduction to multi-objective analysis with engineering and business application*. New York: John Wiley & Sons Inc.

Gozzard, B. 2011. Western australian beach. Perth: Department of Planning and Department of Transport.

Granger, K., T. Jones, M. Leiba, and G. Scott. 1999. Community risk in cairns: A multi-hazard risk assessment. *Australian Journal of Emergency Management* 14 (2):25-26.

Greenfeld, J. 2002. Analytical solution for the amplitude ratio method for determining mean high water in tidal regions. *Journal of Surveying Engineering* 128 (2):61-75.

Griffith, D. A. 1988. *Advanced spatial statistics: Special topics in the exploration of quantitative spatial data series*. Vol. 12. Norwell: Kluwer Academic Publishers.

Gu, Y. H., and M. H. J. Bollen. 2000. Time-frequency and time-scale domain analysis of voltage disturbances. *Power Delivery, IEEE Transactions on* 15 (4):1279-1284.

Guariglia, A., A. Buonamassa, A. Losurdo, R. Saladino, M. L. Trivigno, A. Zaccagnino, and A. Colangelo. 2006. A multisource approach for coastline mapping and identification of shoreline changes. *Annals of geophysics* 49 (1):295-304.

Gupta, P., S. Dutta, and S. Panigrahy. 2010. Mapping of conjunctive water use productivity pattern in an irrigation command using temporal IRS WIFS data. *Water Resources Management* 24 (1):157-171.

Guy Jr, D. E. 1999. Erosion hazard area mapping, Lake County, Ohio. *Journal of Coastal Research* 81 (28):185-196.

Hamann, R., and J. Wade. 1990. Ordinary high water line determination: Legal issues. *Florida Law Review* 42:323.

Hangouët, J. F. 1995. Computation of the Hausdorff distance between plane vector polylines. *Proceedings of American Congress of Surveying and Mapping*, 1995, Charlotte: American Society for Photogrammetry and Remote Sensing.

Hapke, C., and B. Richmond. 2000. Monitoring beach morphology changes using small-format aerial photography and digital softcopy photogrammetry. *Environmental Geosciences* 7 (1):32-37.

Herold, M. 2011. Remote sensing science 2.0. Wageningen: Wageningen University.

Heuvelink, G. B. M. 2006. Analysing uncertainty propagation in GIS: Why is it not that simple? In *Uncertainty in remote sensing and GIS*, edited by G. M. Foody and P. M. Atkinson., 155-165. Chichester: John Wiley & Sons, Ltd.

Hicks, S. D. 1985. Tidal datums and their uses-A summary. *Shore and Beach* 53 (1):27-32.

Hicks, S. D., R. L. Sillcox, C. R. Nichols, B. Via, and E. C. McCray. 1989. *Tide and current glossary*. Silver Spring: National Oceanic and Atmospheric Administration.

Hirst, B., and P. Todd. 2003. Defining boundaries within the tidal interface. *Proceedings of Coastal GIS Conference*, 7-8 July 2003, Wollongong: University of Wollongong.

Hodgson, M. E., and P. Bresnahan. 2004. Accuracy of airborne LiDAR-derived elevation: Empirical assessment and error budget. *Photogrammetric Engineering and Remote Sensing* 70 (3):331-340.

Hodgson, M. E., J. Jensen, G. Raber, J. Tullis, B. A. Davis, G. Thompson, and K. Schuckman. 2005. An evaluation of LiDAR-derived elevation and terrain slope in leaf-off conditions. *Photogrammetric Engineering and Remote Sensing* 71 (7):817.

Holman, R. A. 1986. Extreme value statistics for wave run-up on a natural beach. *Coastal Engineering* 9 (6):527-544.

Holmes, K. W., O. A. Chadwick, and P. C. Kyriakidis. 2000. Error in a usgs 30-meter digital elevation model and its impact on terrain modeling. *Journal of Hydrology* 233 (1):154-173.

Horlin, E. 1994. Water boundaries and legal definitions of high water mark. Bachelor's thesis, Surveying and Land Information, Curtin University, Perth.

Hsu, J. R. C., R. Silvester, and Y. M. Xia. 1989. Generalities on static equilibrium bays. *Coastal Engineering* 12 (4):353-369.

Hu, L., Z. Wang, H. Li, and X. Zhang. 2010. Trust evaluation of cops partners based on wavelet support vector machine model and its application. *Proceedings of International Conference on Management Science and Engineering (ICMSE)*, 24-26 November 2010: IEEE.

Hubbert, G. D., and K. L. McLnnes. 1999. A storm surge inundation model for coastal planning and impact studies. *Journal of Coastal Research* 15 (1):168-185.

Hughes, M. G., A. S. Moseley, and T. E. Baldock. 2010. Probability distributions for wave runup on beaches. *Coastal Engineering* 57 (6):575-584.

Hughes, S. A. 2004. Estimation of wave run-up on smooth, impermeable slopes using the wave momentum flux parameter. *Coastal Engineering* 51 (11):1085-1104.

Humbach, J. A., and J. A. Gale. 1975. Tidal title and the boundaries of the bay: The case of the submerged high water mark. *Fordham Urban Law Journal* 4:91.

Hunter, G. J., and M. F. Goodchild. 1997. Modeling the uncertainty of slope and aspect estimates derived from spatial databases. *Geographical Analysis* 29 (1):35-49.

Huttenlocher, D. P., G. A. Klanderman, and W. J. Rucklidge. 1993. Comparing images using the Hausdorff distance. *Pattern Analysis and Machine Intelligence, IEEE Transactions on* 15 (9):850-863.

Ishizaka, A., and A. Labib. 2011. Review of the main developments in the analytic hierarchy process. *Expert Systems with Applications* 38 (11):14336-14345.

Jacquin, A., D. Sheeren, and J.-P. Lacombe. 2010. Vegetation cover degradation assessment in madagascar savanna based on trend analysis of modis NDVI time series. *International Journal of Applied Earth Observation and Geoinformation* 12, Supplement 1 (0):S3-S10.

Jaganathan, S., J. J. Erinjeri, and J. Ker. 2007. Fuzzy analytic hierarchy process based group decision support system to select and evaluate new manufacturing technologies. *The International Journal of Advanced Manufacturing Technology* 32 (11):1253-1262.

Jaksa, M. B., P. I. Brooker, and W. S. Kaggwa. 1997. Inaccuracies associated with estimating random measurement errors. *Journal of Geotechnical and Geoenvironmental Engineering* 123 (5):393-401.

Jassbi, J., and S. Khanmohammadi. 2010. Determination of the fuzzy weights of criteria in MADM. *Proceedings of 40th International Conference on*

Computers and Industrial Engineering (CIE) 25-28 July 2010, Awaji Island: IEEE.

Jayawardena, A. W., and F. Lai. 1994. Analysis and prediction of chaos in rainfall and stream flow time series. *Journal of Hydrology* 153 (1-4):23-52.

Jian, X., R. A. Olea, and Y. Yu. 1996. Semivariogram modeling by weighted least squares. *Computers & Geosciences* 22 (4):387-397.

Jiang, J., and R. E. Plotnick. 1998. Fractal analysis of the complexity of United States coastlines. *Mathematical Geology* 30 (5):535-546.

Jones, A., and M. Hayne. 2002. Modelling coastal erosion at perth due to long-term sea level rise. *Proceedings of Australia's National Coastal Conference (Coast to Coast) – Source to Sea,* 4-8 November 2002, Tweed Heads: Coast to Coast Australia.

Jong, R., S. Bruin, A. Wit, M. E. Schaepman, and D. L. Dent. 2011. Analysis of monotonic greening and browning trends from global NDVI time-series. *Remote Sensing of Environment* 115 (2):692-702.

Kahraman, C., U. Cebeci, and Z. Ulukan. 2003. Multi-criteria supplier selection using fuzzy AHP. *Logistics Information Management* 16 (6):382-394.

Kalra, R., and M. Deo. 2007. Genetic programming for retrieving missing information in wave records along the west coast of india. *Applied Ocean Research* 29 (3):99-111.

Kangas, A., J. Kangas, and J. Pykäläinen. 2001. Outranking methods as tools in strategic natural resources planning. *Silva Fennica* 35 (2):215-227.

Kay, R. C., and J. Alder. 1999. *Coastal planning and management*. New York: CRC Press.

Kazeminezhad, M., A. Etemad-Shahidi, and S. Mousavi. 2005. Application of fuzzy inference system in the prediction of wave parameters. *Ocean Engineering* 32 (14):1709-1725.

Kearns, F. J. 1980. Waterboundaries. *NewZealandSurveyor* XXXIX (5):470-476.

Kingston, K. S., B. G. Ruessink, I. M. J. Van Enckevort, and M. A. Davidson. 2000. Artificial neural network correction of remotely sensed sandbar location. *Marine Geology* 169 (1):137-160.

Kinsman, B. 2002. *Wind waves: Their generation and propagation on the ocean surface*. New York: Courier Dover Publications.

Kok, M., and F. Lootsma. 1985. Pairwise-comparison methods in multiple objective programming, with applications in a long-term energy-planning model. *European Journal of Operational Research* 22 (1):44-55.

Korner, T. W. 1989. *Fourier analysis*. Cambridge: Cambridge University Press.

Kumar, P., and E. Foutoula-Georgiou. 1997. Wavelet analysis for geophysical applications. *Reviews of Geophysics* 35 (4):385-412.

Kwiatkowski, D., P. C. B. Phillips, P. Schmidt, and Y. Shin. 1992. Testing the null hypothesis of stationarity against the alternative of a unit root: How sure are we that economic time series have a unit root? *Journal of econometrics* 54 (1–3):159-178.

Kwiesielewicz, M., and E. van Uden. 2004. Inconsistent and contradictory judgements in pairwise comparison method in the AHP. *Computers & Operations Research* 31 (5):713-719.

Kyriakidis, P. C., A. M. Shortridge, and M. F. Goodchild. 1999. Geostatistics for conflation and accuracy assessment of digital elevation models. *International Journal of Geographical Information Science* 13 (7):677-707.

Land Services. 2008. Nature boundaries. In *Cadastral Survey Guidelines*. Adelaide.

Landgate. 1995. *Lidar points of Port Hedland (dataset)*. Perth.

———. 2009a. *Digital elevation of Port Hedland (dataset)*. Perth.

———. 2009b. *Port Hedland townsite and environment mosaic (dataset)*. Perth.

———. 2009c. Survey & plan practice manual. Perth: Landgate.

———. 2010. *Metro west mosaic (dataset)*. Perth.

———. 2012. *Digital elevation of South Fremantle (dataset)*. Perth.

Larson, M., and N. C. Kraus. 1994. Temporal and spatial scales of beach profile change, Duck, North Carolina. *Marine Geology* 117 (1):75-94.

Laukkanen, S., A. Kangas, and J. Kangas. 2002. Applying voting theory in natural resource management: A case of multiple-criteria group decision support. *Journal of Environmental Management* 64 (2):127-137.

Leon, J., and C. T. Correa. 2006. Quantification of shoreline change in Salaverry, Peru. *Journal of Coastal Research* (Special Issue 39):1013-1016.

Levy, J. K., J. Hartmann, K. W. Li, Y. An, and A. Asgary. 2007. Multi-criteria decision support systems for flood hazard mitigation and emergency response in urban watersheds1. *Journal of the American Water Resources Association* 43 (2):346-358.

Li, J., and A. D. Heap. 2008. *A review of spatial interpolation methods for environmental scientists*. Vol. 23. Canberra: Geoscience Australia.

Lin, P.-C., B. Wu, and J. Watada. 2010. Kolmogorov-Smirnov two sample test with continuous fuzzy data. *Integrated Uncertainty Management and Applications* 68:175-186.

Lippmann, T., and R. Holman. 1989. Quantification of sand bar morphology: A video technique based on wave dissipation. *Journal of Geophysical Research* 94 (C1):995-1011.

———. 1990. The spatial and temporal variability of sand bar morphology. *Journal of Geophysical Research* 95 (C7):11575-11590.

List, J. H., and A. S. Farris. 1999. Large-scale shoreline response to storms and fair weather. *Proceedings of Fourth International Symposium on Coastal Engineering and Science of Coastal Sediment Processes*, June 21-23, 1999, New York: the American Society of Civil Engineers (ASCE).

Liu, X., J. Xia, C. Blenkinsopp, L. Arnold, and G. Wright. 2012. High water mark determination based on the principle of spatial continuity of the swash probability. *Journal of Coastal Research.* In press, doi:10.2112/jcoastres-d-12-00061.1.

Müller, U. K. 2007. A theory of robust long-run variance estimation. *Journal of econometrics* 141 (2):1331-1352.

Mahoney, R. 2007. Permanent committee on tides & mean sea level. Perth: Department for Planning and Infrastructure.

———. 2009. Coastal demarcation lines for administrative and engineering purposes. Perth: Department of Transport.

Mai, S., H. Schwarze, and C. Zimmermann. 1997. Safety of coastal defense systems: An assessment of the reliability of coastal systems in the event of rising water levels due to climate change. *Proceedings of the 1st International Conference Port Coast Environment*, Varna: Bulgarian Coastal Association.

Maiti, S., and A. K. Bhattacharya. 2009. Shoreline change analysis and its application to prediction: A remote sensing and statistics based approach. *Marine Geology* 257 (1):11-23.

Makarynskyy, O. 2004. Improving wave predictions with artificial neural networks. *Ocean Engineering* 31 (5):709-724.

Makarynskyy, O., A. A. Pires-Silva, D. Makarynska, and C. Ventura-Soares. 2005. Artificial neural networks in wave predictions at the west coast of Portugal. *Computers and Geosciences* 31 (4):415-424.

Maloney, F. E. 1977. The ordinary high water mark: Attempts at settling an unsettled boundary line. *Land and Water Law Review* 13:465.

Maloney, F. E., and R. C. Ausness. 1974a. Use and legal significance of the mean high water line in coastal boundary mapping. *North Carolina Law Review* 53:185.

———. 1974b. The use and legal significance of the mean high water line in coastal boundary mapping. *North Carolina Law Review* 53:185.

Mandelbrot, B. B. 1967. How long is the coast of Britain? Statistical self-similarity and fractional dimension. *Science* 156 (3775):636-638.

———. 1982. *Nature of fractal geometry*. San Francisco: Freeman

Marfai, M., and L. King. 2008. Potential vulnerability implications of coastal inundation due to sea level rise for the coastal zone of Semarang City, Indonesia. *Environmental Geology* 54 (6):1235-1245.

Marpu, P. R. 2009. Geographic object-based image analysis. Doctoral Dissertation, Geosciences, Geo-Engineering and Mining, Technische Universitat Bergakademie Freiberg, Freiberg.

Martins, A. G., D. Coelho, H. Antunes, and J. Clímaco. 1996. A multiple objective linear programming approach to power generation planning with demand-side management (DSM). *International Transactions in Operational Research* 3 (3):305-317.

Mase, H. 1989. Random wave runup height on gentle slope. *Journal of Waterway, Port, Coastal, and Ocean Engineering* 115 (5):649-661.

Masselink, G., and C. B. Pattiaratchi. 2001. Seasonal changes in beach morphology along the sheltered coastline of perth, western australia. *Marine Geology* 172 (3-4):243-263.

Masselink, G., and P. Russell. 2006. Flow velocities, sediment transport and morphological change in the swash zone of two contrasting beaches. *Marine Geology* 227 (3-4):227-240.

MathWorks. 2010. *Matlab: The language of technical computing, version 7.11* (program). Auckland.

McBeth, F. H. 1956. A method of shoreline delineation. *Photogrammetric Engineering* 22 (2):400-405.

McKinley, S., and M. Levine. 1998. *Cubic spline interpolation*. College of the Redwoods [accessed 11 November 2012. Available from http://online.redwoods.edu/INSTRUCT/darnold/LAPROJ/Fall98/SkyMeg/Proj.PDF.

McMaster, R. B. 1986. A statistical analysis of mathematical measures for linear simplification. *Cartography and Geographic Information Science* 13 (2):103-116.

Mendoza, G. A., and H. Martins. 2006. Multi-criteria decision analysis in natural resource management: A critical review of methods and new modelling paradigms. *Forest Ecology and Management* 230 (1):1-22.

Mendoza, G. A., and W. Sprouse. 1989. Forest planning and decision making under fuzzy environments: An overview and illustration. *Forest Science* 35 (2):481-502.

Min, D., L. Zhilin, and C. Xiaoyong. 2007. Extended hausdorff distance for spatial objects in GIS. *International Journal of Geographical Information Science* 21 (4):459-475.

Mitasova, H., T. Drake, R. Harmon, J. Hofierka, and J. McNinch. 2002. Spatio-temporal monitoring of evolving topography using LiDAR, real time kinematic GPS and sonar data. *Proceedings of Open Source Free Software GIS–GRASS Users Conference*, 11-13 September 2002, Trento: University of Trento.

Moore, I. D., R. B. Grayson, and A. R. Ladson. 1991. Digital terrain modelling: A review of hydrological, geomorphological, and biological applications. *Hydrological processes* 5 (1):3-30.

Moore, L. J. 2000. Shoreline mapping techniques. *Journal of Coastal Research* 16 (1):111-124.

Moore, L. J., P. Ruggiero, and J. H. List. 2006. Comparing mean high water and high water line shorelines: Should proxy-datum offsets be incorporated into shoreline change analysis? *Journal of Coastal Research* 22 (4):894-905.

Moore, S. R. 1999. Fractal interpolation techniques. Bachelor's thesis, Mathmatics, The University of Southern Mississippi, Hattiesburg.

Morton, R. A. 1974. Shoreline changes on Galveston Island (Bolivar Roads to San Luis Pass). *Geological Circula* 2:33.

———. 1991. Accurate shoreline mapping: Past, present, and future. *Proceedings of Conference on Quantitative Approaches to Coastal Sediment Processes*, June 25-27 1991, Seattle: American Society of Civil Engineers.

Morton, R. A., M. P. Leach, J. G. Paine, and M. A. Cardoza. 1993. Monitoring beach changes using GPS surveying techniques. *Journal of Coastal Research* 9 (3):702-720.

Morton, R. A., T. L. Miller, and L. J. Moore. 2004. *National assessment of shoreline change: Part 1: Historical shoreline changes and associated coastal land loss along the us gulf of mexico*. Vol. 1043, *US geological survey open file report*. Collingdale: DIANE Publishing.

Morton, R. A., and F. M. Speed. 1998. Evaluation of shorelines and legal boundaries controlled by water levels on sandy beaches. *Journal of Coastal Research* 14 (4):1373-1384.

Muzy, J. F., J. Delour, and E. Bacry. 2000. Modelling fluctuations of financial time series: From cascade process to stochastic volatility model. *The European Physical Journal B-Condensed Matter and Complex Systems* 17 (3):537-548.

U.S. Maritime zones and boundaries. Image. 2012. National Oceanic and Atmospheric Administration (NOAA). http://www.nauticalcharts.noaa.gov/csdl/mbound.htm (accessed 15 August 2012).

———. 2010a. *History of tidal analysis and prediction* [accessed 27 June 2011. Available from http://tidesandcurrents.noaa.gov/predhist.html#Up.

———. 2010b. *Tidal constituent, also known as a constituent tide* [accessed 7 May 2011. Available from http://www.co-ops.nos.noaa.gov/constitu.html.

———. 2010c. *Tide-predicting machine* [accessed 9 June 2011. Available from http://tidesandcurrents.noaa.gov/predmach.html.

Newey, W. K., and K. D. West. 1987. A simple, positive semi-definite, heteroskedasticity and autocorrelation consistent covariance matrix. *Econometrica: Journal of the Econometric Society* 55 (3):703-708.

Nicholls, R. J. 2002. Analysis of global impacts of sea-level rise: A case study of flooding. *Physics and Chemistry of the Earth, Parts A/B/C* 27 (32):1455-1466.

NOAA Coastal Services Center. 2011. *What does accuracy mean in GIS and remote sensing?* [accessed 19 August 2011. Available from http://www.csc.noaa.gov/crs/lca/faq_tech.html.

Nunley, J. C. 2002. Potential for remote sensing to locate the ordinary high water line in Florida: A case study of Lakes Hatchineha and Kissimmee. Master's thesis, Environmental Protection, University of Florida, Gainesville.

Oksanen, J., and T. Sarjakoski. 2005. Error propagation of DEM-based surface derivatives. *Computers & Geosciences* 31 (8):1015-1027.

Oliver, M. A., and R. Webster. 1990. Kriging: A method of interpolation for geographical information systems. *International Journal of Geographical Information Systems* 4 (3):313-332.

Opricovic, S. 2011. Fuzzy VIKOR with an application to water resources planning. *Expert Systems with Applications* 38 (10):12983-12990.

Overton, M., C. Petrina, and J. Fisher. 1996. Determining shoreline position using historical photography and digital softcopy photogrammetry. *Proceedings of American Society for Photogrammetry and Remote Sensing/American Congress on Surveying and Mapping (ASPRS/ACSM) Annual Convention And Expo*, April 22-25 1996, Bethesda: ASPRS/ACSM.

Özger, M., and Z. Şen. 2007. Prediction of wave parameters by using fuzzy logic approach. *Ocean Engineering* 34 (3-4):460-469.

Ozmutlu, H. C., A. Spink, and S. Ozmutlu. 2002. Analysis of large data logs: An application of poisson sampling on excite web queries. *Information Processing & Management* 38 (4):473-490.

Pajak, M. J., and S. Leatherman. 2002. The high water line as shoreline indicator. *Journal of Coastal Research* 18 (2):329-337.

Palisade Corporation. 2009. *@risk for excel, version 5.5* (program). New York.

Palmer, M. W. 1988. Fractal geometry: A tool for describing spatial patterns of plant communities. *Plant Ecology* 75 (1):91-102.

Papathoma, M., and D. Dominey-Howes. 2003. Tsunami vulnerability assessment and its implications for coastal hazard analysis and disaster management planning, gulf of corinth, greece. *Natural Hazards and Earth System Science* 3 (6):733-747.

Parker, B. B. 2003. The difficulties in measuring a consistently defined shoreline—the problem of vertical referencing. *Journal of Coastal Research* (Special Issue 38):44-56.

Pattiaratchi, C., and E. Sarath Wijeratne. 2009. Tide gauge observations of 2004–2007 indian ocean tsunamis from sri lanka and western australia. *Pure and Applied Geophysics* 166 (1):233-258.

Pawlowicz, R., B. Beardsley, and S. Lentz. 2002. Classical tidal harmonic analysis including error estimates in matlab using T_TIDE. *Computers & Geosciences* 28 (8):929-937.

Percival, D. B., and A. T. Walden. 2006. *Wavelet methods for time series analysis*. Vol. 4. Cambridge: Cambridge University Press.

Perron, O. 1907. Zur theorie der matrizen. *Mathematische Annalen* 64:781-798.

Pethick, J. S., and S. Crooks. 2000. Development of a coastal vulnerability index: A geomorphological perspective. *Environmental Conservation* 27 (04):359-367.

Peuquet, D. J. 1992. An algorithm for calculating minimum euclidean distance between two geographic features. *Computers & Geosciences* 18 (8):989-1001.

Phillips, J. D. 1986. Spatial analysis of shoreline erosion, delaware bay, new jersey. *Annals of the Association of American Geographers* 76 (1):50-62.

Phillips, T. 1999. *Harmonic analysis and prediction of tides* [accessed 15 May 2011. Available from https://www.math.sunysb.edu/~tony/tides/harmonic.html.

Phua, M. H., and M. Minowa. 2005. A GIS-based multi-criteria decision making approach to forest conservation planning at a landscape scale: A case study in the kinabalu area, sabah, malaysia. *Landscape and Urban Planning* 71 (2):207-222.

Pohekar, S. D., and M. Ramachandran. 2004. Application of multi-criteria decision making to sustainable energy planning—a review. *Renewable and Sustainable Energy Reviews* 8 (4):365-381.

Priest, G. R. 1999. Coastal shoreline change study northern and central lincoln county, oregon. *Journal of Coastal Research* 81 (28):140-157.

Pugh, D. T. 1996. *Tides, surges and mean sea-level (reprinted with corrections)*. Chichester: John Wiley & Sons Inc.

Pukkala, T. 1998. Multiple risks in multi-objective forest planning: Integration and importance. *Forest Ecology and Management* 111 (2):265-284.

Quadros, N. D., and P. A. Collier. 2008. A new approach to delineating the littoral zone for an australian marine cadastre. *Journal of Coastal Research* 24 (3):780-789.

R Development Core Team. 2012. *R: A language and environment for statistical computing, version 2.15.2* (program). Auckland.

Reikard, G. 2009. Forecasting ocean wave energy: Tests of time-series models. *Ocean Engineering* 36 (5):348-356.

Rooney, J. J. B., and C. H. Fletcher. 2000. A high resolution, digital, aerial photogrammetric analysis of historical shoreline change and net sediment transport along the kihei coast of maui, hawaii. *Proceedings of Thirteenth Annual National Conference on Beach Preservation Technology*, February 2-4, 2000, Melbourne, Florida: Florida Shore & Beach Preservation Association.

Rosner, B., and D. Grove. 1999. Use of the Mann–Whitney U-test for clustered data. *Statistics in Medicine* 18 (11):1387-1400.

Rubner, Y., J. Puzicha, C. Tomasi, and J. M. Buhmann. 2001. Empirical evaluation of dissimilarity measures for color and texture. *Computer Vision and Image Understanding* 84 (1):25-43.

Ruggiero, P., G. M. Kaminsky, and G. Gelfenbaum. 2003. Linking proxy-based and datum-based shorelines on a high-energy coastline: Implications for shoreline change analyses. *Journal of Coastal Research* 81 (38):57-82.

Ruggiero, P., P. D. Komar, W. G. McDougal, and R. A. Beach. 1996. Extreme water levels, wave runup and coastal erosion. *Proceedings of 25th Conference on Coastal Engineering*, 1996, Orlando: American Society of Civil Engineers.

Ruggiero, P., P. D. Komar, W. G. McDougal, J. J. Marra, and R. A. Beach. 2001. Wave runup, extreme water levels and the erosion of properties backing beaches. *Journal of Coastal Research* 17 (2):407-419.

Ruggiero, P., and J. H. List. 2009. Improving accuracy and statistical reliability of shoreline position and change rate estimates. *Journal of Coastal Research* 25 (5):1069-1081.

Saaty, T. 1980. *The analytic hierarchy process*. New York: McGraw-Hill.

Scheffner, N. W. 1992. Stochastic time‐series representation of wave data. *Journal of Waterway, Port, Coastal and Ocean Engineering* 118 (4):337-351.

Schmoldt, D. L., J. Kangas, G. A. Mendoza, and M. Pesonen. 2001. *The analytic hierarchy process in natural resource and environmental decision making*. Vol. 3. Dordrecht: Springer.

Schwimmer, R. A. 2008. A temporal geometric analysis of eroding marsh shorelines: Can fractal dimensions be related to process? *Journal of Coastal Research* 24 (1):152-158.

Shalowitz, A. L. 1964. *Shore and sea boundaries: With special reference to the interpretation and use of coast and geodetic survey data*. Washington: Coast and Geodetic Survey.

Shemshadi, A., H. Shirazi, M. Toreihi, and M. J. Tarokh. 2011. A fuzzy VIKOR method for supplier selection based on entropy measure for objective weighting. *Expert Systems with Applications* 38 (10):12160-12167.

Shepard, F. 1950. Longshore-bars and longshore-troughs. *Beach Erosion Board Technical Memorandum* 15:31.

Shi, W. 2009. *Principles of modeling uncertainties in spatial data and spatial analyses*. Boca Raton: CRC.

Short, A. D. 2004. *Beaches of the Western Australian coast-Eucla to Roebuck Bay: A guide to their nature, characteristics, surf and safety*. Sydney: Sydney University Press.

Short, A. D., and C. L. Hogan. 1994. Rip currents and beach hazards: Their impact on public safety and implications for coastal management. *Journal of Coastal Research* (Special Issue 12):197-209.

Shoshany, M., and A. Degani. 1992. Shoreline detection by digital image processing of aerial photography. *Journal of Coastal Research* 8 (1):29-34.

Silva, V., D. C. Morais, and A. T. Almeida. 2010. Prioritizing complex issues of hydrographic basin committees by group decision approach. *Brazilian Journal of Operations & Production Management* 7 (1):123-139.

Simon, D. 1993. Ordinary high-water mark(OHWM). In *Waterway and Wetland Handbook*. Wisconsin.

Songberg, G. 2004. Accurate mean high water mark determination fact or fiction. *Proceedings of New South Wales Staff Surveyors Association Incorporated Annual Conference*, 2004, Sydney: Association of Public Authority Surveyors NSW.

Southgate, H. N. 1989. A nearshore profile model of wave and tidal current interaction. *Coastal Engineering* 13 (3):219-245.

Spanos, P. T. D. 1983. Arma algorithms for ocean wave modelling. *Journal of Energy Resources Technology, Transactions of the ASME* 105 (3):300-309.

Stockdon, H. F., R. A. Holman, P. A. Howd, and J. A. H. Sallenger. 2006. Empirical parameterization of setup, swash, and runup. *Coastal Engineering* 53 (7):573-588.

Stockdon, H. F., A. H. Sallenger, J. H. List, and R. A. Holman. 2002. Estimation of shoreline position and change using airborne topographic LiDAR data. *Journal of Coastal Research* 18 (3):502-513.

Stubsjøen, S. M., J. Bohlin, E. Skjerve, P. S. Valle, and A. J. Zanella. 2010. Applying fractal analysis to heart rate time series of sheep experiencing pain. *Physiology & Behavior* 101 (1):74-80.

Subasi, A. 2007. Eeg signal classification using wavelet feature extraction and a mixture of expert model. *Expert Systems with Applications* 32 (4):1084-1093.

Tanadtang, P., D. Park, and S. Hanaoka. 2005. Incorporating uncertain and incomplete subjective judgments into the evaluation procedure of transportation demand management alternatives. *Transportation* 32 (6):603-626.

The Intergovernmental Committee on Surveying and Mapping (ICSM). 2009. Australian tides manual. In *Special Publications 9 Handbook*. Wollongong.

———. 2010a. *Note regarding doodson number attributed to Mr. Alan Marshall* [accessed 3 May 2011. Available from http://www.icsm.gov.au/icsm/SP9/links/Doodson_PCTMSL.html.

———. 2010b. *Tides, sea level and water currents* [accessed 13 July 2011. Available from http://www.icsm.gov.au/icsm/SP9/tides.html.

———. 2012. *Tidal interface compendium of terms* [accessed 16 November 2012. Available from http://www.icsm.gov.au/tides/tidal_interface.html.

The Virginia Institute of Marine Science. 2010. *Tide analysis* [accessed 11 April 2011. Available from https://web.vims.edu/physical/research/TCTutorial/tideanalysis.htm.

Theiler, J. 1990. Estimating fractal dimension. *Journal of the Optical Society of America A* 7 (6):1055-1073.

Thieler, E. R., and W. W. Danforth. 1994. Historical shoreline mapping (i): Improving techniques and reducing positioning errors. *Journal of Coastal Research* 10 (3):549-563.

Thompson, J. A., J. C. Bell, and C. A. Butler. 2001. Digital elevation model resolution: Effects on terrain attribute calculation and quantitative soil-landscape modeling. *Geoderma* 100 (1):67-89.

Thyagarajan, K. S. 2011. *Still image and video compression with matlab*. Hoboken: Wiley-IEEE Press.

Titus, J. G., R. A. Park, S. P. Leatherman, J. R. Weggel, M. S. Greene, P. W. Mausel, S. Brown, C. Gaunt, M. Trehan, and G. Yohe. 1991. Greenhouse effect and sea level rise: The cost of holding back the sea. *Coastal management* 19 (2):171-204.

Travers, A. 2009. Low-energy beach morphology with respect to physical setting: A case study from Cockburn Sound, Southwestern Australia. *Journal of Coastal Research* 23 (2):429-444.

Tremarfon Pty Ltd. 2011. *Wave heights and period (dataset)*. Melville.

Triantaphyllou, E., and C. T. Lin. 1996. Development and evaluation of five fuzzy multiattribute decision-making methods. *International Journal of Approximate Reasoning* 14 (4):281-310.

Triantaphyllou, E., and S. H. Mann. 1989. An examination of the effectiveness of multi-dimensional decision-making methods: A decision-making paradox. *Decision Support Systems* 5 (3):303-312.

Triantaphyllou, E., B. Shu, S. N. Sanchez, and T. Ray. 1998. Multi-criteria decision making: An operations research approach. *Encyclopedia of electrical and electronics engineering* 15:175-186.

Trimble Germany GmbH. 2010. *Ecognition developer, version 8.0.2* (program). Sunnyvale.

URS Group Inc. 2006. High water mark collection for hurricane katrina in alabama. Gaithersburg: Federal Emergency Management Agency.

Ustoorikar, K., and M. C. Deo. 2008. Filling up gaps in wave data with genetic programming. *Marine Structures* 21 (2):177-195.

Uunk, L., K. M. Wijnberg, and R. Morelissen. 2010. Automated mapping of the intertidal beach bathymetry from video images. *Coastal Engineering* 57 (4):461-469.

Vaze, J., and J. Teng. 2007. High resolution LiDAR DEM–how good is it? *Proceedings of the MODSIM 2007 International Congress on Modelling and Simulation*, December 2007, Christchurch: Modelling and Simulation Society of Australia and New Zealand.

Verbesselt, J., M. Herold, R. Hyndman, A. Zeileis, and D. Culvenor. 2011. A robust approach for phenological change detection within satellite image time series. *Proceedings of 6th International Workshop on the Analysis of Multi-temporal Remote Sensing Images*, 12-14 July 2011, Trento: IEEE.

Verbesselt, J., A. Zeileis, and M. Herold. 2012. Near real-time disturbance detection using satellite image time series: Drought detection in Somalia. *Remote Sensing and Environment* 123:98 -108.

Von Winterfeldt, D., and G. W. Fischer. 1975. Multi-attribute utility theory: Models and assessment procedures. In *Utility, probability, and human decision making*, edited by D. Wendt and C. A. Vlek, 47-85. Dordrecht: Springer.

Walter, V. 2004. Object-based classification of remote sensing data for change detection. *Journal of Photogrammetry and Remote Sensing* 58 (3):225-238.

Wechsler, S. P., and C. N. Kroll. 2006. Quantifying DEM uncertainty and its effect on topographic parameters. *Photogrammetric Engineering and Remote Sensing* 72 (9):1081.

Weishar, L. L., and W. L. Wood. 1983. An evaluation of offshore and beach changes on a tideless coast. *Journal of Sedimentary Research* 53 (3):847-858.

Whittal, J. 2011. The integrated coastal management act no 24 of 2008 (ICMA) – a professional land surveyor's interpretation. *Proceedings of the Jubilee Congress of the Commission on Legal Pluralism*, 8-10 September 2011, Cape Town: University of Cape Town.

Whittal, J., and F. Fisher. 2011. Implications of the integrated coastal management act no 24 of 2008 on the South African coastal cadastre and its survey and management. *Proceedings of AfricaGEO conference*, 31 May-2 June 2011, Cape Town: AfricaGEO.

Williams-Wynn, C. 2011. Practical examples of the legal position of the high water mark at a specific point in time. *Proceedings of AfricaGEO conference*, 31 May-2 June 2011, Cape Town: AfricaGEO.

Winant, C., D. Inman, and C. Nordstom. 1975. Description of seasonal beach changes using empirical eigenfunctions. *Journal of Geophysical Research* 80 (15):1979-1986.

Wise, S. 2000. Assessing the quality for hydrological applications of digital elevation models derived from contours. *Hydrological processes* 14 (11):1909-1929.

Wong, D. W., L. Yuan, and S. A. Perlin. 2004. Comparison of spatial interpolation methods for the estimation of air quality data. *Journal of Exposure Analysis and Environmental Epidemiology* 14 (5):404-415.

Wood, S. 2005. Determination of high water mark: The Don Wallace method. Bachelor (Hons)'s thesis, Spatial Sciences, Curtin University of Technology, Perth.

Zhang, J., and M. F. Goodchild. 2002. *Uncertainty in geographical information*. London: Taylor and Francis.

Zhou, Y., and G. A. G. Paul. 2005. High-energy noise attenuation of seismic data in the wavelet-transform domain. *Integrated Computer-Aided Engineering* 12 (1):57-67.

APPENDIX I

FIELD WORK PLAN FOR HWM DETERMINATION IN PORT HEDLAND

The aim of this field survey is to identify the position (X, Y, Z) of HWM indicators and the significant swash (wave runup, the maximum horizontal position of water that can reach on the shore) heights by RTK methods using GNSS.

- Scope of the study area

The site extends approximately 2,300m along the coast at Cooke Point, Port Hedland. The Figure 1 shows the extent of the study area with coordinates.

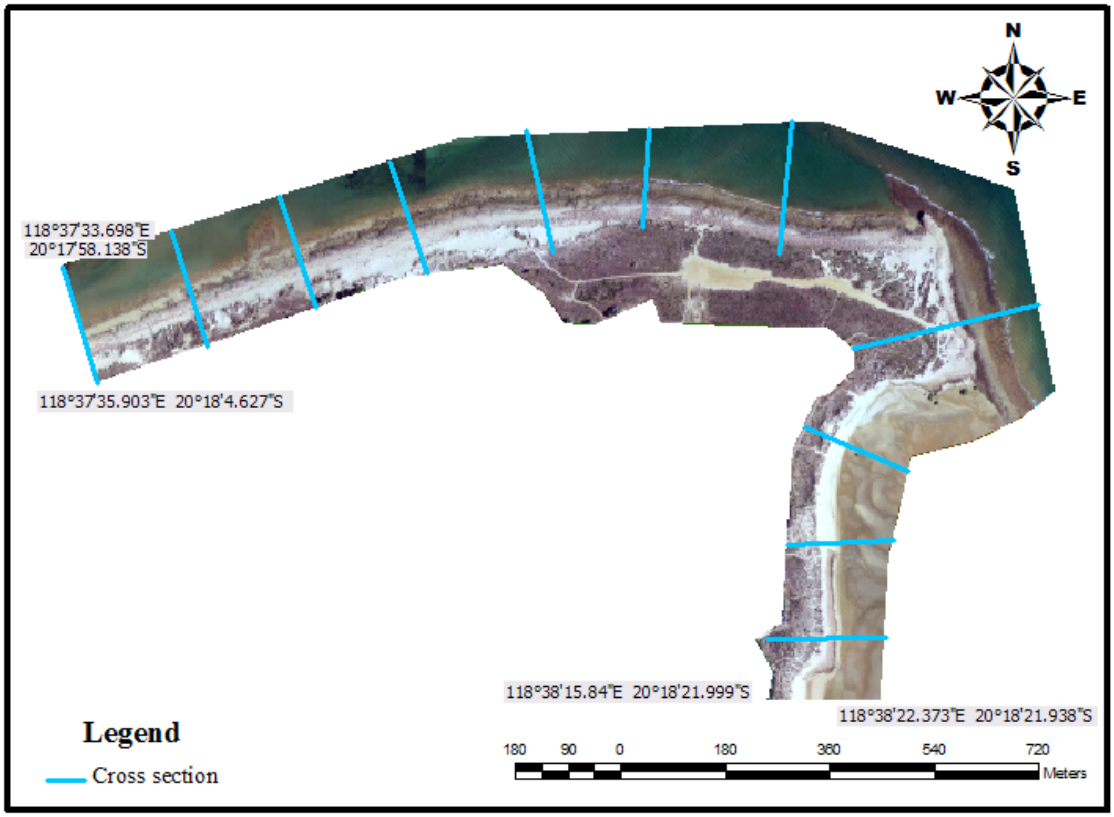

Figure 1 Study area

- Setup cross-sections

To identify the position of HWM indicators, which include high water line (long term mark of wet and dry sand) (Figure 2), frontal dune toe and vegetation line (Figure 3), the cross-shore transects need to be setup at regular intervals (in order to interest with the three onshore features). However, in order to obtain more samples,

the cross-sections may not have the same and fixed interval and as same position as shown in Figure 1.

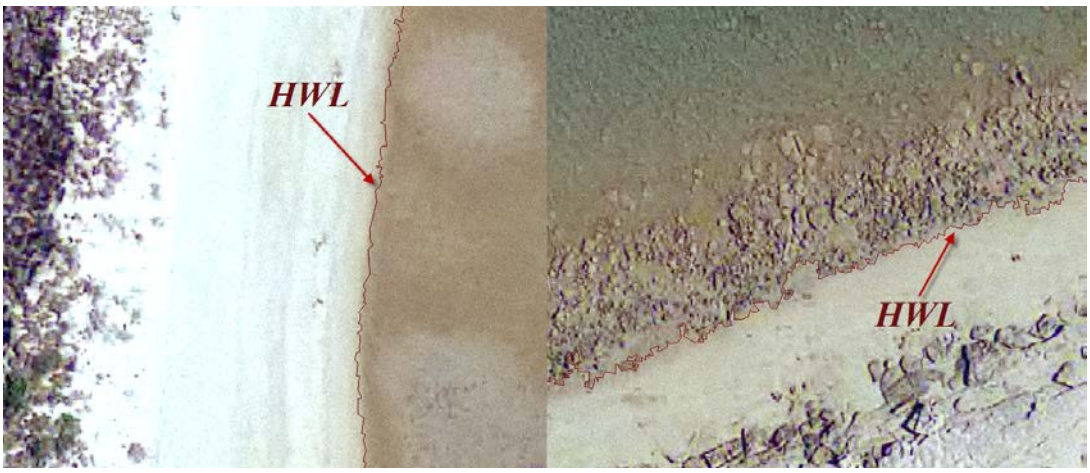

Figure 2 High water lines

Figure 3 The frontal dune toe and vegetation zone

- Onshore features identification

Three types of features' positions are required to be identified: high water line, frontal dune toe and vegetation line. The intersected points of high water line and frontal dune toe with cross sections are recorded as their position, and the X, Y, Z of these points are recorded by the RTK.

Because the vegetation is irregularly distributed, the average height of sparse vegetation zone was defined as the position of vegetation. The sparse zone was

defined as the area where trees are not adjacent, they are scattered and distributed with a certain space interval. However, it was not possible to provide the exact space interval or distance between the trees for the real field work. However, Figures 4 and 5 provide a visual for the vegetation colour. Here dark green indicates the density vegetation and light green or even grey and brown indicates the sparse vegetation. For example, in Figure 5, it can be seen that there are two sparse vegetation zones that intersected with the cross-section (indicated by the red pen). In the field, this could estimate the average heights of those two zones (maybe it is the middle point of those two) and record that position and the height of it.

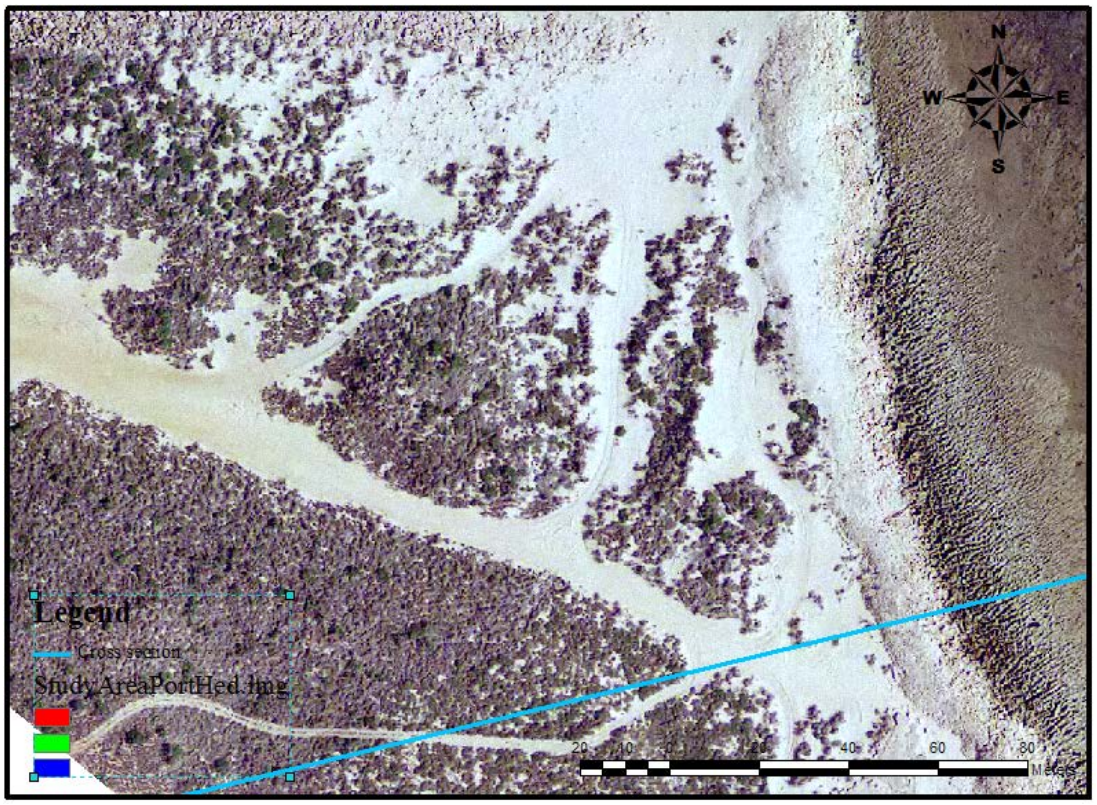

Figure 4 The vegetation shown on the image

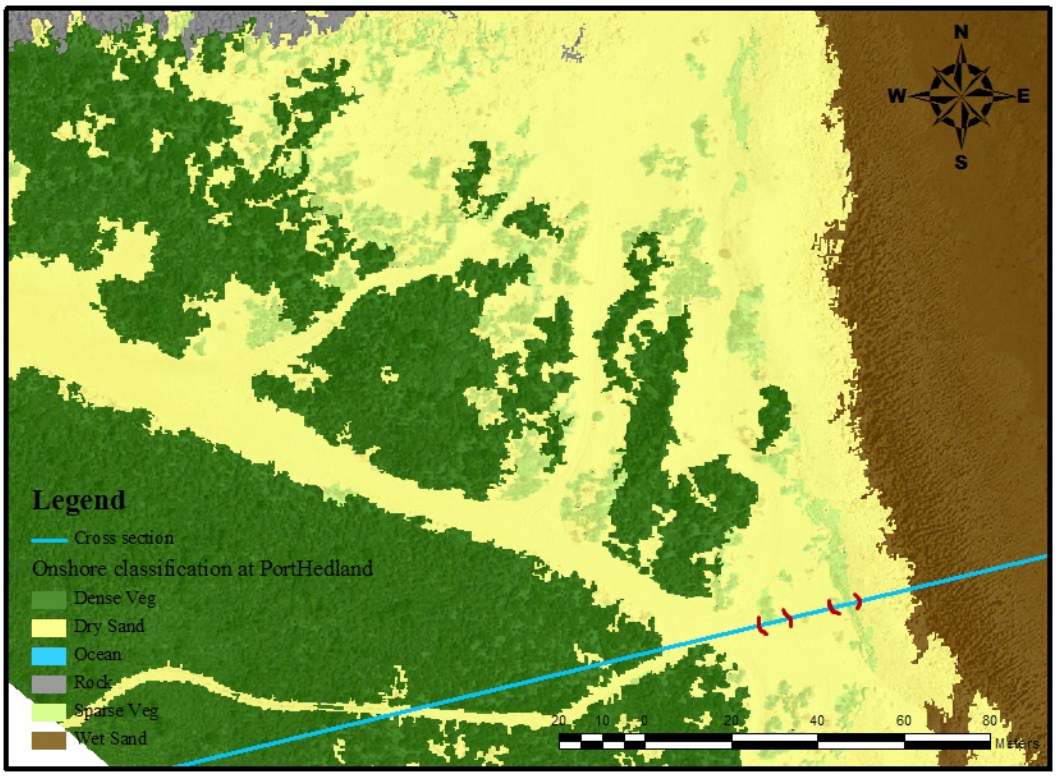

Figure 5 The classification results

- Swash heights observation

The swash heights (associated with time) are required to be continuously recorded for 14 hours along one cross-section of a study area. It is possible to pick up any one that is convenient for surveying. The time interval of the recording is 1 hour, and within the 1 hour, the maximal swash level needs to be recorded.

APPENDIX II

SURVEY FOR THE EVALUATION OF HWM DETERMINATION

Request to Participate in Research

Dear Experts,

I am writing to invite you to take part in the High Water Mark (HWM) indicators evaluation survey. You have been selected for the survey because we believe you are an expert in the coastal research, land management and cartography areas. Your participation in this study will provide valuable information in developing a consistent, stable and precise HWM, which is a boundary that separates water and land. The questionnaire answers will be used to compare the importance of three criteria for HWM determination.

The three criteria to evaluate the HWM include temporal and spatial variation and inundation probability, which could be interpreted as stable, precision and inundation risk for the determined HWM (see the following table) and has been calculated in the previous studies.

Your participation in this study is voluntary. The survey is expected to take no more than 5-10 minutes of your time. The questionnaire is in the following pages.

All information collected will be kept strictly confidential and will be used for this study only. The survey is completely anonymous, thus information collected from the survey will not include names **but will include affiliation information**, which will facilitate in discussion of the survey results. You will be free at any time to withdraw consent to further participation without prejudice in any way. You need give no reason or justification for such a decision. In such cases, any records of your participation in the interview will be destroyed unless you agree otherwise.

This research has been approved by the Human Research Ethics Committee, Research Services, at Curtin University of Technology with approval number RD-47-12.

Should you have any queries about the survey, please do not hesitate to contact Xin Liu at xin.liu2@postgrad.curtin.edu.au or on 08-9266 4255 or Dr. Jianhong (Cecilia) Xia at c.xia@curtin.edu.au or on 08-92667563.

We look forward to your participation in this study and thank you for your co-operation.

Yours sincerely,

Xin Liu

PHD Candidate

310A, Department of Spatial Sciences

Curtin University of Technology

GPO Box U1987 Perth, WA 6845 Australia

Email: xin.liu2@postgrad.curtin.edu.au

Tel:+61 8 9266 4255

	Determine method	Impact
Stability	Compare the difference of two DEMs representing summer and winter coastal morphology that may lead to the variation of shorelines.	The aim of shoreline management is to achieve the shoreline stability (Pethick and Crooks 2000).
Precision	Calculate the precision of the model and data that derives the HWM indicators and the complexity of the HWM indicators when they are identified or levelled off on the beach plane.	A precise method to determine the position of shoreline has been identified as a critical need among policy makers and coastal researchers (Thieler and Danforth 1994).
Inundation risk	Inundation probabilities from swash were determined using empirical models by taking into account the wave and tide records. These heights were then fitted to an appropriate distribution and the probability that swash would reach each HWM indicator was computed, taking into account the effects of waves and tide (Liu *et al.* 2012).	Swash probability of HWM indicates inundation risk, which is an important reference for the coastal protection system (Mai *et al.* 1997).

Research title: Determination of the High Water Mark and its location along a coastline

This research has the Curtin Human Research Ethics Committee approval number RD-47-12 from 28 August 2012 to 28 August 2013.

Questionnaire

1) Criteria evaluation (9 point scale, compare row relative to column, for example, "relative to a criterion on the right top, a criterion on the left is very strongly less important," you can put a "1/7" in the table):

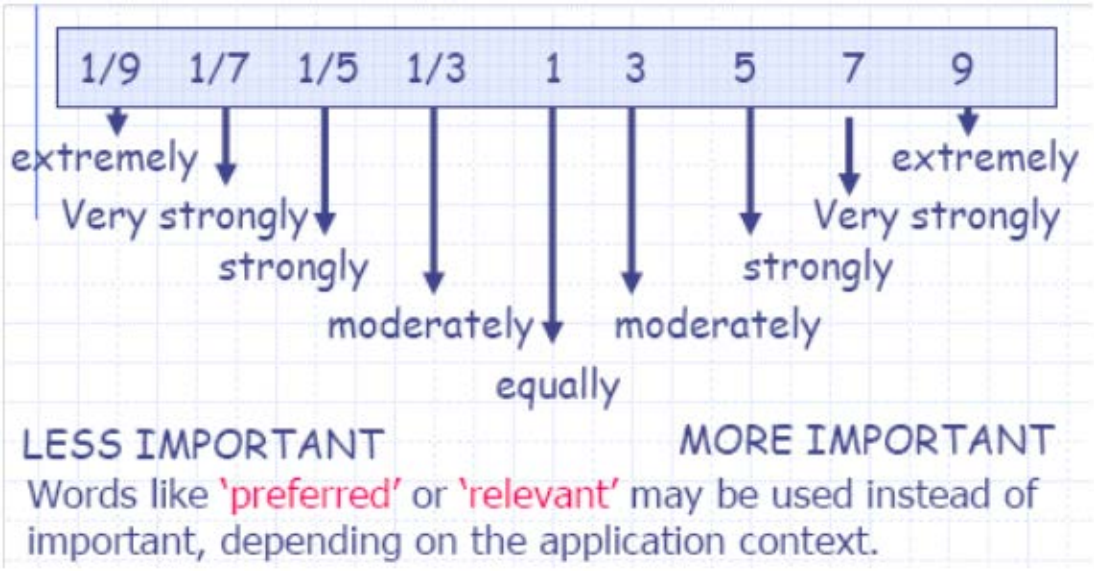

	Stability	Precision	Inundation risk
Stability	1		
Precision		1	
Inundation risk			1

THE END!

Thank you for completing our survey! Your responses and feedback are greatly appreciated.